EPITOPE-TARGETING STRATEGY FOR A VACCINE AGAINST HUMAN IMMUNODEFICIENCY VIRUS TYPE-1: PEPTIDE LIGANDS FOR THE BROADLY-NEUTRALIZING ANTIBODIES b12, 2F5 AND 2G12

by

Alfredo Menendez

B. Sc. University of Havana, 1985

THESIS SUBMITTED IN PARTIAL FULFILLMENT

OF THE REQUIREMENTS OF THE DEGREE OF

DOCTOR OF PHILOSOPHY

in the

Department of Molecular Biology and Biochemistry

SIMON FRASER UNIVERSITY

Summer 2005

APPROVAL

NAME: Alfredo Menendez

DEGREE: Doctor of Philosophy

TITLE OF THESIS: Epitope-targeting strategy for a vaccine against Human Immunodeficiency Virus type-1; peptide ligands for the broadly-neutralizing antibodies b12, 2F5 and 2G12.

EXAMINING COMMITTEE:

CHAIR: Dr. Rosemary Cornell, Professor
Department of Molecular Biology and Biochemistry, SFU

Dr. Jamie K. Scott, Professor, Canada Research Chair
Senior Supervisor, Department of Molecular Biology
and Biochemistry, SFU

Dr. Mark Paetzel, Assistant Professor
Department of Molecular Biology and Biochemistry, SFU

Dr. Dipankar Sen, Professor, Department of Chemistry,
Department of Molecular Biology and Biochemistry, SFU

Dr. Lisa Craig, Assistant Professor, Internal Examiner
Department of Molecular Biology and Biochemistry, SFU

Dr. Richard Wyatt, Chief Structural Virology Laboratory
NIH Vaccine Research Center, Bethesda, MD
External Examiner

Date Approved: May 17, 2005

SIMON FRASER UNIVERSITY

PARTIAL COPYRIGHT LICENCE

ABSTRACT

The research presented here is part of an ongoing effort to develop an epitope-targeted vaccine against the Human Immunodeficiency Virus type 1. We have used phage-displayed peptide libraries, in conjunction with other biochemical and structural techniques, to generate and characterize peptides specific for the broadly-neutralizing, human monoclonal antibodies (Mab) b12, 2F5 and 2G12.

First, peptide ligands for Mab b12 were isolated. One peptide, B2.1, was characterized in detail. The crystal structure of B2.1 in complex with b12 Fab was solved and compared with a model of the antibody docked to gp120. B2.1 was used to immunize mice, seeking to generate a b12-like, neutralizing antibody response. Minimal structural resemblance between the putative b12 epitope and B2.1 peptide was observed, indicating different mechanisms of binding to b12. Moreover, the anti B2.1 response from the immunized mice did not cross-react with gp120, further indicating this difference.

Second, we demonstrate that Mab 2F5, which binds to the sequence ELDKWA on gp41, selects peptides with multiple, different amino acid sequences flanking its three-residues DKW native core epitope. High-affinity binding was achieved by peptides with unrelated flanking sequences C-terminal to the core epitope, with the nature and location of critical binding residues differing between peptides. Our results implicate multiple mechanisms of binding, and suggest the existence of two distinctive functional regions in the 2F5 paratope, one that is DKW-specific and one that is multi-specific.

Finally, a peptide ligand specific for the carbohydrate-binding Mab 2G12 was isolated, characterized and optimized. The peptide competes with carbohydrate ligands

for binding to 2G12. The crystal structure of the 2G12-peptide complex, and its comparison with the 2G12-$Man_9GlcNAc_2$ complex, shows that the peptide is not a mimic of $Man_9GlcNAc_2$. They occupy separate sites in the antibody's paratope, with minimal overlaping, therefore the peptide and $Man_9GlcNAc_2$ make a different set of contacts with the Mab.

In summary, we have observed that peptide mimicry of the b12, 2F5 and 2G12 epitopes is essentially functional, not structural. Our results indicate that these ligands can be used as antibody-specific markers, and that most likely, conventional immunizations with so-called peptide mimics will not elicit these antibodies.

DEDICATION

To Mari, Laura and Alfredo, for making it worthwhile,

and to my parents, for their share in who I am.

ACKNOWLEDGMENTS

Many people have made possible the completion of this work. First of all, I want to thank my wife, Mari Montero for her unconditional love and support and for always believing in me. She has been a constant source of inspiration, as well as an invaluable colleague, with whom I have had countless enjoyable moments of good science.

I am especially indebted to my supervisor, Jamie Scott, who back in 1997 gave me the opportunity that had eluded me for a year, and took me into her lab. Under her guidance, I have learnt to think critically and have gained much knowledge and independence as a scientist. I am particularly grateful to her for always keeping the challenges there for me, and give me the choice to take them. Working with her has been my pleasure.

I have shared much time with past and present members of the Scott lab, who had made working there a memorable experience. I like to thank Pilar Blancafort and Lisa Craig for helping me in the very early days, Lori Bonnycastle, Juqun Shen and Kelly Brown for teaching me around, and make me feel welcome in the lab. To Michael Zwick, I am grateful for the constant brainstorming we always had going, and from which came many good suggestions and ideas. I'd like to thank Oscar Pan, Brett Vanderkist, Keith Chow, John Zuccolo and Sampson Wu for their excellent technical assistant, and my fellow graduate students Sondra Bhar, Melita Irving, Mary Montero and Nienke van Houten for their contributions to this work. I am also grateful to other members of the lab, Martina Mai, Joanna Chodkowska, Xing Wang and Tanika Grant for their help and support. I am indebted to Blair Jonhston (SFU) and Juan Carlos Almagro (Miami, FL) for

their help and patience in my many consultations with them about carbohydrates and antibodies, respectively. I thank Teresa Kitos (SFU) and Louise Creag (UBC) for their help with HPLC and Biacore, respectively.

I had also the pleasure of working with several bright undergraduate students, that while training in the lab, made contributions to the work presented here, thus I'd like to thank Anita Burguess, Sonia Statsny, Rena Astronomo, Amanda Johner and Chao Wang for their excellent work.

This project has greatly benefited from collaboration with other research groups, I would like to acknowledge the contributions from Daniel Calarese, Michael Zwick, Ralph Pantophlet, Erica Ollman-Saphire, Chris Scanlan, Robyn Stanfield, Ian Wilson and Dennis Burton, from The Scripps Reseacrh Institute, CA, and Herman Katinger, Gabriela Stiegler and Renata Kunert, from the University of Agricultural Sciences in Vienna, Austria.

My work was supported by Dr. Scott's NIH/NIAID grants R21-AI49808 and RO1AI49111. I thank the financial support provided by a Graduate Scholarship from the Michael Smith Foundation for Health Research, BC, and a Canada Graduate Scholarship from the Natural Sciences and Engineering Research Council, as well as the President's Research Stipend from SFU. I would also like to acknowledge the donation of valuable reagents by the MRC Centralised AIDS Facility (UK) and the NIH AIDS Research and Reference Reagents Program.

Finally, I would like to thank the members of my Examining Committee for their time and effort in evaluating my research.

TABLE OF CONTENTS

LIST OF TABLES

CHAPTER 2.

CHAPTER 3.

CHAPTER 4.

CHAPTER 5

LIST OF FIGURES.

CHAPTER 1.

CHAPTER 2.

CHAPTER 3.

CHAPTER 4.

CHAPTER 5.

LIST OF ABBREVIATIONS.

ABTS: 2,2'-Azino-bis(3-ethylbenzthiazoline-6-sulfonic acid);
BSA: bovine serum albumin, fraction V;
DTT: dithiothreitol;
H_2O_2: Hydrogen peroxide
HIVIG: Anti-HIV immunoglobulins, from human donors;
HRP: horseradish peroxidase;
Isopropyl β-D-thiogalactopyranoside;
Kd: Dissociation constant at equilibrium;
k_a: Association rate constant;
k_d: Dissociation rate constant;
MAb: monoclonal antibody;
Manα1-2Man: 2-O-(α-D-Mannopyranosyl)-D-Mannopyranose;
MBP: *E. coli* maltose-binding protein;
NZY/Tet/IPTG: NZY media supplemented with 15 ug/ml of tetracycline and 1 mM;
Nt: Neutralizing;
NtAbs: Neutralizing antibodies;
PDPLs: Phage-displayed peptide libraries;
PEG/NaCl: 16.7% Polyethylene glycol 8000, 3.3 M sodium chloride;
pNPP: p-Nitrophenyl phosphate
SDS-PAGE: sodium duodecyl sulphate-polyacrylamide gel electrophoresis;
SHIV: Simian, Human Immunodeficiency Virus;
SPR: Surface plasmon resonance;
TBS: Tris-buffered saline, pH 7.5;
RU: Resonance units;
(-3): amino acid position three residues C-terminal to the Trp residue in the DKW core sequence (Chapter 4).
(+3): amino acid position three residues N-terminal to the Asp residue in the DKW core sequence (Chapter 4).

CHAPTER 1: INTRODUCTION.

1.1. Thesis format.

In this thesis, we present results produced while studying three human monoclonal antibodies (MAbs) against Human Immunodeficiency Virus type-1 (HIV-1), which are capable of efficiently neutralize a broad range of field isolates of HIV-1. These antibodies (b12, 2F5 and 2G12) are attractive targets for prophylactic anti-HIV-1 vaccine design (the aspects of the cellular immune response against HIV-1 and their relevance to vaccine will be occasionally referred to, but not discussed here). The work reported here has been published, or is being prepared for submission.

We have chosen to present our results in this dissertation using the "published manuscript" format based in the characteristics of the work. The antibodies b12, 2F5 and 2G12 represent three independent identities, directed against separate and dissimilar sites of the envelope of HIV-1. MAb b12 reacts with a discontinuous protein epitope on gp120, 2G12 with a unique carbohydrate epitope, and 2F5 with an incompletely-characterized epitope that includes a continuous site on gp41. Thus, although similar general approach has been equally employed for all three MAbs, the challenges in each case are very specific, and so are the type and significance of the results. The "published manuscript" format is very adequate for the independent presentation of each set of results.

The approach we have undertaken to develop an HIV-1 vaccine involves, by necessity, many different scientific aspects and the use of a variety of technologies, without which the work couldn't be advanced beyond the initial phases. Successful

collaborations with other groups were established, as reflected by their contributions to the results discussed here. The self-contained character of the chapters in the "published manuscript" format provides a clear-cut picture of these collaborations and the way in which specific issues were addressed.

This thesis contains a general introduction (Chapter 1), in which I have provided background information that complements the introduction of the other chapters. Chapters 2-5 are self-contained, and each one is devoted exclusively to one of the three aforementioned antibodies. Chapter 2, published in *The Journal of Virology 75:6692-6699, 2001* presents the isolation of B2.1, a peptide specific for MAb b12. Chapter 3 describes functional and structural studies on the binding of B2.1 peptide to MAb b12, as well as immunization studies in animals; it is being prepared for submission to *The Journal of Biological Chemistry*. Chapter 4, published in *The Journal of Molecular Biology 338:311-327, 2004*, presents the isolation and characterization of peptides reactive with MAb 2F5, and our contribution to the identification of the 2F5 epitope. Finally, Chapter 5, which is being prepared for submission to *The Journal of Biological Chemistry*, describes the isolation, structural and functional characterization of peptide ligands for MAb 2G12. A final chapter with general conclusions, and discussing the results from chapters 2-5 is also included.

1.2. Summary of my contribution to Chapters 2, 3, 4 and 5.

The design and execution of the experiments presented here are not exclusively the result of my work. I had a direct involvement in designing and executing about half of the experiments presented in Chapter 2. Some of those experiments were performed

before I entered the PhD program, however the conclusion of the work and writing of the paper was done as part of my studies. I had a leading role in the analysis of the results and the writing and submission of the paper, together with Dr. M. Zwick (TSRI, La Jolla, CA) and my supervisor, Dr. Jamie Scott. My contribution to Chapter 3 involved the execution of one of the experiments presented, and a leading role in the analysis of the results and the writing of the paper, in cooperation with Dr. E. Ollman-Saphire (TSRI) and Dr. Scott. All the experiments in Chapter 4 are the result of my direct execution or supervision; the analysis of results, and writing/submission of the paper was done in collaboration with Dr. Scott. Results in Chapter 5 were also performed by me or under my direct supervision, except the determination of the crystal structure. The writing of the paper, which will be submitted from our laboratory, has been done in collaboration with Dr. Scott and D. Calarese, from TSRI.

1.3. Phage-displayed peptide libraries.

The display of a short recombinant peptide on the surface of a filamentous phage was first reported by George P. Smith, in 1985 (300). From that pioneering work, the ideas of affinity selection (or "biopanning") and phage-displayed peptide libraries (PDPLs) were rapidly developed and implemented (236, 296). A PDPL consists of millions of independent phage clones, with each expressing a different peptide sequence, and displaying it on the surface of the phage particle. Since the DNA sequence encoding the peptide is cloned in frame with a phage coat protein gene, the peptide sequence can be directly deduced from the phage DNA sequence, and target-specific clones can be readily isolated and characterized upon affinity purification with a target molecule.

Most random peptide libraries are built in filamentous phage, like M13 and f1, or derivatives. Display *via* the major coat protein (pVIII) of filamentous phage is highly multivalent, for example, a density of recombinant peptides of up to 10 % of the total pVIII (~ 300 copies per phage particle) can be obtained in f88-4 (294). Other libraries, fused to the minor coat protein pIII, display between 0-5 peptide copies per phage particle (294). Filamentous phage are easy to work with, their biology is relatively well-known, and they are versatile enough as to accommodate the cloning of peptide sequences in several of their structural proteins, thus providing a range of library choices with different properties (106, 108, 152).

The screening of PDPLs is typically carried over several consecutives rounds of selection, which include *(i)* binding of the phage to the target molecule; *(ii)* capture of phage-target complexes; *(iii)* washing to remove unbound phage and *(iv)* the recover of bound phage and their amplification in bacterial cells. Phage clones can be selected from amplified pools by infection at low multiplicity of infection, and are characterized for binding to the screening target and competition with the original antigen (1).

1.4. The concept of epitope-targeted vaccine.

Current experience in vaccine immunology indicates that protection against infectious diseases requires the presence of multiple B- and T-cell epitopes, combined in a single antigenic entity. Epitopes are by definition discrete sites on antigens, which can be recognized and bound by B- or T-cells *via* their antigen receptors (172) (B-cell epitopes can also bind soluble antibodies). The concerted recognition of relevant epitopes by B and T cells serves as the basis of the adaptive immune response.

Regarding the antibody response, there are no specific rules as to the amount and complexity of B-cell epitopes that a single antigen might contain. Antigens can be of very diverse chemical nature, comprising small molecules with one or a few B-cell epitopes (*e.g.*, dinitrophenol), or large and complex molecules with hundreds of different ones (*e.g.*, HIV-1 glycoprotein gp120); they are all characterized by their ability to bind antibodies. Antigens may be *antigenic* and *immunogenic*. Antigenicity refers to the ability of an antigen to be recognized by antibodies, whereas immunogenicity applies to its ability to elicit a specific antibody response (172). These concepts can also be applied to describe any particular epitope; by definition, any immunogenic epitope is also antigenic, but the reverse situation is not always true.

More than 200 years after Edward Jenner's experiments, vaccine research is still a poorly rationalized enterprise that relies essentially on trial and error approaches. Most of the successful vaccines so far, fall into the category of live or inactivated vaccines (http://www.fda.gov/cber/vaccine/licvacc.htm) that share the distinction of being composed of whole organisms, carrying hundreds of epitopes. Despite their success, a clear disadvantage of those types of vaccines is that a significant immune response is made against non-relevant epitopes, along with those needed to confer protection.

Epitope-targeted vaccines are aimed at the elicitation of an oligoclonal, response, based on the use of one or a few well-defined, protective epitopes. They offer the advantage of focusing the immune response to the pathogen's sites relevant for protection, and minimize the generation of responses with potential detrimental effects, like for example, antibodies that mediate infection enhancement, which have been observed with many viruses, including HIV-1 (199, 208, 213, 256). Targeting specific

epitopes is a very general approach that, in principle, is applicable to virtually any scenario, regardless of the chemical nature of the antigen.

The expansion and refinement of epitope discovery tools, such as PEPSCAN (117), synthetic random peptide libraries (116) and phage-displayed peptide libraries (236, 296), have made possible the systematic identification and characterization of epitopes and epitope mimics relevant to many infection models, as well as the establishment of peptide-based epitope-targeting strategies for the development of vaccines (204). The starting element is usually a worthy antibody with a known protective activity, usually a MAb that has been characterized in terms of bactericidal activity, viral neutralization or protection in challenge experiments in animal models. The antibody is then used in a combinatorial approach to isolate reactive peptides, which ideally, will replicate or *mimic* the original protective site on the pathogen. These peptide leads are subsequently characterized, often optimized, and eventually tested for their ability to produce a protective response in an immunization model (Fig 1).

1.5. Peptide mimicry of linear, conformational and carbohydrate epitopes.

The biggest obstacle in the development of epitope-targeted vaccines that are based on peptide mimics of neutralizing or bactericidal sites on pathogens, is the lack of a straightforward translation of *antigenic mimicry* into *immunogenic mimicry*. It seems a natural assumption that if an antibody binds to a particular peptide, there should be a high likelihood that such peptide will induce such antibody upon immunization. However, that assumption doesn't always hold true, especially for mimics of conformational protein epitopes and carbohydrate epitopes.

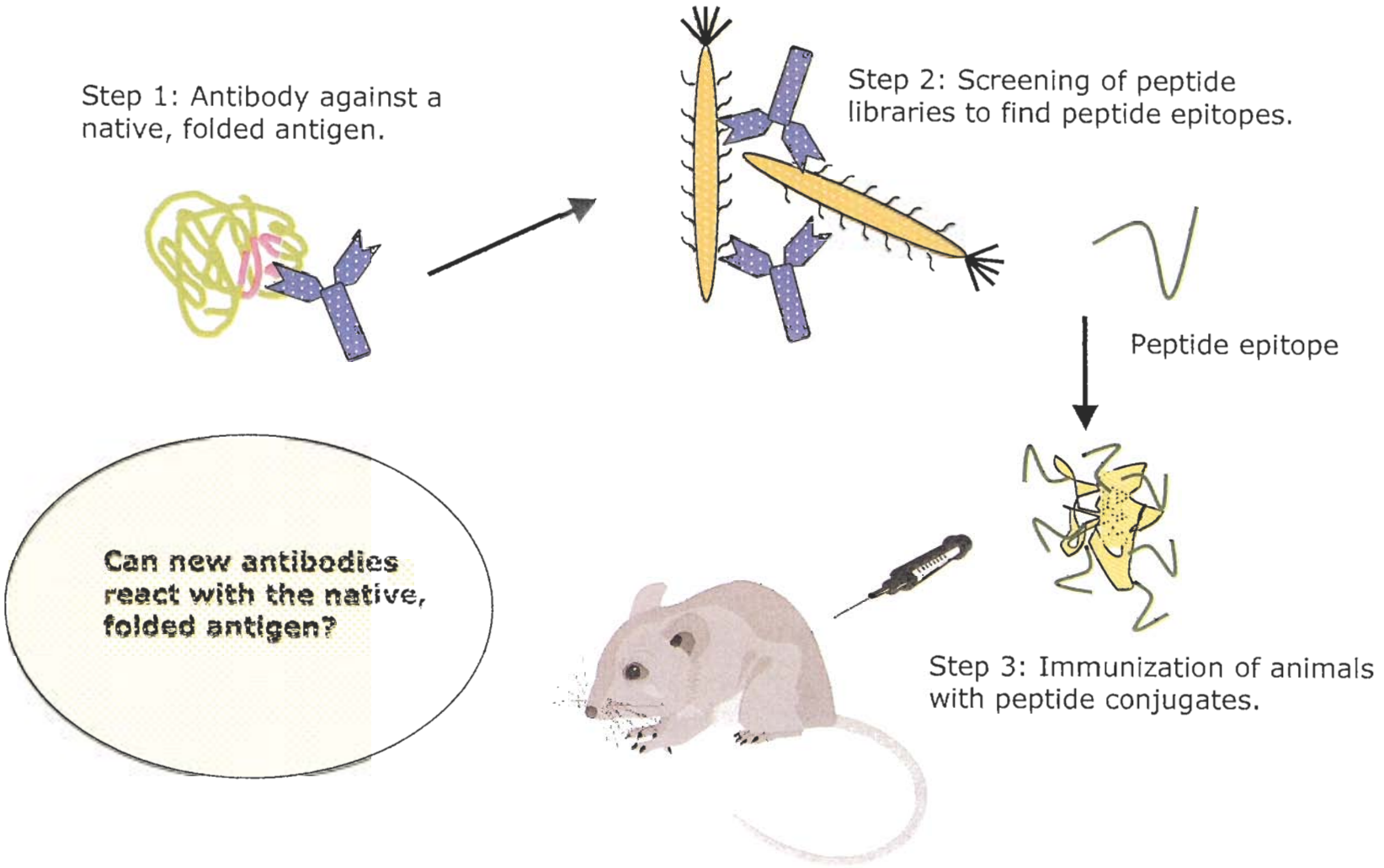

Figure 1. General strategy for the development of an epitope-targeted vaccine.

The distinction between antigenic and immunogenic mimicry may be established as an extension of the concepts of antigenicity and immunogenicity. A peptide that competes with molecule X for binding to the paratope of an antibody is considered a functional antigenic mimic of molecule X (or said to be crossreactive with X), but to be considered an immunogenic mimic, the peptide should elicit an antibody response qualitatively similar to that elicited by molecule X. It is thought that the more an antigenic mimic mirrors the structure of the epitope on molecule X, especially in its contacts with the antibody's paratope, the more likely it will be an immunogenic mimic that can elicit antibodies that crossreact with molecule X.

Antigenic mimicry of continuous and discontinuous protein epitopes by peptides has been extensively documented with the use of peptide libraries (146, 322). Antibodies against discontinuous epitopes dominate in most anti-protein polyclonal responses (20, 67, 141, 147, 155, 193), including that against gp120 in HIV-1 infection (211). However, peptide mimics of continuous sites are more frequently isolated from screenings with polyclonal antibodies (69, 141, 288, 310). This may be partially due to inherent limitations of the screening techniques, but is also a reflection of differences between the paratopes of peptide-binding and protein-binding antibodies and their intrinsic ability to bind peptides. A recent study analyzing 37 crystal structures of antibodies in complex with protein or peptide antigens, found that antibodies against both antigens use essentially the same average number of specificity-determining residues (SDRs), that is, residues involved in direct contact with the antigen (16.6 for protein-bound and 17.2 for peptide-bound antibodies) (8). However, recognition of peptides and proteins seems to require different antigen-binding site topographies (190, 325), for example, it has been

observed that antibodies that contact proteins are more likely to use residues in the apical regions of the hypervariable loops and thus to have a "flat" paratope, whereas antibodies that contact peptides have a stronger tendency to use residues closer to the base of the loops, located in the interior of the binding site and thus to form a "grooved" paratope (8). These differences in paratope topography may limit the ability of protein-binding antibodies to interact with short peptides.

Peptide mimicry of discontinuous epitopes is typically observed with non-detectable, scarce or dispersed sequence similarity between the peptide and the cognate protein antigen (43, 111, 154, 156, 323). Moreover, cross-reactivity between peptides selected from libraries and continuous protein epitopes, frequently occurs with a relatively small number of shared residues, as shown, for example, for hen egg white lysozyme and myohemerythrin (69), glycoprotein S of murine *Coronavirus* (347) and *E. coli* colicin A (68) (see also Chapter 4). These observations suggest that in most cases, peptide mimicry of protein antigens is achieved in the absence of significant *structural mimicry*, and is instead based on contacts different from those of the antibody/protein pair, *i.e. via functional mimicry.*

The mechanism of functional mimicry is further supported by multiple precedents of antibody promiscuity in the recognition of peptide epitopes, which show the ability of one antibody to bind several, unrelated peptide sequences (80, 171, 195, 251, 270, 320). Keitel *et al.* have provided an excellent example of peptide binding promiscuity of an antibody in their studies with the anti-HIV-1 p24 MAb CB4-1, which binds to several peptides of unrelated sequences, selected from a synthetic peptide library. Crystal structures of two of the peptides in complex with CB4-1 showed different peptide

structures with occupancy of the same binding site by both peptides, mediated by different interactions (167, 171). In an elegant extension of that study, Hoffmuller *et al.* (138) evolved one peptide into the other by sequential single amino acid substitutions, without loss of binding to CB4-1 by the intermediates. The crystal structure of one intermediate peptide showed the establishment of new peptide-antibody contacts, including a striking change in the orientation of the side chain of a key Leu residue of the peptide (138).

Peptide mimicry of carbohydrate moieties also seems to occur through functional rather than structural mechanism(s). Although not an antibody, a well-characterized example is the case of Concanavalin A (ConA), a lectin from the jack bean (*Canavalia ensiformis*), specific for Man(α1-6)Man(α1-3)Man tri-mannose cores in mannose-containing carbohydrates (93, 221). ConA crystal structure in complex with a carbohydrate ligand reveals the existence of an extended carbohydrate-binding site, which contacts all three monosaccharide subunits of the tri-mannose core *via* three discrete sub-sites (36, 81, 221). Oldenburg *et al.* and Scott *et al.* isolated ConA-binding peptides displaying the motif YPY, by screening of octapeptide and hexapeptide PDPLs, respectively (229, 295). Crystal structure of one peptide in complex with ConA shows that the peptide binds in two different modes, to two sites different from the mannose and tri-mannose binding sites (149). Moreover, a comparison with two other peptides in complex with ConA shows a situation similar to that of MAb CB4-1 (see above), with all three peptides bound to a common site, but with the contacting residues and interactions rearranged depending on peptide size and sequence (150).

For anti-carbohydrate antibodies, the only direct comparison of the structures of an antibody in complex with the native carbohydrate epitope, and a peptide ligand, comes from the work of Vyas *et al.* (330) with MAb SYA/J6, a murine IgG specific for the polysaccharide O-antigen of the *Shigella flexneri* Y liposaccharide. Peptides that bind to SYA/J6 were isolated by Harris *et al.* by screening of PDPLs (132). Vyas *et al.* solved the crystal structure of a synthetic octapeptide bound to SYA/J6 Fab, and compared it to that of the Fab in complex with a synthetic pentasaccharide (331). They found that the peptide complements the shape of the antigen-binding site of SYA/J6 more closely than does the pentasaccharide; the peptide also makes significantly more contacts with SYA/J6, and most contacts differ between the two ligands. Another remarkable feature was the interaction of the peptide *via* 14 water molecules, which mediate multiple hydrogen bonds with the SYA/J6 Fab (330).

Thus, the evidence indicates that peptide mimicry of discontinuous protein epitopes and carbohydrate epitopes is more functional than structural, that is, peptide binding is satisfied by series of new interactions, with minimal mimicry of the structural properties of the original antigen (see also Chapters 3 and 5). The implications of this for the development of epitope-targeted vaccines are significant, since it is apparent that it may be difficult to elicit a desired antibody response by direct immunizations with antigenic peptide mimics of an epitope.

1.6. Epitope-targeted vaccines, the need for a combined approach.

Screening of PDPLs allows one to explore the binding of a target to millions of short peptides in a single experiment, therefore it is a powerful tool for the discovery and

mapping of antibody epitopes. PDPLs have been extensively used for this purpose, and many successful examples have been reported in the literature (reviewed in (146, 322)). The technology has also been used for the isolation of peptide leads that can later be evolved into vaccine candidates.

However, isolating peptide leads from PDPLs is only the initial step; very often petides isolated from primary PDPLs display low affinities for their cognate antibodies, thus peptides are optimized by construction and screening of semi-defined sublibraries (86, 205). Additional decreases in affinity may be observed in some instances, if a peptide is taken out of the context of the phage, and made as a synthetic, free peptide (58, 79, 86, 309). As a consequence, peptides are often expressed as fusion proteins, or synthesized as multiple antigenic peptides (MAPs), with a higher valency (101, 130, 154, 262, 307).

The concept of epitope-targeted vaccines is inextricably linked with the idea of peptide vaccines. However, as discussed in section 1.5, the basis of peptide crossreactivity with more complex epitopes is not completely understood. It is apparent that functional mimicry plays a predominant role in most cases, but the information is limited due to the lack of structural data comparing antibodies bound to both the native epitopes and peptide mimics. Whereas there are multiple examples of atomic structures of antibodies in complex with peptides mimics of continuous epitopes in proteins (PDB Database, http://www.rcsb.org/pdb/ (21), there are only two cases of solved structures of antibodies bound to peptide mimics of carbohydrate antigens (330, 346). In addition, there is not a single example of a crystal structure of a mimic of a protein conformational site, bound to the cognate antibody (we provide the first one here, see Chapter 3).

Collection of functional data is necessary to complement the information provided by the atomic structures, for example, the identification of critical-binding residues in the peptides and determination of the affinity of antibody-peptide interactions. Resolution of crystal structures of mimics in complex with the antibody, combined with the functional data, are very informative, and can be of great use in structure-based improvement of peptide ligands, as has been demonstrated in previous work (19, 346).

Antibodies produced against peptide mimics, have occasionally shown crossreactivity with the native epitopes and even inhibited the action of pathogens (19, 55, 303, 328). More commonly, significant titers of anti-peptide antibodies are generated, but show poor cross-reactivity with the native epitope (see Chapter 2 of this work). Interestingly, there is not a commercial vaccine yet, based on a peptide mimic, which indicates the need for a deeper understanding of the laws of mimicry, and illustrates the necessity for developing and testing novel immunogen formulations, and immunization strategies. One such immunization strategy is a prime-boost approach, in which native antigen is used to generate a primary response, and the peptide mimics are used for subsequent immunizations. This method has already been validated by Beenhouwer *et al.*, who demonstrated the generation of significant antibody titers against protective epitopes of the glucuronoxylomannan (GXM) component of the capsular polysaccharide *Cryptococcus neoformans* (19). They used a tetanus toxoid conjugate of GXM for priming, followed by boosts with a tetanus toxoid conjugate of a high-affinity peptide that bound to a protective antibody against GXM. Using this approach, they produced an antibody response focused on anti-GXM protective epitopes (19).

1.7. Human Immunodeficiency Virus type-1 (HIV-1).

1.7.1. The biology of HIV-1.

Human Immunodeficiency Virus type 1 (HIV-1) is the causative agent of the Acquired Immunodeficiency Syndrome (AIDS), a disease of pandemic proportions with over 40 million infected persons, and a cumulative mortality of more than 30 million since the recognition of the disease in the early 1980s (319). The virus is transmitted by sexual contact or contact with bodily fluids (*e. g.*, transfusion of infected blood or sharing contaminated needles between intravenous drug users). Based on genome sequence similarities, primary (or clinical) HIV-1 isolates are divided into three subtypes; M (main), N (new) and O (outlier). Group M accounts for most human infections, and it is in turn divided into seven genetic clades and multiple circulating recombinant forms (HIV Molecular Immunology Database, http://hiv-web.lanl.gov/content/immunology).

HIV-1 (Figure 2) is a membrane-enveloped retrovirus from the genus *Lentivirus* that mainly infects human T-helper $CD4^+$ cells, monocytes and macrophages. Its genome is made of two copies of positive-stranded RNA, which code for several structural, regulatory and accessory genes. The life cycle of HIV-1 is characterized by the reverse synthesis of viral DNA by a virally-coded reverse transcriptase that uses the two genome RNA molecules as templates, and the integration of the newly-synthesized DNA into the host cell genome. In the most general model, infection by HIV-1 is initiated by the recognition of its receptor, the CD4 molecule on the host cells, by the viral envelope glycoprotein gp120 (74). Upon binding to CD4, a series of conformational changes are induced on gp120 that result in the exposure (or formation) of the coreceptor-binding site (56, 159, 220, 342), which in turn interacts with the CCR5 or CXCR4 coreceptors (7, 85).

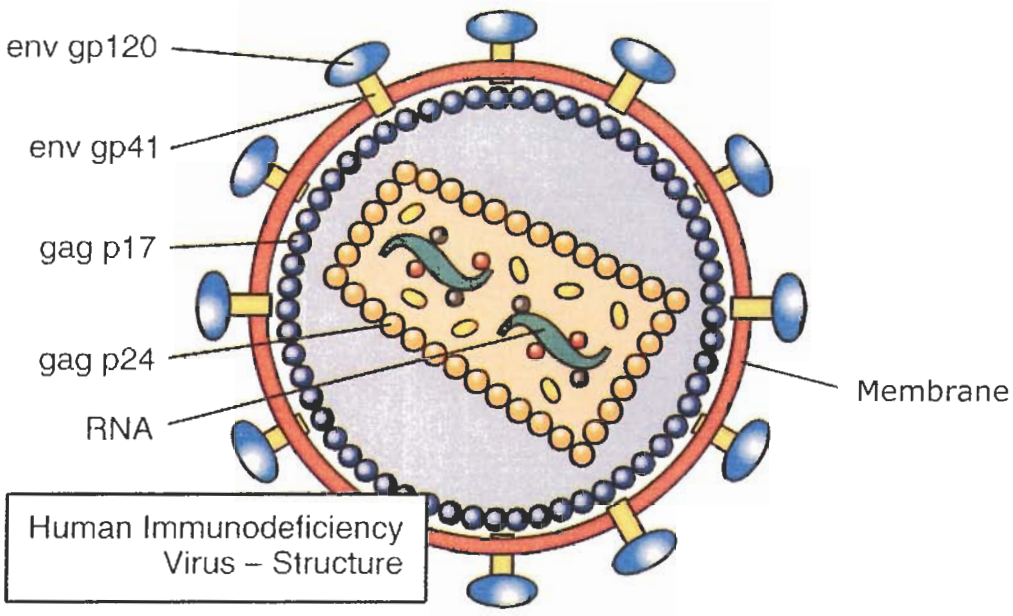

Figure 2. Cartoon representation of the HIV-1 viral particle, (www.avert.org, reproduced with permission).

The structural changes in gp120 induce conformational changes on the viral transmembrane glycoprotein gp41, which releases and inserts its fusogenic region in the host cell's membrane promoting, the apposition of the two membranes, and ultimately cell and viral membrane fusion. After membrane fusion, the viral capsid is released to the cell cytoplasm, the viral RNA genome is reverse transcribed, and the genomic DNA is transported to the nucleus and inserted into the host cell genome. Once inserted, the viral DNA is transcribed and translated; leading to the assembly of new viruses in the vicinity of the cytoplasmic membrane. The viral progeny eventually bud from the cell as immature viral particles, which are enveloped with the cell membrane carrying the viral glycoproteins and multiple cellular proteins (17, 129). Alternatively, after integration into the cell genome, the virus can remain functionally latent for long periods of time, until it is reactivated and the infected cell becomes a virus-producer cell (299).

When HIV-1 infects a new host, it rapidly and irreversibly colonizes and establishes a latent infection in multiple compartments of the immune system (60), thus the host remains chronically infected. After controlling the initial viremia, the host enters a lasting clinically asymptomatic phase that eventually leads to the onset of AIDS and death, caused by opportunistic bacterial, fungal and viral infections. The clinically asymptomatic phase is characterized by a remarkable diversification of the viral genome, that reaches levels of up to 20% nucleotide sequence divergence between isolates within one infected person (332).

HIV-1 posseses the highest genome diversity ever recorded, with estimates of more than 10^{18} worldwide circulating variants (332). The virus is characterized by a very high replication rate, with the production of approximately 10^{10} new viruses every day, as

estimated by studies of perturbations of the equilibrium between virus replication and clearance using anti-retroviral drugs (reviewed in (299)). This high viral replication is accompanied by a high mutation rate, due to the low fidelity of the RT, which accumulates errors at a rate of 10^{-4} per nucleotide site per generation (153, 258). The dynamic nature of HIV-1 replication, as well as the extent of reverse transcriptase error rate, imply that mutations at every single position of the 9500 nucleotide-long genome can arise daily. Genotypic diversity is further increased by a large number of recombination events per replication cycle. Recombination occurs when the reverse transcriptase transfers between the two genomic RNA strands of the diploid virion during reverse transcription, and generates a daughter DNA that is a mosaic of the two parental genomes (223).

Recent findings in a coinfection model *in vitro* have shown that around nine and thirty recombination events occur in T-cells and macrophages, respectively, in a single replication cycle (184). Also, superinfection or coinfection of a cell with divergent strains typically leads to the co-packaging of non-identical genomes in the next generation of viruses, thus creating heterozygous virus and fueling the next diversification cycle. The extraordinarily high level of viral diversity, together with the existence of latent virus reservoirs in resting $CD4^+$ T-cells, are significant factors in the persistency of HIV-1 in infected individuals and the ultimate failure of highly-active anti-retroviral therapies (HAART) to eliminate the virus. Under prolonged treatment, drug-resistant strains are invariably selected and eventually come to dominate the population, rendering that therapy ineffective (62).

It has been clearly shown that both the cellular and humoral arms of the immune system are capable of successfully suppressing HIV-1 replication (34, 35, 110, 118, 139, 196, 201, 238). However, it has also been shown that the virus escapes the immune system, given the persistent appearance of escape variants with mutated epitopes for both cytotoxic T-cells (99, 158) and neutralizing antibodies (NtAbs) (2, 72, 208, 268, 334, 335), resulting in the inability of the immune system to completely clear the virus.

1.7.2. HIV-1 envelope glycoproteins: the targets of antibody-mediated neutralization.

Antibody-mediated neutralization, defined as the inhibition of viral infectivity of host cells in an *in vitro* assay, results from the binding of antibodies to the virus, and interference with the viral attachment and entry processes (237). The targets for HIV-1-NtAbs are the functional glycoprotein spikes on the surface of the viral envelope. The envelope spikes are responsible for the early stages of infection, mediating viral attachment to receptor and coreceptor (mediated by gp120) and membrane fusion and entry to the host cell (mediated by gp41) (74, 91, 159, 255).

The HIV-1 envelope spike (Figure 3) is a heterotrimer comprising three transmembrane glycoprotein subunits (gp41) that are non-covalently associated with three surface glycoprotein subunits (gp120) (51, 90). The envelope is synthesized as a precursor, gp160 (271), that is assembled into trimeric structures, transported to the endoplasmic reticulum, glycosylated, and proteolytically processed into gp41 and gp120 subunits. The number of envelope spikes per viral particle, has been estimated at between 7 and 70, with an unknown fraction of them being functional (57, 114, 179, 253). In the viral spike and on the surface of infected cells, gp41 is inserted on the membrane *via* a

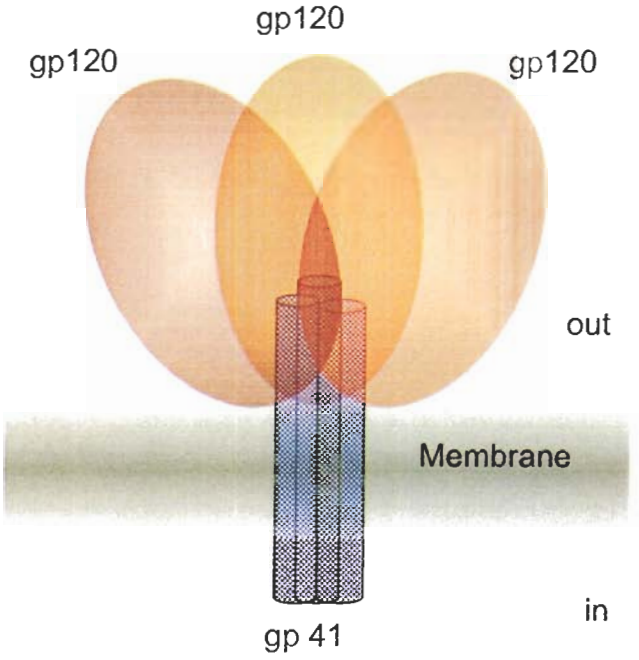

Figure 3. Cartoon representation of the HIV-1 envelope spike in the surface of the virus. The spike is formed by three transmembrane subunits (gp41, in blue) in non-covalent association with three surface subunits (gp120, in shades of brown). The actual structure of the spike is not known but it is thought that gp120 prevents the exposure of most or all of gp41 until it engages the viral receptor and coreceptor. The viral membrane is represented in green, only a section of the 150 amino acids-long "cytoplasmic" tail of gp41 is shown.

transmembrane domain , with an external fragment of about 170 amino acids and an internal (or cytoplasmic) tail of approximately 150 amino acids. The outer or ectodomain of gp41 is divided in three main functional sub-domains: an N-terminal fusogenic peptide responsible of inserting into the host cell membranes, and two heptad repeats that participate in the formation of the pre-fusogenic intermediate (107, 145). In addition, several parts of the ectodomain are responsible for interactions with gp120, and participate in the formation of the spike (134, 192, 340).

The surface glycoprotein gp120 is heavily-glycosylated, with about one half of its molecular weight contributed by carbohydrate. The crystal structure of a de-glycosylated gp120 monomer core, bound to the CD4 receptor and Fab b17, solved by Kwong *et al.* (176) shows a structure unrelated to any other protein structure previously described. The protein can be divided in three general structural domains: (*i*) the inner domain, which is mostly engaged in interactions with the other gp120 subunits of the trimer and with gp41, and thus is not exposed in the trimer; (*ii*) the outer domain, which is heavily glycosylated, and (*iii*) the bridging sheet, which connects the inner and outer domains and participates in the formation of the receptor-binding sites (176). A recent structure of a unliganded, fully glycosylated SIV gp120 core revealed important differences from the HIV-liganded core, the most remarkable of which are the absence of a formed bridging sheet domain, the lack of properly-formed receptor and coreceptor binding sites, and the subdivision of the inner domain into several distinct substructures that seem to move independently from each other upon binding to CD4 (56). The differences found between the two gp120 structures underline the amount of conformational change that occurs in this subunit upon binding to the viral receptor (56, 176).

Epitope mapping of MAbs that bind to gp120 has led to the demarcation of a *non-neutralizing*, a *neutralizing* and a *silent* face in the gp120 monomer (341). The location of these zones roughly corresponds with the three structural domains observed in the core gp120 structure. The *non-neutralizing* face overlaps with the inner domain, which is only accessible to antibodies in the monomeric form but not in the spike. The *neutralizing* face is located in and around the bridging sheet, including areas implicated in receptor and coreceptor binding. The *silent* face, against which a poor antibody response is generally elicited, overlaps with the highly-glycosylated outer domain (341).

The arrangement of gp120 and gp41 in the envelope spike is unknown; it is clear that their structure is different from that of the monomeric subunits. Nonetheless, models of the spike (especially gp120) have been constructed based on the available crystal structures (56, 176, 177). The model of an unliganded trimer by Chen *et al.* proposes that the three CD4-binding sites face a bowl-like cavity around a three-fold axis, at the top of the molecule (and away from the viral membrane), and that the V1-V2 segment of one gp120 subunit interacts with the V3 of a neighboring subunit (56). The putative structure of gp41 in the native envelope is more difficult to picture. It is generally accepted that gp41 undergoes dramatic conformational changes as a result of gp120 binding to the receptor and coreceptor (107, 159). Crystal structures of the external region of gp41, after the formation of the pre-fusion intermediate, reveal that the N- and C-terminal heptad repeats associate to form a metastable six-helix bundle, which is responsible for the apposition of the viral and cellular membranes (53, 336). In addition, structural and biophysical evidence suggests that gp41 not only interacts with gp120 and other gp41

subunits, but that it may also form close associations with membrane lipid bilayers (244, 245, 291, 329).

The envelope spikes that decorate the viral surface appear to have a structurally heterogeneous character, as shown by studies of neutralizing *vs.* non-neutralizing antibodies binding to virus and infected cells. Poignard *et al.* (253) showed that while viral particles can be captured with both anti-gp120 neutralizing and non-neutralizing antibodies, the binding of non-neutralizing antibodies to virus does not prevent its subsequent neutralization by the NtAb. Herrera *et al.* reported that non-neutralizing antibodies to the gp120 CD4-binding site do not interfere with neutralization by b12 (135). These results indicate that two types of envelope spikes exist on the viral surface: one subset that may bind both neutralizing and non-neutralizing antibodies and is irrelevant to neutralization, and a second type of spike that confers neutralization sensitivity, and most likely represents the functional spike population that mediates infection (135, 253). It is not known how many functional spikes are needed by a viral particle to infect a target cell. However, it has been proposed that the binding of one antibody molecule per spike is sufficient to neutralize the virus (237, 344). This model postulates that every spike of the virus should be bound by antibody, rendering a total of 70 antibody molecules (237) or 7-14 (344), depending on the total number of the spikes/particle considered by each study.

1.7.3. The neutralizing antibody response in HIV-1 infection.

NtAbs are readily produced within months after primary HIV-1 infection, but usually at low titers and mainly against autologous strains (2, 169, 187, 209, 268, 335).

NtAb appearance has sometimes been detected early after primary infection, and correlated with the control of viral replication during the initial stages of infection (6, 178, 274). However, more often, a clearer correlation can be established with the cellular cytotoxic response instead, since NtAb are usually detected later, after the clearance of the initial viremia (10, 33, 170, 191, 249). The broadening of the NtAbs response is slow and delayed with respect to viral evolution, as shown by longitudinal studies following neutralization patterns against autologous and heterologous viral isolates. This diversification is apparently driven by selective pressure from the immune system over the virus, and the constant generation of escape variants to which new antibodies are produced (2, 72, 208, 268, 334, 335).

Most antibodies circulating in the serum of HIV-1-infected people do not bind intact virus (50), thus NtAb are only a small fraction of the total antibody response against the viral proteins. It has been suggested that in natural infection, most anti-envelope antibodies are elicited by viral debris or free gp120, which induce a response against sites that are structurally distinct from, or inaccessible, on the trimeric envelope spike (243). This idea is supported by differences in the antigenic and immunogenic properties between monomeric and oligomeric envelope (18, 120, 267), and by the lack of correlation between virus neutralization and antibody binding to monomeric gp120, as compared to oligomeric gp120 (105, 210, 240, 286). Instead, a good correlation between antibody neutralizing capacity and binding to spikes on the surface of infected cells has been observed (240, 269, 286). Neutralization of HIV-1 seems to be dependent upon antibody binding to functional spikes, irrespective of which epitope is recognized (240, 344). It has been shown that several non-neutralizing MAbs can still bind to viral

particles or infected cells, but they apparently target a different, most likely non-functional, subset of spikes (135, 253).

A few broadly-neutralizing monoclonal antibodies, that is, antibodies that neutralize a wide range of circulating strains, have been isolated from infected donors (MAbs b12, 2F5, 2G12, 4E10) (42, 44, 305), but they seem to be rarely produced. They represent exceptional activities found among the majority of non-neutralizing antibodies produced, sometimes even against the same or overlapping sites. For example, many antibodies against the CD4-binding site, which overlaps the epitope of MAb b12, are detected in sera from HIV-infected subjects (52, 211, 317), but most of them are non-neutralizing. Also, antibodies against the membrane-proximal external region (MPER) of gp41, which carries the core epitopes for 2F5 and 4E10, have been repeatedly documented in natural infection (40, 47, 83, 112, 123, 142, 216, 318, 324).

1.8. Development of antibody-based anti-HIV-1 vaccines.

1.8.1. Challenges for the development of an anti-HIV-1 vaccine.

HIV-1 infection is a public health issue of pandemic proportions. Estimates from the Joint United Nations Program on HIV/AIDS and the World Health Organization declared the occurrence of approximately five million new infections in the year 2004 (319). Most of the current forty million people living with HIV/AIDS are in underdeveloped countries, with limited or no access to effective antiretroviral therapy (319). It is clear that the long-term solution to the pandemic lies in the development of a prophylactic anti-HIV-1 vaccine. The beneficial impact of such a vaccine would be considerable, even in the case that it only achieves sub-optimal efficacy (*i.e.* 50 %).

Unfortunately, after 20 years of intensive research, the development of an effective vaccine is still nothing but a hope. HIV-1 is a virus that establishes very complex and diverse interactions with its host, and although its biology is relatively well-understood compared to other viruses, our knowledge is still insufficient even to properly determine the correlates of protection. Historically, HIV vaccine researchers have been divided into those arguing for a predominant role of the cytotoxic T lymphocytes (CTLs) in protection, and those who believe that NtAbs are the key to a successful vaccine. Protection from infection (or the lack of it) has been associated with both types of response in multiple studies (77, 98, 197, 264, 350). However, in recent years, data have emerged suggesting that most likely an effective vaccine should elicit a response from both components of the immune system (297, 313). This is clearly illustrated by the high percentage of the current vaccine trials that are directed to elicit both CTL and antibody responses (298).

The biological property of HIV-1 to colonize the host and establish a persistent infection is a significant factor to consider when designing vaccine candidates; it indicates the need to achieve *sterilizing immunity*, that is, complete protection from infection. Most candidates tested so far in virus challenge models in monkeys, have failed to protect, or have conferred sterilizing immunity to only some individuals from the challenged group. *Non-sterilizing immunity*, manifested in the form of reduced viral loads and attenuated disease progression, has also been obtained in these studies, suggesting that it too, may be an attractive goal (201, 239, 350). The benefits of a non-sterilizing vaccine are not completely obvious though; on one hand there seems to be a clear attenuation of the disease, with a longer asymptomatic phase; on the other, there is still

the problem of the eventual progression to AIDS. Also, a longer asymptomatic phase, if accompanied by changes in the sexual behavior of the immunized population (*i. e.* increased risk behavior), makes the impact of a disease-attenuating vaccine more questionable at the epidemiological level (76).

The genetic variability of HIV-1 is a major challenge for the development of an effective vaccine (109). This is clearly reflected by the ever-evolving amino acid sequence of the viral envelope glycoproteins, and the failure of most broadly neutralizing MAbs to neutralize every viral isolate tested (26). For a vaccine to work, it has to be able to elicit broadly-NtAb. Both envelope glycoproteins possess regions that are relatively-conserved between divergent isolates, and domains that display a high degree of sequence variability. In general, NtAb responses against conserved domains (like the CD4-binding site) are very poor, whereas responses against variable domains (like the V3 loop) are most often isolate-specific (232).

The complex structural properties of the envelope proteins are another major obstacle for a vaccine. As discussed in section 1.7.2 the structure of the native envelope spike is unknown, and neither its structure, nor its antigenic and immunogenic properties, are fully replicated by monomeric (nor by trimeric) recombinants gp41 or gp120. In principle, to elicit a response that recognizes the viral envelope in its native state, it will be necessary to use immunogens that replicate or mimic that structure; and such an immmunogen is not yet available. The technical difficulties associated with obtaining envelope protein preparations that conserve the native spike structure are immense. For example, since the interactions between gp 41and gp120 are non-covalent, gp120 has a

high propensity to shed, resulting in the loss of the native envelope structure (114, 263, 292).

Finally, a complex group of logistical, socioeconomical and ethical issues also conspire against the expedited development and testing of new vaccines, for example, the lack of a simple HIV-1 infection animal model. Most vaccine tests are conducted in non-human primates (primarily macaques), using Simian-Human Immunodeficiency Virus (SHIV) as the challenge strains. Although the macaque-SHIV model recapitulates the central aspects of human HIV-1 infection, and therefore may predict the efficacy of a vaccine candidate, it has not been fully-validated yet with a successful vaccine (128). There are still important differences regarding the short time course of the disease in macaques, and how realistically the routes and doses of challenge mimic natural infection in humans; also, the availability of animals for testing new immunogens is rather limited. HIV-1 vaccine efficacy (phase III) trials are particularly challenging, since they involve large number of individuals. The best places to conduct phase III trials are those areas with high HIV-1 incidence, which are generally the ones with the poorest infrastructure in place. Phase III trials are long and expensive to conduct, and require a strong involvement and support of the governments, public health officials, the media and the community (94).

1.8.2. Approaches for antibody-based anti-HIV-1 vaccine: a brief overview.

Traditional vaccine approaches involving attenuated or inactivated pathogen and subunit vaccines have failed to produce an effective HIV-1 vaccine candidate in animals or humans, so far. Non-pathogenic, genetically-altered SIV live viruses have been tested

in monkeys, and have conferred protection to challenge. However, these attenuated viruses eventually have regained their pathogenic potential, and have promoted progression to simian AIDS (9, 11, 75, 337). Inactivated viral vaccines, depleted of envelope, were tested in HIV-infected volunteers, but failed to produce convincing evidence of efficacy (164, 183, 214). Safety issues associated with the use of attenuated or inactivated HIV-1 have slowed the progress in this area considerably.

As has been observed in the anti-envelope antibody response during natural infection, immunization with recombinant envelope protein subunits elicits mainly antibodies against epitopes that are occluded in the native viral envelope, and therefore, are non-neutralizing. These disappointing results have been consistently observed in both animal immunizations, and human vaccine trials (104, 144, 200, 202, 298). The failure of envelope subunit vaccines to generate a neutralizing response is now understood on the basis of the known functional and structural properties of the viral envelope. It is clear that, most likely, a vaccine based solely on soluble, recombinant envelope proteins will be unable to confer protection.

The failure of traditional approaches to produce an effective HIV-1 vaccine has prompted the exploration of novel vaccine candidates and strategies for immunization. Considerable effort has been placed in engineering recombinant envelope proteins, with the objective of develop immunogens that replicate the structural properties of the trimer, and improve its immunogenicity. The association of gp41-gp120 has been stabilized by addition of an engineered linkage of the two subunits *via* a *de novo* inter-subunit disulfide bridge, without altering the antigenic properties of the complex (25, 100, 293, 343). Furthermore, mutations have been introduced in the N-terminal heptad repeat of gp41, to

promote the formation of trimeric complexes (278). A strategy is currently being explored of blocking immunodominant, non-neutralizing sites on gp120 by coverage of most of its surface with carbohydrates, yet leaving the epitopes for broadly-NtAbs exposed, (234). Other strategies have factored in the possible structural benefit of a membrane-anchored trimer, and have therefore generated proteoliposomes incorporating gp160 (126), viral-like particles displaying gp120 (5, 82), or have developed novel virus inactivation protocols that preserve the antigenic features of the envelope spike (125, 272).

Vaccines using recombinant live vectors and DNA vectors carrying the HIV-1 *env*, *gag* and/or *pol* genes have received special attention, since they can potentially stimulate the T and B cell branches of the immune system. Immunization studies using live recombinant vaccinia virus have consistently generated cellular and humoral responses (122, 143, 246). However, serious concerns remain regarding the safety of such vaccines in immunocompromised individuals, as well as their efficacy due to high prevalence of immunity against vaccinia virus in the smallpox-vaccinated population (182). Other live vectors that are being explored are canarypox (61, 248), Modified Vaccinia virus Ankara (MVA) (16), Adenovirus 5 (Ad5), fowlpox virus (FPV) (73), bacilli Calmette-Guerin (BCG) (345), Semliki Forest virus (215), and Venezuelan equine encephalitis virus (78, 84). DNA vectors usually deliver genes coding for subunits, rather than whole organisms. They use the transcription and translation machinery of the cells to produce the immunogen. Trials of DNA vaccines in seronegative volunteers, have been conducted (38, 97), and several more are currently in progress (for a complete list of trials see http://www.iavireport.org/trialsdb/).

1.9. The broadly-neutralizing, human monoclonal antibodies b12, 2F5 and 2G12 as templates for vaccine development.

1.9.1. The impact of HIV-1 broadly-neutralizing antibodies *in vivo*.

In spite of *in vitro* HIV-neutralizing activity, broadly neutralizing antibodies seem to have a negligible effect on the long-term control of HIV-1 infection *in vivo*, as is suggested by persistent viral escape, and by results from antibody transfer experiments in severe combined immunodeficiency (SCID) mice reconstituted with human peripheral blood lymphocytes (hu-PBL SCID mice), and infected with HIV-1 (254). Furthermore, a Phase I study of passive 2G12 and 2F5 infusion in infected volunteers showed only transient reductions in viral load, with the onset of neutralization escape variants for 2G12 (304).

However, NtAbs b12, 2F5 and 2G12 have been shown to prevent or attenuate primary infection in animal models *in vivo*, if these antibodies are present at sufficient levels before or shortly after infection. Parren *et al.* (238) and Gauduin *et al.* (110) achieved protection using MAb b12 in HIV-1-infected hu-PBL SCID mice. Mascola *et al.* showed protection of rhesus macaques against intravenous challenge with $SHIV_{89.6PD}$ by a triple combination of HIVIG/2F5/2G12 (196). A second study with vaginal challenge, achieved protection in 4 out of 5 animals treated with the triple antibody combination (201). Baba *et al.* reported that the infusion of a triple combination of MAbs 2F5, 2G12 and F105 into macaques, protected them from infection after intravenous or oral challenge with SHIV-vpu^+ (12). Other studies have shown different degrees of protection in neonate macaques (103, 139, 140), which indicate a potential effect of NtAbs in preventing mother to child transmission.

It has been proposed that NtAbs confer sterilizing immunity by inactivation of the initial infecting inoculum at the primary infection site (239, 350). However, very high concentrations of NtAb *in vivo* seem to be required to achieve sterilizing immunity, as shown by Parren *et al.* (239). In order to protect macaques from intravaginal challenge with the R5 virus $SHIV_{162P4}$, using IgG1 b12, the NtAb levels needed *in vivo* were 400-fold greater than the titers required to achieve 90% neutralization *in vitro*. For the case of the broadly-NtAbs b12, 2G12 and 2F5, that titer translates into serum antibody concentrations from 100 μg/ml to 1 mg/ml, which are probably not attainable by vaccination (239). It is possible nonetheless, that sub-NtAb concentrations mediate some protective effects, like antibody-mediated, complement-dependent cytotoxicity (CDC) or antibody-dependent cell cytotoxicity (ADCC). Lysis of HIV-1 and HIV-infected cells by CDC and ADCC has been documented *in vitro*, and has been inferred to occur in vivo (3, 136, 306, 316). ADCC has been documented with the sera of immunized animals and humans, but a clear role in protection has not yet been established (119, 166). In general, the results from passive antibody transfer studies show that NtAb alone can protect against primary HIV-1 exposure, and support the idea that eliciting NtAb should be part of an effective HIV-1 vaccine.

1.9.2. The HIV-1 broadly-neutralizing MAbs IgG1b12, 2F5 and 2G12.

A common theme of the HIV-broadly-neutralizing MAbs is their unusual structural features. MAbs b12, 2F5 and 4E10 have each a very long CDR H3 of 18, 22 and 18 amino acids, respectively (49, 173, 284); the average length for H3 in human antibodies is 13.1 amino acids (257). The long H3 have been shown to be crucial for the

activity of b12 (357) and 2F5 (355). 2G12 has a unique structure that shows domain exchange between the VH chains, and the formation of two additional sugar-binding sites (46). The Nt MAbs are also highly mutated, in contrast with the average number of mutations (7.3 for V_H and 5.8 for Vκ), observed in a large group of rearranged human immunoglobulin genes (312).

1.9.2.1. The anti-CD4 binding site, Nt MAb, IgG1 b12.

MAb b12 was isolated from a Fab phage-displayed library constructed from an asymptomatic, HIV-1 positive donor (44). It is one of the few broadly-neutralizing MAbs, with potent neutralizing activity against primary isolates from several genetic clades (13, 26, 45, 70, 210). MAb b12 recognizes a highly-conserved epitope that overlaps the CD4-binding site of gp120, it competes with other, non-neutralizing CD4 binders (212), and with soluble CD4 for binding to gp120 (13). In addition to its potent HIV-1 neutralization activity, b12 has shown CDC and ADCC effector function activities on HIV-1 infected cells *in vitro* (136).

MAb b12 possesses a long CDR H3 of 18 amino acids, which is crucial for its activity (357). The crystal stucture of b12, solved at 2.7 Å resolution by Saphire *et al.* (284) shows that the long CDR H3 rises 15 Å above the surface of the antigen-binding site in a finger-like extended loop, which probably allows the antibody to probe the recessed CD4-binding site of gp120. In fact, a model of b12 docked to the gp120 core structure (284) suggests that the apical Trp residue from the H3 inserts into the CD4-binding site cavity, in a manner similar to the Phe 43 from CD4 in the CD4-bound gp120 structure solved by Kwong *et al.* (176).

Extensive mutagenesis studies in both b12 (357) and gp120 (233) have delineated some details of their interaction, and have in general, confirmed the information provided by the docked model. An imprint of b12 on gp120 based in the combined analysis of the structural and mutagenesis data reveals the coverage of the CD4-binding site, and interactions that differ from those of the non-neutralizing CD4-binding antibodies b3 and b6. Most gp120 mutations that uniquely affect b12 binding are located towards the neutralizing face, whereas most that only affect b3 or b6 are located in, or oriented towards the non-neutralizing face. This observation lead to the suggestion that b12 binds gp120 at a different angle from b3 and b6, and therefore can interact with the trimer, whereas MAbs b3 and b6 can't (233). However only partial correspondence between binding data and virus neutralization was observed, suggesting that the effect of the mutations is different in the context of the spike. Amino acid substitutions in b12 showed the importance of residues in the long H3 for b12 binding to gp120, and suggested that the rigidity of the long H3 may be a necessary feature for proper contact with the hydrophobic CD4-binding cavity (357).

A striking difference between b12 and other less-potently neutralizing anti-CD4-binding site antibodies lies in their thermodynamics of binding to gp120. A recent study by Kwong *et al.* (175), observed that binding of non-neutralizing MAbs specific for the CD4-binding site, to monomeric gp120, is associated with large unfavorable changes in entropy, that is, a positive $T\Delta S$ component, which implies a negative ΔS. These large, negative entropic changes indicate significant conformational rearrangements of gp120 upon antibody binding. In contrast, such large entropy changes are not observed upon

b12 binding, suggesting that this difference may be associated to the different neutralizing capacity of b12 respect other anti- CD4-binding site MAbs (175).

1.9.2.2. The anti-gp41 Nt MAb, 2F5.

MAb 2F5, which recognizes the transmembrane glycoprotein of HIV-1 (gp41), was obtained by electrofusion of peripheral blood mononuclear cells from HIV-1 infected volunteers and the cell line CB-F7 (42, 219). It binds with high affinity to a linear site on the MPER of gp41, with the residues $D_{664}K_{665}W_{666}$ forming the core of the epitope (64, 219). The core epitope is located in the MEPR, close to the viral membrane and flanked on its C-terminal side by a stretch of highly-conserved hydrophobic residues with a high Trp content, which adopts an alpha-helical structure in lipid micelles (291), and contains a cholesterol-binding domain (329). The MPER of gp41 has been the focus of intense study in recent years, resulting in the expansion of the epitope originally defined, from ELDKWA(662-667) (64, 219) to NEQELLELDKWASLWN(656-671), (235); LELDKWASL(661-669), (311) and ELLELDKWASLWN(659-671), (15). Several lines of evidence suggest that the 2F5 epitope is better exposed after the virus has initiated the attachment events (24, 356).

MAb 2F5 is an unusual antibod, it has an unconventional D segment, and a remarkably long CDRH3 loop of 22 residues (173), which is important to its activity (355). Moreover, its neutralization capacity seems to be unique among a myriad of other antibodies directed against the MPER (40, 47, 83, 112, 123, 142, 216, 318, 324), emulated only by another MAb, 4E10 (26, 168, 356). 2F5 efficiently neutralizes most laboratory and primary isolates from clades A to F at relatively low concentrations (64,

71, 261, 315). A recent, detailed study conducted by Binley *et al.* shows that 2F5 can neutralize primary isolates from most genetic clades, with the exception of clade C (26). In agreement with epitope mapping results, the presence of the DKW residues on gp41 is necessary for 2F5-mediated neutralization of HIV-1 (26, 48, 64, 261, 354). However the DKW core seems to be insufficient to confer sensitivity to 2F5, since 2F5-resistant isolates carrying the DKW motif have been observed (26).

Attempts to elicit 2F5 by immunization with peptides or fusion proteins carrying the core epitope have been made by multiple groups. Muster *et al.* (217) introduced the ELDKWAS and LELDKWAS sequences in the antigenic site B of the influenza hemaglutinin, and used the chimeric viruses to immunize mice intra-nasally. They obtained sera that neutralized the chimeric influenza virus, and several tissue culture-adapted HIV-1 isolates, but failed to neutralize primary HIV isolates (217, 218). Other groups have tested the insertion of the epitope ELDKWA in the surface antigen of hepatitis B virus (92), in different locations of the maltose-binding protein (63), in the heavy chain of an IgG (137), and in the V3 region of gp120 expressed in recombinant, attenuated measles virus (188). Also, DNA immunizations with plasmid constructs with the LLELDKWASL coding-sequence inserted in the V1, V2, V3 and V4 loops of the $gp140_{IIIB}$ (186) have been tested. Most studies have shown the generation of anti-ELDKWA, antibodies that nonetheless, fail to neutralize primary HIV-1 isolates. Immunizations with synthetic peptides have produced similar results (163, 203, 224). These immunization results indicate that although 2F5 binds a linear antigenic determinant, there are other elements involved in the formation of the immunogenic, and very likely the neutralization 2F5 epitopes.

Several studies have shown a lack of correlation between peptides antigenicity and the neutralizing capacity of the antibody response against those peptides (*i.e.*, improved peptide antigenicity does not translate into the generation of a neutralizing antibody response) (163, 203, 311). Moreover, crystal structures of 2F5 in complex with the peptides support the idea of an incomplete epitope (228, 231). According to these crystal structures, large areas of the antibody's paratope are apparently excluded from the interaction, most remarkably the apex of 2F5's long CDR H3; in spite of mutagenesis results showing that residues in the H3 apex are important for 2F5 binding to gp41 and ELDKWAS peptide, as well as for viral neutralization (355). Thus, the identification of the full epitope able to elicit 2F5 is currently one of the most important lines of research with this MAb.

1.9.2.3. The anti-carbohydrate Nt MAb, 2G12.

MAb 2G12 was isolated together with 2F5 and 4E10 by Buchacher *et al.* (42). Initially thought to recognize a mixed protein-carbohydrate epitope formed around the C3/V4 region of gp120 (316), it has been recently shown to react exclusively with terminal mannoses in a cluster of high-mannose glycans on the silent face of gp120 (277, 289). The atomic structure of 2G12 alone, and in complex with the carbohydrates $Man_9GlcNAc_2$ and with the disaccharide Manα1-2Man, has revealed a unique structure never before seen in an antibody. The VH regions of the two Fabs undergo domain exchange and form a novel interface that accommodates two additional $Man_9GlcNAc_2$ moietites (46). The antibody possesses an unusual, extended linear conformation, instead of the normal Y- or T-shaped configuration of the immunoglobulins, which has also been

visualized by electron microscopy (46, 273). MAb 2G12 shows a high level of somatic mutation when compared to the closest germline genes (18 mutations in the light chain and 44 mutations in the heavy chain) with 50% of all mutations in the framework regions (46, 173).

Carbohydrates in gp120 are known to mediate binding to several lectins, most importantly cyanovirin (CVN), a protein isolated from the bacterium *Nostoc ellipsosporum*, and DC-SIGN, a surface protein expressed by dendritic cells in humans. Whereas CVN inhibits HIV-1 replication at nanomolar concentrations *in vitro* (29, 37), DC-SIGN has been implicated in primary HIV-1 infection in facilitating transfer of the HIV-1 by dentritic cells from the submucosa to the secondary lymphoid organs *in vivo* (113, 252). Binding of 2G12 to gp120 is blocked by pre-incubation with CVN, however 2G12 is unable to block binding of CVN to gp120, indicating that 2G12 has a more restricted binding specificity than CVN (*i.e.*, CVN binds multiple glycans on gp120 besides the 2G12 epitope) (96, 289).

Efficient neutralization of primary HIV-1 isolates has been obtained with 2G12 (26, 71, 315). The antibody has potent ADCC activity, and mediates complement deposition in the surface of infected cells, although no clear role in cellular lysis could be established (316). Resistance to neutralization has been observed for isolates from clades C and E (26) and several pediatric isolates (242). Similar to the other broadly-NtAb, 2G12 seems to be rarely-produced in infected subjects (316).

1.10. Objectives of this work.

The work presented here constitutes the initial part of a long-term effort undertaken in the laboratories of Dr. Jamie Scott and her collaborators, to develop an epitope-targeted vaccine that elicits neutralizing antibodies against HIV-1. We have chosen to use the broadly-neutralizing MAbs b12, 2F5 and 2G12 as tools to isolate peptides leads from PDPLs, which could be further developed into effective immunogens. As discussed above, the scientific and technical challenges of this approach are significant.

Our research also fulfills the objective of generating specific peptide markers for these MAbs, which may be an important tool for the detection of b12-, 2F5- and 2G12-like antibody responses in natural infection and vaccine-evaluation trials. Indeed the peptide B2.1, a specific marker for MAb b12 (352), has already been used for this purpose (239). In addition, current research in our laboratory is utilizing some of the peptide ligands described in this work along with so-called "commonly reactive" peptides, to characterize the antibody response in acutely and chronically infected donors.

Finally, with the structural and functional characterization of our peptide ligands, we have also intended to gain a better understanding of the basis of the peptide cross-reactivity with carbohydrate epitopes and discontinuous epitopes on folded proteins. We believe this to be an important issue, whose understanding may contribute significantly to the future development of epitope-targeted vaccines.

CHAPTER 2

Identification and Characterization of a Peptide that Specifically Binds the Broadly HIV-1-Neutralizing, Human Antibody, b12.

Michael B. Zwick[1,†], Lori L. C. Bonnycastle[1,‡], **Alfredo Menendez[1]**, Melita B. Irving[1], Carlos F. Barbas, III[2], Paul W.H.I. Parren[3], Dennis R. Burton[2,3] and Jamie K. Scott[1,*]

[1]Department of Molecular Biology and Biochemistry, Simon Fraser University, Burnaby, B.C. V5A 1S6, Canada; Departments of [2]Molecular Biology and [3]Immunology, The Scripps Research Institute, 10550 North Torrey Pines Road, La Jolla, CA 92037.

* **Corresponding author:** Telephone: 1-604-291-5658; fax: 1-604-291-5583; email: jkscott@sfu.ca.

†Present address: Department of Immunology, The Scripps Research Institute, 10550 North Torrey Pines Road, La Jolla, CA 92037, USA.

‡Present address: Monsanto Corp., 3302 S.E. Convenience Blvd., Ankeny, IA 50021,

Running title: Peptide B2.1 binds MAb b12 specifically.

This work has been published in ***The Journal of Virology 75(14): 6692-6699, 2001*** and is reproduced here with permission.

ABSTRACT

Human monoclonal antibody (MAb) b12 recognizes a conformational epitope that overlaps with the CD-4-binding site of the HIV-1 envelope. MAb b12 neutralizes a broad range of HIV-1 primary isolates, and protects against primary virus challenge in animal models. We report here the discovery and characterization of B2.1, a peptide that binds specifically to MAb b12. B2.1 was selected from a phage-displayed peptide library using IgG1 b12 as the selecting agent. The peptide is a homodimer whose activity depends on an intact disulfide bridge joining its polypeptide chains. Competition studies with gp120 indicate that B2.1 occupies the b12 antigen-binding site. The affinity of b12 for B2.1 depends on the form in which the peptide is presented; b12 binds best to the homodimer as a recombinant polypeptide fused to the phage coat. Originally, b12 was isolated from a phage-displayed Fab library constructed from the bone marrow of an HIV-1-infected donor. The B2.1 peptide is highly specific for b12 since it selected only phage bearing b12 Fab from this large and diverse antibody library.

Anti-HIV-1 neutralizing antibodies (Abs) first appear months after the viremia that follows initial infection (187, 226). This response, however, is highly type-specific. Neutralizing Ab responses may broaden later in the infection (39, 209), but usually remain poor and occur sporadically in the majority of patients, including long-term infected individuals (88, 208).

Only three broadly-conserved, neutralizing epitopes have been identified thus far on the viral envelope; they are defined by the human monoclonal (M)Abs b12, 2G12 and 2F5. MAb b12 binds to a discontinuous epitope that overlaps with the CD4-binding site on gp120. MAb 2G12 recognizes a complex discontinuous epitope involving the C3-V4 region of gp120 and carbohydrate (316). MAb 2F5 binds to a linear epitope on the ectodomain of gp41 (64, 219, 314); however, the simplicity of the this epitope is deceptive, since immunizations with recombinant influenza virus (217) or fusion proteins bearing this epitope (92, 186) have failed to produce significant 2F5-like neutralizing Ab responses, indicating that the native epitope on gp41 is more complex than the 6-residue linear sequence. MAbs b12, 2G12 and 2F5 have shown *in vitro* neutralizing activity against a wide variety of primary isolates (45, 64, 71, 241, 315). Moreover, passive transfer of b12, 2F5 and 2G12 can provide sterile protection if adequate concentrations are achieved before HIV-1 exposure. Studies with 2F5, 2G12 and HIVIG showed that macaques were protected from intravenous (196) and vaginal (201) challenge with the pathogenic SHIV $_{89.6PD}$ (265). Passive immunization with IgG1 b12 protects hu-PBL-SCID mice from HIV-1 primary isolate challenge before and shortly after intravenous viral challenge; (110), and macaques from vaginal challenge with pathogenic R5 SHIV $_{162P}$ (239).

The success of these passive immunization studies indicates an obvious goal in the development of a prophylactic vaccine: to elicit Abs having neutralizing activities similar to those of the currently-known, broadly-neutralizing MAbs (b12, 2G12 and 2F5). Yet, all recombinant envelope-based vaccine candidates tested so far in clinical trials have been unable to elicit significant, neutralizing responses against HIV-1 primary isolates (66, 200, 202), even in cases in which b12, 2F5 and 2G12 bound well to the immunizing subunit antigen, indicating that their respective epitopes are antigenic on these forms of the envelope proteins. Furthermore, these neutralizing epitopes are not recognized to any significant degree during natural infection; instead, as mentioned above, serum Abs having only weak cross-neutralizing titers are typically produced. Out of the large number of MAbs cloned from infected donors, b12, 2G12 and 2F5 are the only ones reported so far that neutralize a broad spectrum of primary HIV-1 isolates. Thus, although the epitopes known to mediate broad neutralization are present on recombinant envelope proteins, and on envelope proteins produced during natural infection, they do not elicit significant neutralizing Ab responses against primary isolates.

The low apparent immunogenicity of these neutralizing epitopes on the envelope proteins may be circumvented if suitable small molecules mimicking them could be generated (*i.e.*, molecules that bind tightly to the combining sites of the neutralizing MAbs), and then presented in such a form that they elicit the cognate Abs. Our approach in developing a vaccine against HIV-1 has been to identify peptides that are specific for b12, 2F5 and 2G12, and to develop these into a vaccine that will actively target the production of broadly-neutralizing Ab responses having specificities that are similar to these MAbs. This work describes the identification and characterization of a peptide that

binds specifically to MAb b12.

We used biotinylated IgG1 b12 (44, 45) to screen a panel of 11 peptide libraries displayed on the major coat protein of filamentous bacteriophage (pVIII), as described in (30). Two clones, Ed1 and Ed2, were identified that bound b12; DNA sequencing revealed the amino-acid sequences of their displayed peptides, as shown in Table 1. The peptides displayed by these clones share the motif: SDLX3CI; however the Ed1 sequence bears two Cys residues, whereas Ed2 bears only a single Cys whose position is shared in both clones. Thus, a set of two phage sublibraries displaying the shared residues, and reflecting the Cys content of the two Ed clones, was constructed following (30). The resulting sublibraries bear the random-peptide sequences: XCX_3SDLX_3CI (B1 sublibrary, two fixed Cys) and X_7SDLX_3CI (B2 sublibrary, one fixed Cys), respectively. These sublibraries were screened with biotinylated IgG1 b12, yielding phage bearing the B1 and B2 peptide sequence families shown in Table 1. All but one of the selected phage clones bear two Cys residues, and all clones bound IgG1 b12 by direct phage ELISA, performed as described in (30).

The deduced amino-acid sequences of the peptides displayed by the phage clones isolated from the sublibraries revealed a more detailed consensus for both the B1 peptides alone and the B1 and B2 peptides. Almost all clones selected from the B1 library contain Leu followed by an aromatic amino acid (usually Tyr) N-terminal to the fixed Ser.Asp.Leu sequence. Similarly, clones from the B2 library most often bear a hydrophobic residue (usually Leu) followed by an aromatic one (usually Trp) at this site. Most clones from the B2 sublibrary screening have a second Cys (selected for in the screening). The peptide displayed by only one clone, B2.1, contains a single Cys residue;

Table 1. Sequences and ELISA signals of peptide phage clones affinity-selected by biotinylated IgG1 b12.

Clone	Peptide Sequence[#]	$OD_{405-490}$		
		IgG1 b12	Fab b12	
		37°C	4°C	37°C
Ed1	T C LW SDL RAQ CI	nd	nd	nd
B1 library	**X C XX SDL XXX CI**			
B1.2	G **C** LY **SDL** LAT **CI**	1.321	0.013	0.019
B1.11	N **C** LY **SDL** TQS **CI**	1.236	0.016	0.018
B1.9	N **C** LY **SDL** YAR **CI**	1.223	0.013	0.015
B1.20	K **C** MY **SDL** LGI **CI**	1.153	0.012	0.021
B1.10	D **C** LY **SDL** ESR **CI**	0.818	0.015	0.021
B1.4	S **C** LY **SDL** LEL **CI**	0.750	nd	nd
B1.3	E **C** MW **SDL** ELR **CI**	0.571	nd	nd
B1.12	N **C** LW **SDL** EQF **CI**	0.343	nd	nd
Ed2	REKRWIF SDL THT CI	nd	nd	nd
B2 library	**XXXXXXX SDL XXX CI**			
B2.1	HERSYMF **SDL** ENR **CI**	1.236	1.071	0.219
B2.11	CSRNQLW **SDL** HGS **CI**	1.207	0.012	0.016
B2.12	NNQGCLW **SDL** TAS **CI**	1.189	0.013	0.017
B2.18	STTRCTW **SDL** YDS **CI**	1.141	0.011	0.016
B2.8	QSSSCMW **SDL** FQQ **CI**	0.992	0.016	0.018
B2.6	AQKQCTW **SDL** LSR **CI**	0.903	0.019	0.018
B2.7	RPCRGVY **SDL** LDK **CI**	0.886	0.016	0.020
B2.10	SSDHCLW **SDL** TMT **CI**	0.644	nd	nd
B2.3	LPSSCSW **SDL** LNR **CI**	0.276	nd	nd
B2.15	HTCAGTW **SDL** LST **CI**	0.252	nd	nd
gp120	positive control	1.121	0.863	1.166
f88-4	negative control	0.075	0.014	0.019

[#] Bold residues indicate the fixed residues in the sublibraries
nd indicates the experiment was not done

this peptide sequence shares similarities with those of other clones from the B2 sublibrary, and even more similarity to the Ed2 sequence, in the region N-terminal to the fixed Ser.Asp.Leu sequence. The B2.1 phage was significant in binding more tightly to b12 than the other clones. ELISA signals for almost all the clones were strong in assays performed with IgG1 b12; whereas binding was much reduced in assays using Fab b12 when reacted with phage at 4°C, and still lower when reacted at 37°C (Table 1). Fab b12 bound only the B2.1 and Ed2 peptides with signals above background, and in a side-by-side titration experiment it was further demonstrated that binding of b12 to B2.1 significantly stronger than to Ed2 (data not shown), so the Ed2 peptide was not further characterized.

The ability of the B2.1 peptide to bind to the antigen-binding site of b12 was assessed in a competition ELISA. Biotinylated IgG1 b12 (1 nM) was pre-incubated either with $gp120_{Ba\text{-}L}$ (100 nM) and reacted with plate-adsorbed B2.1 phage. Results in Figure 1 show that gp120 blocked the binding of IgG1 b12 to immobilized B2.1 phage, indicating that the peptide binds to the antigen-binding site of IgG1 b12. The binding to B2.1 phage was also blocked by B2.1 synthetic peptide (300 mM), non-biotinylated IgG1 (100 nM) and the recombinant B2.1 phage, but not by f88-4 phage or the unrelated synthetic peptide, G45B.

The specificity of the B2.1 peptide for b12 was also assessed. MAb b12 was originally isolated from a phage-displayed Fab library constructed from the bone marrow of the HIV-1-infected donor, M, and subsequently screened with recombinant gp120 (44). To study the specificity of the B2.1 peptide for b12, we tested whether B2.1 would select phage bearing b12 out of the repertoire of expressed Fabs from donor M. Table 2 shows

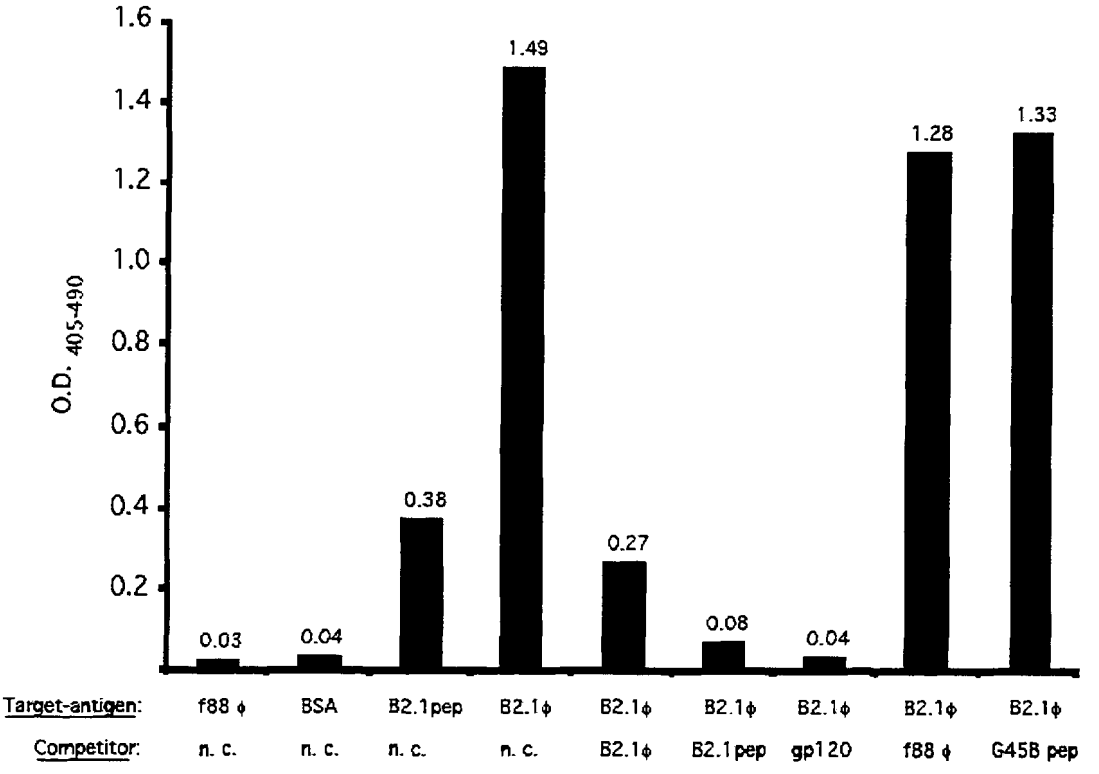

Figure 1. Binding of biotinylated IgG1 b12 to B2.1 phage (B2.1 ϕ) and B2.1 synthetic peptide (B2.1 pep) by ELISA. Competition for IgG1 b12 binding to plate-adsorbed B2.1 phage by "in solution" competitors: 2 x 10^{10} B2.1 phage, 300 uM B2.1 synthetic peptide, 100 nM gp120 Ba-L (gp120), f88-4 phage (f88 ϕ) and G45B unrelated peptide (G45B, sequence is VERSKAFSNCYPYDVPDYASLRS). BSA is bovine serum albumin and n. c. indicates no "in solution" competitor.

that yields of 10^{-1} % were obtained after four rounds of panning the M phage library on B2.1 phage. Moreover, the Fabs from all twelve independent phage clones that were sequenced from this phage pool were identical to b12. Thus, even though the M library contains a large number of other Fabs that recognize the CD4-binding site of gp120 (14), B2.1 selected only phage bearing the Fab b12.

To produce synthetic peptides bearing the B2.1 sequence, we investigated the condition of the thiol group of the single Cys residue that is present in the B2.1 sequence. As multiple copies of the peptide-pVIII fusion protein are incorporated into the phage coat, the single Cys residue of B2.1-pVIII may potentially be in a reduced form (as a reduced thiol group) or disulfide-bridged to a second copy of the B2.1-pVIII fusion protein. If the B2.1 peptide-pVIII fusion protein existed as a homodimer on the phage surface, it would have roughly twice the molecular weight of the pVIII monomer. Thus, B2.1 phage were analyzed by SDS-PAGE using Tris-Tricine buffer as described (358). Phage samples were initially treated with the thiol-reactive reagent, N-ethylmaleimide (NEM) (Figure 2A) which blocks free thiols that might be present on the phage coat, and would prevent the formation of pVIII dimers after solubilization of the phage coat proteins with heat and SDS. Hence, if B2.1-pVIII fusions bear free thiols and are monomeric, reaction with NEM should prevent them from dimerizing after dissociation of the phage. Alternatively, if the B2.1-pVIII fusions exist on the phage coat as dimers (produced by disulfide bridging between displayed B2.1 peptides), treatment of the phage with NEM, followed by boiling in the presence of SDS, should not affect their migration as dimers. The results shown in Figure 2A reveal that the recombinant pVIII from B2.1 phage migrates as a dimer that is not affected by NEM treatment; whereas it migrated as

Table 2. Percent yields for four successive rounds of affinity selection of the phage-displayed Fab library M with B2.1 phage.

Round	Immobilized on plate	Input (TU x 10^9)	Output (TU x 10^4)	% Yield
1	B2.1 phage	62	4.8	9.2×10^{-5}
	f88-4 phage	62	4.0	7.8×10^{-5}
	gp120	62	9.6	1.8×10^{-4}
2	B2.1 phage	6.6	2.4	3.6×10^{-4}
	f88-4 phage	6.6	1.6	2.4×10^{-4}
	gp120	6.6	140	2.1×10^{-2}
3	B2.1 phage	2.1	14	6.8×10^{-3}
	f88-4 phage	2.1	14	6.8×10^{-3}
	gp120	2.1	3200	1.5
4	B2.1 phage	2.7	400	1.5×10^{-1}
	f88-4 phage	2.7	19	8.8×10^{-3}
	gp120	2.7	110	4.1×10^{-1}

For the panning, 400 ng of $gp120_{SF2}$ and $5x10^{10}$ recombinant B2.1 or f88-4 phage were immobilized to the plate. Input and output phage are given in ampicillin-resistant transfecting units (TU)

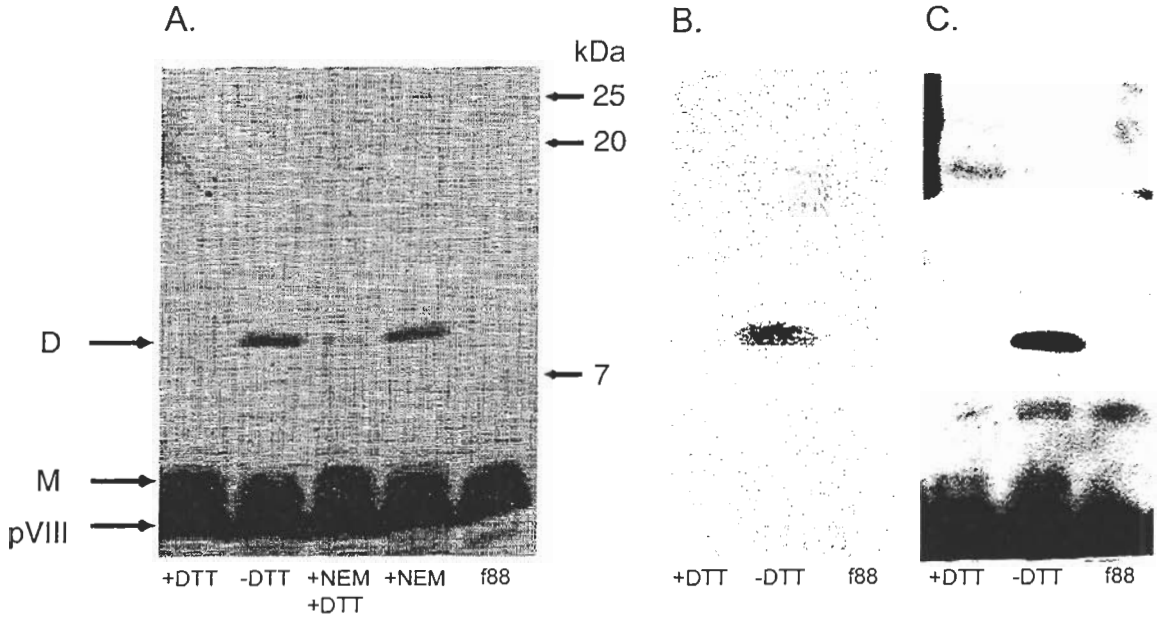

Figure 2. SDS-PAGE analysis of the f88-4 wild type phage (f88) and recombinant B2.1 phage (all others). Phage were untreated or treated with dithiothreitol (DTT), N-ethylmaleamide (NEM) or NEM followed by DTT, then analyzed by SDS-PAGE. Monomeric (M) and dimeric (D) recombinant pVIII are shown. Similar gels were either silver stained or the proteins were transferred to a membrane and subjected to western blotting with anti-phage Ab or IgG1 b12. Silver-stained gel (**A**); western blot using IgG1 b12 to show the reactive dimer (**B**); western blot using rabbit anti-phage Ab to show the wild type and recombinant pVIII proteins (**C**).

a monomer in samples treated with the reducing agent dithiothreitol (DTT). Samples sequentially treated with NEM and DTT also behaved as monomers. This proves that most or all of the B2.1 peptide displayed on the phage surface is homodimeric.

In contrast to the B2.1 dimers, the clones that display peptides containing two Cys residues produced monomer or, less often, a mixture of monomer and dimer, with monomers predominating (data not shown). This result suggests that, as opposed to B2.1, these clones bear mostly intra-chain disulfide bridges, consistent with the results of Zwick *et al.* (358). Their survey of phage displayed peptides bearing one and two Cys residues showed that almost all containing two Cys residues are cyclic, whereas all of those bearing a single Cys residue form homodimers.

The requirement for an intact disulfide bridge for the antigenicity of B2.1, and of clones bearing cyclic peptides, was assessed by western blot experiments (131), using IgG1 b12 or rabbit, polyclonal anti-phage Ab for detection. Figure 2B shows that IgG1 b12 binds only to the B2.1-pVIII fusion in its dimeric form. Staining with IgG1 b12 was present at the site of the dimer, but not at the monomer; whereas both forms were detected by anti-phage Ab (Figure 2C). A clone selected from the B1 sublibrary, bearing a peptide-pVIII fusion containing two Cys residues, was also tested by western blot with IgG1 b12. It produced a much weaker band than that of the B2.1 phage, whereas blotting with anti-phage Ab produced a recombinant band with similar intensity to the B2.1 clone (data not shown). This supports the conclusions drawn from the ELISA data (Table 1), indicating that IgG1 b12 does not bind as tightly to peptides containing two Cys residues as it does to the B2.1 homodimer. Moreover, as with B2.1 homodimer, reduction by DTT of the intra-chain disulfide bridge of clones containing peptides bearing two Cys

residues ablated b12 binding in ELISA; thus, disulfide-bridging is also required for their antigenicity (data not shown).

The location of the Cys residue (and hence the disulfide bridge) in the B2.1 sequence is crucial to its reactivity with b12. Phage bearing mutations in the B2.1 peptide sequence were prepared, and assayed for their ability to bind IgG1 b12 and to produce homodimer and/or monomer bands on analysis by SDS-PAGE. As shown in Table 3, substitution of Cys_{14} with Ser ablated dimer formation and Ab binding. Interestingly, substitution of Ser_4 with Cys ablated binding, regardless of whether the residue at position 14 was Cys; even the dimeric form of this mutant peptide did not bind b12 significantly. Thus, the antigenicity of B2.1 is strongly affected by the presence and location of the disulfide bridge that produces homodimers.

To study the affinity of the B2.1 homodimer out of the context of the phage coat, a synthetic version of the B2.1 peptide was prepared as a disulfide-bridged homodimer, with the sequence: NH_3-HERSYMFSDLENRCIAAEGK-NH_2 (Multiple Peptide Systems, San Diego; monomer MW = 2354.6; >95% pure and >95% dimer). This synthetic B2.1 peptide was used as a target to isolate phage bearing b12 Fab from the M library; but no phage were selected (data not shown), indicating that the synthetic peptide does not bind b12 as tightly as the phage-borne one. To verify the relatively weak interaction of the synthetic peptide with b12 compared to phage-borne B2.1, a panning reconstruction experiment was performed in which phage bearing Fab b12 were mixed with various amounts of phage bearing the unrelated Fab AD27/A47 (as background control phage). The Fab phage were panned side-by-side in wells coated with gp120, B2.1 phage or B2.1 peptide. The results in Table 4 show that gp120 and B2.1 phage

Table 3. Binding of b12 IgG to mutants of the B2.1 phage.

		IgG1 b12 *		SDS-PAGE †		WB #
Clone	Peptide sequence	3 nM	30 nM	Dimer	Monomer	b12 binding
B2.1	HERSYMFSDLENRCI	1.00	1.04	(+)	(+)	(+)
B2.1-Δ Cys	HERSYMFSDLENRSI	0.02	0.04	(-)	(+)	(-)
B2.1-5'Cys	HERCYMFSDLENRSI	0.02	0.05	(+)	(+)	(-)
B2.1-CC	HERCYMFSDLENRCI	0.03	0.13	(-)	(+)	(-)
f88-4	---	0.02	0.03	(-)	(-)	(-)
No phage	---	0.02	0.03	n.a.	n.a.	n.a.

* Values are OD $_{(405\text{-}490)}$ from direct phage ELISA.
† Wild type and mutant B2.1 phage were subjected to SDS-PAGE in the presence and absence of dithiothreitol (DTT); the "Dimer" and "Monomer" columns show the results for non-treated and DTT-treated phage, respectively. The plus sign (+) indicates the detection of recombinant B2.1-PVIII fusion band on silver-stained gels, the minus sign (-) indicates no band observed.
# A plus sign (+) indicates reactivity with IgG1 b12 in western blot (WB), the minus sign (-) indicates no reactivity.
n.a. is not applicable.

Table 4. Reconstruction panning of Fab b12 phage (b12 ϕ) vs. B2.1 peptide, B2.1 phage (B2.1 ϕ) and gp120 Ba-L. Decreasing amounts of Fab b12 phage were mixed with DP47/AD27 phage (DP47/AD27 ϕ), to a total of 10^{10} particles and screened one single round with the three antigens. Results are expressed as percent yields of ampicillin-resistant transfecting units.

b12 ϕ	10^{10}	10^{9}	10^{8}	10^{7}	10^{6}	10^{5}	10^{4}	---
DP47/AD27ϕ	---	$9x10^{9}$	10^{10}	10^{10}	10^{10}	10^{10}	10^{10}	10^{10}
B2.1 peptide	2.7 e-3	3 e-3	1.5 e-4	1.6 e-4	4.5 e-4	1.2 e-4	3.4 e-4	1.6 e-4
B2.1 ϕ	2.1 e-1	1.4 e-1	7.7 e-2	3.1 e-4	5.8 e-5	1.3 e-4	2.7 e-4	2 e-4
gp120 Ba-L	3.2 e-1	2 e-1	2.8 e-2	1 e-3	2.7 e-4	1.2 e-4	3.1 e-4	4.9 e-4

enriched b12 phage 50-100 fold better than that of the synthetic B2.1 peptide. Thus, the affinity of the phage-borne B2.1 for the b12 Fab appears stronger than that of the synthetic peptide.

A biotinylated, synthetic version of the B2.1 peptide was also prepared, having the sequence: NH_3-HERSYMFSDLENRCIAAE-Orn(biotin)-KK-NH_2 (Multiple Peptide Systems; monomer MW = 2767.6; >95% pure and 80% dimer). This peptide (bio-B2.1) was biotinylated so that it could be bound to immobilized streptavidin in ELISA wells, and directly detected during the production of conjugates for immunization, regardless of its IgG1 b12 antigenicity. The relative affinity of Mab b12 for the B2.1 sequence presented in different forms was assessed by direct titrations using Fab and IgG1 b12. The titrations were performed on streptavidin-captured and plate-immobilized bio-B2.1 peptide, as well as with recombinant B2.1 phage (and gp120 as positive control). Figure 3A shows that the binding of Fab b12 to both plate-immobilized and streptavidin-captured synthetic B2.1 peptide was almost undetectable over background. In contrast, Fab binding to recombinant B2.1 phage was strong and followed a titration curve similar to that of gp120 (Figure 3A), suggesting that the affinities of b12 for gp120 and phage-displayed peptide are similar. (Kds of 3 nM ($gp120_{MN}$) and 9.1 nM ($gp120_{LAI}$) have been reported by Roben *et al.* (269) and Parren *et al.* (242), respectively.) Although the results were somewhat different when IgG1 b12 was used instead of Fab for the titration ELISA (which was most likely due to the avidity inherent to the IgG), a similar trend was observed (Figure 3B). The IgG1 b12 reacted with both phage-displayed and synthetic B2.1 peptide; however, it bound more tightly to recombinant B2.1 phage than to either form of the synthetic peptide. Moreover, the Ab showed better binding to the plate-

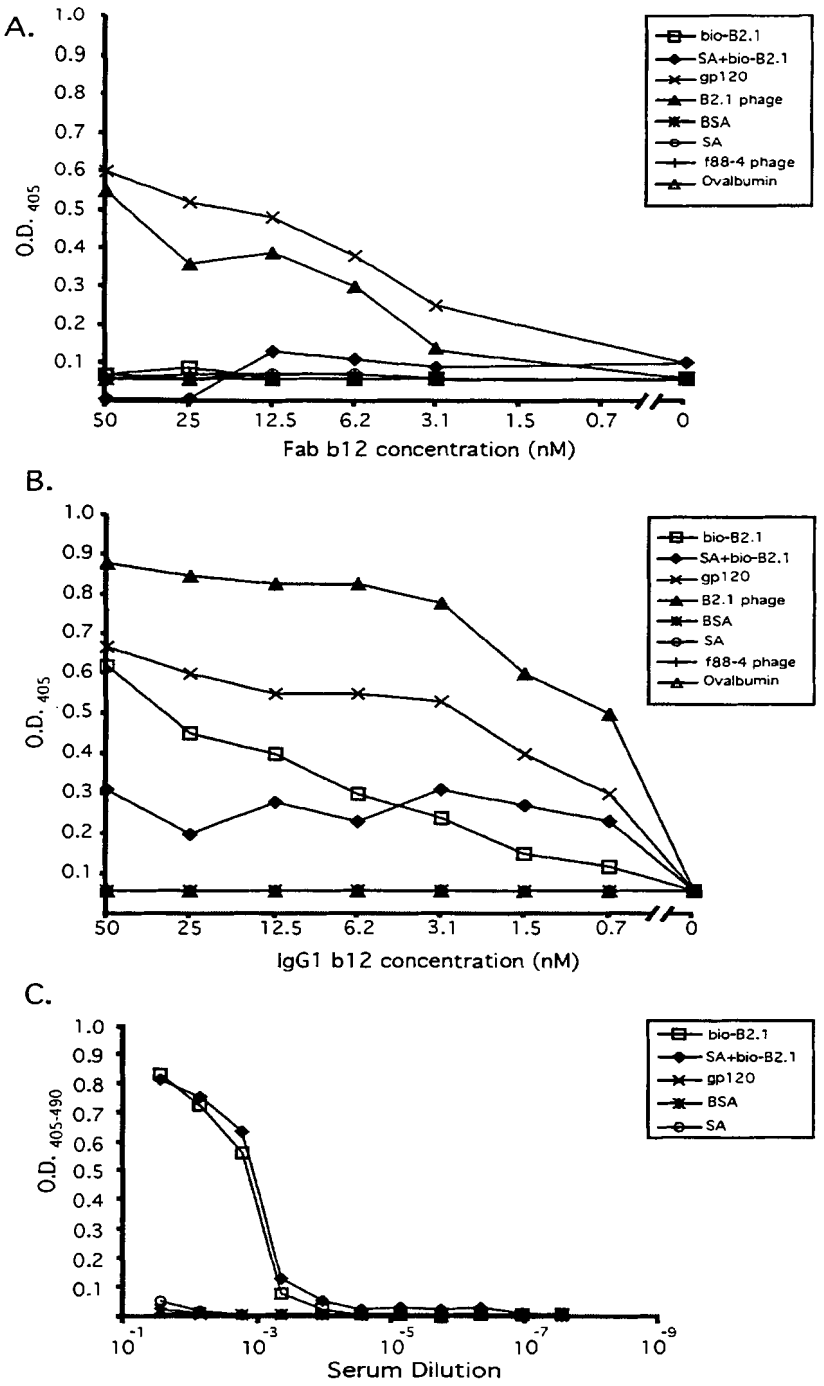

Figure 3: Titration of Fab b12 (A), IgG1 b12 (B) and murine anti-B2.1-peptide serum (C) on different immobilized antigens. Serial dilutions of Fab, IgG1 b12 and mouse serum were reacted with bio-B2.1 adsorbed to ELISA wells (bio-B2.1), bio-B2.1 bound to immobilized streptavidin (SA+ bio-B2.1), $gp120_{Ba-L}$, B2.1 recombinant phage, f88-4 phage, bovine serum albumin (BSA), ovalbumin and streptavidin (SA).

adsorbed peptide than to the streptavidin-captured one, thus it was able to discriminate between these two means of presenting the peptide. In contrast to IgG1 b12, the IgG from a mouse who had been immunized with a B2.1 conjugate vaccine (see below) showed no discrimination between the streptavidin-bound and plate-adsorbed forms of bio-B2.1 (Figure 3C), and binding to gp120 was undetectable. These results indicate that ability of b12 to discriminate between plate-immobilized and streptavidin-captured peptide is linked with its capacity to bind gp120, again, suggesting that a specific B2.1 structure (or set of structures) is responsible for its antigenicity for b12. It is apparent from these titration experiments that the most antigenic structure of the B2.1 sequence is best represented by the recombinant peptide in the context of the phage coat.

To assess the range of affinities of the different peptides for b12, the in-solution binding affinity of IgG1 b12 for the B2.1 peptide was determined using a KinExA 3000 (Kinetic Exclusion Assay) instrument (Sapidyne Instruments, Inc., Boise, ID) (27), as described in (69). KinExA measurements involving in-solution monovalent antigen yields affinity constants that are independent of the Ab valency. The data in Figure 4 show that the interaction between IgG1 b12 and the free peptide closely follow a 2.5-μM Kd best-fit, theoretical curve derived from a simple, second-order kinetic model (Fig. 4A). Comparison of the % root-mean square deviation errors (Figure 4B), produced from the fit of these data to the best-fit curves calculated for a range of Kds, reveal the accuracy of the Kd found for b12 and B2.1 in solution. This Kd is ~200-fold higher than the 9.1-nM Kd measured for the interaction between Fab b12 and recombinant gp120 from HIV-1_{LAI} as determined by surface plasmon resonance (269). However, the Kd is lower than the ~100 μM one found for a synthetic, cyclic peptide made from one of the

A.

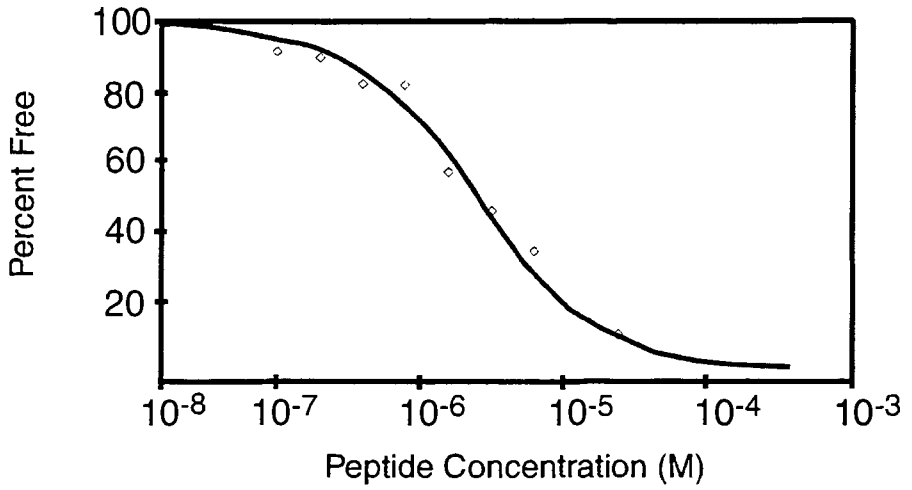

B.

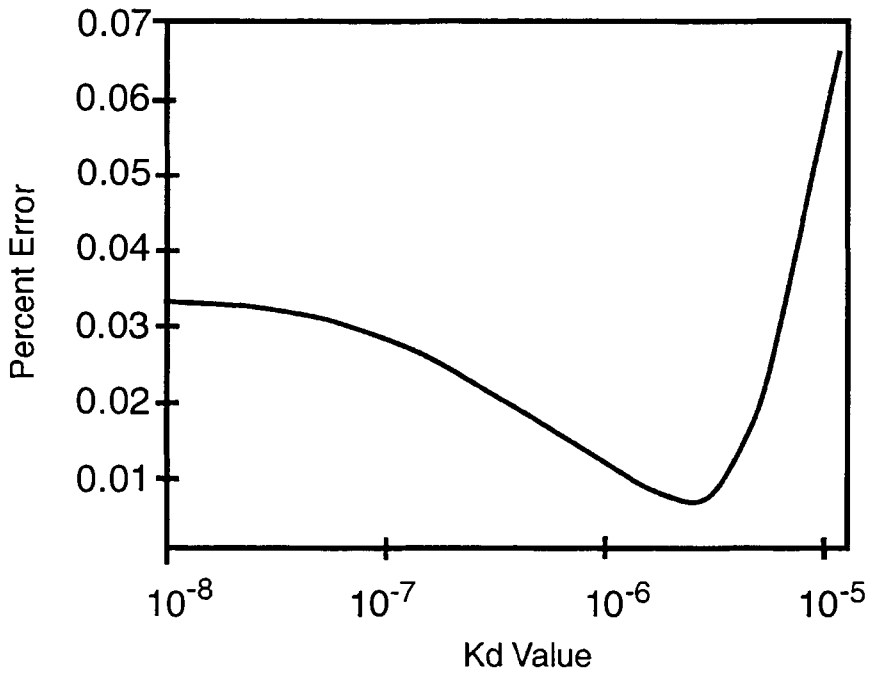

Figure 4. Binding of IgG1 b12 to B2.1 peptide in-solution, determined by KinExA. Percent free Ab *vs.* molar concentration of peptide; data (diamonds) and best-fit theoretical curve (A). Percent error from fit of the data in 3A to the best-fit curves calculated for a range of Kds (B). The 95% confidence interval calculated for this experiment is: 1.3-3.7 μM.

clones isolated from the B1 library, by competition ELISA of that peptide with Fab b12 (A. Satterthwait and J.K.S., unpublished data).

The Fab and IgG1 titration data and the in-solution affinities of b12 for B2.1 and gp120 may be used to provide very rough reference values from which the affinity of the plate-bound and phage-displayed peptides could be interpolated. Given the range of 9 nM for $gp120_{LAI}$ and ~3 mM for the free peptide (and assuming that the affinity of free B2.1 is similar to that of bio-B2.1 captured on streptavidin), we speculate that the plate-adsorbed peptide binds with a Kd ranging between 20 nM and 500 nM. The phage-displayed, recombinant peptide shows the highest affinity for binding to Fab b12, with the data suggesting a Kd value close to that of b12 for gp120.

Taken together, our results support the idea that the affinity of B2.1-b12 interaction is dependent on the environment in which the peptide is presented to b12. The data suggest the existence of different structures of the B2.1 homodimer, and indicate that the predominant structure of B2.1 in solution (and tethered, *via* biotin, to streptavidin) is either "unfolded" or "unstable", and different from the one(s) that it assumes in the context of the phage coat. Our results with synthetic and recombinant B2.1 peptides indicate that the structure of the homodimer could be further optimized to maximize its antigenicity. B2.1 binds b12 preferentially when fused to the pVIII coat protein and displayed on the phage surface, perhaps, because the highly structured phage coat provides a more rigid and/or stable environment to the peptide. This would be in keeping with the work of Jelinek *et. al.* (151), which shows that antigenic peptides fused to pVIII produce NMR-definable structures, even though the peptide in solution doesn't.

The sequences of the peptides we have discovered (Table 1), especially B2.1, show significant homology to the D-loop region of gp120 (residues 273-285). The residues of the B2.1 sequence that are shared with D-loop sequences from a number of gp120s are bolded in: HERSYMFSDLENRCI. The D loop region of gp120 contains a number of residues that are highly-conserved among HIV-1 isolates from different clades. Frequencies in gp120s from all clades for the bolded residues in the B2.1 sequence are 96% for Arg273, 96% for Ser274, 52% for Phe277, 99% for Ser or Thr at position 278, 99% for Asp or Asn at position 279 and 98% for Ile285 (frequency data were taken from the Los Alamos Env sequence database at: http://hiv-web.lanl.gov/). As well, residue Asp279 of the D loop also makes contact with CD4, and thus, forms part of the CD4 binding site on gp120 (176).

Figure 5 shows the sequence and structure of the D loop of HXB2 gp120; it appears to be partially stabilized by the interaction between the side chains of Val275 and Ile284. The b12-selected clones that contain two Cys residues most often have loop lengths of eight residues (Table 1). If the sequences of the cyclic peptides having 8-mer loops are overlaid on the D loop, with their N- and C-terminal Cys residues being placed where Val275 and Ile284 of the D loop are located, respectively, homologous residues shared between the two are perfectly aligned. The location of the FSD sequence aligns with that of the D loop's FTD sequence, and the N-terminal Ile of the peptides aligns with the gp120 Ile285.

The homologies between residues in B2.1 and conserved residues in the D loop, as well of the structural homologies with the cyclic peptides, lead us to predict that the D loop of gp120 is involved in binding the b12 Ab, with the residues RS, FSD and I being

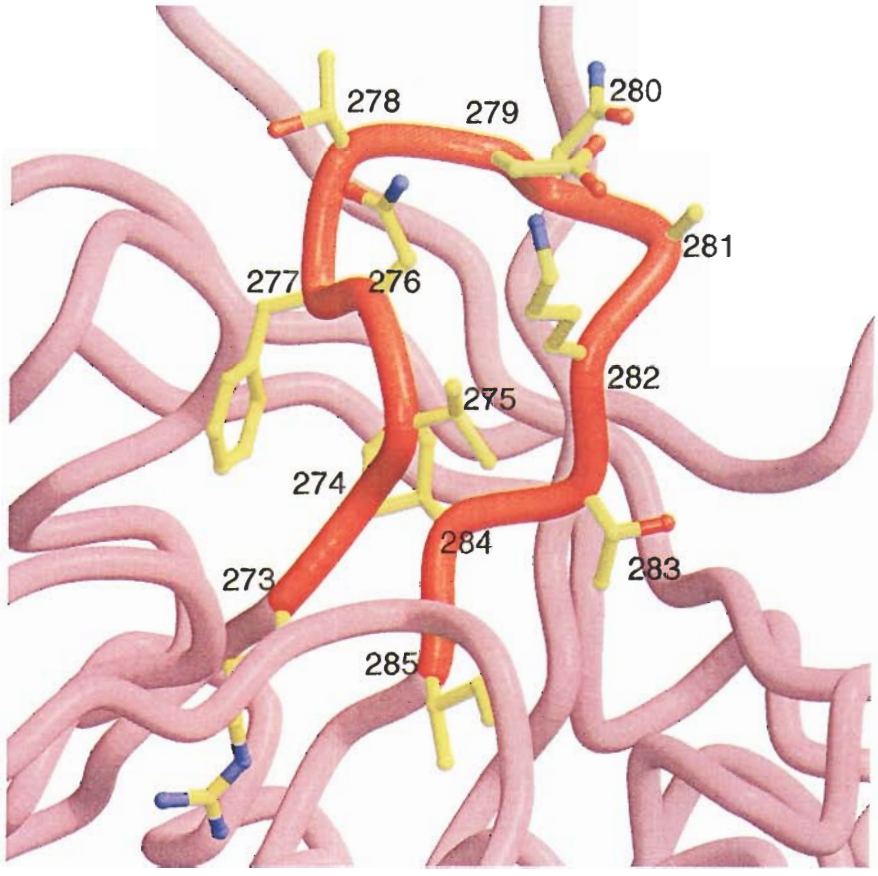

Figure 5. Structure of the D loop of gp120, residues 273-285, taken from the HXB2 HIV-1 isolate. The sequence of this region, shown in red, is: **RS**VN**FTD**NAKTI**I**. Residues shared with the B2.1 peptide, HE**RS**YM**FSD**LENRC**I**, are in bold.

important in maintaining a D-loop-like structure and/or in making direct contacts with the b12 Ab. The crystallographic structure of IgG1 b12 has been elucidated, both in the free form and bound to the B2.1 peptide (pers. comm. E. O. Saphire, The Scripps Research Institute). These structures should prove useful in directing further optimization of the B2.1 peptide, as a b12-ligand and as a gp120 mimic, and in characterizing the gp120-epitope for b12 at the atomic level.

Our goal in developing a peptide mimic of the b12 epitope is to use it in a vaccine against HIV-1 infection, to elicit b12-like, neutralizing Abs. We conjugated the biotinylated synthetic peptide to wild-type phage and ovalbumin using BS3 as cross-linker. The conjugates bound IgG1 b12 by western blot, ELISA and immunoprecipitation, indicating that the antigenic structure of B2.1 was conserved after the conjugation. We found that both conjugates were immunogenic in mice and rabbits, but did not elicit significant gp120-cross-reactive Ab titers, indicating that b12-like Abs were not produced at detectable levels (data not shown). At least two reasons may account for this: (1) the relatively low affinity of b12 for the synthetic version of the peptide and/or (2) the species barrier (b12 has an 18-residues long H3 and Abs with such features are not produced in mice). We also carried out immunizations with B2.1 recombinant phage, which produced only moderate anti-peptide Ab titers, accompanied by high anti-phage Ab responses. In addition to the species problem mentioned above, we believe that the relatively low copy number of B2.1 homodimer displayed on the phage surface (~ 200 copies/phage) explains this result.

Thus, the isolation and characterization of the B2.1 peptide constitutes the first stage of a new strategy for targeting the production of Abs against a single pre-specified,

neutralizing epitope on HIV-1. However, the generation of a successful B2.1 immunogen will require further optimization at several levels. The results described here indicate that the structure of the homodimer displayed on the phage coat is best for binding b12; thus the recombinant phage is the primary target for our efforts in structure-based optimization of B2.1 as an antigen and immunogen. We are currently assessing the peptide residues that are critical for b12 binding in the context of the phage. These functional data, coupled with the crystollographic data mentioned above, should provide insight into further optimization of the B2.1 peptide. Such optimization also requires knowledge of the phage-borne structure of B2.1. Thus, we are also making efforts to raise the copy number of the B2.1 homodimer on the phage coat, to allow NMR-based analyses, and to generate soluble B2.1 fusion proteins, so that the dimer can be studied in a "monovalent" protein format (as compared phage particles, which bear multiple copies of the dimer). Other immunization strategies (a prime-boost approach) and species (monkeys and XenoMouse™) will also be explored.

ACKNOWLEDGEMENTS

This work was supported by grants from NHRDP (J.K.S.), MRC (MT-14562 to J.K.S.), and the NIH (R21-AI44395 to J.K.S., AI42653 to P.W.H.I.P. and AI33292 to D.R.B.). M.B.Z. was supported by a predoctoral scholarship from NSERC, and J.K.S. was supported in part by a fellowship from BCHRF. We thank Edward Leong, Kelly Brown, Nienke van Houten, Firmin Hung and Ann Hessell for their excellent technical contributions to this work, and Bret Vanderkist for his help with the figures. We

gratefully acknowledge Arnold Satterthwait for his cyclic peptide studies, and Tim Fouts for providing gp120.

CHAPTER 3

Crystal Structure of a Broadly Neutralizing Anti-HIV-1 Antibody in Complex with a Peptide: Mechanism of gp120 Cross-Reactivity.

Erica Ollmann Saphire[2§], Marinieve Montero[4§], **Alfredo Menendez**[4], Nienke E.van Houten[4], Ralph Pantophlet[2], Michael B. Zwick[2], Paul W.H.I. Parren[2†], Dennis R. Burton[1,2], Jamie K. Scott[4]* and Ian A. Wilson[1,3]*

[1]Departments of Molecular Biology, [2]Immunology, and [3]The Skaggs Institute for Chemical Biology, The Scripps Research Institute. 10550 North Torrey Pines Road, La Jolla, California 92037, USA. [4]Department of Molecular Biology and Biochemistry, Simon Fraser University, Burnaby, British Columbia V5A 1S6, Canada.

***Correspondence should be addressed to:** J.K.S. E-mail: jkscott@sfu.ca or to I.A.W. E-mail: wilson@scripps.edu

†Present address: Genmab, Jenalaan 18a, 3584 CK Utrecht, The Netherlands.

[§]These authors contributed equally to this work.

Running title: Anti-HIV-1 Fab:peptide complex and gp120 cross-reactivity.

This work is being prepared for submission to ***The Journal of Biological Chemistry.***

ABSTRACT

IgG b12 recognizes a discontinous epitope on gp120 and is one of the rare monoclonal antibodies that neutralize a broad range of primary HIV isolates. We present the crystal structure at 1.8 Å resolution of a complex between Fab b12 and B2.1, a dimeric peptide that binds with high specificity to b12 and competes with gp120 for b12 binding. The peptide inserts into a canyon in the light chain that abuts the third complementarity-determining region of the heavy chain of b12, occupying about half of the antibody paratope. Alanine substitution experiments reveal that six of the fifteen residues of B2.1 are critical for b12 binding. Structural data differentiate residues that form critical contacts with b12 from those required for maintenance of the antigenic structure of the peptide. Affinity of B2.1 was improved 40-fold, to within an order of magnitude of that of gp120, by fusing it to the N-terminus of a soluble protein.

B2.1 and the gp120 D loop share sequence homology and occupy the same region in the b12 paratope. However, only a few critical binding residues are shared between B2.1 and gp120, and immunization with B2.1 fails to yield gp120 cross-reactive sera. Thus, although the binding sites of B2.1 and the gp120 D-loop roughly overlap, molecular mimicry is limited to only a few shared residues. The results underscore challenges to HIV-1 vaccine design and the necessity of combining complementary experimental approaches in analyzing the immunogenic properties of molecular mimics.

INTRODUCTION

A major obstacle to HIV-1 vaccine design is the difficulty in generating a protective humoral immune response against the viral envelope proteins (Env) gp120 and gp41. One strategy in developing such a vaccine is to emulate the properties of the rare human antibodies that are highly effective at neutralizing primary HIV-1 isolates (*e.g.*, IgG1 b12, 447-52D, 2G12, 2F5 and 4E10), but so far have been difficult to elicit with recombinant envelope proteins. Antibody b12 was isolated from a phage displayed Fab library that was produced from the bone marrow of an HIV-1 infected man who had been seropositive, yet asymptomatic for six years (269). IgG1 b12 recognizes the CD4 binding site of gp120 and neutralizes a wide range of primary HIV-1 isolates from diverse geographic origin (45, 315) *in vitro* . It also protects against HIV-1 infection in passive immunization experiments in animals (110, 238), whether provided intravenously (110, 238, 239, 326) or in a topical gel (326).

The crystal structure of intact, uncomplexed IgG1 b12 was previously determined at 2.7 Å resolution (284), revealing a 15 Å vertical projection of complementarity determining region (CDR) H3 ringed by two canyons: one formed between CDRs L1, L3 and H3, and the other between CDRs H1, H2 and H3 (285). Docking experiments of b12 onto gp120 illustrate a striking complementarity of fit between surfaces of b12 and the outer domain of gp120 (284). Mutagenesis studies have highlighted CDRs L1 and H3 as the key regions for b12 interaction with gp120 (357), and defined critical binding residues on both antibody (357) and antigen (233). In our docking model, the b12 epitope is created by the confluence of at least six separate peptide segments in the primary

sequence of gp120, with participation of D loop residues 276-280 and the ridge formed by residues Ser 365-Gly 367 (284),.

Phage-displayed peptide libraries can be highly effective tools in selecting peptide ligands for antibodies against linear and conformational protein epitopes (146). By screening a group of phage-displayed peptide libraries, we previously isolated and characterized a peptide, termed B2.1, which is specific for IgG b12. B2.1 does not react with non-neutralizing antibodies that compete with b12 for binding to gp120, suggesting that B2.1 recognizes unique features of the neutralizing b12 paratope. Partial sequence homology of B2.1 with the D-loop of gp120 (residues 271-285, HxB2 strain) suggested that B2.1 might mimic this region of the b12 epitope (352).

Here, we present the first crystal structure of a peptide thought to mimic a conformational epitope in complex with its corresponding antibody. The structure of Fab b12 in complex with the B2.1 peptide was determined at 1.8 Å resolution. The structure of B2.1-bound Fab b12 is very similar to the free Fab (284), indicating that no gross conformational changes accompany peptide binding. The B2.1 peptide inserts into a canyon in the light chain and covers about half of the putative b12 paratope. Six residues required for binding to b12 were identified on B2.1 by alanine-substitution mutagenesis. Only two of these residues make direct contact with b12, indicating that the remaining residues support the antigenic structure of B2.1. Comparison of the b12-B2.1 structure with the b12-gp120 docked model suggests that B2.1 occupies the same region of the b12 paratope as the gp120 D-loop. It is plausable that Asp 9, a critical binding residue in B2.1, mimics Asp 279, a critical binding residue of gp120 identified in mutagenesis studies (233, 284). However, few other residues shared between B2.1 and gp120 appear

to mimic each other. In addition, immunization of mice with a B2.1 peptide-ovalbumin conjugate resulted in high titers of anti-B2.1 antibodies that do not cross-react with gp120. In addition, the pattern of binding of these sera to the panel of Ala-substitution mutants differs from that of b12. Our results shed light on the mechanism of peptide mimicry of protein epitopes and its relevance to epitope- and antibody-targeted vaccines.

METHODS

Protein Expression and Peptide Synthesis.

IgG1 b12 was expressed in CHO K1 cells as previously described (283). Fab fragments were obtained by papain cleavage and purified with protein A and protein G affinity chromatography (338). The B2.1 peptide used in crystallization experiment was synthesized by AnaSpec, Inc. of San Jose, CA, and is encoded by the sequence HERSYMFSDLENRCIAAE-Orn(biotin)-KK. The biotinylated ornithine-lysine-lysine sequence was incorporated into the synthetic peptide for detection in separate ELISA experiments.

Crystallization and Data Collection.

Plate-like crystals were obtained from 17 mg/ml Fab, a five-fold molar excess of B2.1 peptide, 1.7 M ammonium sulfate, 200 mM lithium sulfate, and 100 mM CAPS buffer, pH 10.5. The crystals are monoclinic $P2_1$ with two Fabs and one dimeric peptide per asymmetric unit (V_M= 2.4) (Table 1). For cryoprotection, crystals were soaked in a solution of mother liquor containing increasing concentrations of glycerol (from 1-16%)

and flash-cooled in liquid nitrogen. Data were collected at 100K to 1.75 Å resolution at SSRL beamline 11-1 (Table 1), and integrated and scaled with DENZO (230) and SCALEPACK (230).

Structure Determination and Refinement.

Fab structures were determined by molecular replacement in AMoRe (222) using the Fab fragments of the intact IgG1 b12 structure (284) as search models. The R-value after molecular replacement was 37.4 for 15-4 Å data. Peptide and ligand molecules were built using the modeling programs TOM/FRODO (157, 160) and O (161), and the structure was refined to 1.8 Å using CNS (41) (Table 1). Clear electron density is visible for residues 1-214 of antibody light chain L, residues 1-128 and 137-228 of antibody heavy chain H, residues 1-214 of antibody light chain M and residues 1-127 and 136-230 of antibody heavy chain K. Heavy chain residues 127-137 comprise a solvent exposed loop in the constant region of the Fab that is frequently disordered in antibody structures (301). Coordinates and structure factors have been deposited in the Protein Data Bank (http://www.rcsb.org/pdb/, accession code 1N0X). Figures 1 and 4 were created using Molscript (95). Figure 3 was created in PMV (279, 280) with molecular surfaces generated using a 1.4 Å probe radius in msms (281).

Site-directed Mutagenesis of B2.1 Phage.

All residues of the B2.1 peptide, with the exception of the cysteine, were singly replaced by alanine in the context of B2.1. Alanine substitution of the cysteine residue on B2.1 phage has been previously described (352). Single-stranded DNA from phage B2.1

was used as template for site-directed mutagenesis using a set of fourteen oligonucleotides as previously described (174).

Direct-Binding ELISAs.

To assess binding of b12 to B2.1 mutant phage by ELISA, phage were adsorbed to microtiter wells, blocked, washed, incubated with either 0.1 nM IgG b12 or 10 nM Fab b12 for 2 to 4 hours at room temperature, and detected with goat anti-human Fab antibody conjugated to HRP. Replica, phage-coated wells were reacted with a rabbit polyclonal anti-phage antibody to verify that similar amounts of phage particles were adsorbed to the plate. The relative binding of b12 IgG and Fab to phage mutants bearing alanine substitutions were calculated as the percent binding with respect to binding to B2.1 wild-type phage (100%).

Sera from immunized mice were reacted with B2.1 peptide, phage bearing mutations of the B2.1 peptide, gp120 or OVA, with each serum dilution duplicated on BSA-coated wells as a control for background signal. ELISAs were performed essentially as described above, except that 1 mg OVA, 200 ng B2.1 peptide or 100 ng of gp120 (Ba-L isolate, kindly provided by Tim Fouts) were adsorbed overnight to wells. After blocking with BSA, serially-diluted mouse sera were added to each well and incubated for two hours at room temperature. The wells were washed six times and incubated with goat anti-mouse IgG (Fc)-HRP conjugate (Pierce). Serum titers were measured as the dilution at which the half-maximal $OD_{405-490}$ signal for B2.1 peptide and OVA were observed. Data for gp120 binding were reported as $OD_{405-490}$ at a 1:50 dilution.

B2.1-MBP Fusion Protein Production and Affinity Measurement.

B2.1-maltose binding protein (MBP) fusion protein was prepared as described (358). The affinity at equilibrium of dimeric B2.1-MBP for IgG1 b12 was measured using a KinExA 3000 instrument (Sapidyne Instruments, Boise, ID) as described (69) and by surface plasmon resonance (SPR) using a Biacore 3000 instrument (Biacore AB, Uppsala, Sweden) following the manufacturer's kinetics method. The affinity of free B2.1 peptide for b12 was determined by SPR by a binding-inhibition procedure (165, 225) as described (206) and also by using the steady state affinity model of BiaEvaluation 3.1 software (Biacore AB).

Coupling of synthetic B2.1 peptide to f1.K and OVA

f1.K is an engineered f1 phage carrying a Lys at the N-terminus of every copy of the pVIII major coat protein. The B2.1-f1.K conjugate was prepared with an 11-fold molar excess of peptide to pVIII phage protein: 8.5 x 10^{12} particles/ml f1.K phage, 2 mg/ml synthetic B2.1 peptide and 3 mg/ml Bis(sulfosuccinimidyl)suberate (BS^3) crosslinker (Pierce) in PBS pH 7.4. Conjugation reactions were rotated slowly at room temperature for one hour and quenched with 0.1 vol. 1M Tris-HCl, pH 7.4. Phage were precipitated with 0.15 vol PEG/NaCl, overnight incubation at 4°C and centrifugation at 13,000 x g for 40 min at 4°C. Pellets were resuspended in sterile PBS and aliquots were removed and analyzed by electrophoresis on a 4x GBB, 0.8% agarose gel (31).

The B2.1-OVA conjugate was prepared by mixing a 60-fold molar excess of B2.1 peptide with ovalbumin (OVA), allowing ~3.5 molecules of peptide per each of 20 Lys residues followed by addition of BS^3: 298 μg/ml OVA, 2 mg/ml synthetic B2.1 peptide

and 3 mg/ml BS^3. The conjugation reaction was as described above, except that the conjugates were washed three times using a Centricon-30 ultrafiltration device (Amicon, Inc., Beverly, MA) rather than precipitated by PEG.

Immunization of Mice with B2.1 Peptide-Bearing Immunogens.

Groups of five eight-week old female BALB/c mice were immunized by intraperitoneal injection with either 100 μg recombinant B2.1 phage, 10 μg B2.1-OVA conjugate or 10 μg OVA. All samples were diluted in a total volume of 100 μl PBS. No adjuvant was used. For all groups, the mice were immunized on days 0, 14, 28, 42, 63, 98 and 119. The mice were bled from the tail vein on days 0, 14, 28, 42, 63, and 77, just prior to immunization. Subsequent tail bleeds were not performed due to tail scarring. The final bleed for the B2.1-OVA conjugate or OVA immunized mice was performed on Day 140 by cardiac puncture under CO_2 anesthesia. The final bleed for the B2.1 phage-immunized group was performed on day 77, also by cardiac puncture under CO_2 anesthesia. After collection, each blood sample was heated to 37°C for 60 min, allowed to clot overnight at 4°C, and centrifuged at 12,000 x g for 15 min. Serum samples were then transferred to fresh microfuge tubes and stored at -20°C.

In a separate study, groups of four of eight-week old female BALB/c mice received 10 μg f1.K/B2.1 conjugate or 10 μg f1.K unconjugated phage by subcutaneous injection at two different sites. Immunogens were injected in a total volume of 100 μl PBS with or without adjuvant. Immunizations were given on days 0, 21, 42, 63, 92, 147, and 210. Tail bleeds were conducted two weeks after each immunization (days 0, 14, 35, 56, and 105). Bleeds were not taken after the fourth and the sixth immunizations due to

tail scarring. The final bleed was taken on day 224 by cardiac puncture as described above. After collection, blood was treated as described above.

Construction and Screening of the B1.2/D-loop Mixed-sequence Library.

The b12-binding phage clone, B1.2 (352), expressing the cyclic peptide GCLYSDLLATCI, was used as a template for the construction of a limited library according to the alignment with the D-loop of gp120 (HXB2 env 274-285, SVNFTDNAKTII). Note that B1.2 is very similar to B2.1, but is cyclic rather than linear, and monomeric rather than dimeric. A degenerate, synthetic oligonucleotide with the sequence ATC-ACC-TTC-TGC-AGC-AGA-ACC-GAT-G(C/A)(A/T)-GGT-T(G/T)(C/T)-C(A/G)(G/C)-(C/G)(A/T)(G/T)-GTC-GG(A/T)-A(T/A)A-(C/G)(A/T)(G/T)-A(C/A)(A/C)-A(C/G)(C/A)-ACC-AGA-GGC-AAA-GCT-TAG-CAT-AGG-AAC was cloned into the recombinant *gene 8* site of f88-4 as described (30). Each residue in the displayed peptides of the resulting library was either: *(i)* the original residue of B1.2, *(ii)* the corresponding residue from the D-loop of gp120, or *(iii)* one of several additional amino acids. All positions in the peptide were diversified in this way except residues Asp 6, Thr 10 and Ile 12, which are conserved between B1.2 and the D loop and hence, fixed in the library. One Gly and one Ser residue served as spacers and were introduced at both ends of the sequences for all clones. A control B1.2 phage incorporating the Gly and Ser spacers (named MMB1.2) was also constructed. The phage library was screened with b12 IgG as described (205).

RESULTS

Antibody Structure

The b12-B2.1 structure was determined to 1.8 Å by molecular replacement using Fab regions of the IgG b12 structure as search models and refined to an R_{cryst} of 22.0 and an R_{free} of 25.2 (Table 1). The asymmetric unit of the crystals consists of one disulfide-bonded B2.1 peptide dimer (chains P and R) in simultaneous contact with two opposing Fab fragments (LH, MK) (Figure 1A). The two Fabs in the asymmetric unit are essentially identical in structure, with only minor variation in side chains that are not involved in peptide contact. In addition, the structures of the two b12 Fab regions in complex with B2.1 peptide are nearly identical to the unliganded b12 Fab fragments contained within the intact b12 IgG (284, 285). Interestingly, the only significant difference is for CDR H3s of the peptide-bound b12 structures, which have a slightly taller vertical projection than the CDR H3s of the unbound b12 structures. Otherwise, the overall similarity in structures between the bound and free b12 Fabs (average r.m.s.d. of 0.74 Å for all main-chain atoms in all possible permutations) implies that no gross conformational changes accompany peptide recognition, and that the b12 surface topography is complementary to both gp120 (as determined by computational docking; 12) and the B2.1 peptide (as determined from the crystal complex).

Approximately 610 $Å^2$ of B2.1 peptide and 650 $Å^2$ of b12 antibody molecular surface are buried by the interaction (as calculated with ms (65)). For comparison, 1030 $Å^2$ of gp120 and 1040 $Å^2$ of b12 antibody molecular surface are buried by the gp120-b12 interaction in our docking studies (284). Thus, a little more than half of the putative b12

Table 1. Summary of crystallographic data and refinement statistics.

Data collection

Wavelength (Å)	0.965 Å
Space group	$P2_1$
Unit cell dimensions	a=51.6Å, b=184.4Å, c=56.2Å, β=103.1°
Resolution (Å)[1]	45-1.78 (1.81-1.78)
# reflections	215,495 observed; 94,383 (4468) unique
Completeness[1] (%)	92.0 (87.1)
R_{sym} [1,2] (%)	6.0 (38.5)
I/σ(I) [1]	17.6 (1.5)

Refinement statistics

Number of reflections		84,895		
Number in test set[3]		9419, 1967		
R_{cryst} [4] (%)		22.0		
R_{free} [5] (%)		25.2		
Number of residues		876 antibody, 41 peptide		
Number of other atoms[6]		83 ligand atoms, 725 waters		
Average B values (Å^2)				
Fab fragments	31.3			
Peptide	47.0 (35.7 in contact hairpin[7])			
Ramachandran plot (%)			R.m.s.deviations	
Most favored		89.0	Bond lengths (Å)	0.005
Additional allowed		10.5	Angles (°)	1.4
Generously allowed		0.2	Dihedral (°)	26.7
Disallowed[8]		0.2	Improper (°)	0.80

[1]Numbers in parentheses refer to highest resolution shell.

[2]$R_{sym} = \Sigma| I - \langle I \rangle | / |\langle I \rangle|$, where $\langle I \rangle$ is the mean intensity of a set of equivalent reflections

[3]A 10% test set was used for initial rounds of refinement, and a 2.3% test set was used for the final round of refinement, as studies indicate that the deviation in R_{free} is roughly proportional to its value divided by the square root of the number of excluded reflections. Reflections in the final, smaller test set were also in the original, larger test set.

[4]$R_{cryst} = \Sigma_{hkl} |F_o - F_c| / \Sigma_{hkl} |F_o|$

[5] R_{free} was calculated as for R_{cryst}, but on the test set portion of the data excluded from the refinement.

[6] 14 atoms from a CAPS molecule, 48 atoms from glycerols, 20 atoms from sulfate ions, and 1 potassium atom

[7]The contact hairpin includes residues Ser P8 – Leu P10 and Ile P15.

[8]Includes Val L51 of both Fab light chains. This residue exists in a well-defined γ turn in almost all antibody structures, but still continues to be designated by PROCHECK as an outlier despite its inclusion in a well-defined and well-documented secondary structure

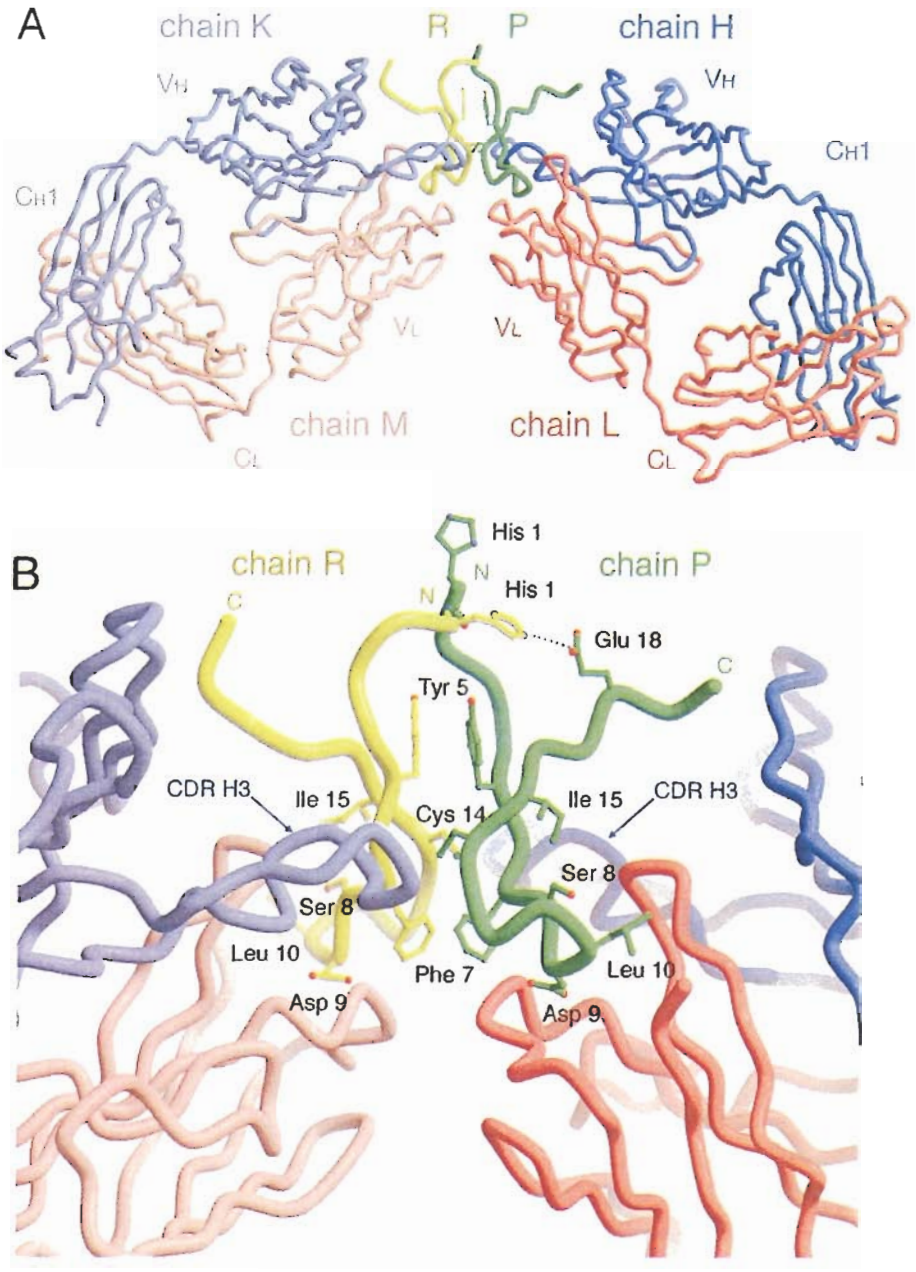

Figure 1. Crystal structure of the b12-B2.1 complex. (A) The peptide dimer is formed by chains P (green) and R (yellow). Peptide chain P (green) is bound to Fab #1 which is designated in the deposited coordinates by heavy chain H (blue) and light chain L (red). Peptide chain R (yellow) is bound to Fab #2 which is designated by heavy chain K (blue) and light chain M (light pink). (B) Each of the two monomers of the B2.1 dimer independently contact one of the two b12 Fabs. Key side chains of the B2.1 dimer are illustrated in ball-and-stick. The extended CDR H3s of the b12 antibody reach across each peptide monomer, yet form no contact to the opposing monomer. Figure was made using MolScript.

paratope interacts with the B2.1 peptide. However, this interaction surface is larger than that observed for most antibody-peptide complexes (on average, 480 $Å^2$ of peptide and 550 $Å^2$ of antibody surface (302, 339)), owing to the longer length of the B2.1 peptide (20 ordered residues as compared to an average of 9-10 ordered residues in typical antibody-peptide structures in the Protein Data Bank.

Peptide Structure

Clear electron density was present in the antibody-combining site for the first eighteen residues of the 21-mer peptide sequence, whereas the density for Orn 19, Lys 20, and Lys 21 was only interpretable for the polypeptide backbone. These residues have been built in as alanines. The biotin moiety is not defined in the electron density maps. Each monomer of the B2.1 peptide forms a hairpin structure with the N-terminal arms of the two hairpins extending roughly in parallel to each other and the C-terminal arms angling outwards from each other (Figure 1B). The hairpin turn contains B2.1 peptide residues Ser P8, Asp P9, and Leu P10 and twists upwards at Phe P7, towards Ile P15 in the C-terminal arm. Each hairpin turn curls into the antigen-binding site of each one of the two opposing antibodies. Hence, in the $SDLX_3CI$ motif borne by phage selected by b12 (including the B2.1 peptide (352)), the Ser, Asp, and Leu form antibody contacts (see below), whereas the Cys forms the intrapeptide disulfide bridge that holds the dimer together and main chain atoms of the Ile forms hydrogen bonds connecting the N and C termini within each peptide monomer (Figure 1B). The B2.1 dimer interface is formed mainly by peptide residues Tyr P5 and Cys P14 (Figure 1B). The Tyr P5 side chains on the N-terminal arms of the hairpins form aromatic face-to-face π-stacking interactions

Table 2. Peptide:peptide and peptide:antibody contacts observed in the crystal structure complex of the dimeric B2.1 peptide bound to two b12 Fab fragments.

Intrapeptide (P:P and R:R)	Interpeptide (P:R)	Antibody:peptide		
		Fab LH:Peptide P	Fab MK:Peptide R	Fab MK: Peptide P
Hydrogen-bonds †	**Hydrophobic contacts**	**Hydrophobic contacts**	**Hydrophobic contacts**	**Hydrogen bonds**
Ser 4 O:Ala 17 N	Tyr 5(P):Tyr 5 (R)¶	Glu 1(L) CA:Leu 10(P) CD1	His 27(M) CE1:Leu 10(R)CD1	Ser302,100c(K)OG:Asn12(P)O
Met 6 N:Ile 15 O	Cys 14(P)SG:Cys 14(R)SG	Ser 30(L) CB:Asp 9(P) CG	Glu 1(M) CB:Leu 10(R)CD1	
Met 6 O:Ile 15 N	Met 6(R)C:Cys 14(P)SG	Ile 28A(L) CG2:Asp 9(P) CG	Ser 30(M) CB:Asp 9(R)CG	
Ser 8 N:Arg 13 O	Met 6(R)CA:Cys 14(P)SG	Ile 28A(L) CA:Asp 9(P) CG	Ile 28A(M) CG2:Asp 9(R)CG	
Ser 8 Og:Glu 11 N	Met 6(P)C:Cys 14(R)SG	Arg 29(L) CD:Phe 7(CZ) §	Ile 28A(M) CA:Asp 9(R)CG	
Ser 8 O:Asn 12 N	Cys 14(R)CB:Tyr 5(P)CB	Arg 29(L) CD:Phe 7(CE2) §	Arg 29(M) CB:Phe 7(R)CE2§	
	His 1(R)CE1:Arg 3(P)CG	Arg 29(L) CG:Phe 7(CE2) §	Ala 93(M) CA:Met 6(R)SD	
		Arg 29(L) CB:Phe 7(CE2) §	Ala 93(M) CB:Met 6(R)CG	
	Hydrogen bonds	Asn 56(H) CG:Ala 20(P) CA	Asn 56(K) CG:Ala 19(R)CB**	
	His 1(R)N: His 1(P)O	Asn 56(H) CB;Ala 20(P) CA	Asn 56(K) CB:Ala 19(R)CB**	
	His 1(R)NE2:Glu18(P)OE2	Glu 58(H) CG:Ala 21(P) C	Trp 50(K) CH2:Ala 19(R)CB	
		Gln 304,100E(H)CD:Met 6(P)CE	Lys 57(K) C:Ala 19(R)CA	
		Gln 304,100E(H)CD:Met 6(P)SD	Asn 56(K) CB:Ala 19(R)CA**	
			Glu 58(K) CD:Glu 18(R)CG	
		Hydrogen bonds	Glu 58(K) CD:Glu 18(R)CB	
		Ser 30(L) N:Asp 9(P) OD2	Glu 58(K) CB:Glu 18(R)CB	
		Arg 29(L) N:Asp 9(P) OD2	Gln 304,100e(K)CD:Met 6(R)CE	
		Arg 29(L) NE:Asn 12(P) OD1	Gln 304,100e(K)CD:Met 6(R)SD	
		Arg 29(L) NH2:Asn 12(P) OD1	Gln 304,100e(K)CG:Met 6(R)SD	
		Ser 30(L) OG:Asp 9(P) OD1	Gln 304,100e(K)CB:Met 6(R)SD	
		Arg 32(L) NH2:Phe 7(P) O	Pro 303,100d(K)CG:Ser 4(R)CB	
		Arg 32(L) NH1: Phe 7(P) O	Pro 303,100d(K)CB:Ser 4(R)CB	
		Asn 56(H) OD1:Ala 20(P) N		
			Hydrogen bonds	
			His 27(M) ND1:Leu 10(R) O	
			Ser 30(M) N:Asp 9(R) OD2	
			Ser 30(M) OG:Asp 9(R) OD1	
			Arg 32(M) NH2:Phe 7(R) O §	
			Arg 32(M) NH1:Phe 7(R) O §	
			Asp 301,100b(H)O:Arg13(R)NH2	
			Asp 300,100a(H)O:Arg13(R)NH2	

with each other, whereas the Cys P14 residues form a disulfide bridge. The B2.1 hairpin structure appears to be further maintained by six hydrogen bonds within each monomer that connect the N terminus to the C terminus (Table 2).

Single Ala substitutions within phage-displayed B2.1 peptide were performed to identify the residues that are critical or important to b12 binding (Figure 2A). The mutations were verified by DNA sequencing and equal expression levels of the recombinant mutant proteins on the phage surface were confirmed by SDS-PAGE (data not shown). Critical binding residues are defined here as those that, if substituted with Ala, produce a decrease in binding to both IgG and Fab of >90%. Important residues are defined as those whose substitution to Ala causes a >80% drop in binding to Fab without significantly affecting IgG binding (IgG has higher avidity than Fab). Figure 3 summarizes the main contacts observed in the crystal structure, along with the classification of each B2.1 residue as critical, important or unimportant to b12 binding, according to the Ala-substitution data in Figure 2A. Taken together, the structural and Ala-substitution data reveal the importance of both intra- and inter-peptide interactions for the functional activity of B2.1. Tyr P5 and Cys P14 which form interchain contacts and Ile 15 which forms intrachain contacts are all critical for binding to b12, even though they do not directly interact with the antibody. Thus, these three residues most likely serve a critical role in maintaining the antigenic structure of B2.1.

Peptide Contact to Antibody

The two peptide monomers make essentially identical contacts to their respective Fabs. The three N–terminal residues of B2.1 are positioned above CDR-H1, but do not

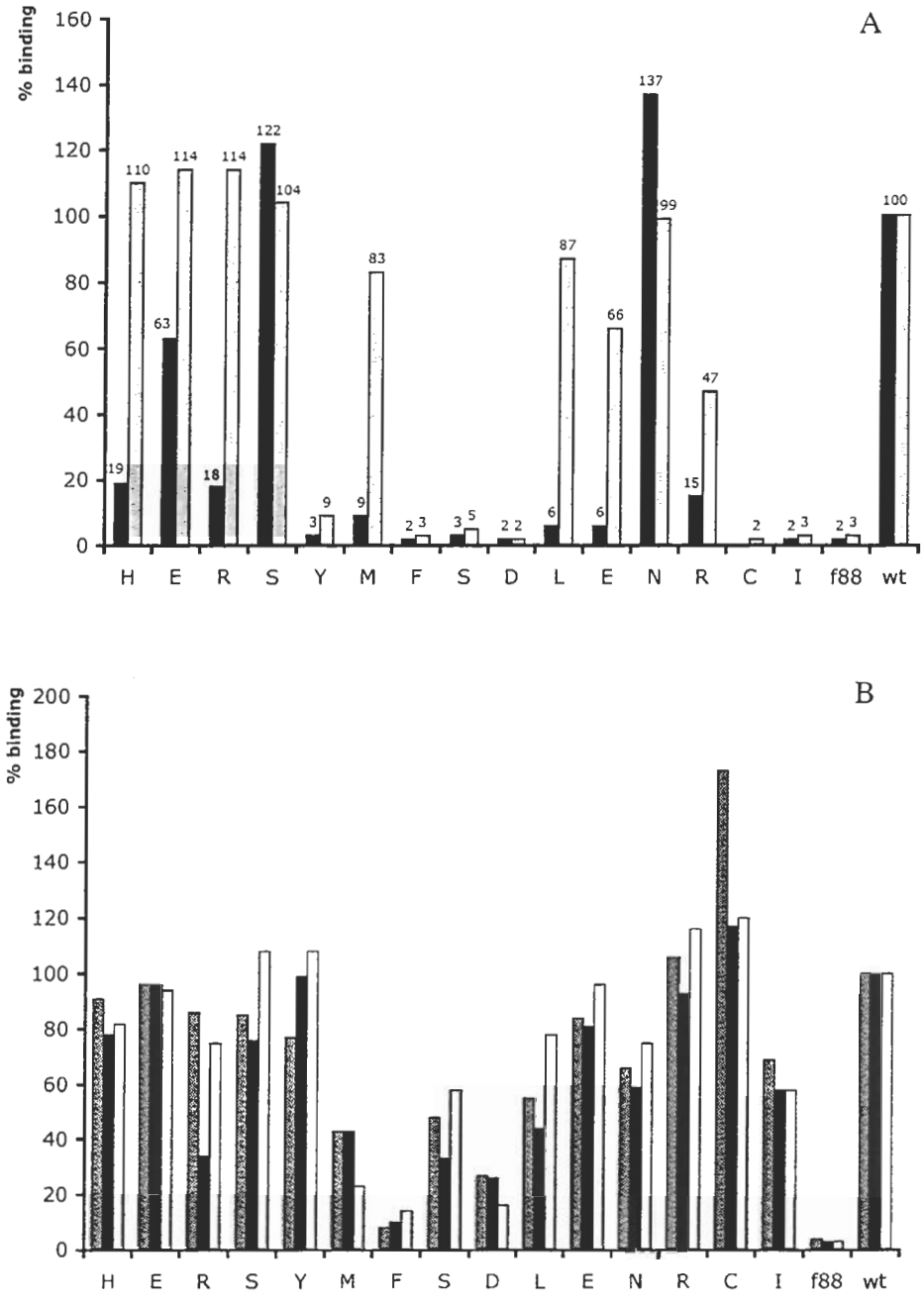

Figure 2. Alanine-substitution scanning of the B2.1 peptide. (A) Binding of IgG b12 (grey bars) and Fab b12 (black bars) to mutant B2.1 peptides. (B) Binding of sera from each of three mice (grey, black, and white bars) immunized with B2.1 peptide-Ovalbumin conjugate. Results are expressed as % binding of each mutant phage with respect to wild-type (wt) B2.1 phage, the f88 is a negative control for phage expressing no peptide.

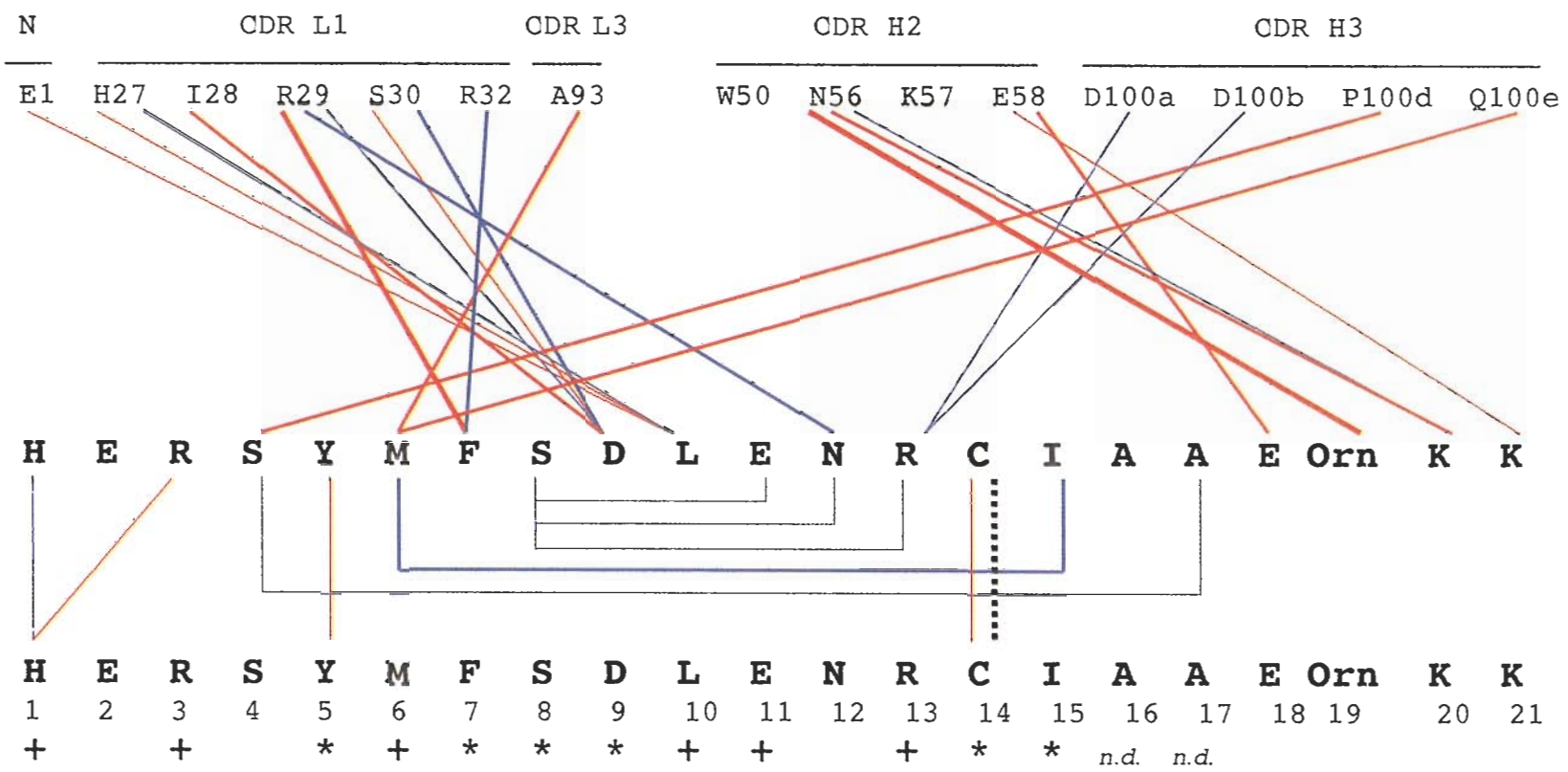

Figure 3. Schematic representation of direct contacts between one B2.1 peptide monomer and b12 (top panel) and contacts between the two monomers of the peptide dimer (bottom panel). Red lines represent hydrophobic contacts, blue lines represent hydrogen bonds, and the dotted black line represents the single intrapeptide disulfide bridge. Thin lines represent a single pair of contacting atoms. Thick lines represent 2-4 atomic contacts per residue. Contacts mediated by water are not represented here. Peptide residues (as determined by Ala substitutions) critical for binding to b12 are indicated by *; important residues are indicated by +.

contact it. Antibody interaction begins with Ser P4 as the peptide monomer descends down along one side of CDR H3 towards CDR L1, then continues as the peptide forms a hairpin, reverses direction, and extends across CDR L3 to terminate at CDR H2 (Figure 4A). The most significant region of peptide interaction is within the depression between CDRs L1, L3 and the light chain N terminus (Figure 4B). Here, Asp P9 contacts Ile 28a, Ser 30, and Arg 32 of CDR L1, and Leu P10 contacts Glu L1 (Table 2 and Figure 3). Ser P8 contacts Ala L93 and Ser L94 indirectly *via* water molecules (Figure 4C). Phe P7 forms side chain hydrophobic contacts to Arg 29, and hydrogen bonds between its main chain carbonyl oxygen to the side chain nitrogens of Arg 32 of CDR L1 (Figure 4C). Interaction with CDR-H3 is mediated by N-terminal residues of the peptide, where Met P6 contacts Gln 100e and Ser P4 abuts Pro H100d (Figure 4D). In addition, the side chain of Arg P13 hydrogen bonds to the main chain of Asp 100a and Asp 100b in CDR H3, although this interaction is only observed for one of the two peptide chains. Hydrophobic contact to CDR H2 is made by various C, Ca, and Cb atoms of the Orn-Lys-Lys C-terminal extension to B2.1 (Figure 4D). However, these contacts are probably crystal contacts rather than specific binding contacts as they differ for each peptide chain. The Ala-substitution data (Figure 2) show that Phe P7, Ser P8 and Asp P9 are critical for binding to b12, whereas other contacting residues (Met P6, Leu P10 and Arg P13) are important but not critical for b12 binding. Although Ala-substitution of Ser P8 abrogates b12 binding, its side chain only contacts b12 indirectly via a water molecule. Thus, Phe P7 and Asp P9 were classified as critical contact residues.

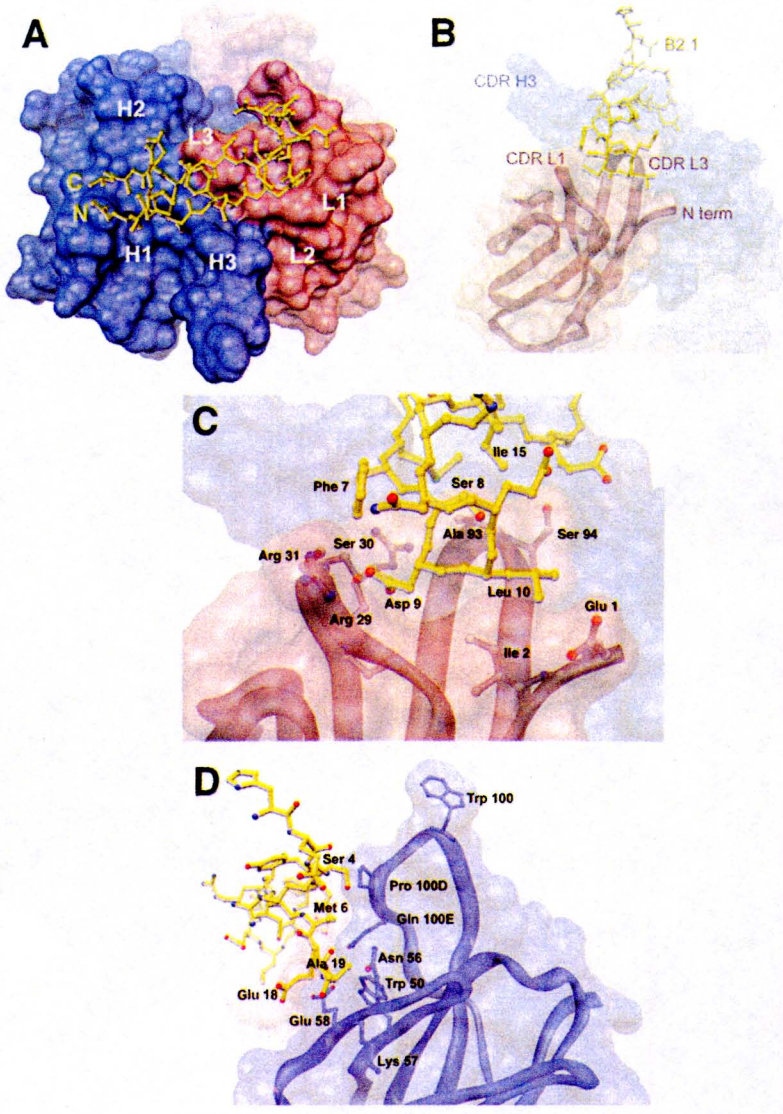

Figure 4. B2.1-b12 interactions. In all panels, the light chain of b12 is colored pink and the heavy chain colored blue. Only one monomer is shown bound to its respective Fab b12. Panels (a-d) illustrate contacts between the peptide chain R and Fab #2, as this peptide chain is characterized by slightly lower B values. (A) Top view of the Fab b12 antigen-binding site with the bound B2.1 peptide illustrated in yellow ball and stick with the N and C termini of the peptide indicated. The b12-combining site is illustrated as a molecular surface with locations of the six CDRs (L1, L2, L3, H1, H2, and H3) indicated. (B) Side view of the b12 antibody-combining site. B2.1 dips into a canyon formed between CDRs L1, L3 and H3. (C) Specific contacts between B2.1 and the light chain involve the residues SDL of the original selected $SDLX_3CI$ consensus motif. (D) Alternate view of the b12 combining-site highlighting interaction of the B2.1 peptide with the heavy chain (blue Cα ribbon) underneath the transparent molecular surface.

Potential for mimicry of the gp120 D loop by B2.1-related peptides

As B2.1 and the D loop of gp120 (residues 279-285) share some sequence homology (HE**RS**YM**FSD**LENRC**I**AAE vs. **RS**VN**FTD**NAKTI**D**), we previously hypothesized that B2.1 and related peptides could mimic the D-loop of gp120 (352). Superposition of b12 Fab molecules in the B2.1 co-crystal and the gp120 docked model (284) reveals that the peptide and the D loop occupy the same general region of the paratope (Figure 5). In addition, alanine mutagenesis of CDR L1 of b12 and the corresponding contact residues in B.1 and gp120 D loop underscore the importance of this region in contacting both gp120 and the B2.1 peptide. Mutation of any of Arg 29, Ser 30, Arg 31, or Arg 32 of CDR L1 of b12 almost completely abrogates binding to $gp120_{IIIB}$, $gp120_{JR\text{-}FL}$, and the B2.1 peptide alike (357). In addition, alanine substitution of Asp 279 in $gp120_{JR\text{-}CSF}$ (284), $gp120_{JRFL}$ or $gp120_{IIIB}$ (233) abrogates b12 binding.

Effects of mutagenesis of the gp120 D loop and corresponding B2.1 residues are summarized in Figure 6. As previously described, Asp P9 of B2.1 and Asp 279 of gp120 are both critical for binding b12 and align in sequence and in structure. The extent of mimicry is less clear for other homologous pairs, as several residues align only in linear sequence, but not in structure, and/or are part of glycosylation motifs unique to gp120. For example, Arg P3 of B2.1 and Arg 273 of gp120 align in linear sequence and are both important for b12 binding. However, neither residue appears to contact the b12 paratope directly (Figure 3). Ile P15 and Ile 285 align in linear sequence but not in the structures, and Ile P15 does not contact b12. In contrast, Phe7 contacts b12 and aligns with Phe 277. In addition, although Asn P12 and Asn 276 do not align in linear sequence, they do align in structure. Asn 276 is part of a glycosylation motif in gp120, whereas Asn P12 appears

unimportant for b12 binding. As a fifth example, Ser P8 of B2.1 and Thr 278 of gp120 align in the linear sequence and roughly align in the structures. However, Ala substitution of Ser P8 abrogates b12 binding, whereas Ala substitution of Thr 278 increases b12 binding. However, note that the T278A mutation ablates a NXT glycosylation motif, and loss of this glycan may increase b12 affinity by exposing more of the D loop or surrounding regions to b12 binding. Thus, of the homologous residues, only Phe P7 and Asp P9 remain as a clear potential mimics of critical binding residues Phe 277 and Asp 279 on the D loop.

Construction of phage-displayed peptide/D loop chimeras

To further test the mimicry hypothesis experimentally, we designed a phage-displayed peptide library, using the sequence from a previously-identified, monomeric b12-binding peptide as template, together with the incorporation of partially-randomized residues from the gp120 D-loop. Our reasoning was that if there is a shared binding mechanism, the addition of D-loop residues into the peptide sequence should increase its affinity for b12, and thus favor the selection of new, optimized clones.

As the B2.1 peptide homodimer requires maintenance of the C-terminal disulfide bridge for binding to b12 (352), we used the monomeric cyclic peptide, B1.2 (352) for the library template. Clones B2.1 and B1.2 were both selected by b12 IgG from phage-displayed peptide libraries that share the $SDLX_3CI$ motif. In both peptides, two sequential hydrophobic residues were selected by b12 to precede the SDL motif (Table 3a). Clone B1.2 and all of its sibling cyclic clones bind IgG b12 but not Fab b12, indicating an affinity lower than that of B2.1 (352). The resulting library, comprising 3×10^7

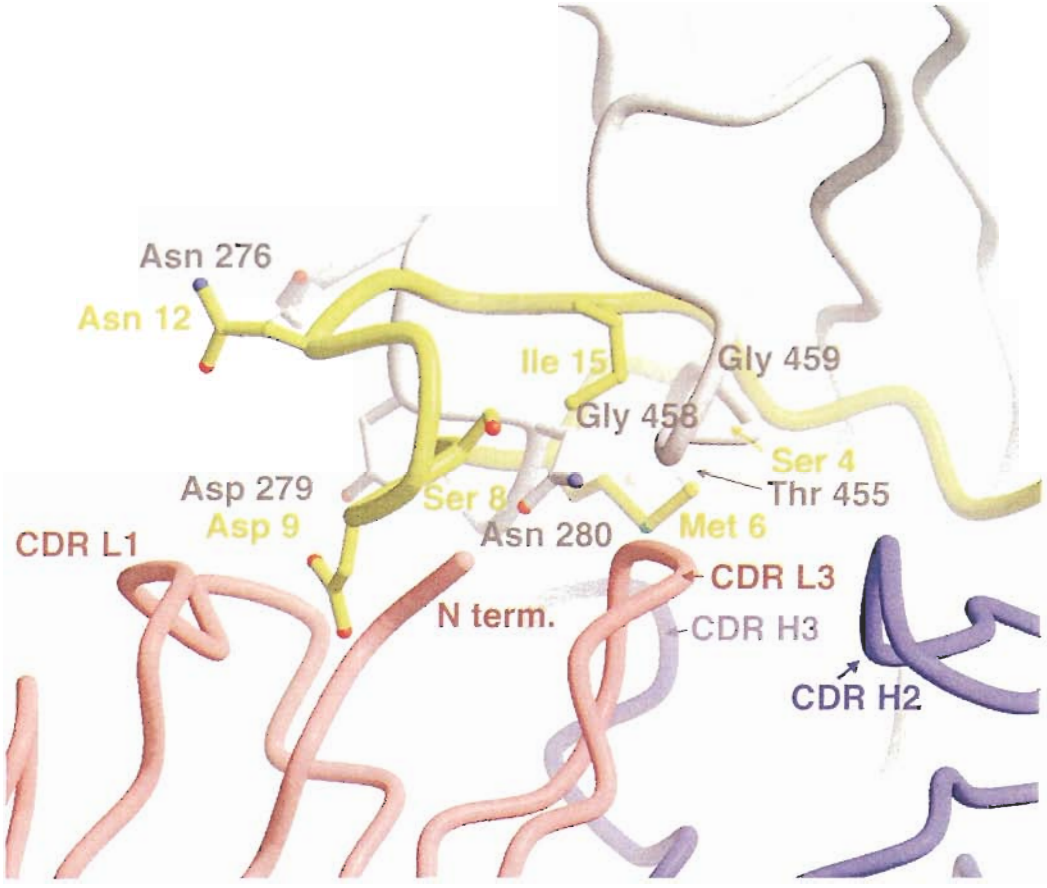

Figure 5. Alignment of b12-B2.1 crystal structure with b12-gp120 docked model. The B2.1 peptide is illustrated in yellow, gp120 in grey, the b12 antibody light chain in pink and the heavy chain in blue. Although the structural scaffolding of contact residues presented by B2.1 and by gp120 are very different, the chemical nature of certain atomic contacts is similar (for example, Asp P9 and Asp 279). The pairs of Asn P12 and Asn 276, Ser P4 and Thr 455, and the side chain terminal oxygens of Ser P8 and Asn 280 also roughly align, but the individual importance of each of these contacts to b12 binding is unclear as Asn 276 is glycosylated in gp120 and the position of other atoms may shift somewhat between a docked model and an actual b12-gp120 complex.

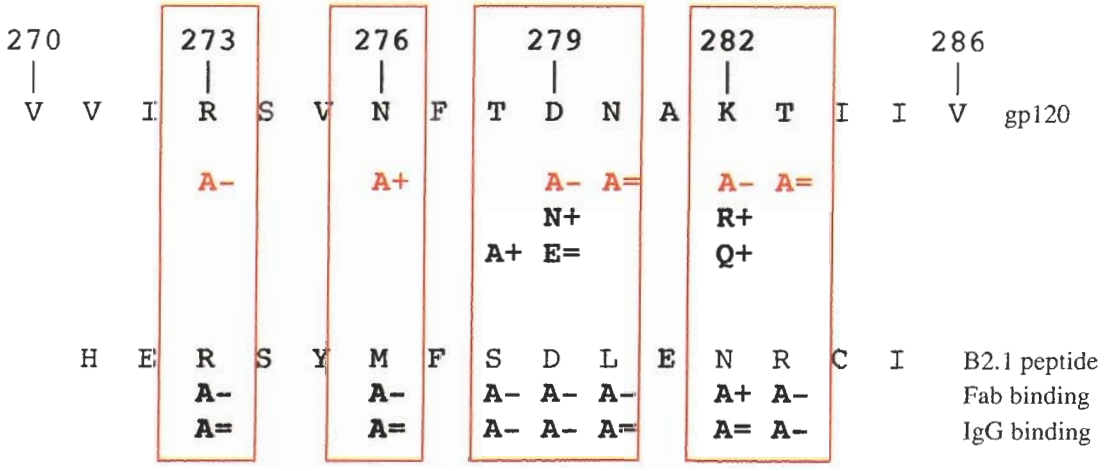

Figure 6. b12 binding to gp120 and B2.1 phage mutants. The gp120 mutations in red letters, shown under the sequence of HXB2 gp120, are described elsewhere (231). Binding of IgG and Fab b12 to mutant B2.1 phage, relative to the B2.1 wild type, is indicated under the sequence of B2.1 peptide. Mutants represented in black letters were generated in this study. (+) indicates increase, (-) decrease and (=) no effect on binding .

independent clones, includes peptides bearing linear and constrained versions of original and variant sequences of the D loop and the B1.2.

Table 3b shows the deduced amino acid sequence of the phage-borne peptides selected from the B1.2/D loop library with b12 IgG and their relative binding to b12 IgG. Only one clone, termed C1, showed detectable binding to b12 IgG in ELISA. The C1 amino acid sequence includes three substitutions encoded by the library design, although none of them are related to the D loop. The most striking feature of C1 is that the C-terminal Cys is shifted three residues toward the C terminal end thereby increasing the Cys-constrained loop length from 8 to 10 residues. Although C1 phage binds Fab b12 more strongly than does B1.2 by titration ELISA, C1 phage does not bind Fab b12 as well as B2.1 phage. Hence, the amino acid substitutions and/or extension of the loop in clone B1.2 improve binding, but not to the level of B2.1. Not a single clone was selected that had increased sequence homology to the D-loop, suggesting that the incorporation of residues from the D-loop will not improve binding to b12. Moreover, in a separate experiment, b12 did not bind a cyclic D-loop sequence that was fused to the pVIII molecule (data not shown). Thus, it appears that binding to peptides bearing the SDL consensus sequence cannot be improved by becoming more like the D-loop.

Comparison of the b12 Antibody with Antisera Against the B2.1 Peptide

The B2.1 peptide is a specific marker for b12 (352). Thus, it is of interest to determine whether immunizations with B2.1 would elicit a b12-like antibody response. BALB/c mice were immunized with synthetic B2.1 peptide conjugated to OVA at a ratio of ~10 peptide molecules per OVA molecule (data not shown). Sera on day 140 (after

Table 3. (A) Amino acid sequence of peptides B1.2 and B2.1, and the HXB2 gp120 D-loop (env 273-285). (B) Deduced amino acid sequence and b12 IgG reactivity of clones selected from the B1.2/D-loop mixed library.

A.

Sequence name	Amino acid sequence[1]
MZB1.2	GCL**YSDL**LA**T**C**I**AAE
MMB1.2	SGGCL**YSDL**LA**T**C**I**GSAAE
HXB2 gp120 D-loop	**RS**VN**FTD**NAK**TII**
B2.1	HE**RS**YM**FSDL**ENRC**I**AAE
B1.2/D-loop library design[2]	SGxxxxxDxxxTxIGSAAE GCLYS LLA C SVNFT NAK I AFH HPE F CGQ QVT L M M S I I K K

(1) Similar or identical residues between peptides and gp120 are in bold.
(2) The design of the B1.2/D-loop mixed library is shown. Positions coding for more than one residue are represented by X; the amino acids coded in each position are listed below; residues fixed in the library are underlined.

B.

Clones	Sequence	b12 IgG ELISA[3]
B2.1	HERSYMFSDLENRCI	1.16
MZ B1.2	GCLYSDLLATCI	0.18
MMB1.2	SGGCLYSDLLATCIGS	0.10
C1	SG**A**CLYSDL**AATFIC**S	1.26
20-2	SG**A**CLYSD**H**LATCIGS	0.12
20-3	SG**S**CLYSD**H**LATCIGS	0.10
20-4	SG**S**CL**F**SD**M**LATCIGS	0.02
20-5	SGGCLYSD**HA**ATCIGS	0.02
4-3	SG**AG**LYSDL**GKTF**IGS	0.01
0.8-3	SGG**FHFTD**K**PTTI**IGS	0.01
0.8-3	SG**SFIFPTSVATF**IGS	0.01
f88-4	n.a.	0.02

(3) Values are $OD_{405-490}$.

seven immunizations) react strongly with B2.1 peptide (Table 4), with an average half-maximal titer of 73,000, indicating that B2.1 is immunogenic in this context. However, these sera react poorly with HIV-1 gp120 $_{Ba\text{-}L}$, even at the low dilutions tested (1:50) (Table 4). Immunization with B2.1-expressed on the surface of phage or with B2.1 synthetically conjugated to phage also produce a range of anti-peptide and anti-phage titers in BALB/c mice, but fail to elicit gp120 reactivity (Table 4). Similar results were obtained with C57BL/6 mice (data not shown). One mouse, immunized with B2.1-expressing phage, produced a titer of ~13,000 against the B2.1 peptide, yet failed to produce significant gp120 reactivity (data not shown). Mice immunized with the B2.1-f1.K conjugate produced somewhat higher anti-B.1 peptide titers than mice immunized with B2.1-expressing phage, probably because of the increased B2.1 copy number (~1200 copies per B2.1-f1.K phage compared to ~200 copies per B2.1 phage). Taken together, these results demonstrate that the B2.1 peptide does not elicit antibodies that are functionally similar to b12, indicating that it is not an immunogen mimic in mice.

A comparison of the anti-B2.1 sera with b12 for binding to the panel of B2.1 Ala-mutant phage (Fig 2B) also supports this interpretation. Whereas the contact residue Phe P7 seems to be important for binding to both b12 and the mouse antibodies, remarkable differences were observed for the structural critical binding residues Tyr P5 and Cys P14. Substitution of these two residues ablates binding to b12, but does not affect significantly the reactivity with the anti-B2.1 peptide mouse sera, indicating that most antibodies elicited by the B2.1/OVA conjugate in mice are different from b12.

Table 4. Anti-gp120 and anti-B2.1 antibody response in mice immunized with synthetic B2.1 peptide conjugated to OVA (OVA-B2.1), peptide fused to f1.K phage (f1.K-B2.1), or B2.1 recombinant phage (B2.1 phage).

			vs. gp120		*vs.* OVA	
Immunogen	anti-B2.1 peptide	*vs.* BSA	in BSA	in NFDM	in BSA	in NFDM
OVA-B2.1	**73510** ***(13022)***	**0.08** ***(0.02)***	**0.18** ***(0.06)***	**0.06** ***(0.00)***	**nd**	**nd**
OVA	0	0.08 *(0.02)*	0.16 *(0.04)*	0.05 *(0.00)*	nd	nd
f1K-B2.1	**106298** ***(34564)***	**0.05** ***(0.01)***	**0.14** ***(0.03)***	**0.10** ***(0.02)***	**0.23** ***(0.07)***	**0.17** ***(0.09)***
f1K	0	0.03 *(0.00)*	0.11 *(0.03)*	0.11 *(0.03)*	0.05 *(0.00)*	0.02 *(0.00)*
f1K-B2.1-Adj	**112935** ***(33812)***	**0.09** ***(0.03)***	**0.20** ***(0.02)***	**0.12** ***(0.01)***	**0.48** ***(0.17)***	**0.36** ***(0.19)***
f1K-Adj	0	0.08 *(0.02)*	0.16 *(0.05)*	0.11 *(0.00)*	0.13 *(0.03)*	0.04 *(0.03)*
B2.1 phage	**4682** ***(2294)***	**0.17** ***(0.02)***	**0.17** ***(0.02)***	**nd**[(i)]	**nd**	**nd**

Sera diluted, 1/50, in TBS/Tween buffer containing 1% w/v BSA or 5% non-fat dried milk (NFDM), and tested for binding to gp120 or ovalbumin (OVA)) as a measure of non-specific binding. Values are expressed as $O.D._{405\text{-}490}$, with standard errors in parentheses. All immunogens were administered in 10 μg doses, with the exception of recombinant B2.1 phage for which 100 μg was administered.

Affinity of B2.1 peptide and B2.1-MBP fusion protein

In previous work, we reported qualitative observations that B2.1 bound more tightly to Fab b12 in ELISAs when adsorbed onto plastic or fused to maltose binding protein (MBP) than as the free synthetic peptide captured by biotin-streptavidin interactions (352). We also reported an in-solution affinity of the free synthetic peptide for b12 measured by KinExa (Kd = 2.5 μM). Here, we report that the affinity of B2.1 for b12 as measured by surface plasmon resonance (SPR) is similar to that determined by KinExA: Kd = 5.0 μM (352) and kd = 6.9 μM for the binding-inhibition and steady-state models, respectively (Table 5). Here, we also report experimental measurement of the improved affinity of B2.1-MBP over free B2.1: Kd = 60 nM, and Kd = 20 nM as determined by KinExa and SPR, respectively (Table 5). We also report here that the affinity of synthetic B2.1peptide immobilized on a Biacore CM5 chip is 160 nM, over an order of magnitude stronger than that of the free peptide in solution (as measured by KinExA). It is possible that some of the observed increase in the binding affinity resulted from Fab re-binding, a phenomenon known to artificially slow down off-rates during the measurement of binding constants in solid phase SPR experiments (225). Nevertheless, taken together, the results confirm that the mode of presentation of B2.1 to b12 significantly influences the affinity of their interaction, and that tethering one terminus to a protein or artificial substrate improves its antigenic structure.

Table 5. Binding constants (Kd) obtained for B2.1 synthetic peptide and B2.1/MBP fusion protein by kinetics exclusion assay (KinExA) and surface plasmon resonance (SPR).

Reactants[(a)]	Method[(b)]	Sequence	Kd (M)
B2.1 peptide- IgG b12[(c)]	KinExA, Equil/soln	NH_3-HERSYMFSDLENRCIAAE-Orn(biotin)-KK-NH_2	2.5×10^{-6}
B2.1 peptide- Fab b12	SPR, Equil/soln	NH_3-HERSYMFSDLENRCIAAE-Orn(biotin)-KK-NH_2	5.0×10^{-6}
Fab b12-B2.1 peptide	SPR, Steady-state	NH_3-HERSYMFSDLENRCIAAE-Orn(biotin)-KK-NH_2	6.9×10^{-6}
B2.1 peptide- Fab b12	SPR, Kinetics	NH_3-HERSYMFSDLENRCIAAE-Orn(biotin)-KK-NH_2	1.6×10^{-7}
IgG b12-B2.1/MBP	KinExA, Equil/soln	HERSYMFSDLENRCIAAEE-MBP	6.0×10^{-8}
IgG b12-B2.1/MBP	SPR, Kinetics	HERSYMFSDLENRCIAAEE-MBP	2.0×10^{-8}

(a) For the kinetic and the steady-state methods in the Biacore (SPR), the first of the reactants in each pair listed is the one immobilized on the chip, the second is the in-solution analyte.

(b) Method: In SPR, soluble analyte is flowed over immobilized ligand. In kinetics analysis by SPR, association and dissociation rates are determined and Kd at equilibrium is calculated. In steady-state analysis by SPR, the Kd is measured at equilibrium. The Equil/soln method (Equilibrium solution, described for both KinExA and SPR) determines concentration of free antibody at equilibrium using several concentrations of in-solution peptide. For Equil/soln, on and off rates are not obtained.

(c) Results from Zwick *et al.* (353).

DISCUSSION

There is a common assumption about the connection between structural mimicry and immunogenic mimicry, which holds that the closer an immunogen comes to having the structure of a given epitope, the greater the likelihood that it will be able to elicit antibodies against that epitope. A second assumption is that if a ligand binds an antibody paratope where cognate epitope does, and with similar affinity to the cognate epitope, the ligand will very likely mimic the contacts made by that epitope. The structure presented here is the first example of a peptide bound to an antibody against a discontinuous protein epitope. It is of importance because the epitopes recognized by most anti-protein antibodies are discontinuous. We have characterized the mechanism of peptide binding to b12, and have compared that mechanism to what we can deduce about the mechanism by which b12 binds to gp120, based on a docked model and extensive mutagenesis of b12 and gp120. Our hypothesis was that B2.1 mimics the D loop of gp120, in making identical contacts with b12 to those made by the D loop. The peptide occupies only about half of the cognate paratope, and, although a crystal structure of the b12 Fab-gp120 complex is not available for direct comparison, we have shown that the peptide occupies a site of the paratope that binds a limited region (the D loop) of the cognate protein antigen (gp120). Yet on closer inspection, the mechanism of binding at this site (defined by the residues critical for binding of the peptide or the D loop to Fab) appears to differ for the peptide and the cognate antigen, gp120. While the Ala substitution of many of the D loop residues indicates that Asp279 is perhaps the only critical binding residue there (there are no data for Phe 277), there are three critical contact residues in the B2.1 peptide

(Phe7 and Asp9, with Ser8 acting through a bound water). The overlap between critical binding residues in the D loop and the B2.1 peptide indicates that there may be some shared mechanism of binding by critical contact residues, particularly in their shared Asp, and perhaps, Phe. The results of Ala substitution studies on the b12 Fab, particularly in the light-chain CDR-L1 residues, Arg 29, Arg 31, and Arg 32, lend indirect support for this notion; however, it also appears that the Ala-substitution of residues in b12, which do not even contact B2.1, can affect binding of b12 to both peptide and gp120 (357). Thus, even given the limited nature of the mimicry of the D loop by B2.1, there may be a more global, shared mechanism of binding that is not easily defined.

So far there is only one previous study testing the hypothesis that a peptide can mimic the gross structure and contacts with antibody made by a cognate eptiope, and it involves a peptide mimic of a carbohydrate epitope (330). Side-by-side structures of the peptide and oligosaccharide bound to an anti-carbohydrate Fab showed that both bind in the same gross region, but by different structural mechanism in terms of the contacts that the Fab makes with each antigen. Interestingly, the intrinsic affinities of each antigen for Fab differed by only two-fold. Thus, in both cases, it appears that antibodies select peptides to fit their cognate paratope, or part of it, but may accomplish binding through different, and partially overlapping, contacts for peptide and cognate epitope. This may have important consequences for the use of peptides as immunogenic mimics of a cognate epitope.

A recent study (86) describes the identification of phage displaying b12-binding peptides (in low copy number *via* pIII). The peptides have a binding motif (V(W/F)SD) similar to the one we previously described, and shared by B2.1 (352). While no affinity

studies were performed on the peptides, immunization of mice with whole phage elicited low gp120 binding titers that lacked HIV-1-neutralizing activity (the anti-peptide antibody response was not measured). This is in contrast to the results of the immunizations reported here, which repeatedly produced strong anti-peptide titers, yet no appreciable gp120 reactivity. Moreover, the critical binding residues in B2.1 that are recognized by the highest-titer anti-peptide sera are quite different from those recognized by the b12 antibody (Fig. 2). Perhaps the difference in the gp120 reactivity of anti-peptide antibodies in the two studies is due to sequence differences among the peptides. The work of Dorgham *et al.* (86) is important in suggesting that b12-binding peptides elicit gp120 cross-reactivity. However, to definitively prove that these serum antibodies specifically bind the b12 epitope on gp120, it should be clearly demonstrated that b12 blocks serum cross-reactivity with gp120.

There are several other possible explanations for the failure of B2.1 to act as an immunogenic mimic for the b12 epitope on gp120. First, it is possible that the higher-affinity B2.1-MBP fusion proteins would elicit b12-like reactivity with gp120 (in contrast to the lower affinity B2.1-OVA or phage conjugates). This seems unlikely since recombinant phage displaying B2.1 elicited significant titers against B2.1, but no cross-reactivity with gp120. Second, perhaps BALB/c mice cannot produce b12-like antibodies, since murine antibodies, in general, do not have long CDR-H3 loops ion contrast to many human antibodies, including b12. To address this, we plan to immunize transgenic mice that produce human antibodies, including those having long CDR-H3s (124) with recombinant B2.1. Third, it may be that b12 is such an unusual antibody that it cannot be produced after a few rounds of immunization; it has 28 mutations and an 18-

residue CDR-H3 (13) and the reversion of several residues to germline sequence affect gp120 binding (357). We have screened the sera of a number of HIV-infected people from whom samples have been collected over time, and who followed different clinical courses, and we have yet to observe specific binding to the B2.1 peptide. This indicates that B2.1 may be "too specific" to b12, and/or that b12-like antibodies are rarely produced in natural infection (unpublished data, C. Wang, X. Wang, and J.K.S.).

More success has been seen with an engineered version of gp120 that selectively binds to b12. Importantly, this gp120 variant does not bind well to CD4, and thus, is very different from native gp120 at this site. Our studies showed that the binding of HIV+ serum antibodies to this gp120 could, in part, be blocked by the b12 Fab, indicating the possibility of other, b12-like antibodies in the sera of HIV-infected people (unpublished data, ibid). Such antibodies could be affinity purified on the engineered gp120, and further tested for their ability to compete with b12 and to neutralize HIV-1. Since the serum samples tested were taken during the first year after initial infection, neutralizing antibodies obtained from them should have fewer somatic mutations. The identification of antibodies capable of neutralizing even a limited range of primary HIV-1 isolates may be of value to HIV-1 vaccine design.

Peptide ligands, such as B2.1, which are specific for antibodies against discontinuous epitopes may play an important role in the development of epitope-targeted vaccines *via* prime-boost immunizations (322). In this scenario, a priming immunization with cognate antigen (in this case, gp120 or a particle bearing gp120) would elicit a polyclonal B cell response, with only a small fraction of those cells producing the desired antibody. A second boosting immunization, this time with the antibody-specific peptide,

would serve to selectively enhance the production of the targeted antibody. To be successful, a prime-boost immunization strategy such as this must fulfill two criteria: *(i)* a common T cell epitope must be present and functional in both the prime and the boost to drive B cell proliferation and differentiation, and *(ii)* the priming immunization must activate B cells that produce the targeted antibody, so that these clones can be selectively re-stimulated in the boost. Both these criteria are achievable goals. In fact a successful prime-boost immunization using a peptide mimic of a carbohydrate epitope has been recently reported by Beenhouwer *et al.* (19). Thus, an antibody-targeting ligand may not have to mimic the binding mechanism of a cognate epitope *per se* to selectively enhance the production of a targeted antibody. Several laboratories are pursuing such prime-boost strategies in one form or another (*e.g.*, (19, 228, 352) The development such highly-targeted immunization strategies could be of great significance to HIV-1 vaccine research.

ACKNOWLEDGEMENTS

We thank the staff of SSRL Beamline 11-1, and M. Irving, O. Pan and B. Vanderkist for excellent technical assistance. We thank Tim Fouts (Institute of Human Virology, Baltimore, MD) for providing HIV-1 Ba-L gp120. We gratefully acknowledge NIH grants GM46192 to IAW, AI33292 to DRB, AI49808 to JKS, and AI40377 to PWHIP, the Universitywide AIDS Research Program (EOS), a Career Award in the Biomedical Sciences from the Burroughs Wellcome Fund (EOS), the Elizabeth Glaser Pediatric AIDS Foundation (MBZ), The Michael Smith Foundation for Health Research

(MM and AM) and the Natural Sciences and Engineering Research Council of Canada (MM and AM), The Skaggs Institute for Chemical Biology (IAW and EOS), and The International AIDS Vaccine Initiative (IAW and DRB) for support. This is publication No. 15160-MB from The Scripps Research Institute.

APPENDIX.

Surface Plasmon Resonance and affinity determination.

The interaction of macromolecules can be followed in real time using biosensors that exploit the optical phenomenon of surface plasmon resonance (SPR). SPR is a simple and direct sensing technique that probes refractive index in the very close vicinity of a thin metal film surface. For example, the accumulation of molecules in an aqueous layer close to a metal surface causes changes in the refractive index that can be observed as a shift in the properties of the detectable SPR.

The biosensor system developed by Biacore AB (Uppsala, Sweden) uses a miniaturized sensor chip composed of a glass surface with a thin gold layer, which creates the physical conditions required for SPR, and coated with an active surface (*e. g.* dextran), to which ligand molecules can be immobilized. The immobilized molecule is exposed to a flow chamber through which an analyte solution is injected at a controlled flow rate. Binding of the analyte to the ligand increases the mass whereas dissociation decreases it, these changes are detected as arbitrary resonance units (RU) that are plotted against time, creating a sensorgram (for details see www.biacore.com). In the Biacore, the association and dissociation of the analyte and the ligand can be observed in real time.

Typically, a Biacore kinetic experiment involves the independent injection of several concentrations of analyte over an immobilized ligand. The association and dissociation of the analyte are recorded as a set of sensorgrams, from which association (*ka*) and dissociation (*kd*) rates can be derived by fitting the data to any of several affinity models described (23). From these rates, the constants at equilibrium (Ka and Kd) can be calculated. Several basic experimental conditions must be meet for the kinetic data to be accurate: (*i*) the range of analyte concentrations tested should include the Kd value of the interaction, (*ii*) the density of immobilized ligand should be kept at a minimum that gives a detectable response and (*iii*) the flow rate of injection should be as high as practically possible (22). A low density of immobilized ligand and a high flow rate are required to avoid limitation of analyte mass-transfer from the buffer to the solid phase, allowing the interaction rates to be driven by the affinity. Another important experimental consideration is the valency of the analyte; (for example IgGs have two antigen-binding sites), and the avidity caused by this bivalency would artificially increase the affinity of the interaction. Thus, IgGs should not be used as analytes in kinetic assays. Even though the IgG bivalency problem can theoretically be resolved by the use of a monovalent analyte (like a Fab), other factors have to be taken into account before choosing Ab as analytes in kinetic experiments.

Immobilization of antigens in a Biacore chip, followed by injection of an Ab analyte may produce experimental artifacts, and thus artificial Kds. Two main problems inherent to this set up are the potential heterogeneity of the immobilized ligand (as a result of the immobilization procedure), which may lead to a mixture of binding/dissociation constants (for a good description of surface-associated artifacts see

(227)); and analyte re-binding effects that occur during the dissociation phase, even with monovalent analytes (225). One way to minimize these problems is by using the Ab instead as the immobilized ligand.

Methods for the determination of real Kds "in-solution" have been developed, which essentially rely on the measurement of free analyte concentration in a reaction in solution with ligand at equilibrium, under conditions of mass-transfer limitation (59, 225, 266). When the transfer of the analyte from the unbound, in-solution state to the bound, solid phase state is limited, the association rate is driven by the free analyte concentration and not by the affinity of the interaction. The experimental conditions for such assays are therefore opposite to those for kinetic assays; *i.e.* the ligand is immobilized on the chip at the highest possible density, and the injection flow rate is the lowest possible. Binding data are collected early in the association phase, when mass-transfer limitation is at the highest. Since the dissociation phase is not considered in this method, re-binding of the analyte does not affect the data significantly. The disadvantage of the in-solution inhibition method with respect to the kinetic one is that it only provides Kd at equilibrium, and not ka or kd rate constants.

In keeping with these considerations, we have detected differences between the in-solution inhibition and kinetic methods, similar to the results described by Nieba *et al.* (225). Three examples of Kd heterogeneity are provided in Table 6: one with a b12 Fab and B2.1 peptide pair (see Chapters 2 and 3), a second example involving gp160 and 2F5 IgG, and a third one with E4.6 peptide and 2F5 IgG.

Table 6. Binding constants obtained by surface plasmon resonance may be strongly influenced by the experimental set up.

Exp #	Ligand[a]	Analyte[b]	Method[c]	$\mathcal{K}a$ (1/Ms)	$\mathcal{K}d$ (1/s)	Kd[d]
1	B2.1 peptide	b12 Fab	Kinetics	3.9 e4	6.1 e-3	160 nM
2	B2.1 peptide	b12 Fab	Equil/Sln			5.0 μM
3	b12 Fab	B2.1 peptide	Steady			6.9 μM
4	B12 IgG-B2.1 peptide		KinExA			2.5 μM
5	$gp160_{IIIB}$	2F5 IgG	Kinetics	1.1 e5	2.1 e-7	1.8 pM
6	$gp160_{IIIB}$	2F5 IgG	Equil/Sln			720 nM
7	E4.6 peptide	2F5 IgG	Kinetics	2.6 e6	1.9 e-3	710 pM
8	E4.6 peptide	2F5 IgG	Equil/Sln			0.95 μM
9	E4.6 peptide	2F5 IgG	Equil/Sln			0.84 μM
10	E4.6 peptide	2F5 IgG	Equil/Sln			1.10 μM

a. Ligand refers to the reactant immobilized on the chip in the kinetic experiment.
b. Analyte refers to the reactant in-solution, which is injected on the chip in the kinetic experiment.
c. Method refers to the procedure used for the experiment or analysis; Kinetics involves the flowing of analyte over the immobilized ligand and calculation of association ($\mathcal{K}a$) and dissociation ($\mathcal{K}d$) rate constants, in this instance the constants at equilibrium are calculated from the rate values. Equil/Sln is based on the determination of free antibody in a set of reactions at equilibrium in solution, for which a fixed antibody concentration is reacted with a several concentrations of peptide/protein inhibitor; in this type of experiment only the association and dissociation constants are obtained. Steady refers to data obtained using the steady-state affinity model on a kinetic-like experimental set up. KinExA is an independent method that does not rely on SPR (see text). For specific details in experiments 1 and 2 see Chapter 3, for experiment 4 see Chapter 2, for experiments 5 to 10 see Chapter 5.
d. Kd: dissociation constant at equilibrium.

B2.1 peptide-b12 Fab: Kinetic assays with immobilized peptide and Fab analyte (Exp # 1 in Table 6) produced higher affinity (Kd = 160 nM) than that observed by the in-solution inhibition method (Exp # 2, Kd = 5 μM), the steady-state method with Fab ligand and peptide analyte (Exp #3, Kd = 6.9 μM), and also by KinExA (Exp #4, Kd = 2.5 μM, see Chapter 2). The similarity of Kds obtained with the in-solution inhibition, the steady-state method, and KinExA (see below) suggests that the real Kd for the B2.1-b12 interaction is ~ 5 μM and that the lower Kd observed with the kinetic method is an experimental artifact, likely due to Fab re-binding as described by Nieba *et al.* (225). It should be noted that the analysis at steady-state (Exp # 3) was performed with data generated by the same experimental conditions as the kinetic method, except that the immobilized ligand was the b12 Fab and the analyte in-solution was the B2.1 peptide, a situation reversed from Exp #1. Since the affinity of this interaction is low, typical association and dissociation curves were not observed in Exp # 3, preventing the generation of kinetic data.

The KinExA instrument differs from Biacore in that it is not based on SPR. The instrument is a flow spectrofluorimeter on which free Ab from a reaction at equilibrium is captured with an antigen-coated bead pack, and quantified with a second fluorescently-labeled antibody (27). Data generated by Biacore and KinExA are comparable, as has been reported by Drake *et al.* (87) for several antigen-antibody pairs with Kds ranging from nM to pM. In addition to the b12 Fab-B2.1 peptide pair, we have also observed good agreement between rate constants determined by both KinExA and Biacore for 2G12-2G12-binding peptides (see Chapter 5).

gp160-2F5 IgG: An artificial, very high affinity was observed for this interaction if gp160 was used as immobilized ligand, and 2F5 IgG as analyte (Exp #5, see also Chapter 4). This high affinity was based on the lack of dissociation of 2F5 IgG from gp160 over a time period of 15 minutes. However, in-solution inhibition assays (Exp #6) produced a Kd that was five orders of magnitude higher. It should be noted that recombinant gp160 preparations are usually multimeric (and therefore multivalent) to some extent, which may contribute to aberrant data, even with the in-solution method. Also, it is not clear whether there are significant differences in the antigenicity of multimeric and monomeric gp160 for 2F5.

E4.6 peptide-2F5 IgG: This example shows the same trend as the B2.1 peptide-b12 Fab pair, with even more marked differences between the two methods, since bivalent IgG was used (compare Exp #7 *vs.* 8,9 and 10 and see Chapter 4).

We have therefore, favored the use of the "in-solution" inhibition method in most instances (see also Chapters 4 and 5). Our results confirm the validity of those by Nieba *et al.* (225), and add a cautionary note to the determination of Kd by simple derivation from kinetic data.

CHAPTER 4

Human Immunodeficiency Virus type 1-Neutralizing Monoclonal Antibody 2F5 is Multispecific for Sequences Flanking the DKW Core Epitope.

Alfredo Menendez, Keith C. Chow, Oscar C. C. Pan and Jamie K. Scott

Department of Molecular Biology and Biochemistry, Simon Fraser University, Burnaby, BC, Canada

Corresponding Author:
Jamie K. Scott
Department of Molecular Biology and Biochemistry
Simon Fraser University
8888 University Drive
Burnaby, BC,
Canada V5A 1S6

E-mail: jkscott@sfu.ca
Tel: (604) 291-5658
Fax: (604) 291-5583

Running title: Multispecificity of HIV-1-neutralizing antibody 2F5.

Keywords: Mab 2F5, HIV-1, phage-displayed peptide libraries, epitope, neutralizing antibody,

This work has been published in ***The Journal of Molecular Biology 338: 311-327, 2004*** and is reproduced here with permission.

SUMMARY

2F5 is one of a few human antibodies that neutralize a broad range of HIV-1 primary isolates. The 2F5 epitope on gp41 includes the sequence ELDKWA, with the core residues, DKW, being critical for antibody binding. HIV-neutralizing antibodies have never been elicited by immunization with peptides bearing ELDKWA, suggesting that important part(s) of the 2F5 paratope remain unidentified. The use of longer peptides extending beyond ELDKWA has resulted in increased epitope antigenicity, but neutralizing antibodies have not been generated.

We sought to develop peptides that bind to 2F5, and that function as specific probes of the 2F5 paratope. Thus, we used 2F5 to screen a set of phage-displayed, random peptide libraries. Tight-binding clones from the random peptide libraries displayed sequence variability in the regions flanking the DKW motif. To further reveal flanking regions involved in 2F5 binding, two semi-defined libraries were constructed having twelve variegated residues either N-terminal or C-terminal to the DKW core (X_{12}-AADKW and AADKW-X_{12}, respectively). Three clones isolated from the AADKW-X_{12} library had similar high affinities, despite a lack of sequence homology among them, or with gp41. The contribution of each residue of these clones to 2F5 binding was evaluated by Ala-substitution and amino-acid-deletion studies, and revealed that each clone bound 2F5 by a different mechanism. These results suggest that the 2F5 paratope is formed by at least two functionally distinct regions: one that displays specificity for the DKW core epitope, and another that is multispecific for sequences C-terminal to the core epitope. The implications of this second, multispecific region of the 2F5 paratope for its unique biological function are discussed.

INTRODUCTION

Human monoclonal antibody (MAb) 2F5 is one of the few HIV-1-broadly neutralizing antibodies identified so far (71, 315). Passive transfer of 2F5, in combination with other neutralizing human MAbs, has conferred sterilizing protection to viral challenge in several animal models (140, 196, 201). 2F5 binds with high affinity to a conserved site on the extracellular region of the transmembrane protein gp41 (residues 662-667, amino acid sequence ELDKWA) (64). Results from screening of phage-displayed peptide libraries and from 2F5 IgG binding studies to substituted synthetic peptides have shown that the tri-peptide DKW is required for binding, and thus constitutes the core of the epitope (64, 261). The crystal structure of 2F5 in complex with the short synthetic, peptide ELDKWA, revealed a type I β-turn formed by the residues DKW. It also showed that extensive regions of the putative antigen-binding site on the antibody, more specifically the apex of the long H3, did not contact the peptide, indicating sites of potential interaction with other parts of the envelope spike and/or lipid on the surface of the virus (231).

Direct binding of 2F5 to viral particles and infected cells has been observed by Sattentau *et al.* (287) and Zwick *et al.* (356), suggesting that the epitope is expressed and accessible on the pre-fusogenic viral envelope. However, other studies indicate that the 2F5 neutralization-sensitive epitope is exposed or formed only after the virus has contacted the cellular receptors, and triggered the cascade of events leading to fusion of the cellular viral membranes (24, 121). This contradiction can be explained by the work of Poignard *et al.* (253), which indicates that the viral envelope spikes exist in both

infectious and non-infectious forms; very probably 2F5 binds to both forms. Thus, the unique neutralizing properties of 2F5 reside in its specificity for a cryptic site on the infectious spike that is probably exposed during infection.

The potency and breadth of 2F5's neutralizing capacity suggest an important biological role for the membrane-proximal ectodomain of gp41, making it an attractive candidate for vaccine purposes. However, multiple efforts to elicit antibodies with the specificity and neutralizing activity of 2F5 by immunization with different forms of the ELDKWA fragment have repeatedly failed (63, 92, 102, 186). Several studies have tested the antigenicity and immunogenicity of larger peptide epitopes based on the gp41 sequence, as well as peptides having novel structural constraints that optimize antigenicity (15, 163, 203, 311). However, even with these improvements, the antibodies generated bind to synthetic peptides and/or to recombinant envelope, but do not neutralize primary HIV-1 isolates (163, 203). These disappointing results suggest that the ELDKWA fragment and extensions of it do not represent the entire 2F5 epitope, or that the neutralizing epitope, if present, is not immunodominant. In addition, it is not clear whether the failure to elicit 2F5-like antibodies results from the presence of an incomplete epitope in the immunogens used so far, and/or because antibodies having the unusual structure of 2F5; (30 somatic mutations and a very long, 22 residue, H3 loop) (173) are difficult to elicit by conventional immunization strategies. Antibodies functionally similar to 2F5 are rarely produced in natural infection (173, 198, 218), even though reactivity against ELDKWA-containing peptides has been consistently observed in the serum of HIV-1-infected subjects (40, 47, 112).

In the work reported here, we screened several primary and semi-defined phage-displayed peptide libraries with MAb 2F5 with the objective of finding peptide antigens with more extensive coverage of the 2F5 paratope than that of gp41-based peptides. We analyzed the sequence requirements of 2F5 by using it to screen a panel of random peptide libraries. Our data led us to postulate that if we reduced binding to the DKW core and extended the randomized regions flanking it, we could produce libraries that would identify unique, nearby regions in the antibody paratope that have the potential to bind protein. We found that the residues flanking the DKW core on the C-terminal side are required for high-affinity binding to 2F5, and that the antibody binds tightly to several unrelated sequences in this region, making the 2F5 paratope multispecific. Thus, our results indicate that the 2F5 paratope comprises two regions: one that is highly selective for the core sequence DKW, and another that binds C-terminal to the core and is multispecific. We discuss how these results pertain to 2F5's unique biological properties, and to epitope-targeted and antibody-targeted vaccine development.

MATERIALS AND METHODS

Materials:

Seventeen "primary" phage libraries displaying fully-randomized peptides (with some libraries containing 1-2 fixed Cys residues) (30) were screened with MAb 2F5 IgG. Semi-defined peptide libraries were constructed using the vector f88-4 (351), according to Bonnycastle *et al.* (32). MAb 2F5 IgG and HIV-1 envelope proteins were obtained from the NIH AIDS Research and Reference Reagent Program and the MRC Centralised

Facility for AIDS Reagents. MAb 2F5 was also donated by H. Katinger (University of Agricultural Sciences, Vienna). 2F5 Fab was kindly donated by M. Zwick and D. Burton (The Scripps Research Institute, La Jolla, CA), it was produced in *E. coli* using a pCOMB-3-based expression system developed by Zwick *et al.* (355). Oligonucleotides were synthesized "in house" using an ABI 392 synthesizer, or by the NAPS Unit at the University of British Columbia, Vancouver, Canada. Peptides E7.3, SCPPES**DRW**SCFAEGK(bio); E8.3, SC**DKW**VPYCAAEGK(bio); E9.6, ARANTC**DKWA**LPCNTGNAEGK(bio); E10.10, ALGTNC**DKWA**CMHYAEGK(bio); E11.6, YCTAPLNA**DKW**SCTAEGK(bio); H2.5, SRK**ELDKWAS**TDC**MQC**QAEGK(bio) and ME2F5, GG**ELDKWA**GGGK(bio) were synthesized using a multi-pin system from Chiron Mimotopes PTY Ltd (Victoria, Australia) and Fmoc chemistry, according to the manufacturer's instructions. Peptide E4.6, LHEESM**DKW**SNLMQCCTAAEGK(bio) was purchased from Multiple Peptide Synthesis (San Diego, CA). Synthetic peptide concentrations were determined by measuring their absorbance at 280 nm, and calculating concentration using an extinction coefficient of 5560 for each Trp residue in the peptide seqeunce. Protein concentrations were determined with the Protein Assay kit from Biorad (Hercules, CA).

HRP-conjugated, goat anti-human Ig G (Fab-specific) and HRP-conjugated Neutravidin were purchased from Pierce (Rockford, IL). A MAb against the maltose-binding protein of *E. coli* (MBP) was from New England Biolabs (Beverly, MA). Dialyzed BSA, dithiothreithol, H_20_2 and ABTS were purchased from Sigma (St. Louis, MO).

Bacterial strains and culture media:

E. coli strain K91 was used for phage production, following the procedures described in Bonnycastle *et al.* (31). NZY Tet/IPTG was routinely used for phage amplification. Electrocompetent *E. coli* strain MC1061 was used to produce mutant phage in site-directed mutagenesis studies, and for the production of peptide libraries (32). *E. coli* strain ER2507, a gift from New England Biolabs, was used for the production of the MBP fusion proteins.

DNA manipulations:

The generation of deletion mutants was performed using linear, single stranded phage DNA as template, following the procedure described in Bonnycastle *et al.* (30). Site-directed mutagenesis for the generation of amino acid substitutions and deletions were made with closed, circular single strand phage DNA as described in Sambrook *et al.* (276). The transfer of peptide coding sequences to the MBP fusion system pMALX and the conditions for culture and purification of the protein have been described by Zwick *et al.* (353). DNA sequencing from partially purified phage clones was performed with the Thermo Sequenase II Dye Terminator Cycle kit (Amersham Biosciences, NJ) following the manufacture's instructions. DNA fragments from the sequencing reactions were resolved using an ABI 373 apparatus and analyzed with EditView 1.0.1 software.

Screening of peptide libraries and characterization of peptides:

The biotinylation of antibodies was performed as described in Menendez *et al.* (205). The seventeen primary phage-displayed peptide libraries were screened "in

solution" with 100 nM 2F5 IgG, according to Menendez *et al.* (205). Phage-antibody complexes were captured out of solution with streptavidin-coated magnetic beads (Dynal, Lake Success, NY). The semi-defined libraries were subjected to three separated screenings with three different, low concentrations of biotinylated 2F5 Fab (0.1, 1 and 10 nM). Starved K91 cells were infected with pools of phage selected after the third rounds of screening, and individual clones were isolated and amplified in 2 ml NZY Tet/IPTG as described in Bonnycastle *et al.* (31). Phage were partially purified and concentrated by precipitation with PEG/NaCl and re-suspension in TBS containing 0.02% (w/v) sodium azide. Phage concentrations were estimated by agarose gel electrophoresis and optical density determination as described in Bonnycastle *et al.* (31). PEG-purified phage clones were used for ELISAs and DNA sequencing.

ELISA:

Phage ELISA were performed as described in Zwick *et al.* (30). Briefly, 2 x 10^{10} phage particles were adsorbed to microtiter wells at 4°C overnight, followed by blocking with 200 µl TBS containing 2% (w/v)BSA for one hour at 37 °C. The plates were washed three times with TBS containing 0.1% Tween (v/v), and incubated with the target antibody for 2 to 4 hours at room temperature. The plates were washed six times, and 35 µl of a 1:500 dilution of goat anti-human (Fab specific) antibody conjugated to HRP were added for one hour at room temperature. The plates were washed six times, and the reaction was developed with 0.03% (v/v) H_2O_2 and 400 µg/ml ABTS in citrate/phosphate buffer. Optical density was measured in a Biotek EL 312e plate reader at 405 and 490 nm for a time period of up to 45 minutes. Values of absorbance at 405 nm minus absorbance

at 490 nm are reported. Replica, phage-coated wells were reacted with a rabbit polyclonal anti-phage antibody to verify that similar amounts of phage particles were adsorbed to the plate. Bound anti-phage antibody was detected with a protein A-HRP conjugate (Pierce) and the H_2O_2/ABTS mixture described above.

For synthetic peptide ELISAs, 35 µl TBS containing 1 µg streptavidin (Roche Diagnostics, QC, Canada) were added to the microtiter wells and incubated at 4 °C overnight. Next day, after blocking with TBS/2% BSA at 37°C for one hour, an excess of biotinylated peptide (100 ng in 35 µl TBS) was added to each well and captured for 30 minutes at room temperature. The addition and detection of bound antibody were performed as described for the phage ELISA.

Reducing ELISA included an additional step of treatment with 100 nM DTT for 1 hour at 4 °C after the BSA-blocking step. The incubation with 2F5 was carried out in the presence of 5 mM DTT to prevent re-formation of the disulfide-bridges in the peptides.

For peptides- and MBP-titration ELISAs, we used a procedure that captured the antigen out of solution in a monovalent fashion, thus minimizing avidity. 2F5 IgG (100 ng in 35 µl TBS) was adsorbed to microtiter wells at 4°C overnight. Next day, the antibody was removed, and the wells were blocked with 200 µl of 2% BSA in TBS at 37 °C for one hour. The wells were washed three times with TBS/0.1% Tween, and 35 µl of serial dilutions of the synthetic peptides or the MBP fusions were added and incubated for two hours at room temperature. The wells were washed six times with TBS/0.1% Tween. For detection in the peptide titrations, 35 µl 1µg /ml Neutravidin-HRP were added and incubated for 30 minutes at room temperature. For detection in the MBP fusion titrations, 10 nM of a biotinylated anti-MBP monoclonal antibody was added and

incubated for one hour at room temperature, the plates were washed six times, and 35 µl of 1µg /ml Neutravidin-HRP were added and incubated for 30 minutes at room temperature. The reactions were developed with H_2O_2 and ABTS as described above.

Affinity determinations.

The affinity of 2F5-antigen interactions was studied at the University of British Columbia Centre for Biological Calorimetry using a Biacore 3000 apparatus (Biacore AB, Uppsala Sweden). The binding-inhibition procedure described in Nieba *et al.* (225) and Karlsson (165) was followed. CM5 sensor chips were covalently coated at high density with synthetic E4.6 peptide using the Biacore amide coupling kit and following the manufacture's instructions. Independent reactions of 2F5 Ig G and peptide or protein analytes were incubated at 4 °C overnight in buffer HBS-EP (Biacore) to allow them to reach equilibrium. The final 2F5 concentration used was 5 nM for all experimental points; six or seven analyte (synthetic peptides or MBP fusion proteins) concentrations, ranging from 27 nM to 5.4 µM, were routinely explored in a single experiment. Equilibrium reactions were injected in duplicate over a E4.6-coated chip at a flow of 3 µl /minute. Under these conditions, binding of the antibody to the chip is limited by mass transfer, thus the reaction is driven by free antibody concentration, and not by the affinity for the immobilized ligand (266, 348). Bound antibody was recorded as resonance units very early in the association phase (ten seconds after the start of the injection). The concentration of free antibody for each reaction was estimated by comparison of the experimental data with an antibody calibration curve generated with 2F5 concentrations of 1.25 to 20 nM, in the absence of antigen. Free antibody concentrations were plotted

against their respective analyte concentration, and the curves were fitted to the "in solution" affinity model provided with the BiaEvaluation 3.1 software (Biacore).

RESULTS

2F5 selects phage bearing peptides with multiple DKW-flanking sequences from primary phage-displayed peptide libraries.

IgG 2F5 was used to screen seventeen phage libraries displaying fully-randomized peptides of varying length (30). The phage libraries are built in the f88-4 vector, which allows a single phage particle to display 30 to 300 copies of the same peptide fused to the N-terminus of the major coat protein pVIII. The displayed peptides in many of the libraries also bear one or two fixed Cys residues. Sequence analysis of clones, shown in Table 1, revealed that 2F5 mostly selected phage carrying a short core epitope sequence homologous to that of HIV-1-gp41 (DKW, LDKW or DKWA). Some variations as DRW and DPW were also observed. The clones neither displayed significant homology to gp41, nor formed an identifiable consensus sequence in the regions flanking the DKW, indicating that the selection was primarily based on the presence of the DKW motif. However, DKW-flanking sequences apparently determined overall binding affinity, since large differences in ELISA signals were observed among clones sharing the DKW motif. Interestingly, phage bearing peptides with potentially Cys-constrained loops of different length were also selected, the shortest loop being four residues long. Clones E6.5 and E4.6 showed the strongest 2F5 reactivity. The tighter binding of 2F5 to these clones was not a result of increased peptide expression (nor of

Table 1. Phage-displayed peptides selected by MAb 2F5 contain the core sequence DKW and display sequence variability in the regions flanking DKW. The core DKW sequence is in bold. The Ala residue corresponding to the first amino acid of the phage pVIII protein is indicated in parenthesis. Values are expressed as the optical density at 405 nm minus that at 490 nm.

Clone	ELISA	Sequence
E6.5	0.98	MV**LDKW**(A)
E4.6	0.96	LHEESM**DKW**SNLMQCCT
E9.6	0.73	RANTC**DKWA**LPCNTGN
H2.5	0.68	SRK**ELDKWAS**TDCMQCQ
E11.6	0.67	YCTAPLNA**DKW**SCT
E10.10	0.58	LGTNC**DKWA**CMHY
E8.3	0.54	SC**DKW**VPYCA
E6.7	0.54	NS**LDKW**(A)
E11.9	0.42	DCLTP**DRW**VSFPSGCM
E8.1	0.40	TC**DKW**VARCE
E11.1	0.36	VCPKSAQM**DRW**YCL
E10.1	0.28	LDALC**DKW**SCAKMN
E9.8	0.27	HYETC**DKW**HLCDSHS
H2.6	0.25	RCAQVLACLPTHD**LDKW**(A)
E9.9	0.23	AGLYC**DKW**QTNCKISE
E7.3	0.15	SCPPES**DRW**SCF
E7.6	0.14	KC**DKWA**YDEDCL
f88-4	0.05	parental vector

peptide dimerization for clone E4.6), as evaluated by reducing and non-reducing SDS-PAGE of phage clones, which separates recombinant pVIII proteins from wild-type ones (data not shown). Thus, 2F5 binds to a large array of peptide sequences that contain the DKW core epitope, demonstrating both a strict requirement for the DKW motif, and the tolerance of multiple sequences in the DKW flanking regions that contribute to affinity.

We focused on a group of clones bearing the DKW motif flanked by Cys residues, whose structure is potentially constrained by disulfide bridging (Table 1 clones E7.3, E8.3, E9.6, E10.10 and E11.6). The introduction of disulfide or β-lactam bridges in 2F5-binding peptides has, in several instances, improved affinity for 2F5 (203, 311). Our previous experience has shown that, in most cases, if two Cys residues are present in a phage-displayed peptide they usually form an intra-chain disulfide bond, and therefore the peptide is displayed as monomer on analysis of whole phage by non-reducing SDS-PAGE (358). In contrast, peptides bearing a single Cys residue (and some containing two Cys) have a strong tendency to form inter-molecular bridges, and thus the peptides are typically displayed as homo-dimers instead of monomers (352, 358). SDS-PAGE performed in the presence or absence of the reducing agent DTT confirmed the monomeric status of the peptides expressed by the phage clones E7.3, E8.3, E9.6, E10.10 and E11.6. Phage ELISA under reducing conditions indicated that disulfide bridges were required for 2F5 binding to all of the clones (data not shown).

A set of synthetic peptides was produced (H2.5, E4.6, E7.3, E8.3, E9.6, E10.10, E11.6 and H2.5) for the experiments described below. The peptides were designed so that their C-terminal sequences would include N-terminal residues (AEG or AAEG) of the phage major coat protein, pVIII. Also, a biotinylated Lys was introduced at the

C terminus to facilitate immunochemical assay. A peptide (ME2F5) containing the sequence of the native, six-mer epitope (ELDKWA) was also made as a control. Binding of 2F5 to streptavidin-captured synthetic peptides was analyzed by direct ELISA, with results similar to those from phage ELISAs (data not shown). Thus, the behavior of the synthetic peptides was similar to that of their phage-displayed counterparts.

These ELISAs were again performed under reducing conditions (Table 2a) to assess the role of potential disulfide bridges in the binding of 2F5 to the cyclic peptides. Biotinylated peptides were captured on immobilized streptavidin and treated with 100 mM DTT. The peptides were then reacted with 2F5 IgG in the presence of a low (5 mM) concentration of DTT, which allowed binding of 2F5 to the peptides, but prevented re-formation of disulfide bridges in the peptides. Dependency of an intact disulfide bridge was observed for all peptides having the DKW sequence bordered by Cys residues (E8.3, E9.6 and E11.6), and was not detected in similarly-treated clones bearing "linear" peptides (DKW outside the Cys loop or no Cys residues). Substitution of Cys to Ser in clone E8.3, by site-directed mutagenesis, confirmed these findings and ruled out artifacts of the assay in the observed DTT sensitivity (Table 2b). The results showed that, for most peptides containing two Cys, the constraint(s) imposed by a disulfide bridge are important for binding of 2F5 to phage-displayed peptides or to their synthetic-peptide counterparts.

To detect differences in binding affinity that could have been suppressed in the direct ELISAs (due to bivalent binding of the IgG to multivalent peptide on phage), in-solution titration assays were performed, in which the 2F5 IgG was immobilized onto microtiter wells and synthetic peptides were captured from solution in a monovalent

Table 2. (a) ELISA on 2F5-binding synthetic peptides under non-reducing and reducing conditions. (b) 2F5 ELISA on wild type and Cys-substituted mutants of clone E8.3. Values are expressed as the optical density at 405 nm minus that at 490 nm.

a.

Peptide	Sequence	No DTT	DTT
E9.6	ARANTC**DKWA**LPCNTGN(AEGK)-bio	**.851**	**.285**
E11.6	YCTAPLNA**DKW**SCT(AEGK)-bio	**.570**	**.205**
E8.3	SC**DKW**VPYCA(AEGK)-bio	**.742**	**.118**
E10.10	ALGTNC**DKWA**CMHY(AEGK)-bio	**.571**	**.242**
E7.3	SCPPES**DRW**SCF(AEGK)-bio	.106	.064
E4.6	LHEESM**DKW**SNLMQCCT(AEGK)-bio	.893	.907
H2.5	SRKEL**DKW**ASTDCMQCQ(AEGK)-bio	.796	.865
ME2F5	GG**ELDKWA**GGGK(AEGK)-bio	.772	.799
No peptide	---	.032	.017

b.

Phage clone	Sequence	ELISA 2F5	ELISA anti-phage
E8.3 wild type	SCDKWVPYCA	**1.00**	0.76
E8.3C5'/S	S**S**DKWVPYCA	0.08	0.77
E8.3C3'/S	SCDKWVPY**S**A	0.07	0.79
f88-4	---	0.01	0.00
No phage	---	0.01	0.01

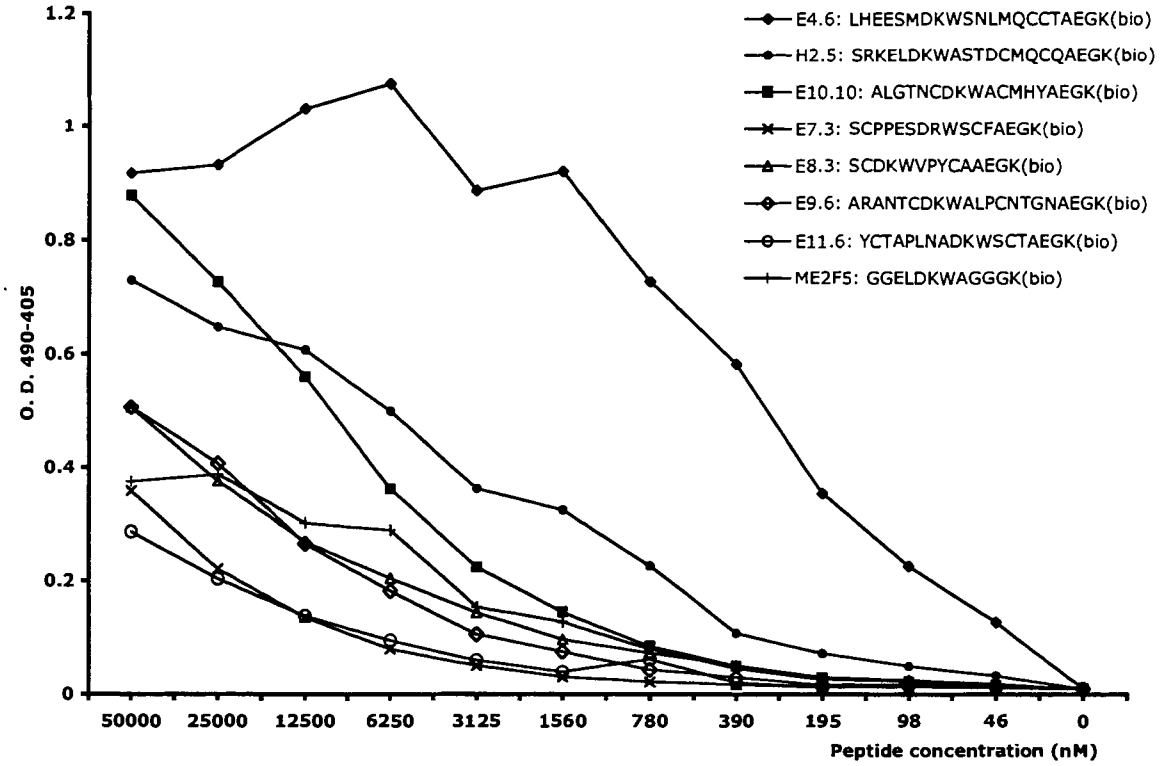

Figure 1. A synthetic peptide bearing the displayed sequence from the E4.6 phage clone binds 2F5 IgG tighter than the native hexa-peptide epitope (ME2F5) in titration ELISA. 2F5 IgG was adsorbed to microwells and used to capture biotinylated peptides from solution at the concentrations indicated; bound peptides were detected with Neutravidin-HRP and ABTS. Values are expressed as the optical density at 405 nm minus that at 490 nm.

fashion. Bound peptides were then detected *via* their biotin group using a Neutravidin-HRP conjugate. The results in Figure 1 show that peptide E4.6 was the tightest binder, even though H2.5 carries the complete ELDKWAS sequence present in gp41. Different from gp41, in which hydrophobic (Leu) and acid (Glu) residues predominate proximal to the N-terminal side of the DKW core, peptide H2.5 has two basic amino acids (Arg and Lys) that could negatively influence its reactivity. The control peptide ME2F5 showed poor reactivity as compared to E4.6 and H2.5.

Taken together, these results show that the DKW core is essential for binding of MAb 2F5 to synthetic and phage-displayed peptides. Moreover, 2F5 has increased affinity for peptides bearing a diversity of sequences flanking the DKW motif, even though those sequences do not share homology to HIV-1 gp41. Thus, for each clone, 2F5 binding is determined by its flanking sequences and/or by the presence of constraints imposed by disulfide bridging.

The flanking region C-terminal to the DKW motif is important for strong peptide reactivity with MAb 2F5.

We wanted to further explore the specificity of the 2F5 paratope with regard to the level of sequence variation permitted around the DKW core. Thus, we constructed two phage-displayed, semi-defined peptide libraries containing the minimal-binding sequence, DKW, flanked by twelve variegated residues at either the N or C terminus, to investigate the extent to which the N- and C-terminal regions are involved in binding to the antibody. The rationale of the design was to produce two libraries with minimal binding to 2F5, and to select flanking residues that would increase the affinity of

Table 3. Sequences of peptides displayed by phage clones isolated by high stringency screening of the X_{12}-DKW and DKW-X_{12} libraries. Binding refers to phage reactivity with 2F5 IgG in ELISA, and is represented in arbitrary binding units based on two independent ELISAs, normalized with the signal from clone E4.6. X_{12}D sub and DX_{12} sub refer to the X_{12}-DKW and DKW-X_{12} sublibraries before the screening, respectively. The sequence AAEGD corresponds to the N-terminus of the phage major coat protein.

Clone	Binding	Sequence
X_{12}D sub	-	XXXXXXXXXXXXAA**DKWS***AAEGD*
XD10.1	++++	IEADM**LDRWA**YYAA**DKWS***AAEGD*
XD10.2	++++	TSPHASLHMW**DLDKWS***AAEGD*
XD1.2	++++	EGPYVDYP**LDKWA**EWS*AAEGD*
XDR4.24	+	SNGAASLLNNYLAA**DKWS***AAEGD*
XDR4.44	+	RERDKTSLAPPFAA**DKWS***AAEGD*
XD10.3	-	DPWNDRGSELAIAA**DKWS***AAEGD*
XD10.4	-	GIRTPMTEIEWLAA**DKWS***AAEGD*
XD10.5	-	EYGESFDSYWPLAA**DKWS***AAEGD*
DX_{12} sub	-	AA**DKWS**XXXXXXXXXXXXX*AAEGD*
DX1.1	++++	AA**DKWS**HLSLTEFSPSHQ*AAEGD*
DX10.5	++++	AA**DKWS**DWPNIAQYTTTL*AAEGD*
DXR4.22	++++	AA**DKWS**FWPWGDDSPLLT*AAEGD*
DXR4.14	++	AA**DKWS**KLGYTPDLPTSP*AAEGD*
DXR4.17	+	AA**DKWS**DFIIYSTIPFRL*AAEGD*
DX10.1	+/-	AA**DKWS**TEAHNLMAV**DKWA***AEGD*
DX10.3	+/-	AA**DKWS**LWDSQSEVRMLT*AAEGD*
DX10.4	+/-	AA**DKWS**DWSSNGSILGTR*AAEGD*
DX1.3	+/-	AA**DKWS**LWADAPTLGDAM*AAEGD*
DX1.5	+/-	AA**DKWS**GWDHSPVTTVLT*AAEGD*
E4.6	++++	LHEESM**DKWS**NLMQCCT*AAEGD*
gp41		SQNQQEKNEQELLEL**DKWA**SLWNWFNITNWLWYI

interaction with the antibody. Two Ala residues were introduced at the N-terminal side of the DKW core to prevent selection of the native Glu and Leu residues at those positions; a Ser was fixed C-terminal to the DKW based on the sequence from clone E4.6. These three substitutions decreased binding to 2F5 to undetectable levels, as revealed by ELISA on phage clones that were picked from the libraries at random, and the whole libraries (Table 3). Thus, the affinity of tight-binding clones selected from the libraries by 2F5 should depend upon both the DKW core, and sequences selected from the variegated N- or C-terminal flanking regions.

The libraries X_{12}-AADKW and AADKW-X_{12} (comprising ~10^9 independent clones each) were subjected to three rounds of high-stringency affinity selection using biotinylated 2F5 Fab in-solution. The deduced amino acid sequences of the selected clones are shown in Table 3. As observed in clones selected from the primary libraries, the sequences of the DKW-flanking regions shared little homology with the native sequence of gp41, nor could they be formed into consensus groups. However, some general patterns were observed: A hydrophobic amino acid was always selected at position (–3) (*i.e.*, three residues N-terminal to the Asp in DKW) from the X_{12}-AADKW library, and Leu was the most frequent residue selected. Nevertheless, the selection of a Leu at this position was not sufficient to recover high-affinity binding in the context of the clones. All clones carrying Leu (-3) showed only marginal reactivity with 2F5 in ELISA; in fact, Tyr or Trp were present at this position in the tightest-binding clones (XD10.1, XD10.2 and XD1.2). Clones selected from the AADKW-X_{12} library showed selectivity for a hydrophobic residue at the position (+3) (*i.e.*, three residues C-terminal to the Trp in DKW), where a Leu or a Trp were preferentially selected. Again, the presence

of a hydrophobic residue at this position appeared to be required, but was not sufficient to achieve high-affinity binding to MAb 2F5. We also noticed a marked prevalence of acidic residues (Asp and Glu) on both sides of the DKW core epitope.

Most of the clones isolated from the two libraries showed relatively poor binding to 2F5 IgG in ELISA, as compared with clone E4.6 (Table 3). Rare mutational events dominated selection from the X_{12}-AADKW library, as the tight-binding clones duplicated the epitope at a position closer to the N-terminus, and thus acquired a longer C-terminal flanking region (clone XD10.1, IEADM**LDRWA**YYAA**DKW**S*AAEG*), or mutated the Ala residues and created an expanded epitope (clone XD10.2, TSPHASLHMWD**LDKW**S*AAEG*), or expanded and moved the epitope toward the N terminus and acquired a Trp in position (+3) (clone XD1.2, EGPYVDYP**LDKWA**EWS*AAEG*). These results indicate that binding to 2F5 cannot be improved significantly through this means of optimizing sequences flanking the N-terminus of AADKW.

In contrast, strong reactivity of 2F5 to several clones from the AADKW-X_{12} library was based solely on differences in their C-terminal sequence, indicating that there are specific requirements for binding that can be localized to the region C-terminal to DKW. One clone with a second DKW motif in the randomized region, (DX10.1, AA**DKW**STEAHNLMAV**DKWA***AEG*) was selected, but it was a relatively weak binder. Clones DX1.1, DX10.5 and DXR4.22 were especially tight binders, and did not display homology in their flanking regions, indicating that tight binding to 2F5 can be achieved by more than one particular sequence flanking the C-terminal side of the DKW core. To confirm and further explore the binding properties of the selected peptides to

MAb 2F5, the peptide-coding sequences of several clones were transferred to an MBP fusion expression system, and the peptides were expressed as N-terminal fusions to MBP. This allowed the peptides to be analyzed for binding to 2F5 IgG in a monovalent fashion, out of the multivalent context of the phage coat. As shown in Figure 2, clone XD1.2 from the X_{12}-AADKW library showed the strongest reactivity with 2F5; this clone was heavily mutated with respect to the original library design, and bears the native LDKWA sequence plus hydrophobic residues at (–3) and (+3) positions. The reactivity of MBP fusions DX1.1, DX10.5 and DXR42.2, from the AADKW-X_{12} library was stronger than DX10.4, XD10.3 and XD10.4, in keeping with the results from the phage ELISA.

In summary, these results revealed that 2F5 displays multispecificity for sequences flanking the DKW core, and suggest that binding can be achieved by a diversity of sequences, which likely establish different contacts with 2F5. Phage clones bearing peptides with the DKW sequences were selected from the libraries, regardless of the nature of their DKW flanking regions; but tight-binding clones typically required a hydrophobic residue at positions (-3) and/or (+3), and were more effectively selected on the basis of their C-terminal DKW-flanking region.

MAb 2F5 displays similar binding affinity for DX-MBP fusions with different DKW C-terminal sequences.

With the objective of learning whether the observed 2F5 multispecificity would significantly influence the affinity of MAb-peptide interaction, we determined the intrinsic binding affinity of the tight-binding clones by surface plasmon resonance. We

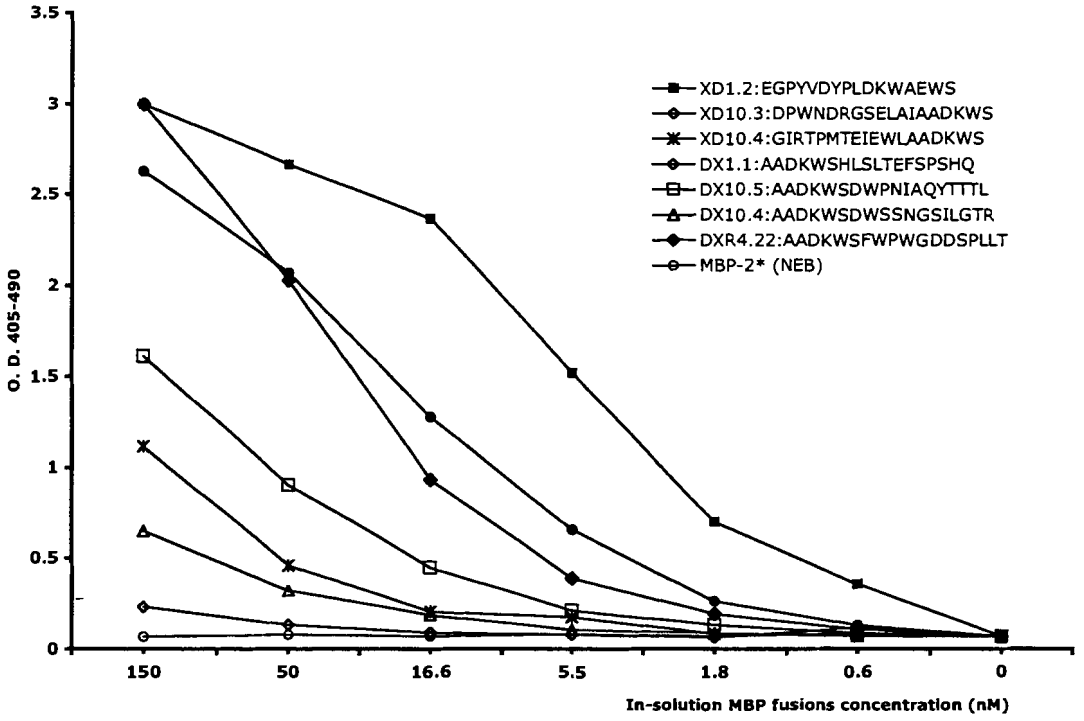

Figure 2. Titration ELISA on MBP fusions produced from XD and DX clones. 2F5 IgG was adsorbed to microwells and used to capture MBP fusion proteins from solution at the concentrations indicated. Bound proteins were detected with a biotinylated anti-MBP monoclonal antibody and Neutravidin-HRP and ABTS. MBP-2* is a purified maltose-binding protein preparation purchased from New England Biolabs (NEB). Values are expressed as optical density at 405-490.

also wanted to compare the affinity of the MBP fusions with those of gp160 and gp41, as well as synthetic peptides carrying the full ELDKWA sequence. The initial experimental design involved the immobilization of MAb 2F5 to the chip and flowing the analyte proteins samples over them. In this way, real-time kinetic data are reliably collected. Several conditions were tested for immobilizing 2F5 and regenerating the surface after each use, but they all were unsatisfactory. The opposite arrangement (*i.e.*, antigens immobilized on the chip and injected antibody) was not explored, since it has been described as generating unreliable data, due to the avidity effect inherent in bivalent molecules and the re-binding events that take place during the dissociation phase (225, 353). Thus, even though this experimental design is widely used for the determination of *on* and *off* rates, kinetic data generated with this procedure may be questionable. We favored the alternative of determining the in-solution affinity at equilibrium as described by Nieba *et al.* (225). In this method, the antibody is at a fixed concentration and is reacted to equilibrium with increasing antigen concentrations. The concentration of free antibody is then determined by injecting the reactions over an antigen-coated sensor chip, and comparing the data against an antibody calibration curve.

In control experiments with MAb b12 and B2.1 peptide, we demonstrated that direct kinetic analysis under conditions in which the peptide was immobilized to the chip and the antibody was used as analyte, did not provide accurate Kds even if Fab was used (not shown). Significant differences in Kd between the two methods were also observed for the E4.6 synthetic peptide (see Table 4, Kinetics *vs* Equil/Sln data for E4.6 peptide-2F5-IgG). The in-solution affinity of 2F5 IgG for the E4.6 synthetic peptide was determined using analyte concentrations ranging from 5.4 μM to 27 nM, and the Kd from

Table 4. Kds obtained for synthetic peptides and fusion proteins by surface plasmon resonance. (a) For the Kinetic method, the first of the reactant in a pair is the one immobilized on the chip. (b) Method refers to the procedure use for the determination; Kinetics involves the flowing of analyte over the immobilized ligand and determination of association and dissociation rates; in this instance, the Kd at equilibrium is calculated from the rate values. Equil/Sln is based on the determination of free antibody at equilibrium, with one fixed antibody concentration and several concentrations of peptide/protein analyte. In this case kinetic data are not obtained. na indicates not applicable.

Reactants[a]	Method[b]	Sequence	Kd
gp160-2F5 IgG	**Kinetics**		1.8 pM
gp160-2F5 IgG	Equil/Sln	n.a.	720 nM
gp41-2F5 IgG	Equil/Sln	n.a.	23 nM
ME2F5 peptide-2F5 IgG	Equil/Sln	GG**ELDKWA**GGGK(bio)	7.1 μM
E4.6 peptide-2F5 IgG	**Kinetics**	LHEESM**DKW**SNLMQCCTAAEGK(bio)	0.7 nM
E4.6 peptide—2F5 IgG	Equil/Sln	LHEESM**DKW**SNLMQCCTAAEGK(bio)	950 nM
E4.6MBP—2F5 IgG	Equil/Sln	LHEESM**DKW**SNLMQCCTAAEE-**MBP**	380 nM
DXR4.22MBP-2F5 IgG	Equil/Sln	**AADKW**SFWPWGDDSPLLT-**MBP**	1.8 μM
DXR4.22**EL** MBP-2F5	Equil/Sln	**ELDKW**SFWPWGDDSPLLT-**MBP**	92 nM
DX10.5MBP-2F5 IgG	Equil/Sln	**AADKW**SDWPNIAQYTTTL-**MBP**	2.3 μM
DX10.5**EL** MBP-2F5 IgG	Equil/Sln	**ELDKW**SDWPNIAQYTTTL-**MBP**	73 nM
DX1.1MBP-2F5 IgG	Equil/Sln	**AADKW**SHLSLTEFSPSHQ-**MBP**	1.7 μM
DX1.1**EL** MBP-2F5 IgG	Equil/Sln	**ELDKW**SHLSLTEFSPSHQ-**MBP**	60 nM
DX10.4MBP-2F5 IgG	Equil/Sln	**AADKW**SDWSSNGSILGTR-**MBP**	23 μM
DX10.4**EL** MBP-2F5 IgG	Equil/Sln	**ELDKW**SDWSSNGSILGTR-**MBP**	190 nM

three independent experiments was 840-950 nM. The Kd for the control peptide, ME2F5, was about one order of magnitude higher than that of E4.6, indicating a stronger 2F5-peptide interaction for E4.6 than for ME2F5. The coding sequence for clone E4.6 was also transferred to the pMALX vector and expressed as an N-terminal fusion to MBP. The purified product was used to determine the Kd at equilibrium, and this Kd was compared to that of the free peptide. As shown in Table 4, the Kd of the E4.6-MBP fusion was three-fold higher than that of the synthetic peptide; in agreement with our previous, unpublished observations and those of Jouault *et al.* (162), which have shown that peptides fused to a scaffold protein often display a better affinity for their cognate antibody than their free, synthetic peptide counterparts.

Also shown in Table 4 are the equilibrium Kds for the MBP fusion proteins corresponding to the tight-binding clones DX1.1, DX10.5 and DXR4.22, along with the Kd of the MBP fusion from the weak-binding clone DX10.4. The Kds for IgG 2F5 and clones DX1.1, DX10.5 and DXR4.22 fusions are very similar, and fall within the range of 1.7 to 2.3 μM, whereas the Kd for the DX10.4-MBP fusion was 23 μM, indicating a weaker interaction with MAb 2F5. These results demonstrate that sequences flanking the C-terminus of DKW can greatly influence the affinity of 2F5 binding to peptide and protein antigens. The data also show that high-affinity binding to 2F5 can be supported by diverse DKW-flanking sequences that are different from the sequence at the corresponding location in HIV-1 gp41, thus suggesting that the 2F5 paratope is multispecific for sequences outside the region binding the DKW core.

To further optimize their antigenicity, the sequences of the three tight-binding DX clones were engineered to expand the native core epitope sequence to ELDKW, by

substituting the two N-terminal Ala residues preceding the DKW in the DX clones to Glu and Leu. The coding regions for these sequences were transferred to pMALX, and the Kds for their interaction with 2F5 were determined. The data in Table 4 show that the re-introduction of Glu and Leu resulted in 20-30-fold increases in affinity for the tight-binding clones (DX1.1-EL, DX10.5-EL and R4.22-EL), and a 100-fold increase for the weak binder, DX10.4-EL. Thus, optimization decreased, but did not eliminate, the difference in affinity between clone DX10.4-EL and the three other clones. We obtained again very similar affinities for clones DX1.1-EL, DX10.5-EL and R4.22-EL, which were also stronger than the equilibrium Kd for $gp160_{IIIB}$, and in the same range as $gp41_{MN}$ (see below).

The affinity at equilibrium of MAb 2F5 for HIV-1 gp 160_{IIIB} was also determined. Surprisingly, we obtained a much lower affinity value (720 nM) than the ones previously reported by Conley *et al.* (64) for gp41 and a synthetic peptide (4.2 nM and 0.7 nM, respectively). We tried to replicate the results of Conley *et al.* (64), using their experimental conditions, and obtained low picomolar Kd values, based on a total lack of dissociation of 2F5 IgG from gp160, over a dissociation time of 15 minutes. We believe that the basis for this discrepancy is that Conley *et al.* (64) used a kinetic assay with gp41 as ligand on the chip and MAb 2F5 (presumably IgG) as analyte. Thus the kinetic Kd may be an artifact produced by the mechanisms mentioned aboved. Moreover, we used gp160 instead of gp41, thus basic differences between 2F5 binding to gp160, gp41 and synthetic peptides, may be at play. Also, variations in the protein samples (*e.g.*, oligomerization state) may lead to differences in epitope accessibility, as shown by Zeder-Lutz *et al.* (349). Experiments are currently underway to clarify these observations.

Amino acid residues critical for binding to MAb 2F5 are found in regions flanking the DKW core.

To investigate the contribution of particular residues to 2F5 binding, we generated a set of Ala-substitutions and deletion mutations in clones DX1.1, DX 10.5 and DXR4.22. Mutant phage clones were analyzed for their ability to bind 2F5 Fab (Figure 3 and Table 5) and to 2F5 IgG (Table 6) in a direct ELISA format. Similar results were obtained in both assays; however, due to the possibility of bivalent binding of IgG to multicopy peptide on the phage, moderate differences in binding are typically masked in the IgG-based assay. Moreover, IgG binding will be more sensitive to peptide copy number than Fab, because peptide spacing will affect the binding avidity. The data in Figure 3 and Tables 5 and 6 show that mutation of any residue in the DKW core significantly decreased binding of all of the DX clones to 2F5; this agrees with previous results obtained with a peptide with the sequence ELDKWA (163, 261, 311). In addition, Tables 5 and 6 show that Ala substitution of D and W in the DKW core of clone E4.6 ablated binding completely. Also crucial to binding in every case was the hydrophobic residue at the (+3) position (Figure 3 and Tables 5 and 6). The (+3) residue in the native gp41 (L_{669}) is highly conserved, (present on 98% of the sequences in the Los Alamos HIV Database). Ala substitution at this site did not affect binding in previous work by Joyce *et al.* (163), however, Tian *et al.* (311) showed by two independent means that Leu at this site affected binding significantly. Thus, our results, showing an absolute requirement for DKW and a hydrophobic residue at the (+3) position, agree with previous studies involving gp41-derived sequences. We conclude from this that all four peptides (E4.6, DX1.1, DX 10.5 and DXR4.22) are similar to the gp41 sequence in being "seated" in the

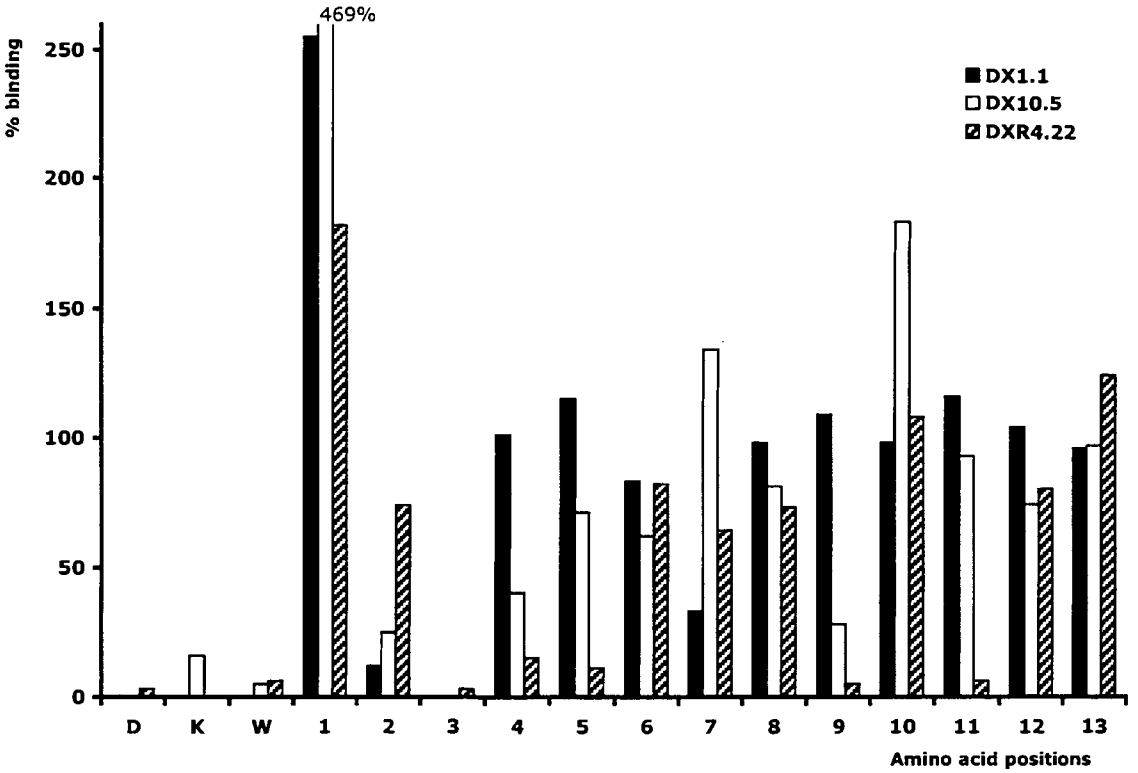

Figure 3. Residues flanking the DKW core epitope are involved in the binding of 2F5 Fab to DX1.1, DX10.5 and DXR4.22 phage. ELISA data were converted to % binding relative to phage bearing non-mutated sequences. The sequences C-terminal to the DKW core are: DX1.1: SHLSLTEFSPSHQ; DX10.5: SDWPNIAQYTTTL; DXR4.22: SFWPWGDDSPLLT. The % binding to the Ala substitution of the fixed Ser at position (+1) of clone DX10.5 was 469% and is indicated on the graph.

DKW-binding region of 2F5. Highly variable sequences outside of the DKW core contribute to affinity; consequently, binding to 2F5 by these regions appears to be multispecific.

The effect of Ala substitution in regions outside the DKW core varied significantly between clones. As summarized in Table 5, binding decreased by over 50% from Ala substitution at positions (+2 and +7) of clone DX1.1, positions (+2, +4 and +9) of clone 10.5, and positions (+4, +5, +9 and +11) of clone DXR4.22; there was no selection for shared residues at these sites. Interestingly, the change of Ser (+1) (which was a fixed residue in the library) to Ala, the residue present in native gp41, significantly increased binding (200-400%); this indicates a previously underestimated role of this Ala in binding affinity. Ala substitutions in clone E4.6 that decreased Fab binding by 50% or more were at positions (-5, -4, -3, -2, and –1) from the N-terminal side of the DKW core and (+3) from the C-terminal side, indicating that those residues are important for binding. The IgG binding data in Table 6 largely supported these findings, though, as noted above, differences in binding (increases and decreases) seen in the Fab assay were muted in assays with IgG. In conclusion, a number of different residues outside the DKW core were important for reactivity. With the exception of the (+3) position, the location and type of these residues varied greatly among the clones. Thus, in each clone studied, residues at different positions C-terminal to the DKW core, and in several cases, C-terminal to the (+3) site, were important for binding to 2F5. Moreover, for residues outside the DKW core and the (+3) position, that appear to play a role in binding, there was little similarity between clones in the type of amino acids selected or their position relative to DKW.

We generated a set of deletion mutants for clones DX1.1, DX10.5 and DXR4.22 by serially removing three residues at a time from the C-terminal end, resulting in C(-3), C(-6) and C(-9) mutants for each clone (three, six or nine residues deleted, respectively). We also constructed a C(-12) clone having only the sequence AADKWS, fixed in the libraries. Binding to 2F5 Fab was assayed as described above for the Ala substitutions, and the data are shown in Tables 5 and 6. The results demonstrate that binding of 2F5 to the DX phage is dramatically affected by deletion of the C-terminal residues, confirming their role for binding in this context. The effect of deletion was strongest for clone DX10.5. Deletion of the three C-terminal residues affected binding moderately (compare Fab to IgG data), even though Ala substitution of each of the residues in this region did not affect binding significantly. Deletion of six residues, which included Tyr (+9), dropped binding to 4% of wild type for both Fab and IgG. Ala replacement had only a moderate effect on Tyr (+9), as it decreased Fab binding significantly, but not IgG binding. Deletion of nine residues, including Tyr (+9), did not. Thus, the deletion of multiple residues, which singly had small effects on binding, appeared to produce larger effects when deleted together. This may indicate the presence at this site of a larger binding motif that depends on the combined effect of multiple residues, including Tyr (+9).

This trend was also observed with clone DX1.1. Ala substitution of Glu (+7) affected binding moderately, whereas substitution of any of the last six C-terminal residues did not affect binding significantly. Deletion of three residues from the C-terminus caused a moderate drop in binding (52% drop in Fab binding and a 19% drop in IgG binding), even though Ala substitution of the residues in this region had little effect.

Table 5. Percent binding of Ala-substituted and deletion mutants of E4.6 and DX phage clones to 2F5 Fab. The sequence of the clones and $gp41_{HXB2}$ are provided for reference. The core DKW sequence is in bold. Ala (+7) in clone DX10.5 was substituted by Gly. nd indicates not done.

HXB2gp41	**E**	**L**	**D**	**K**	**W**	**A**	**S**	**L**	**W**	**N**	**W**	**F**	**N**	**I**	**T**	**N**	**W**	**L**
Position						+1	+2	+3	+4	+5	+6	+7	+8	+9	+10	+11	+12	+13
DXR4.22	A	A	**D**	**K**	**W**	S	F	W	P	W	G	D	D	S	P	L	L	T
DXR4.22-Ala			3	0	6	182	74	3	15	11	82	64	73	5	108	6	80	124
DXR4.22-Del						0			7			18			41			
DX1.1	A	A	**D**	**K**	**W**	S	H	L	S	L	T	E	F	S	P	S	H	Q
DX1.1-Ala			0	0	0	255	12	0	101	115	83	33	98	109	98	116	104	96
DX1.1-Del						0			37			20			48			
DX10.5	A	A	**D**	**K**	**W**	S	D	W	P	N	I	A	Q	Y	T	T	T	L
DX10.5-Ala			0	16	5	469	25	0	40	71	62	134	81	28	183	93	74	97
DX10.5-Del						0			59			4			16			

HXB2gp41	**Q**	**E**	**L**	**L**	**E**	**L**	**D**	**K**	**W**	**A**	**S**	**L**	**W**	**N**	**W**	**F**	**N**
Position	-6	-5	-4	-3	-2	-1				+1	+2	+3	+4	+5	+6	+7	+8
E4.6	L	H	E	E	S	M	**D**	**K**	**W**	S	N	L	M	Q	C	C	T
E4.6-Ala	99	44	34	15	40	39	0	nd	0	269	52	0	99	80	111	111	nd
E4.6-Del			79	101		0	----	----	----	9				76	121	128	

Table 6. Percent binding of Ala-substituted and deletion mutants of E4.6 and DX phage clones to 2F5 IgG. The sequence of the clones and $gp41_{HXB2}$ are provided for reference. The core DKW sequence is in bold. Ala (+7) in clone DX10.5 was substituted by Gly. nd indicates not done.

HXB2gp41	**E**	**L**	**D**	**K**	**W**	**A**	**S**	**L**	**W**	**N**	**W**	**F**	**N**	**I**	**T**	**N**	**W**	**L**
Position						+1	+2	+3	+4	+5	+6	+7	+8	+9	+10	+11	+12	+13
DXR4.22	A	A	**D**	**K**	**W**	S	F	W	P	W	G	D	D	S	P	L	L	T
DXR4.22-Ala			10	0	0	115	96	0	71	28	108	110	117	20	113	29	109	108
DXR4.22-Del						0			5			67			85			
DX1.1	A	A	**D**	**K**	**W**	S	H	L	S	L	T	E	F	S	P	S	H	Q
DX1.1-Ala			0	0	2	103	45	1	100	99	94	68	93	100	93	93	93	89
DX1.1-Del						0			62			58			81			
DX10.5	A	A	**D**	**K**	**W**	S	D	W	P	N	I	A	Q	Y	T	T	T	L
DX10.5-Ala			0	23	15	132	18	6	26	59	84	99	73	71	100	70	82	81
DX10.5-Del						0			2			4			81			

HXB2gp41	**Q**	**E**	**L**	**L**	**E**	**L**	**D**	**K**	**W**	**A**	**S**	**L**	**W**	**N**	**W**	**F**	**N**
Position	-6	-5	-4	-3	-2	-1				+1	+2	+3	+4	+5	+6	+7	+8
E4.6	L	H	E	E	S	M	**D**	**K**	**W**	S	N	L	M	Q	C	C	T
E4.6-Ala	91	43	28	9	43	34	0	nd	0	106	49	3	85	93	100	100	nd
E4.6-Del			76	95		0	----	----	----	1				67	86	100	

The removal of all six terminal amino acids in this clone resulted in a larger drop in binding, even though Ala substitution, again, did not affect any single residue in this region.

In contrast to clones DX1.1 and DX10.5, the effect of Ala substitution was strongest for clone DXR4.22, (especially for residues Trp (+5), Ser (+9) and Leu (+12)), and deletion of regions covering these positions produced progressively larger drops in binding (59%, 82% and 93% drops in Fab binding to clones carrying the (–3), (-6) and (–9) deletions, respectively). This indicates that clone DXR4.22 contains residues in the C-terminal region that most likely have stronger individual effects on binding than the C-terminal residues in clones DX1.1 and DX10.5. Thus, binding to 2F5 appears to depend on particular residues in the C-terminal region of clone DXR4.22, whereas binding to clones DX1.1 and DX10.5 appears to depend on more global effects produced by multiple residues within this region. These global effects can not be provided by any random C-terminal sequence, but are rather specific, since 2F5 did not bind to clones chosen at random from the library, nor to the library as a whole.

The Ala substitution and deletion mutants of clone E4.6 revealed that sequences N- and C-terminal to the DKW core were important for binding. Residues Glu (-4), Glu (-3) and Leu (+3) were strongly affected by Ala substitution. However, binding to E4.6 was ablated only by deletion of both Glu (-4) and Glu (-3) on the N-terminal side, or a deletion on the C-terminal side including Leu (+3). Thus, with this clone, but not clones selected from the X_{12}-AADKW library, residues N-terminal to the DKW core were important for binding. Perhaps this is due to the presence of Leu in the (+3) position in the E4.6 clone, but not in clones in the X_{12}-AADKW library.

Taken together, our results show that the DKW core and a hydrophobic residue at the (+3) position are absolutely required for binding by tight-binding clones from the AADKW-X_{12} library. Moreover, C-terminal sequences beyond (+3) are also involved in binding, but they fall into two general categories: (i) those in which particular residues appear to play a significant role in binding (*e.g.*, clone DXR4.22), and (ii) those in which multiple residues produce a more global effect, but do not individually affect binding significantly (*e.g.*, clones DX1.1 and DX10.5). Besides this, residues N-terminal to the DKW core also can play a significant role in binding (*e.g.*, in clone E4.6), but this may rely upon the presence of a hydrophobic residue in the (+3) position.

DISCUSSION

In this work, we have shown that MAb 2F5 binds to multiple peptides bearing the DKW motif, and that sequences C-terminal to this motif are required for high-affinity binding in the context of phage-displayed peptides. We document differences in binding strength between phage expressing distinct peptides, and show that some degree of restriction is imposed by the nature of the sequences flanking the DKW core, as well as sequence length and constraints imposed by disulfide bridging (see Table 1). In agreement with previous reports, phage selected by 2F5 contained the DKW motif (64, 219). However, we found that in the context of N-terminal fusion to phage major coat protein or to the MBP of *E. coli*, the motif is necessary but not sufficient for high-affinity binding to MAb 2F5. Surface plasmon resonance studies using MBP fusion showed that tight binding in this context is recovered by extension of the C-terminal flanking region

with sequences not necessarily homologous to gp41. Peptides with distinct sequence composition displayed similar affinities, yet possessed different distributions of critical binding residues, indicating that the requirements for binding to 2F5 can be resolved in a variety of ways. This behavior illustrates a significant degree of functional plasticity of the 2F5 antibody, and indicates that its paratope comprises at least two regions: one that is highly selective for the core sequence DKW, and another that binds C-terminal to the core and is multispecific.

The epitope for MAb 2F5 was originally defined as the sequence ELDKWA on gp41 (64, 219). Using synthetic peptides, Purtscher *et al.* (261) found that the N-terminal Glu and the C-terminal Ala residues could be changed to any amino acid without major effect on 2F5 binding. In addition, the N-terminal Leu tolerated most substitutions, although the reactivity was reduced in most cases. Replacements in the Asp, Lys and Trp were much more restrictive, indicating that these three residues were absolutely required for binding. However, work by Tian *et al.* (311) has reported that, to obtain maximal antigenicity, the epitope must be extended to a nonapeptide sequence running from (and including) Leu_{661} to Leu_{669} of gp41 (LELDKWASL), whereas Barbato *et al.* (15) described an even larger fragment of 13-15 residues (659-671/673). Furthermore, Parker *et al.* (235) digested SOS gp140-2F5 complexes with protease, and found that the sequence from Asn_{656} to Asn_{671} of the gp140 (NEQELLELDKWASLWN) was protected by antibody binding. McGaughey *et al.* (203) observed that not only the extension of the epitope, but also the inclusion of a lactam-bridge constraint, were necessary to achieve maximal binding of 2F5 to synthetic peptides. In addition to these epitope-mapping studies, several immunizations with variations of the six-mer sequence (ELDKWA)

failed to produce a 2F5-like, neutralizing antibody response, even though high titers of peptide-, gp160- or gp41-binding antibodies were routinely produced (63, 92, 102, 186). Collectively, these results indicate that the complete 2F5 epitope is formed by more than the six-mer sequence.

Using a protein-fusion system in which minimal binding to the antibody was initially defined by the presence of the core DKW tri-peptide, we showed that 2F5 selected C-terminal sequences that significantly boost affinity. We found that tight-binding to 2F5 was associated with well-defined sequence patterns; hydrophobic residues were selected at position (-3) with respect to the DKW in clones from the X_{12}-AADKW library, and at position (+3) in clones from the AADKW-X_{12} library, indicating that hydrophobicity at those positions is required for high-affinity binding. The importance of hydrophobic residues at positions (-3) and (+3) was highlighted by clones E4.6 (which follows the hydrophobic (+3) rule) and XD1.2 (which follows the hydrophobic (-3) and (+3) rules). Fusions of the E4.6 and XD1.2 sequences to MBP displayed very similar behavior in titration assays (data not shown); for example, they were tighter binders than clone H2.5, which contains the full seven-mer ELDKWAS sequence found on gp41, but does not follow the hydrophobic (–3) or (+3) rules. If the sequences of the XD and DX clones are superimposed onto the sequence of HIV-1 gp41, the Leu (-3) in the XD peptides aligns with Leu $_{661}$ in gp41 and the (+3) position in the DX clones aligns with Leu $_{669}$. Those two Leu residues are highly conserved in HIV-1 isolates, and are considered part of the high-affinity, extended epitope reported by Parker *et al.* (235), Tian *et al.* (311) and Barbato *et al.* (15). Ala substitution studies on clones E4.6, DX1.1, DX10.5 and DXR4.22 confirmed the importance of the DKW motif as well as the (–3)

and (+3) hydrophobic residues. Surprisingly, the introduction of an Ala at position (+1) increased binding significantly in all clones, suggesting an important role of that residue, which had not been previously appreciated by Purtscher *et al.* (261) in the context of synthetic peptides.

We found that several of the peptides, including a short loop of four residues, are dependent on an intact disulfide bridge for binding to 2F5. Constraint of peptides containing the DKWA region by disulfide or beta-lactam bridges converts the random-coil structure of ELDKWASL peptides to beta-turn structures, and in general, improves the affinity of binding (163, 203). Crystallographic data show that the bound structure of the DKW sequence within the ELDKWA peptide forms a type I β-turn (231), a common feature found on antibody-bound peptides (308). Apparently, this particular structure is required for binding, which may in turn explain the strict requirement for the DKW motif.

We confirmed previous findings by others regarding the necessity of the core DKW sequence for binding to 2F5, and the positive effect of an extended epitope, as well as hydrophobic residues at positions (-3) and (+3) of the core. Nevertheless, the screening of our X_{12}-AADKW and AADKW-X_{12} libraries also showed that high affinity binding is achieved *via* the selection of sequences beyond the (+3) residue on the C-terminal side of DKW. Antibody selection for residues (+4) to (+14), C-terminal to the DKW, was evident by the Ala-substitution and the deletion-mutagenesis results from clones DX1.1, DX10.5 and DXR4.22. Residues having a significant effect on binding (as assessed by Fab and IgG binding, Tables 5 and 6) were identified in the C-terminal flanking region of clone DXR4.22, demonstrating that tight-binding to 2F5 is supported by residues

downstream to the DKW core. Ala substitutions on clones DX1.1 and DX10.5 had a lesser effect on binding, and provided evidence of an unequal number of influential residues within each clone, as well as differences in their positioning in the sequence.

In some instances the results of the deletion mutagenesis did not support those from the single Ala substitutions. Deletion of residues from the C terminus of clone DXR4.22 decreased binding in a manner that followed loss of residues that were sensitive to Ala substitution. In contrast, similar deletions in clones DX1.1 and DX10.5 decreased binding significantly, even though the deleted residues were not strongly affected by Ala substitution. The meaning of this latter discrepancy is difficult to interpret but it indicates the necessity of a larger sequence for 2F5 binding. The existence of a secondary binding site in the C-terminal region of clones DX1.1 and DX10.5 may be inferred, but is not proven by our data. The apparent lack of critical binding residues in clones DX1.1 and DX10.5, and their sensitivity to deletion could also indicate that these residues are required to present the correct core to the antibody, rather than participate in specific side-chain contacts, as has been observed by Barbato *et al.* (15). In contrast, clone DXR4.22 behaves differently. In this case, the presence of several critical binding residues may reflect a stronger structural constraint of the peptide, or direct contact(s) with the 2F5 paratope. The latter alternative, the establishment of side chain contacts, would imply an essentially different mechanism of binding between DXR4.22 and DX1.1/DX10.5. It is worth noting that in spite of the sequence diversity of the DX clones, their MBP fusions displayed very similar affinity for 2F5 (Figure 2 and Table 4). These results indicate that the requirements for high-affinity interaction with 2F5 can be satisfied by DKW flanked by diverse C-terminal sequences.

There is no direct information on how the structural features of the cognate epitope for 2F5 (*i.e.*, in the context of the native viral envelope) influence the antigenicity of potential 2F5 ligands. The notion of a larger epitope is supported by biochemical evidence, and by the solved structure of the antibody in complex with the ELDKWA peptide from Pai *et al.* (231). This peptide only covers a fraction of the putative paratope, leaving open the possibility that 2F5 makes additional contacts with other regions of the complete epitope. Based on the structural and functional properties of the N-terminal (53, 54, 336) and the C-terminal (275, 291) regions flanking DKW, it can be assumed that in the viral spike, the 662-667 region of gp41 must have a well-defined structure. Whatever this structure is, it is likely to be important for both antigenicity (the binding of 2F5) and immunogenicity (the elicitation of neutralizing antibody), and it is unlikely to be replicated by peptide immunogens bearing the ELDKWA sequence alone.

Our results show that 2F5 is multispecific, in that it can bind with high affinity to multiple non-homologous sequences. It is also functionally distinct from other human and non-human antibodies capable of binding to ELDKWA peptides, since it neutralizes a wide spectrum of primary HIV-1 isolates *in vitro*. In general, virus neutralization does not correlate with the binding of antibody to recombinant envelope (135), nor even with binding to infectious viral particles (253). A recent study by Poinard *et al.* (253) showed that non-neutralizing antibodies F105 and b6 bind to infectious viral particles, but do not affect the ability of a neutralizing antibody b12 to block infection, even though F105 and b6 compete with b12 for binding to gp120 envelope protein *in vitro*. They suggest that the envelope exists in two different forms on the viral surface: a functional form involved in the infection process (and hence, a target for neutralization by antibody) and a non-

functional one that does not participate in infection (and is irrelevant to virus neutralization), and allows binding of both neutralizing and non-neutralizing antibodies.

Recent results indicate that the neutralization-sensitive binding site for 2F5 is formed only after the fusion process is triggered (24, 121). It is reasonable to assume that the ability of 2F5 to neutralize the virus lies in a unique determinant that allows it to bind to its epitope on infectious viral spike, whereas other non-neutralizing ELDKWA-binders do not. This elusive feature of 2F5 has not yet been biochemically or structurally characterized; it probably resides in regions of the paratope not involved in binding to the extended DKW core. The identification of such determinant(s) bears relevance to vaccine design. The binding studies with our peptides and, our Ala substitution results demonstrated that 2F5 is capable of binding to a variety of peptide sequences, suggesting multiple mechanisms of binding by the C-terminal region of our peptides. Such plasticity may be a unique characteristic distinguishing 2F5 from other ELDKWA-binders, and could be involved in its unique functional properties. We are currently conducting studies with sera from animals immunized with the ELDKWA region to assess whether the binding to our DX peptides is an exclusive trait of 2F5. Peptides having highly restricted specificity for 2F5 have potential as structural probes of unique regions of the 2F5 paratope.

MAb 2F5 has a high level of somatic mutation (16 mutations on VH and 14 on VL) (173) and a very long H3 of 22 residues, which very likely arose from sustained antibody evolution in the presence of persistent antigen stimulation (327). The crystal structure of 2F5 bound to ELDKWA peptide (231) shows that most of the amino acids on the apex of the H3 are not contacted by peptide. However, recent functional studies, in

which residues of the 2F5 H3 were mutated to Ala, showed that the amino acids in the apex of H3 are important for the binding of 2F5 both to gp41 and to synthetic peptides, as well as being critical to neutralization (355). Elucidation of the structure of R4.22 and 10.5 peptides bound to 2F5, coupled with mutagenesis studies similar to those of Zwick *et al.* (355), may reveal site(s) on the antibody involved in its unique neutralizing properties.

Peptide immunogens tested so far have failed to produce a neutralizing response, very likely due to their inability to present the appropriate, complete neutralizing epitope (63, 92, 102, 186). The ideal immunogen for eliciting antibodies having 2F5-like neutralizing properties would comprise the neutralizing epitope on the infectious spike in the absence of other immunodominant epitopes. Some approaches to engineering such an immunogen might include designed peptides in the context of lipid (*e.g.*, Schibli *et al.* (291)), virus-like particles bearing such a structure, and/or larger fragments of gp41 in which irrelevant, immunodominant sites have been obscured (*e.g.*, by glycosylation; Pantophlet *et al.* (234)). Peptide-immunogens containing regions relevant to the neutralization-sensitive site on 2F5 may serve to enhance the production of 2F5-like antibodies in such a scenario, following a prime-boost immunization strategy. In keeping with the strategy of Beenhouwer *et al.* (19), neutralization may be enhanced by a priming immunization using an immunogen that contains the neutralizing epitope, followed by boosting immunization with an immunogen that selectively cross-reacts with the targeted antibody. However, as 2F5 contains a large number of somatic mutations, as well as an unusually-long CDR-H3 loop, such an immunization approach may not elicit antibodies having all of 2F5's structural features. Nevertheless, peptides, such as those described in

this work, may serve as probes in revealing the site(s) on the virus that are required for neutralization, and perhaps, as immunogens that will enhance the production of neutralizing antibodies.

ACKNOWLEDGMENTS

We thank A. Burguess, R. Astronomo, A. Johner, H. Sarling, B. Gangadhar, B. Vanderkist and S. Wu for their technical assistance. We are also grateful to M. Zwick, D. Burton, H. Katinger, the MRC Centralised AIDS Facility (UK) and the NIH AIDS Research and Reference Reagents Program for the donation of materials. We thank L. Creagh (UBC) for help with the Biacore studies. This work was supported by NIH/NIAID grants R21-AI49808 and RO1-AI49111. A. M. was supported by a Graduate Scholarship from the Michael Smith Foundation for Health Research, BC, Canada, and a Canada Graduate Scholarship from the Natural Sciences and Engineering Research Council of Canada.

CHAPTER 5

Peptide ligands for 2G12, a neutralizing antibody that recognizes a carbohydrate epitope on the envelope of the Human Immunodeficiency Virus type 1.

Alfredo Menendez[1*], Daniel A. Calarese[2*], Chris N. Scanlan[3], Keith C. Chow[1], Renate Kunert[5], Robyn L. Standfield[2], Herman Katinger[5], Dennis R. Burton[2,3], Ian A. Wilson[2,4,¶] and Jamie K. Scott[1,¶]

[1]Department of Molecular Biology and Biochemistry, Simon Fraser University, Burnaby, BC, V5A 1S6, Canada. Departments of Molecular Biology[2], Immunology[3], and The Skaggs Institute for Chemical Biology[4], The Scripps Research Institute, 10550 North Torrey Pines Road, La Jolla, CA 92037, USA. [5]Institute of Applied Microbiology, University of Natural Resources and Applied Life Sciences, Muthgasse 18B, A-1190 Vienna, Austria.

[¶]Correspondence should be addressed to J.K.S. or I. A. W.

E-mail: jkscott@sfu.ca or wilson@scripps.edu

* These authors contributed equally to this paper.

Running title: Peptide ligands for the HIV-1-neutralizing antibody 2G12.

This work is being prepared for submission to ***The Journal of Biological Chemistry.***

ABSTRACT

MAb 2G12 is a potent HIV-1-neutralizing antibody. It binds with high affinity to a conserved epitope in the envelope of HIV-1, formed exclusively by carbohydrate. By screening a set of phage-displayed peptide libraries with MAb 2G12, we have isolated one peptide ligand that binds 2G12 specifically, with a 200 μM Kd.

The atomic structure of the peptide in complex with 2G12 Fab was determined at 2.7 Å resolution. Comparison of the peptide-2G12 complex with a previously-solved $Man_9GlcNAc_2$-2G12 structure shows the peptide bound at a site adjacent to, but different from, the primary carbohydrate-binding site of the antibody, with only two antibody residues involved in interactions with both ligands. The peptide establishes 61 van der Waal interactions and 2 hydrogen bonds with 9 residues in the antibody's hypervariable loops. Alanine substitutions along the peptide sequence revealed that most peptide residues contribute to binding.

The affinity of the synthetic peptide was improved ~7-fold by fusing it to a monomeric protein. The peptide was optimized by the screening of a semi-defined sublibrary and the affinity of the optimized peptide in the form of a protein fusion improved a further 70-fold to 340-400 nM. We propose to use these peptides as templates for structure-based design of glycopeptide immunogens meant to elicit 2G12-like antibodies.

INTRODUCTION

Human monoclonal antibody (MAb) 2G12 was isolated from an HIV-1-infected, asymptomatic donor by Buchacher *et al.* (42). It efficiently neutralizes a broad range of HIV-1 primary isolates (26, 71, 315), and confers protection from SHIV challenge in macaques when administered in combination with other antibodies (12, 196, 201, 239). MAb 2G12 binds with high affinity to a unique, conserved epitope formed by a cluster of N-linked, high-mannose glycan groups on the "silent" face of gp120, of the HIV-1 envelope (277, 290, 316).

The crystal structures of 2G12 Fab alone, and in complex with the oligosaccharide $Man_9GlcNAc_2$, and with the disaccharide Manα1-2Man show that two Fabs assemble into an interlocked, V_H domain-swapped dimer, forming an extensive, multivalent binding surface (46). A total of four $Man_9GlcNAc_2$ molecules were observed bound to the domain-swapped dimer in the crystal structure, occupying the two conventional antigen binding sites, as well as two novel sites created at the interface of the two VH domains. Several lines of biochemical and biophysical evidence implicate the domain-swapped dimer as the dominant form that recognizes gp120 (46).

Since the identification of its carbohydrate epitope, MAb 2G12 has received significant attention as a template for HIV-1 vaccine development. Considerable effort has been directed at the characterization of the saccharide-binding profile of 2G12 (4, 180, 333), and the generation of novel antigens in the form of synthetic oligomannoses (180, 185) or short, synthetic glycopeptides (89, 115, 194). We have taken a different approach in generating immunogens meant to elicit 2G12-like antibodies; it relies on the isolation of peptide that crossreact with the native oligomannose epitope. Immunogenic

mimicry of carbohydrates by peptides has been reported (19, 181, 189, 247, 250, 259, 260), indicating that it is indeed, a reasonable goal.

We present here the first detailed characterization of peptide ligands specific for the HIV-1-neutralizing antibody 2G12. It is also the second example of a side-by-side crystal structure of a carbohydrate-binding antibody, in complex with a peptide and carbohydrate ligands. The peptide 2G12.1 bound 2G12 MAb with a Kd of ~ 200 μM, and competed with gp120 and Manα1-2Man for binding to 2G12. The crystal structure of the peptide in complex with 2G12 Fab indicated that there is only partial overlap between the areas in the antigen-binding site occupied by these two antigens; there is no overlap with bound Manα1-2Man. Thus peptide 2G12.1 is a functional but not a structural mimic of 2G12's oligomannose epitope on gp120.

Fusion of the 2G12.1 peptide coding sequence to the gene for the maltose-binding protein of E. coli (MBP) improved the affinity of 2G12.1 by ~7-fold, to at least 28 μM. The 2G12.1 sequence was used to produce a semi-defined phage-displayed peptide library, which was screened for optimized peptide ligands. Optimized peptide 2G12.1-D10 fused to MBP bound 2G12 with a Kd of 400 nM. Here we propose to use these peptides to generate glycopeptide immunogens to elicit protective 2G12-like antibodies.

MATERIALS AND METHODS

Materials

Fifteen phage-displayed random peptide libraries were used in this study: X_6, X_{15}, X_8CX_8, $X_{15}CX$, XCX_{15}, LX_4, LX_6, $LX_{6\text{-}b}$, LX_8, LX_{10} and LX_{12} are described in (30); Cys3,

Cys4, Cys5 and Cys6 were kindly provided by George Smith (University of Missouri-Columbia). Biotinylated, synthetic 2G12.1 peptide (2G12.1, sequence NH_3-ACPPSHVLDMRSGTCLAAEGK(biotin)-NH_2) was from Multiple Peptide Synthesis (San Diego, CA). Cyanovirin-N (CVN) and an anti-CVN polyclonal antibody were generous gifts of J. McMahon, (NCI-Frederic, MD). $gp120_{Ba\text{-}L}$ was a gift from T. Fouts (Baltimore, MD). Oligonucleotides were synthesized "in house" using an ABI 392 synthesizer (Foster City, CA), and by the NAPS Unit (University of British Columbia, Vancouver) and purified by polyacrylamide gel electrophoresis. Protein concentrations were determined with the Protein Assay Kit from Biorad (Hercules, CA). Goat anti-human IgG (Fab-specific), alkaline-phosphatase-conjugated goat anti-human IgG (Fab-specific), horseradish (HRP)-conjugated, goat anti-human IgG (Fab-specific), HRP-conjugated protein A and HRP-conjugated Neutravidin were from Pierce (Rockford, IL). Protein A-coated paramagnetic beads were from Dynal (Lake Success, NY). A MAb against MBP was from New England Biolabs (Beverly, MA). Dialyzed bovine serum albumin (BSA), Tween 20, mannose, hydrogen peroxide and 2,2'-Azino-bis(3-ethylbenzthiazoline-6-sulfonic acid) (ABTS) were from Sigma (St. Louis, MO). Streptavidin was from Roche Diagnostics (QC, Canada), and Mannose α1-2 Mannose was obtained from Dextra Laboratories Ltd (Reading, UK).

Bacterial strains and DNA constructs.

Phage were produced in *E. coli* K91 cells, grown on NZY media supplemented with 20 μg/ml tetracycline and 1 mM isopropyl β-D-thiogalactopyranoside (IPTG) (NZY/ Tet/IPTG), following Bonnycastle *et al.* (30). Electrocompetent, F' *E. coli*

MC1061 cells were transformed with the products of site-directed mutagenesis reactions, and were also used for the production of the phage-displayed peptide sublibrary. *E. coli* strain CJ236 was used to produce phage used as a source of single-stranded viral DNA for site-directed mutagenesis. *E. coli* ER2507 (a gift from New England Biolabs) was used for the production of MBP fusion proteins.

The 2G12.1 peptide sublibrary was constructed in f88-4 phage (351) using single stranded, covalently-closed circular DNA as template, using the procedure described in (30). A degenerated oligonucleotide was synthesized using a two-column "divide-couple-recombine method" described by Haaparanta *et al.* (127). In the resulting library, the amino acids at each position in the peptide sequence were either the original from the 2G12.1 sequence, or a random residue coded by the DNA triplet NNK. Also, the original 2G12.1 DNA sequence was modified to optimize the codon usage for *E. coli.*

Site-directed mutagenesis for the alanine substitutions were made with closed, circular single strand phage DNA as template, essentially as described in (174). The procedure to transfer the peptide coding sequences to pMALX, and the conditions for culture and protein purification have been described by Zwick *et al.* (353). DNA sequencing from partially-purified phage clones was performed with the Thermo Sequenase II Dye Terminator Cycle Kit (Amersham Biosciences, NJ) following the manufacturer's instructions. DNA fragments from the sequencing reactions were resolved using an ABI 373 apparatus and analyzed with EditView 1.0.1 software (ABI).

Screening of the phage-displayed peptide libraries.

The fifteen phage-displayed peptide libraries were mixed in Tris-buffered saline (TBS) containing 1% BSA and 0.5% Tween 20. A total of 10^{12} phage particles were used in the first round of screening. Theoretically, about 60-80 copies of every clone from each library were represented in this mixture. To minimize the selection of protein-A-binding phage, 12 µl of protein-A beads were added to the library mixture, and incubated for 4 hours at 4°C, with gentle shaking. The beads were removed from the phage with a magnet (Dynal) and discarded. IgG 2G12 was added to the remaining phage to a final concentration of 200 nM, and the mixture was incubated at 4°C overnight. Phage-antibody complexes were captured out of solution with 12 µl of protein-A beads for 1 hour at 4°C. The beads were separated from the unbound phage with the magnet and subjected to five washes with 1 ml of TBS containing 0.5% Tween 20. The recovered beads were used to directly infect 75 µl of starved K91 cells (1), and the infected cells were grown for 20 hours at 37 °C in 3 ml NZY/ Tet/IPTG. Amplified phage were partially purified and concentrated by precipitation with PEG/NaCl (1), then re-suspended in TBS containing 0.02% (w/v) sodium azide, and stored at 4°C. A second round of selection was carried out essentially as the first round, but used 10^{10} phage particles from first round, and 2G12 IgG at a concentration of 1 nM. Eluted phage pools were used to infect starved K91, and individual clones were isolated by plating the infected cells on NZY plates supplemented with 40 µg/ml tetracycline and incubation overnight at 37 °C. Independent phage clones were transfer to liquid NZY/ Tet/IPTG media, and grown and purified as described above. Phage concentrations were estimated

by agarose gel electrophoresis as described in (30). PEG-purified phage clones were used for ELISAs and DNA sequencing.

The 2G12.1 sublibrary was subjected to three successive rounds of screening with increasing stringency (200 and 100 nM of 2G12 IgG for rounds one and two, respectively, and 100 nM 2G12 Fab for round three. Phage-IgG complexes were captured out of solution with protein-A beads as described above, whereas Fab-bound phage were captured by protein-A beads coated with goat anti-human IgG (Fab-specific). The isolation of clones was performed as described above.

Enzyme-linked immunosorbent assay (ELISAs).

Phage ELISAs were performed essentially as described in (206, 352). Briefly, $2x10^{10}$ PEG-purified phage particles were adsorbed to microtiter wells at 4°C overnight, followed by blocking with 200 µl TBS containing 2% (w/v) BSA for one hour at 37 °C. The plates were washed three times with TBS containing 0.1% (v/v) Tween 20, and incubated with 50 nM 2G12 for 3 hours at 4°C. The plates were washed six times with cold (4°C) TBS containing 0.1% (v/v) Tween 20, and 35 µl of a 1:500 dilution of protein-A or goat anti-human (Fab specific) antibody conjugated to HRP were added for 2 hours at 4°C. The plates were washed six times with cold buffer, and the reactions were developed at room temperature with 0.03% (v/v) H_2O_2 and 400 µg/ml ABTS in citrate/phosphate buffer (1). Optical density was measured using a Biotek EL 312e plate reader at 405 and 490 nm for up to 45 minutes. Values of absorbance at 405 nm minus absorbance at 490 nm were recorded. Replicate, phage-coated wells were reacted with a rabbit, polyclonal anti-phage antibody to verify that similar amounts of phage particles

were adsorbed to the plate. Bound anti-phage antibody was detected with a protein-A-HRP conjugate (Pierce) and H_2O_2/ABTS. Also, replicate, phage-coated wells were reacted with the conjugates to control for non-specific binding to the secondary reagent. For phage competition ELISAs, 50 nM 2G12 was incubated overnight at 4°C with 300 nM of soluble Ba-L gp120, and then reacted with the phage as described above.

Capture ELISAs with MBP fusions were performed essentially as described by Menendez *et al.* (206). Capture ELISAs with biotinylated, synthetic peptide (2G12.1) were done in an analogous fashion, except that the bound peptide was detected with Neutravidin-HRP (Pierce) and H_2O_2/ABTS. For peptide titration ELISA, 200 ng of 2G12.1 peptide were captured in microwells coated with 1 μg streptavidin, followed by BSA blocking and incubation with 2G12 Fab or IgG as described above. Bound antibodies were detected with a goat anti-human (Fab specific) antibody conjugated to alkaline phosphatase and a substrate solution containing 5mg/ml of p-nitrophenyl phosphate (pNPP) in the manufacturer's recommended buffer. Optical density (OD) was read at 405 nm. For peptide competition ELISAs, 200 ng of the 2G12.1 peptide were captured in each streptavidin-coated microtiter well, and reacted with 2G12 IgG pre-incubated for 16 hours at 4°C with glucose, fructose, mannose, Manα1-2Man and 2G12.1 peptide. Bound antibody was detected with the alkaline phosphatase conjugate. Competitions with gp120 were performed in a similar fashion, except that 100 ng of gp120 (Ba-L isolate) were adsorbed directly to each microwell overnight at 4°C.

Determination of the crystal structure of Fab 2G12-peptide complex.

Human MAb 2G12 (IgG1, κ) and its Fab fragment were produced as described (46). Fab 2G12 was mixed with peptide 2G12.1 at a 5:1 (ligand:Fab) molar ratio. Fab 2G12 + peptide 2G12.1 crystals were grown by the sitting drop vapor diffusion method with a well solution (1 ml) of 1.33 M Na/K phosphate pH 7.8 and 0.2 M isopropanol. For crystallization, 0.6 μl of protein was mixed with an equal volume of reservoir solution. Data were collected at the Advanced Light Source (ALS) beamline 5-1 at 100K. Crystals were cryoprotected by a quick plunge into a reservoir solution containing 25% glycerol. Data for the Fab-peptide complex were reduced in the monoclinic space group $P2_1$ with unit cell dimensions a = 66.0 Å, b = 171.1 Å, c = 119.5 Å, and β = 105.6°. All data were indexed, integrated, and scaled with HKL2000 using all observations >3.0 σ.

The Matthews coefficient (*V*m) for the Fab-peptide complex was estimated to be 3.24 $Å^3$/dalton (corresponding to a solvent content of 62% in the crystal), with four Fab molecules per asymmetric unit. Rotation and translation solutions, using a previously determined 1.75 Å structure of Fab 2G12 as a molecular replacement model, were found using AMoRe. Positional refinement of the four individual Fab molecules in the asymmetric unit gave an overall correlation coefficient of 60.6% and an R-value of 43.4%. The Fab 2G12 + peptide 2G12.1 model building was then performed using TOM/FRODO, and refined with CNS version 1.1 and REFMAC using TLS refinement. Refinement and model building were carried out using all measured data (with $F > 0.0$ σ). Tight noncrystallographic symmetry restraints were applied early on in the model building and released gradually. Electron density maps for model building included 2

$F_{obs} - F_{calc}$ and F_{obs}- F_{calc} maps. An R_{free} test set, consisting of 5% of the reflections, was maintained throughout the refinement.

Affinity determinations.

The affinity of 2G12 for various antigens was studied at the University of British Columbia Centre for Biological Calorimetry, using a Biacore 3000 apparatus (Biacore AB, Uppsala Sweden). The binding-inhibition procedure for in-solution affinity determinations described in (165, 225) was followed for the 2G12.1 synthetic peptide, due to suspected low affinity of interaction, combined with the low molecular weight of the peptide. Peptide 2G12.1 was immobilized at high-density on SA (streptavidin-coated) sensor chips (Biacore) by two sequential injections of 1 μg of peptide. Saturation of the chip was observed after the first injection with a total of ~800 resonance units (RU) captured. The 2F5-binding peptide E4.6 (206), with the amino acid sequence NH_3-LHEESMDKWSNLMQCCTAAEGK(biotin)-NH_2, was immobilized in the reference cell, as a non-specific binding control. Separate reactions of 2G12 IgG mixed with 2G12.1 peptide in buffer HBS-EP (Biacore) were allowed to reach equilibrium by incubation at 4 °C for 20 hours. The final 2G12 IgG concentration was 40 nM, which consistently produced approximately ~100 RU upon injection over the 2G12.1-coated surface. Concentrations of competitor, ranging from 1 mM to 3 μM peptide, were explored in every experiment. After reaching equilibrium, the reactions were injected in duplicate for 100 seconds over the 2G12.1-coated chip at a flow rate of 3 μl/min at 25 °C. Under these conditions, antibody binding is limited by mass transfer; thus the reaction is driven by the free antibody concentration, and is independent of the affinity for the

immobilized ligand (266, 348). Bound antibody was recorded as RU early in the association phase. After each injection, the chip was regenerated with a one-minute pulse of 50 mM NaOH. The concentration of free antibody for each reaction was estimated by comparison of the experimental data with an antibody calibration curve generated with 2G12 IgG concentrations of 2.5 to 80 nM, in the absence of antigen. Free antibody concentrations in the reactions were plotted against their respective competitor concentration, and the curves were fitted to the "in-solution" affinity model provided in the BiaEvaluation 4.1 software (Biacore).

For the 2G12.1 and 2G12.1-D10 MBP fusion proteins, affinity was determined using a kinetic assay. In this case, the kinetic method was favored since some of the the potential complications expected with the 2G12.1 peptide should not apply for the MBP fusions (MW= 52.8 kDa). MAb 2G12 was immobilized on a CM5 sensor chip using the amine-coupling kit supplied by Biacore, and following the manufacturer's instructions. Serial two-fold dilutions of the MBP fusions, from 2 mM to 31 nM, were flowed over the chip for 2 minutes at a flow rate of 50 µl/min at 25 °C. RUs were recorded during the association phase and for the first 20 minutes of the dissociation phase. After each cycle, the surface was regenerated with a 50-µl injection of 3M $MgCl_2$. Data were analyzed using the BiaEvaluation 4.1 software.

RESULTS

Isolation of phage bearing 2G12-binding peptides.

Two consecutive rounds of screening of the primary phage-displayed peptide libraries with 2G12 IgG yielded pools enriched in 2G12-binding phage. Isolation and sequencing of 30 independent clones revealed three distinctive groups of peptide sequences (Table 1): a first group with the consensus sequence QSYP, a second group with the consensus QPCF, and a third group comprising several unrelated sequences. ELISAs with 50 nM 2G12 IgG and control ELISAs without the MAb showed that several clones were reactive with 2G12, but not with the protein-A-HRP conjugate, indicating that the clones are specific for 2G12 MAb, and were not protein A-binders. Clone 2G12.1 had the strongest 2G12 reactivity in the direct ELISA.

To further verify the specificity of the clones, a competition ELISA was performed in which 30 nM 2G12 IgG was incubated with 300 nM HIV-1 gp120 overnight at 4°C, then reacted with selected phage clones. As shown in Table 2, binding 2G12 IgG to gp120 blocked MAb reactivity with clone 2G12.1. This indicates that clone 2G12.1 and gp120 bind to identical, adjacent or overlapping sites on the antibody. In contrast to this, other phage tested showed poor (clones 2, 6 and 15) or no competition (clone 14) with gp120, indicating that their binding to 2G12 occurs at sites other than the antigen-binding site of the antibody. Furthermore, we have previously observed the motif QSYP, in phage from screenings with other antibodies (207), and Jacobs *et al.* (148) have shown that this motif is specifically selected by bovine antibody contaminants present in many MAb preparations. Thus only clone 2G12.1 was further characterized.

Table 1. Deduced amino acid sequence of peptides displayed by phage clones isolated in the screening of the primary phage-displayed peptide libraries with 2G12 IgG.

Clone	Deduced amino acid sequence[(a)]	2G12 ELISA[(b)]	Protein A ELISA[(c)]
2G12.7	VCNH**QSYP**CI(GGPAEGD)	0.28	0.04
2G12.9	G**QSYP**DPLHPDRIAR(AAEGD)	0.29	0.04
2G12.19	S**QSYP**DPILRLPAVA(AAEGD)	0.36	0.05
2G12.15	RCPTVQT**QSYP**NPMCL(AAEGD)	0.36	0.04
2G12.20	TCSN**QSYP**CR(GGPAEGD)	0.32	0.04
2G12.14	Y**QSYPI**(AAEGD)	0.41	0.10
2G12.17	NAF**MSYP**NREIQRSA(AAEGD)	0.25	0.04
2G12.2	QEAMY**ESYP**PPSTYF(AAEGD)	0.43	0.05
2G12.18	QCLE**QSHP**CR(GGPAEGD)	0.16	0.03
2G12.10	KCTR**QSSP**CP(GGPAEGD)	0.22	0.03
2G12.6	TCLKDY**QPCF**(GGPAEGD)	0.50	0.04
2G12.12	HCTSNG**QPCF**(GGPAEGD)	0.31	0.02
2G12.8	SCISDG**QPCF**(GGPAEGD)	0.18	0.03
2G12.1	ACPPSHVLDMRSGTCL(AAEGD)	0.85	0.03
2G12.3	SCPHIPSVCI(GGPAEGD)	0.35	0.03
2G12.5	RFRTGD(AAEGD)	0.28	0.03
2G12.11	NCKWNGLLCR(AAEGD)	0.27	0.03
2G12.4	TCDRTSSPCL(GGPAEGD)	0.24	0.03
f88-4	--	0.15	0.02
gp120	--	1.10	0.02

(a): Consensus sequences are in bold, and the first amino acids from the phage major coat protein are shown in parentheses. *(b)*: reactivity with 50 nM 2G12 IgG, detected with protein A-HRP conjugate and ABTS, values are $OD_{405\text{-}490}$. *(c)*: reactivity with protein A-HRP conjugate as negative control, values are $OD_{405\text{-}490}$.

Table 2. HIV-1 gp120 competes with phage clone 2G12-1 for binding to 2G12 IgG.

Clone[(a)]	Sequence	2G12 IgG[(b)]	2G12 IgG-gp120[(c)]
2G12.1	ACPPSHVLDMRSGTCL(AAEGD)	0.41	0.03
2G12.15	RCPTVQT**QSYP**NPMCL(AAEGD)	0.19	0.11
2G12.14	**YQSYP**I(AAEGD)	0.13	0.13
2G12.2	QEAMY**ESYP**PPSTYF(AAEGD)	0.15	0.09
2G12.6	TCLKDY**QPCF**(GGPAEGD)	0.08	0.04
f88-4	--	0.07	0.03
gp120	--	1.34	0.16

(a): Adsorbed to the microtiter wells. *(b)*: reactivity with 30 nM 2G12 IgG, values are $OD_{405\text{-}490}$.
(c): reactivity with 30 nM 2G12 IgG preincubated with 300 nm gp120, values are $OD_{405\text{-}490}$.

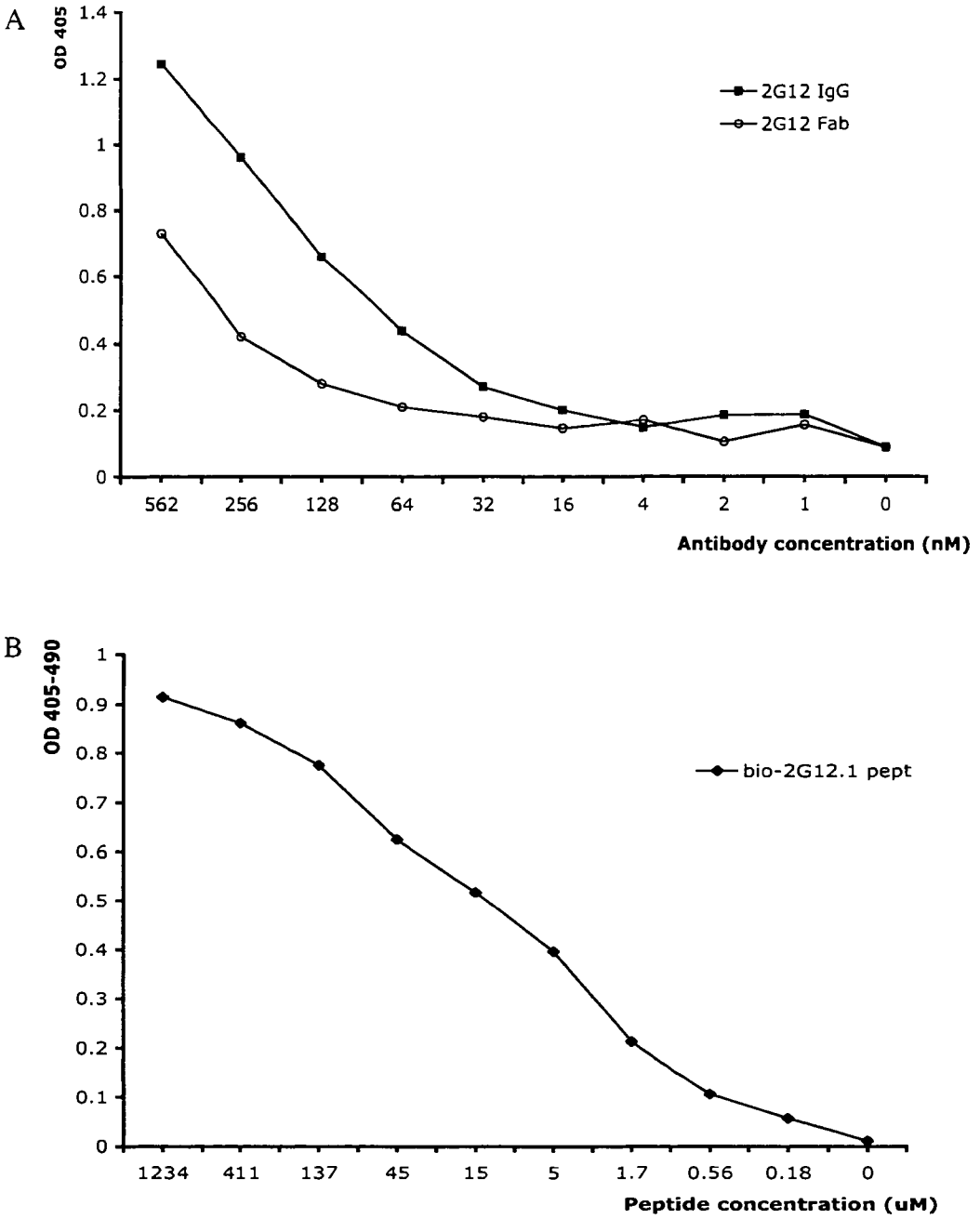

Figure 1. Binding of 2G12 MAb to the bio-2G12.1 peptide. (A) Titration ELISA of bio-2G12-1 peptide captured with streptavidin, and reacted with 2G12 IgG and Fab at the concentrations indicated. Bound antibodies were detected with a goat anti-human antibody conjugated to alkaline phosphatase and pNPP. Values are expressed as optical density at 405 nm. (B) Titration of bio-2G12.1 peptide by capture from solution with plate-adsorbed MAb 2G12. Bound peptide was detected with Neutravidin-HRP and ABTS. Values are expressed as optical density at 405-490 nm.

Synthetic, biotinylated 2G12.1 peptide reacts with MAb 2G12.

A synthetic, biotinylated peptide (2G12.1), with the amino acid sequence NH_3-ACPPSHVLDMRSGTCLAAEGK(bio)-NH_2, was made and tested for binding to 2G12 IgG and Fab. As shown in Figure 1, both the 2G12 IgG and Fab reacted with streptavidin-captured peptide (Figure 1A); furthermore, plate-adsorbed 2G12 IgG captured 2G12.1 peptide out of solution, with a half-maximal concentration of 10 μM (Figure 1B). These results indicate that the antigenic structure of the peptide is maintained in solution, and out of the context of the phage coat. It is noteworthy that the titration curves for IgG and Fab are very similar, most likely as a consequence of the predominantly dimeric nature of our 2G12 Fab preparation (46).

Cyanovirin-N (CVN), an 11-KDa protein isolated from the bacterium *Nostoc ellipsosporum*, binds to high-mannose-type oligosaccharides in the HIV-1 envelope (29, 289). It has been reported that CVN blocks binding of 2G12 to gp120, but in contrast, 2G12 doesn't prevent binding of CVN to gp120, indicating shared oligosaccharide epitopes on gp120, as well as the presence on gp120 of multiple CVN binding-sites (96, 289). In addition to this, CVN and 2G12 have shown partial overlap of their carbohydrate-binding profiles when tested against oligosaccharides captured in microarrays (4, 28). Thus, we decided to investigate if these similarities extend to the 2G12.1 peptide. Reactivity of CVN with the 2G12-1 synthetic peptide was assayed against 2G12.1 synthetic peptide and several MBP fusions bearing optimized derivatives of 2G12.1 (see below) in ELISA. We also tested CVN-2G12.1 reactivity in Biacore, by injection of up to 5 μM CVN over a 2G12.1-coated chip. No binding of CVN was detected with either technique (data not shown). Thus, in spite of the overlap between

CVN and 2G12 in carbohydrate specificity, 2G12.1 peptide failed to react with CVN, indicating that it is specific for MAb 2G12. This specificity of 2G12.1 peptide is further suggested by fact that sera from more than 30 infected donors, though highly-reactive with gp120, do not bind phage bearing the 2G12.1 peptide or derivatives of it (C. Wang, X, Wang, JK Scott, unpublished).

MAb 2G12 binds terminal Manα1-2Man groups present in a cluster of high-mannose carbohydrates in the silent face of HIV-1 gp120 (277, 289). 2G12 also reacts with less complex sugars like mannose and Manα1-2Man, albeit with lower affinity (46, 289). We decided to investigate whether 2G12 binding to the 2G12.1 peptide could be blocked by carbohydrates, as an indication of the degree to which 2G12.1 occupies the carbohydrate-binding sites of MAb 2G12. The peptide was captured in streptavidin-coated microtiter wells and reacted with 100 nM 2G12 IgG pre-incubated with glucose, fructose, mannose or 2G12.1. The results in Figure 2 (open symbols) show that pre-incubation of 2G12 with mannose, fructose or 2G12.1 peptide, blocks the IgG's ability to react with 2G12.1 peptide, whereas the negative control, glucose, had no effect on antibody binding. Furthermore, a concentration of 64 μM Manα1-2Man, reduced 2G12 binding to the peptide by 75%, whereas 300 nM gp120 completely ablated binding (data not shown). An analogous experiment, using plate-adsorbed gp120 and 1 nM 2G12 IgG (Figure 2, closed symbols) shows the same inhibition pattern for glucose, mannose and fructose. Manα1-2Man at 64 μM concentration caused only a 50% reduction in binding to gp120. However, pre-incubation of 2G12 IgG with 1 M 2G12.1 peptide caused only a modest reduction (30%) in gp120 binding. Nevertheless, from these experiments it can be concluded that binding of mannose, fructose and Manα1-2Man to MAb 2G12 prevents

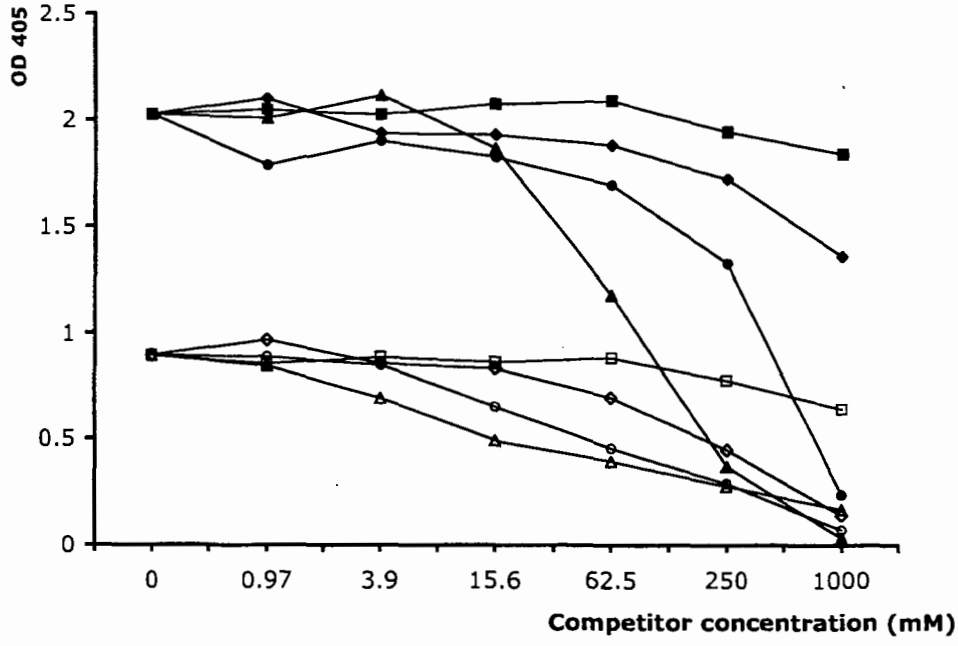

Figure 2. Inhibition of 2G12 binding to bio-2G12.1 peptide (open symbols) and to gp120 (solid symbols) in the presence of monosaccharides and bio-2G12.1 peptide. Binding of 2G12 was assayed after pre-incubation of 1 nM or 100 nM IgG (for gp120 and peptide binding assay, respectively) with serial dilutions of mannose (circles), fructose (triangles), bio-2G12.1 peptide (diamonds) and glucose (squares). Values are expressed as optical density at 405 nm.

its interaction with 2G12.1 peptide, as well as to gp120, thus suggesting that carbohydrates and the peptide bind in the same or overlapping site on 2G12.

The affinity of 2G12 IgG for the 2G12.1 peptide was determined by surface plasmon resonance (SPR) using an "in-solution" inhibition method. The results from Figure 1A suggested a low affinity of interaction, also, preliminary experiments using a KinExA instrument revealed a Kd at equilibrium of 180 μM (data not shown). SPR experiments showed that the affinity of 2G12 for the 2G12.1 synthetic peptide was 200 μM (Table 3), very similar to that found by KinExA and in contrast with the half-maximal binding of 10 μM observed in titration ELISA (1B).

Crystal structure of the 2G12.1 peptide in complex with the 2G12 Fab.

The crystal structure of Fab 2G12 bound to the 2G12.1 peptide was determined at 2.75Å resolution (Table 4). The crystal showed strong anisotropic diffraction, which is reflected in the overall anisotropic B values. As previously observed, Fab 2G12 is in an unusual conformation in which two parallel Fab molecules exchange their variable heavy domains, creating a tightly-packed dimer of Fabs. This domain-swapped architecture has been shown to be the functional, and therefore biologically relevant, conformation of the 2G12 antibody (46).

As shown in Figure 3, the cyclic 2G12.1 peptide is clearly observed bound to both Fabs of the domain-swapped dimer. The 2G12.1 peptide does not bind within the primary carbohydrate-binding site of 2G12, but rather adjacent to it. Eighteen of the peptide residues could be reliably built into the electron density, using the first alanine (Ala1) residue and long C-terminal strand (starting at Leu16) to set the register of the cyclic

Table 3. Association and dissociation rates (k_a and k_d, respectively), and association and dissociation constants at equilibrium (Ka and Kd, respectively), for synthetic bio-2G12.1 peptide (2G12.1 peptide), 2G12.1 and 2G12.1-D10 MBP fusion proteins, determined by SPR. (a) kinetic data fitted with the 1:1 (Langmuir) binding model; (b) kinetic data fitted with the "two stages reaction (conformation change)" model.

(a)

Reactants	Sequence	k_a (1/Ms)	k_d (1/s)	Ka(1/M)	Kd (M)	χ^2
2G12.1 peptide[¶]	H-ACPPSHVLDMRSGTCLAAEGK(bio)-NH_2	n.a.	n.a.	5.0×10^3	2.0×10^{-4}	8×10^{-18}
2G12.1-MBP	ACPPSHVLDMRSGTCL-**MBP**	12.9	3.6×10^{-4}	3.6×10^4	2.8×10^{-5}	1.01
2G12.1.D10-MBP	ACPPSH**Y**LDM**K**SGTC**R**-**MBP**	1.6×10^3	5.0×10^{-4}	2.5×10^6	4.0×10^{-7}	5.96

¶ Results for bio-2G12.1 peptide are from equilibrium experiments; other data are from kinetic assays.

(b)

Reactants	Sequence	k_a1	k_d1	k_a2	k_d2	Kd(M)*	χ^2
2G12.1-MBP	ACPPSHVLDMRSGTCL-**MBP**	16.4	9.4×10^{-4}	1.6×10^{-3}	3.4×10^{-5}	1.2×10^{-6}	0.88
		$KD_1 = 5.7 \times 10^{-5}$		$KD_2 = 2.1 \times 10^{-2}$			
2G12.1-D10-MBP	ACPPSH**Y**LDM**K**SGTC**R**-**MBP**	1.4×10^3	4.7×10^{-3}	5.3×10^{-3}	6.3×10^{-4}	3.4×10^{-7}	1.74
		$KD_1 = 3.3 \times 10^{-6}$		$KD_2 = 1.2 \times 10^{-1}$			

* Apparent dissociation constant.

Table 4. Summary of crystallographic data and refinement statistics.

Data Collection

Wavelength (Å)	1.0
Resolution (Å)	50-2.70
No. of molecules in asymmetric unit	4
No. of observations	222449
No. of unique reflections	71495
Completeness (%)	98.3 (95.5)
R_{sym} (%)	11.8 (58.4)
Average I/σ	14.2 (2.0)

Refinement statistics (all reflections > 0.0σF)

Resolution (Å)	50-2.70
Total no. of reflections used	65232
No. in test set	3488
No. of Fab atoms	13,120
No. of ligand atoms	500
Ramanchandran plot (%)	
Most favored	78.0
Additionally allowed	19.6
Generously allowed	1.5
Disallowed	0.9
Rms deviations	
Bond lengths (Å)	0.030
Angles (°)	2.780

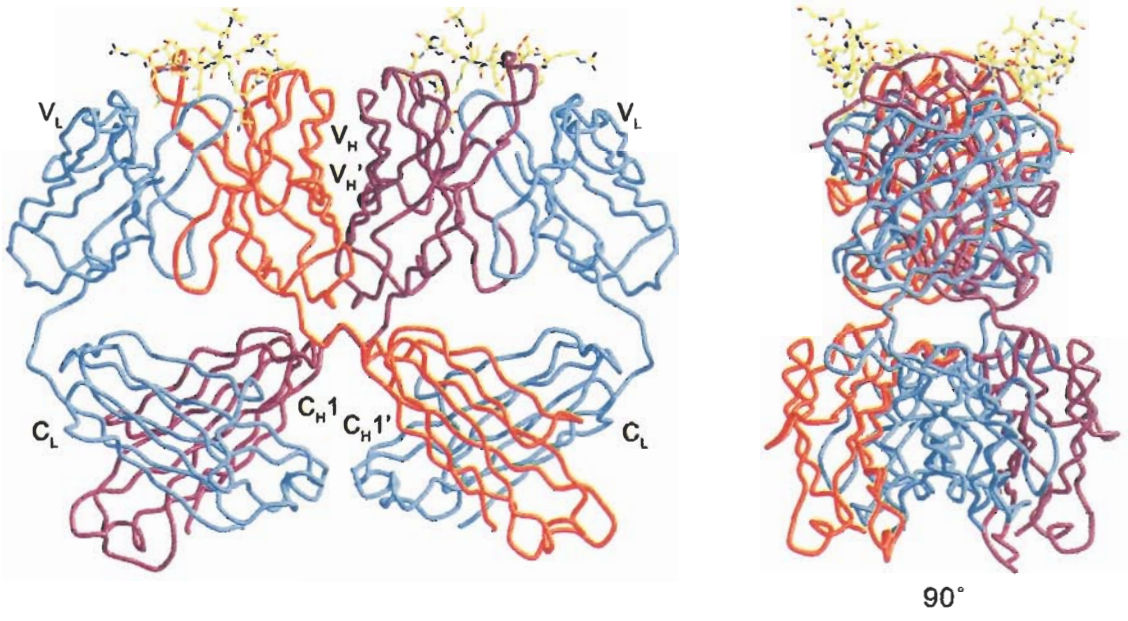

Figure 3. Overall structure of the Fab 2G12 dimer bound to bio-2G12.1 peptide. Each Fab molecule has one 2G12.1 moiety bound near the primary carbohydrate-binding site. Both light chains are shown in cyan, the heavy chains from the separate Fabs are shown in red and purple.

peptide (Figure 4). The cyclic conformation of the 2G12.1 peptide is stabilized by a disulfide bridge between residues Cys2 and Cys15, as well as two turns and several hydrogen bonds. These hydrogen bonds are mostly in the two major turns (Pro3O:His6N, Pro4O:His6ND1, Val7N:Leu16O, Asp9OD2:Ser12OG, Arg11O:Ser12OG, Ser12O:Ser12OG, Ser12O:Thr14N and Thr14OG1:Cys15O). The most significant of these interactions involve residues His6 and Ser12, which form residue-to-backbone hydrogen bonds across the turns, with Pro3 and Asp9, respectively, and are underlined above.

Overall, two segments of the cyclic 2G12.1 peptide, comprising about half of it, face the antibody (Figure 5). A total of 454 $Å^2$ of the Fab's molecular surface and 386$Å^2$ of the peptide's molecular surface are buried in the complex. Two hydrogen bonds and 61 van der Waal interactions are present between Fab 2G12 and the 2G12.1 peptide. The two hydrogen bonds occur between backbone nitrogens of peptide residues Ala1 and Cys2 and the side chains of the H2 loop residues AspH59 and TyrH57, respectively. The bulk of the van der Waal interactions and buried molecular surface contributed from the 2G12.1 peptide, belong to the residues on the side of the cyclic peptide facing the Fab. These residues include Ala1-Pro3 and Met10-Cys15. In addition, Leu8, which is on the side of the cyclic peptide facing away from the Fab, faces down and towards the antibody, its side chain contributes to the peptide-Fab interaction. The peptide contacts the CDR loops L1, L3, H2, and H3. A schematic representation of the intra-peptide and Fab-peptide interactions is shown in Figure 6.

The conformation of the primary combining pocket of 2G12 is slightly perturbed in the Fab-peptide complex relative to its conformation in the $Man_9GlcNAc_2$- and the

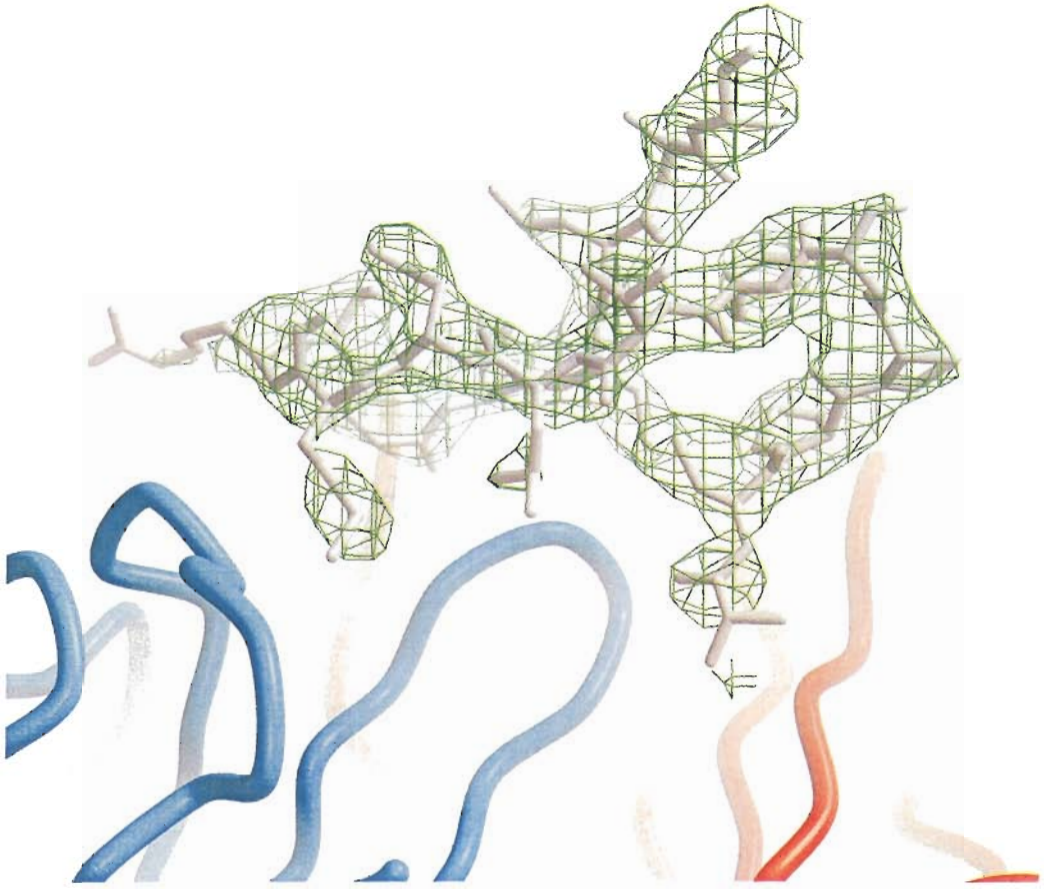

Figure 4. Peptide bio-2G12.1 bound to 2G12 Fab. The corresponding $2F_{obs}$-F_{calc} electron density for the peptide is also shown contoured at 1.6σ. The peptide is in gray, the 2G12 light chain in cyan and heavy chain in red.

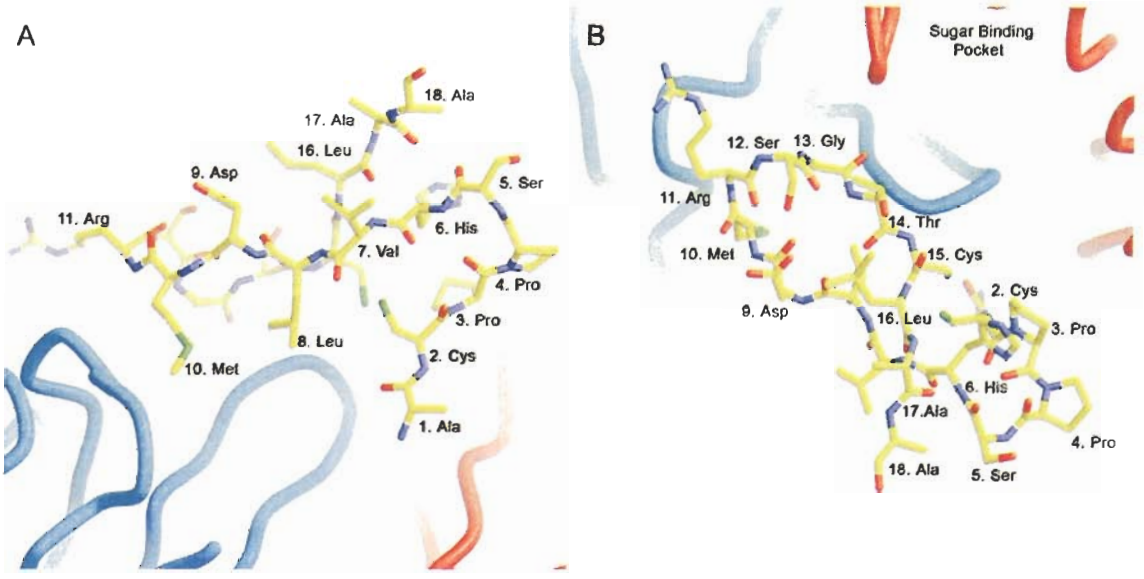

Figure 5. (A) Side view of the bio-2G12.1 peptide-Fab complex. (B) Top view of the peptide bound adjacent to the primary sugar-binding pocket of Fab 2G12.

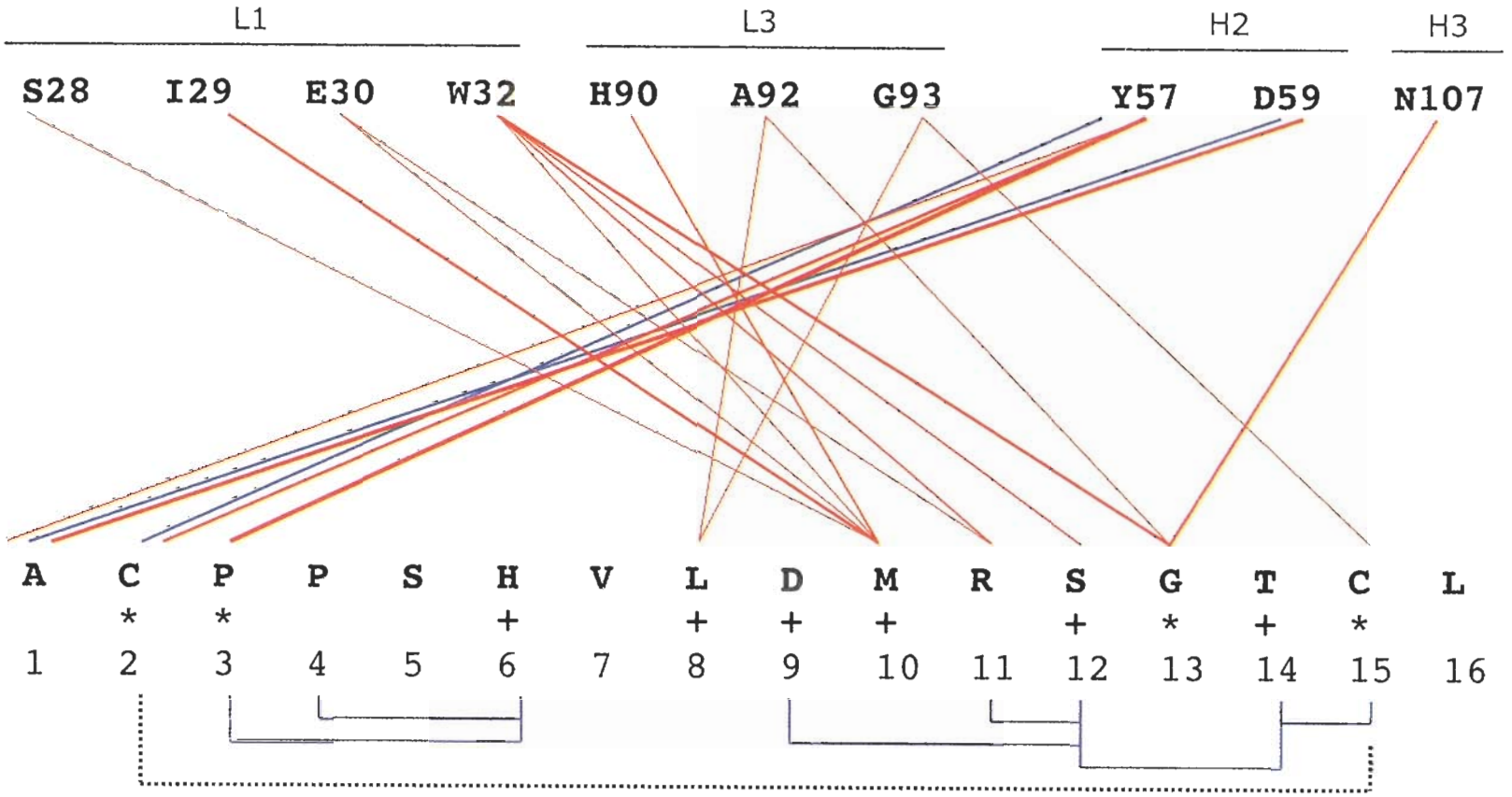

Figure 6. Schematic representation of direct contacts between bio-2G12 peptide and 2G12 Fab (top panel) and intrapeptide hydrogen bonds (bottom panel). Red lines represent van derWaal interactions, blue lines represent hydrogen bonds, and the dotted black line represents the intrapeptide disulfide bridge (the Ser12O:Ser12OG hydrogen bond is not shown here). Thin lines represent 1 to 4, and thick lines represent 5 to 10 pairs of contacting atoms. Peptide residues critical for binding to 2G12 are indicated by *; important residues are indicated by +.

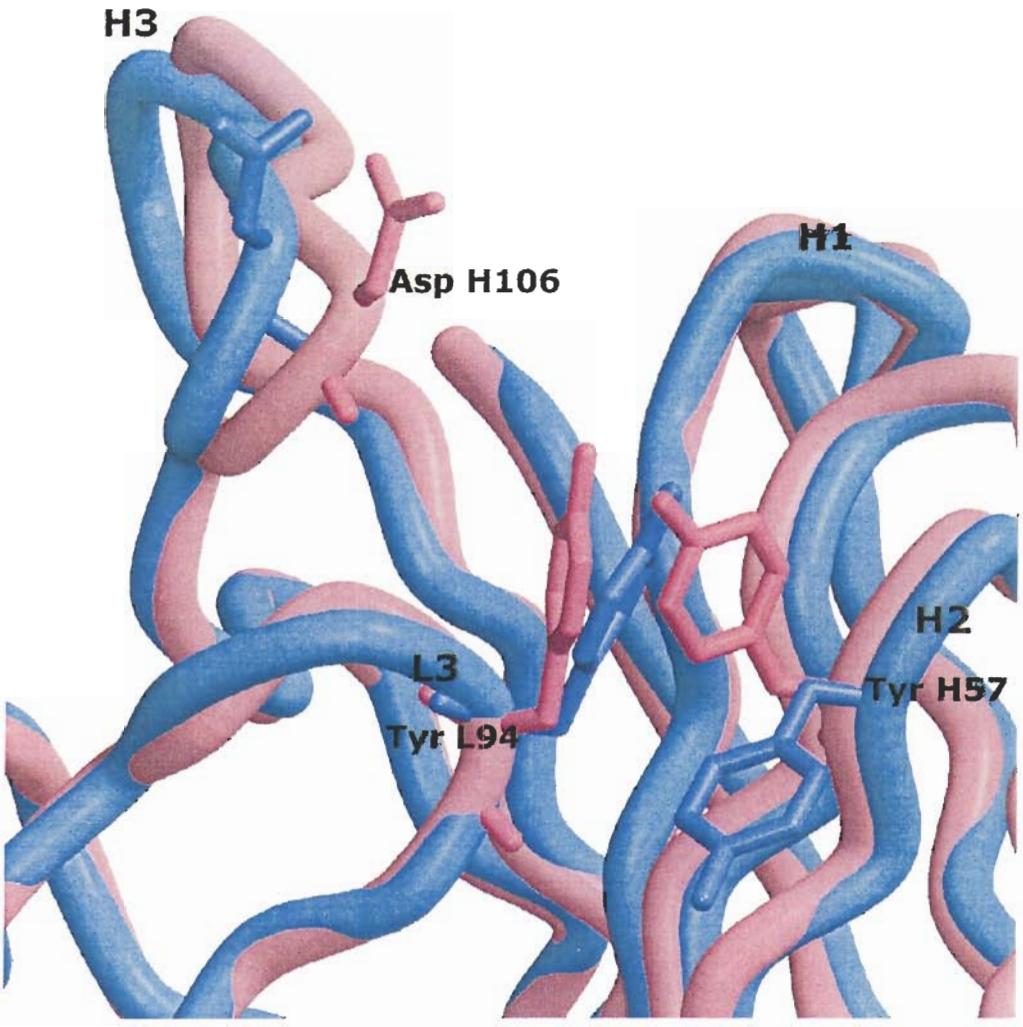

Figure 7. Alignment of the 2G12 structure around the CDRs H1, H2, H3 and L3, from the Fab-peptide complex (blue), and 2G12- $Man_9GlcNAc_2$ complex (purple). TyrH57 side chains are in different rotamers. TyrL94 of the L3 loop, and the displacement of AspH106 carbon and side chain are also shown.

Manα1-2Man-bound structures (Figure 7). TyrH57 in the H2 loop of 2G12 hydrogen bonds to the 2G12.1 peptide, this tyrosine side chain is in a different rotamer, facing up in most of the solved 2G12 structures, in which it pressed up against TyrL94 of the L3 loop which makes up part of the primary mannose binding-site (46). Thus by affecting TyrL94, TyrH57 has an indirect role in sugar binding. A displacement of about 2.2Å is observed for GlyL93, AspH102 and AspH106 backbones, between the 2G12.1- and the $Man_9GlcNAc_2$-bound structures. These displacements are less obvious if the 2G12.1-bound is compared with the Manα1-2Man-bound structure, suggesting that they may be functionally irrelevant.

Optimization of peptide 2G12.1 sequence.

Results from KinExA and Biacore experiments revealed a low-affinity interaction between the 2G12.1 peptide and the antibody. With the objective of optimizing the affinity of clone 2G12.1, we built a phage-displayed peptide sublibrary of 10^9 independent clones. Table 5 shows the results from screening the library with 2G12 IgG and Fab. Clones with a range of reactivities for 2G12 were isolated (clones 1, 2, 5 and D3, D10, respectively), as well as clones that conserve the parental sequence (clones 3 and 10). The majority of selected sequences differed in only one or two residues from the parental clone 2G12.1.

We have previously observed that the apparent affinity of phage clones in ELISA can be influenced by the amount of peptide displayed on the surface of the phage (unpublished results). Since our display system is highly multivalent (up to ~300 copies of peptide/phage particle), large differences in peptide copy number between different

Table 5. Deduced amino acid sequence of peptides displayed by phage clones isolated in the screening of the 2G12.1 sublibrary.

Clone	Deduced amino acid sequence[(a)]	2G12 binding[(b)]
2G12.1-1	**S**CP**SSS**VLDMRSGTCL	-/+
2G12.1-2	ACPP**H**HVLDM**P**SGTCL	-/+
2G12.1-5	ACPPS**TA**LDMRSGTC**K**	-/+
2G12.1*	ACPPSHVLDMRSGTCL	+
2G12.1-3*	ACPPSHVLDMRSGTCL	+
2G12.1-10*	ACPPSHVLDMRSGTCL	+
2G12.1-6	**T**CPPSHVLDMR**R**GTCL	++
2G12.1-C11	**Q**CPP**T**HVLDMRSGTCL	++
2G12.1-D11	**G**CPP**TL**VLDMRSGTCL	++
2G12.1-8	ACPPSHVLDMRSGTC**V**	+++
2G12.1-4	ACPPSHVLDMRSGTC**I**	+++
2G12.1-9	**G**CPP**T**HVLDMRSGTCL	+++
2G12.1-C2	**G**CPPSHVLDMRSGTCL	+++
2G12.1-C12	**G**CPPSH**R**LDMRSGTC**I**	+++
2G12.1-D3	**S**CPPSHVLDMRSGTCL	++++
2G12.1-D10	ACPPSH**Y**LDM**K**SGTC**R**	++++

(a) Amino acids different from the parental 2G12.1 clone are in bold.
(b) Relative binding to 2G12 IgG with respect to the parental clone 2G12.1, as determined by phage ELISAs.
* Same sequence as the 2G12.1 parental clone.

clones are possible. Furthermore, the bivalent binding of IgG may mask differences in peptide affinity, due to the avidity effect. Thus the coding sequences of several peptides (2G12.1, 2G12.1-4, 2G12.1-D3 and 2G12.1-D10) were cloned into the MBP gene, expressed and purified as MBP-fusion proteins, using the system developed by Zwick *et al.* (353). The purity and the monomeric status of the MBP fusion proteins were verified by non-reducing SDS-PAGE (not shown). The binding of MBP fusions to 2G12 IgG was tested by a capture ELISA with plate-adsorbed antibody, in which binding occurs in a monovalent fashion. The results shown in Figure 8 confirmed that the sublibrary clones 2G12.1-4, 2G12.1-D3 and 2G12.1-D10 bound MAb 2G12 more tightly than the parental 2G12.1, with clone 2G12.1-D10 showing the highest signal, thus revealing a binding-optimized peptide.

The affinity of 2G12 IgG for recombinant fusions 2G12.1-MBP and 2G12.1-D10-MBP was determined by SPR, using a kinetic method (Table 3). Control injections of purified, recombinant MBP (New England Biolabs, Beverly, MA) ruled out any detectable interaction of 2G12 with the carrier (MBP) domain of the protein (data not shown). The sensorgrams were fitted to the 1:1 (Langmuir) binding model provided in the BiaEvaluation 4.1 software. As described for other phage-display derived peptides (206, 282), the 2G12.1-MBP fusion protein displayed a higher affinity than the 2G12.1 synthetic peptide, in this case by almost one order of magnitude ($Kd_{MBP\ fusion}$ = 28 μM *vs.* $Kd_{synt.pept}$ = 200 μM). However, only a modest fit could be obtained for 2G12.1-D10-MBP with the 1:1 (Langmuir) binding model (χ^2= 5.96), which produced a Kd of 400 nM, almost two orders of magnitude lower than that of 2G12.1-MBP (Table 3a). Since the fit to the 1:1 binding model was not optimal, and the residual plots show non-dispersed

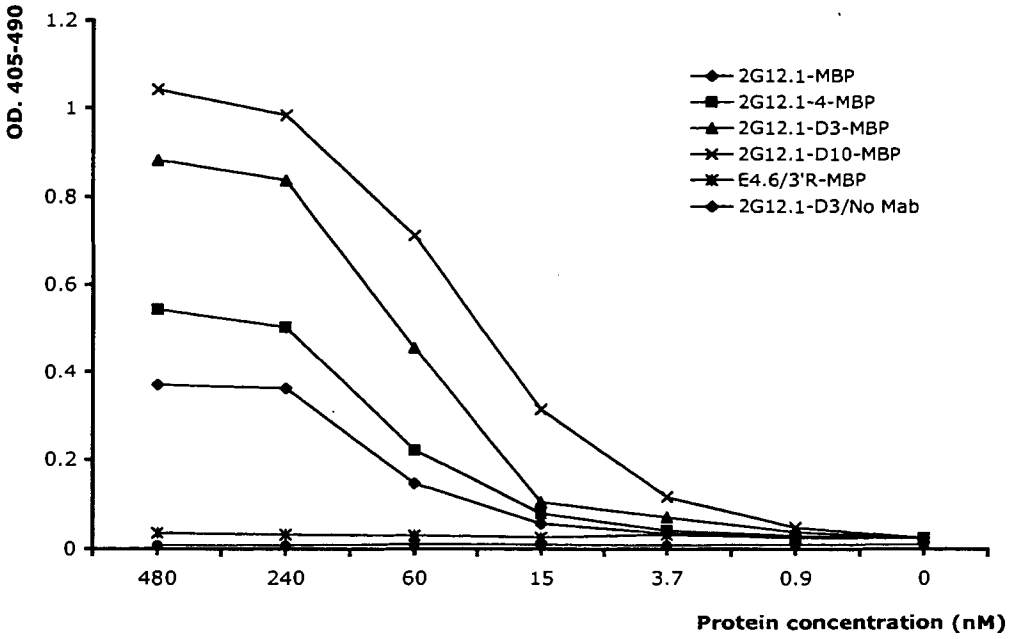

Figure 8. Titration ELISA on MBP fusions produced from 2G12.1 sublibrary clones. 2G12 IgG was adsorbed to microwells and used to capture MBP fusion proteins from solution at the concentrations indicated. Bound proteins were detected with a biotinylated anti-MBP MAb, and Neutravidin-HRP and ABTS. E4.6 is a 2F5-specific MBP fusion used as negative control. Values are expressed as optical density at 405-490.

deviations from the model (not shown), the two sets of data were fitted to other affinity models available on the BiaEvaluation 4.1 software. The "two-stages reaction" model produced a much better fit for the 2G12.1-D10-MBP data (χ^2= 1.32, Table 3b); however, only a slight improvement was observed for the 2G12.1-MBP fit ($\chi^2_{Langmuir}$ = 1.01 *vs.* $\chi^2_{two\ stages}$ = 0.88). Using this model, the overall Kd for the 2G12.1-D10-MBP was 340 nM, only slightly lower than the 400 nM calculated with the 1:1 (Langmuir) binding model. Taken together these analyses produced Kd ranging from 1.2 μM to 28μM for 2G12.1-MBP and 340 nM to 400 nM for the 2G12.1-D10-MBP.

The "two-stages reaction" model describes a 1:1 binding of analyte to immobilized ligand, followed by a reversible conformational change in the complex, which can be expressed as A + B = AB = AB* (23). The model produces two sets of association and dissociation rates, (k_a1/k_d1, and k_a2/k_d2), which correspond to the first (A + B = AB) and the second (AB = AB*) stages of the reaction, respectively. Poor fit to the 1:1 (Langmuir) model, accompanied with good fit to the "two stages model" may be interpreted as an indication of complex binding dynamics. Interestingly, poor fit with the 1:1 (Langmuir) binding model was also observed by Dudkin *et al.*, in SPR assays of 2G12 binding to dimeric Man_9 glycopeptides (89). Their sensorgrams bear strong resemblance to ours, with two apparent association phases and two apparent dissociation phases (not shown). However, deviations from the Langmuir model are often observed in systems conforming with the assumed 1:1 stoichiometry, most frequently because of heterogeneity of the ligand as a result of the immobilization procedure (227). Thus, more intricate binding kinetics than the 1:1 (Langmuir) model can't be assigned based solely on SPR data; instead they must be verified by other methods. Thus, while our data fits a two-

stage model, the possible relevance of this to the mechanism of peptide binding is unclear.

Critical binding residues on the 2G12.1 peptide.

Single substitutions of every residue of the 2G12.1 sequence were generated by site-directed mutagenesis in the context of the phage. Most amino acids were changed to alanine with the exception of Ala1, which was changed to Gly, and Cys2 and Cys15, which were changed to Ser. PEG/NaCl-purified phage were assayed for binding to 2G12 IgG in ELISA using two concentrations of IgG. The results, expressed as % 2G12 binding of the 2G12.1 wild type, are shown if Figure 9.

Several types of substitutions can be identified based on their effect on 20 and 5 nM 2G12 IgG binding: (*i*) substitutions that do not affect reactivity or have only a modest effect (Ala1, Pro4, Ser5, Val7, Arg11 and Leu16), (*ii*) substitutions that have a significant effect (His6, Leu8, Asp9, Met10, Ser12 and Thr14), and (*iii*) those that ablate binding and thus define residues that are critical for binding (Cys2, Pro3, Gly13, Cys15). These results are in good correspondence with those shown in Table 5 for the clones selected from the 2G12.1 sublibrary. Most sequence differences from the 2G12.1 parental clone are concentrated at sites that are not strongly affected by amino acid substitutions.
We have previously observed that moderate binding differences between phage clones may go unnoticed in an IgG-based assay, most likely due to bivalent binding of IgG to multicopy peptide on the phage, whereas those differences become apparent if the assay is performed with Fab (206). This could not be done, since our preparation of 2G12 Fab is composed of 80-100 % dimer, and is therefore mainly bivalent (46). Thus, it is possible

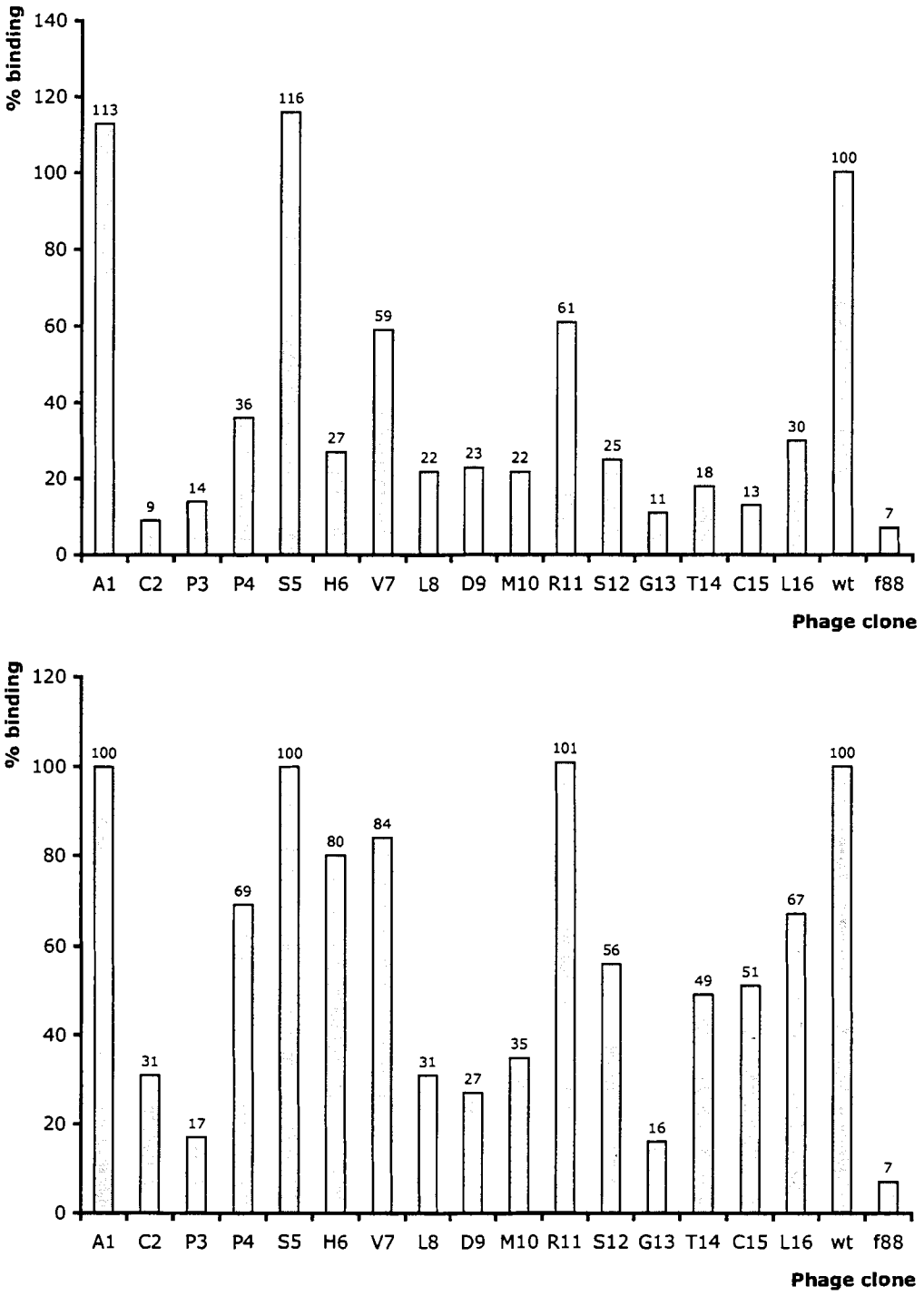

Figure 9. Alanine-substitution scanning of the 2G12.1 peptide in the context of the phage. The relative binding of 20 nM (top) and 5 nM (bottom) 2G12 IgG to the alanine substituted phage is expressed as % binding of each mutant phage with respect to wild-type (wt) 2G12.1 phage. The f88 is a negative control for wild-type phage expressing no peptide.

that were a monovalent fab available for assay some of the substitutions conferring only a significant effect in our assay, may actually define additional critical binding residues.

DISCUSSION

Our results show that the 2G12.1 peptide is not a mimic of the 2G12 oligomannose epitope on gp120. The peptide binds to Fab 2G12 at a site near to, but different from the primary carbohydrate-binding site, as evidenced by the crystal structure presented here. Furthermore, binding to Manα1-2Man and peptide occurs through different antibody-ligand contacts; MAb 2G12 contacts Manα1-2Man through 16 amino acids, 14 of which are located in the VH (46), whereas only ten antibody residues, all located on the CDRs, and most from the VL domain, are involved in contacting nine residues on the 2G12.1 peptide (Figure 6).

Nonetheless, competition ELISAs between peptide and mannose, fructose and Man α1-2Man (Figure 2) showed that pre-incubation with the sugars inhibits subsequent 2G12 binding to 2G12.1, similar to their inhibition of binding to gp120. Only partial inhibition of 2G12 binding to gp120 was observed upon preincubation of 2G12 with a high concentration of 2G12.1 peptide (1 M). This may be explained by the differences in affinity of MAb 2G12 for 2G12.1 peptide and gp120 (micromolar *vs.* nanomolar), which would favor 2G12 binding to the plate-adsorbed gp120 in the competition ELISA. In addition, the 2G12 dimer has four combining sites for the $Man_9GlcNAc_2$ moieties present in gp120, whereas the 2G12-2G12.1 peptide co-crystal structure shows peptide bound only to two sites on the Fab dimer (at the VH-VL interface). Thus, there is the possibility that residual interaction of gp120 $Man_9GlcNAc_2$ with the secondary binding sites on

2G12 (at the VH-VH interface) allows binding to gp120, and thus blocks the peptide binding indirectly. The structure of the Fab-peptide complex illustrates how 2G12.1 can compete with large oligomannose structures on gp120 for binding to 2G12. The superimposition of the peptide-Fab structure with the previously-determined structure of Fab in complex with $Man_9GlcNAc_2$ (46), suggests that the D2 and D3 arms of $Man_9GlcNAc_2$ would sterically clash with the 2G12.1 peptide, if they were bound simultaneously (not shown).

Steric hindrance, however does not explain why smaller molecular-weight sugars like mannose, fructose or Manα1-2Man inhibit 2G12 binding to 2G12.1 peptide; the basis for this inhibition remain unclear. Superimposition of the Manα1-2Man- and the 2G12.1 peptide-bound structures shows that Manα1-2Man and the peptide do not occupy the same space (not shown); furthermore, there is minimal overlap between the footprints of Manα1-2Man and the 2G12.1 peptide on the 2G12 paratope (Figure 10). Nonetheless, two Fab contacts are shared between Manα1-2Man and 2G12.1: GlyL93 (CDR L3) and AsnH107 (CDR H3) (see Figures 6 and 10). Thus it is possible that once engaged in an interaction with one ligand (the saccharide or the peptide), GlyL93 and AsnH107 would no longer be available to contact a second ligand, and thereby prevent binding. If this is the case, it can be predicted that mutations on 2G12 GlyL93 and/or AsnH107 would significantly decrease the reactivity of 2G12 with the 2G12.1 peptide. In support of this explanation, alanine substitution of the AsnH107 on the Fab causes a 1000-fold drop in reactivity with gp120, indicating that AsnH107 is important for binding to the carbohydrates on gp120 (46). On the other hand, alanine substitution of GlyL93 does not affect binding (46). Alternatively, we can speculate that binding to the peptide and the

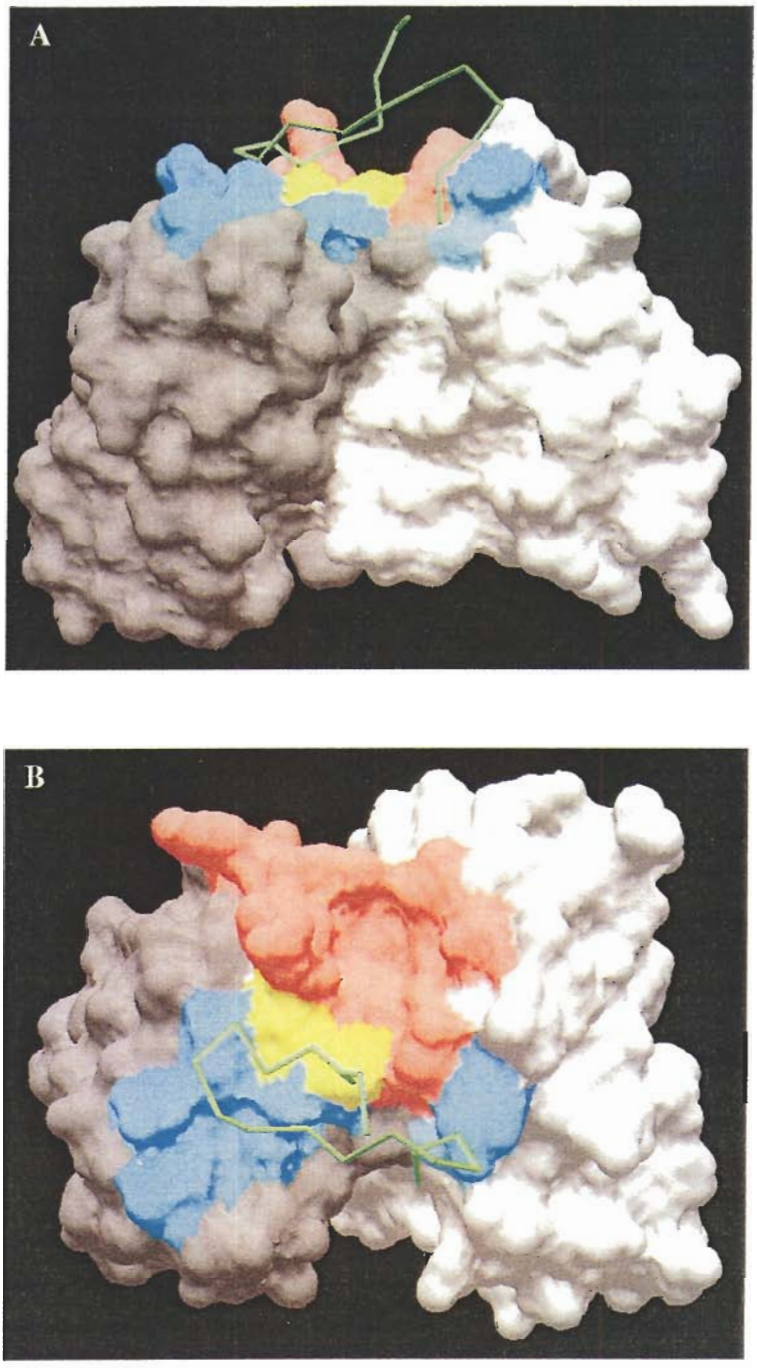

Figure 10. Molecular surface representation of a 2G12 monomer showing antibody areas in contact with 2G12.1 peptide (cyan) and Manα1-2Man (pink), residues that contact both ligands are in yellow. The backbone of 2G12.1 peptide is shown in green. (A) side view; (B) top view. The antibody light chain is shaded in dark gray, the heavy chain in lighter gray. Contacts with Manα1-2Man were taken from Calarese *et al.* (46). Contacts with 2G12.1 peptide are from this work. Figure prepared with Swiss PDB Viewer.

carbohydrates requires different, and probably mutually-exclusive structures of the 2G12 paratope, which may allosterically perturb one another. However, a comparison between the antibody's backbone in the 2G12.1-bound and the Manα1-2Man-bound structures did not provide much support for this idea, since only slight differences of the carbohydrate-binding site were observed between these two structures (not shown).

Alanine substitutions along the 2G12.1 peptide sequence demonstrated that nearly all of the residues in the peptide are somehow important for 2G12 binding. The amino acids least critical for 2G12 binding are Ser5, Val7, and Arg11, which correlates well with the crystal structure. Peptide residues Ser5 and Val7 are both found on the side of 2G12.1 that is away from the Fab, and make no interactions with it. In addition, these side chains do not play a role in any of the internal hydrogen bonds of 2G12.1. Arg11, though calculated to make van der Waal interactions with Fab 2G12, has poorly defined electron density, and therefore these interactions may be insignificant. The frequent substitutions of those residues in phage clones selected from the sublibrary screening (Table 5) also supports this.

The residues in the 2G12.1 peptide that are most critical for 2G12 binding are Cys2, Pro3, Gly13 and Cys15. Cys2 and Cys15 form the disulfide bond, giving 2G12.1 a cyclic structure. Not only do Pro3 and Gly13 make van der Waal contacts with Fab 2G12, but they also appear in the turns of the cyclic peptide; thus their unique phi/psi restraints (or lack of in the case of Gly13) most likely play an important role in its overall structure. In summary, many of the peptide residues are important for Fab binding because they play a role in contacting the Fab directly (through hydrogen bonding or van der Waal interactions), or in stabilizing the peptide's structure, whether by forming the

disulfide bond, internal hydrogen bonds, or conferring specific phi/psi restraints on the turns.

The results reported here are in keeping with the findings of Vyas *et al.* (330) for an octapeptide ligand of the SYA/J6 antibody. Neither of the two peptides are structural mimics of their cognate carbohydrate antigens, but bind to the antibodies using different contacts. In that study, the peptide binds to the carbohydrate-combining site on the antibody, with the same affinity as the pentasaccharide, but the contacts and the thermodynamics of binding are different (330). A third structure, of a peptide ligand bound to MAb 2H1, a protective antibody directed against the glucoronoxylomannan (GXM) of *C. neophormans*, has been reported by Young *et al.* (346). Although there is no carbohydrate-bound structure to compare with in this case, there is indirect evidence suggesting that this peptide is not a structural mimic of GXM. In the structure, most peptide-antibody interactions are established with the VL, however immunizations with the peptide elicited antibodies with the same or related VL genes but VH genes different from 2H1. None of those antibodies crossreacted with GXM, indicating that the usage of the proper VH is critical for reactivity with the carbohydrate (321).

Multiple groups have isolated peptide ligands for antibodies against carbohydrate antigens in pathogens, in most cases, as an attempt to overcome the poor immunogenicity of carbohydrates (132, 181, 247, 250, 260, 320). While this approach assumes that peptides can act as structural mimics of carbohydrates, the structural studies mentioned above indicate that this is probably a rare occurrence. Very likely, most, if not all the peptides isolated are functional rather than structural mimics, and therefore, it is very unlikely that they can be effective immunogens for conventional immunization strategies.

The structure described here provides an opportunity for structure-based design of immunogens to elicit 2G12-like antibodies; for example to design high affinity glycopeptides that would span both the peptide- and the mannose-binding site of the antibody. In addition, further affinity improvements may be obtained by composite peptides, as suggested by modeling a Ser in position 1 (as in clone 2G12.1-D3) in the structure of 2G12.1 peptide, which indicates the establishment of at least one additional hydrogen bond with the antibody. A significant effort is being made by others to develop synthetic carbohydrate immunogens, to elicit 2G12-like, neutralizing antibodies (89, 115, 185, 194, 333), yet most compounds suffer from the handicap of a low affinity of interaction with 2G12. Monomeric $Man_9GlcNAc$ and $Man_9GlcNAc_2$-Asn have an ELISA IC_{50} of 0.95 mM; whereas a tetrameric oligomannose cluster, synthesized on a galactopyranoside scaffold, has an IC_{50} of 13 μM (333). A trimeric $Man_9GlcNAc_2$-Asn structure, assembled on cholic acid, has produced an IC_{50} of 21 μM (185). Our affinity studies show that we can achieve Kds ~ 400 nM, for an optimized sequence fused to MBP. Thus a strategy of glycopeptide design based on the peptides presented here, or their derivatives, could provide a significant starting affinity boost, based on the antibody's specificity for the peptide domain.

AKCNOWLEDGEMENTS

This work was supported by NIH/NIAID grants R21-AI49808 and RO1AI49111. A. M. was supported by a Graduate Scholarship from the Michael Smith Foundation for Health Research, BC, Canada, and a Canada Graduate Scholarship from the Natural Sciences and Engineering Research Council, Canada. We thank A. Burguess, B.

Vanderkist and S. Wu for technical assistance. We are grateful to T. Fouts (Institute of Human Virology, Baltimore, MD), J. McMahon, (NCI-Frederic, MD), B. Johnston (SFU), the MRC Centralised AIDS Facility (UK) and the NIH AIDS Research and Reference Reagents Program for the donation of materials.

6. GENERAL CONCLUSIONS.

In this work, we have presented results pertaining to the isolation, and functional and structural characterization of specific peptide ligands for the broadly HIV-1 neutralizing MAbs b12, 2F5 and 2G12. In Chapters 2 and 3, we described the isolation and characterization of B2.1, a peptide that competes with gp120 for binding to MAb b12, and that shares partial sequence homology with the D-loop of HIV-1 gp120, which is located within the CD4-binding site. The B2.1 peptide is highly specific for b12 since it selected phage carrying this antibody from the phage-displayed antibody library from which b12 was originally isolated. We have presented the crystal structure of the b12-B2.1 peptide complex at 1.7 Å resolution, the first structure of an antibody against a conformational site in complex with a peptide ligand. The B2.1 peptide and the gp120 D-loop occupy the same general spatial location if our structure is superimposed with a b12-gp120 docked model. However, fine structure comparisons, together with functional data suggest that the B2.1 peptide binds to b12 in a way that involves replication of only one or perhaps two, of the putative high-energy contacts that b12 may establish with the D-loop of gp120.

Chapter 4 describes the isolation of peptides specific for MAb 2F5 and their use to explore the sequence requirements for peptide binding to 2F5, and therefore to more fully understand the epitope for 2F5. We have provided evidence that MAb 2F5 displays multispecificity for sequences flanking the DKW core epitope, and that the region C-terminal to the core is important for high-affinity binding. The amino acid sequence in this region may be diverse, and unrelated to the native sequence of gp41. Thus we

defined the existence of two functionally different regions in the paratope of MAb 2F5, one that is highly specific for the DKW core epitope, and another that interacts with the C-terminal region of our peptides in a multispecific fashion. New, interesting evidence has accumulated, which points to the complexity of the epitope for 2F5. Structural results by Ofek *et al.* (228) have shown that regions of 2F5 that are important for its activity are not engaged on binding to a 17-mer peptide derived from the gp41 sequence, and containing DKW (228). Furthermore, Zwick *et al.* (354) found that the only mutations on $gp41_{(660\text{-}680)}$ that confer 2F5 neutralization resistance to pseudotyped viruses, map to the $DKW_{(664\text{-}666)}$ core epitope (354). Grundner *et al.* (126) found a ten-fold better reactivity of 2F5 with gp160 in the context of lipids than without lipids, in a proteoliposome format. More recently, Haynes *et al.* (133) reported that 2F5 binds the phospholipid cardiolipin (albeit at much lower affinity) and suggested that 2F5 may be a polyspecific, autoreactive antibody (133).

A complex epitope for 2F5, in which the membrane phospholipids are involved in interactions with the antibody, would integrate our results (206), with those of Ofek *et al.* (228), Grundner *et al.* (126), Zwick *et al.* (354) and Haynes *et al.* (133). First, 2F5 binds better in the context of lipids (126). Second, the structure solved by Ofek *et al.* (228) shows a "hydrophobic foot" at the top of the CDR H3 of the antibody, which could potentially interact with the viral membrane. Third, the two functional regions of the 2F5 paratope detected by us may correspond to a DKW-binding domain and a membrane-binding one, respectively, the C-terminal regions of the peptides we isolated could extend to reach the CDR H3 hydrophobic foot described by Ofek *et al.* (228). Fourth, the results of Zwick *et al.* (354) indicate that only DKW, and no other gp41 protein residues in the

MEPR are required for neutralization. Fifth, Haynes *et al.* (133) have provided evidence of 2F5 interaction with an endogenous phospholipid. A membrane-protein mixed epitope would also explain the failure of past peptide immunizations to elicit 2F5, since the real epitope would have always been incomplete on those immunogens (see p. 35 for relevant citations). These considerations indicate the necessity of evaluating both the antigenicity and immunogenicity of the gp41 membrane-proximal region in the context of biological or model membranes.

In Chapter 5, we have described the identification of peptide sequences that are specific for the anti-carbohydrate MAb 2G12. One of those (bio-2G12.1) was made as a synthetic peptide and its crystal structure solved in complex with the MAb. A comparison with previously solved structures of the MAb alone or in complex with carbohydrate ligands showed that the peptide binds to a site adjacent to and only partially overlapping the primary carbohydrate-binding site of the antibody. Two antibody residues are involved in contacts with both the peptide and Manα1-2Man, whereas the rest of the interactions are unique to each ligand. Competition between the peptide and Manα1-2Man was observed, most likely determined by their competition for contacting these two antibody residues, since there is no steric hyndrance between the two ligands in the antibody-bound structures.

General conclusions about the mechanism(s) of peptide mimicry of protein and carbohydrate epitopes can be deduced from our results. Ideal peptide mimicry of a conformational site could be defined as that obtained with a mimic that can cover all or most of the paratope, displays the same general shape of the native epitope, and establishes the same high-energy contacts with the antibody. The first condition would be

difficult to fulfill by a peptide epitope, since most antibodies posses a paratope area larger than that of a peptide, thus the most common case would be that a peptide epitope interacts with only a subregion of the antibody's paratope. On the other hand, a peptide may replicate the general structural shape of a part of the native epitope. However, this is not what our results with the B2.1 peptide indicate.

Peptides in our study required most of their amino acids for binding to the antibodies, as evidenced from the alanine substitution or deletion experiments; critical-binding residues (CBRs) were found distributed over the sequence of peptides. The two crystal structures presented here indicate that only a subset of peptides CBRs are involved in antibody contact, many are also heavily engaged in maintaining the complex structures of the peptides. The crystal structures also suggest that the B2.1 and bio-2G12 peptide ligands establish only one or two contacts similar to those made by the native epitopes, which constitute the only elements indicating structural mimicry.

Our results also address the issue of the feasibility of developing an epitope-targeted vaccine that can elicit b12-, 2F5- and 2G12-like, broadly Nt antibodies. Immunization experiments described in Chapter 3 show that gp120 crossreactive antibodies were not produced upon immunization with B2.1 in different formats, even though high titers of anti peptide antibodies were obtained. This outcome is somewhat similar to results with 2F5-binding peptides, reported by others, which have induced high titers of anti-peptide or anti-gp41 antibodies that failed to be neutralizing. It is apparent that peptide antigenic "mimics" of neutralizing sites in the envelope of HIV-1 are unlikely to produce a HIV-neutralizing response by direct immunizations, since they do not fully replicate the structural features of the cognate epitopes on the functional

envelope spike, and therefore induce the production of different antibodies. However, peptide mimics may still be an attractive choice for focusing a pre-existing antibody response to relevant epitopes.

We have explored here three variations of the same theme, and consequently, our strategy has produced peptide ligands with dissimilar characteristics, which relate to the complexities of their respective antibodies. For the domain-swapped, carbohydrate-binder 2G12, a peptide that binds adjacent to the cabohydrate binding site was isolated, whereas for b12 the peptide still binds to the putative gp120-binding site, but seemingly, through limited mimicry of a subsite of the epitope. MAb 2F5, whose activity depends upon the presence of a linear determinant, showed a significant degree of multispecificity for other region(s) of its paratope. What seems to be clear from our results is that each antibody will require its own particular approach for the generation of immunogenic mimics that will elicit neutralizing antibody responses.

The known neutralizing HIV-1 MAbs are molecules characterized by unconventional or exceptional features, which reflect their unique functional properties, and the complexities of their corresponding epitopes on the viral envelope. One such site, the membrane proximal region of the gp41, is particularly attractive since more than one broadly-NtAb against it has been isolated; in fact, the epitopes for the two most potent neutralizing antibodies, 2F5 and 4E10, which have a linear component, map to that area. The strategy described here should prove useful for the characterization of these and other epitopes, and for the development of epitope-targeted vaccines against HIV-1.

REFERENCES

1. 2001. Phage display: A laboratory manual. Cold Spring Harbor Laboratories Press, Cold Spring Harbor, New York.

2. Aasa-Chapman, M. M., A. Hayman, P. Newton, D. Cornforth, I. Williams, P. Borrow, P. Balfe, and A. McKnight. 2004. Development of the antibody response in acute HIV-1 infection. Aids **18:**371-81.

3. Aasa-Chapman, M. M., S. Holuigue, K. Aubin, M. Wong, N. A. Jones, D. Cornforth, P. Pellegrino, P. Newton, I. Williams, P. Borrow, and A. McKnight. 2005. Detection of antibody-dependent complement-mediated inactivation of both autologous and heterologous virus in primary human immunodeficiency virus type 1 infection. J Virol **79:**2823-30.

4. Adams, E. W., D. M. Ratner, H. R. Bokesch, J. B. McMahon, B. R. O'Keefe, and P. H. Seeberger. 2004. Oligosaccharide and glycoprotein microarrays as tools in HIV glycobiology; glycan-dependent gp120/protein interactions. Chem Biol **11:**875-81.

5. Akahata, W., Z. Y. Yang, and G. J. Nabel. 2005. Comparative immunogenicity of human immunodeficiency virus particles and corresponding polypeptides in a DNA vaccine. J Virol **79:**626-31.

6. Albert, J., B. Abrahamsson, K. Nagy, E. Aurelius, H. Gaines, G. Nystrom, and E. M. Fenyo. 1990. Rapid development of isolate-specific neutralizing antibodies after primary HIV-1 infection and consequent emergence of virus variants which resist neutralization by autologous sera. Aids **4:**107-12.

7. Alkhatib, G., C. Combadiere, C. C. Broder, Y. Feng, P. E. Kennedy, P. M. Murphy, and E. A. Berger. 1996. CC CKR5: a RANTES, MIP-1alpha, MIP-1beta receptor as a fusion cofactor for macrophage-tropic HIV-1. Science **272:**1955-8.

8. Almagro, J. C. 2004. Identification of differences in the specificity-determining residues of antibodies that recognize antigens of different size: implications for the rational design of antibody repertoires. J Mol Recognit **17:**132-43.

9. Almond, N., K. Kent, M. Cranage, E. Rud, B. Clarke, and E. J. Stott. 1995. Protection by attenuated simian immunodeficiency virus in macaques against challenge with virus-infected cells. Lancet **345:**1342-4.

10. Ariyoshi, K., E. Harwood, R. Chiengsong-Popov, and J. Weber. 1992. Is clearance of HIV-1 viremia at seroconversion mediated by neutralising antibodies? Lancet **340:**1257-1258.

11. Baba, T. W., Y. S. Jeong, D. Pennick, R. Bronson, M. F. Greene, and R. M. Ruprecht. 1995. Pathogenicity of live, attenuated SIV after mucosal infection of neonatal macaques. Science **267:**1820-5.

12. Baba, T. W., V. Liska, R. Hofmann-Lehmann, J. Vlasak, W. Xu, S. Ayehunie, L. A. Cavacini, M. R. Posner, H. Katinger, G. Stiegler, B. J. Bernacky, T. A. Rizvi, R. Schmidt, L. R. Hill, M. E. Keeling, Y. Lu, J. E. Wright, T. C. Chou, and R. M. Ruprecht. 2000. Human neutralizing monoclonal antibodies of the IgG1 subtype protect against mucosal simian-human immunodeficiency virus infection. Nat Med **6:**200-6.

13. Barbas, C. F., 3rd, E. Bjorling, F. Chiodi, N. Dunlop, D. Cababa, T. M. Jones, S. L. Zebedee, M. A. Persson, P. L. Nara, E. Norrby, and et al. 1992. Recombinant human Fab fragments neutralize human type 1 immunodeficiency virus in vitro. Proc Natl Acad Sci U S A **89:**9339-43.

14. Barbas, C. F., 3rd, T. A. Collet, W. Amberg, P. Roben, J. M. Binley, D. Hoekstra, D. Cababa, T. M. Jones, R. A. Williamson, G. R. Pilkington, N. L. Haigwood, E. Cabezas, A. C. Satterthwait, I. Sanz, and D. R. Burton. 1993. Molecular profile of an antibody response to HIV-1 as probed by combinatorial libraries. J Mol Biol **230:**812-23.

15. Barbato, G., E. Bianchi, P. Ingallinella, W. H. Hurni, M. D. Miller, G. Ciliberto, R. Cortese, R. Bazzo, J. W. Shiver, and A. Pessi. 2003. Structural analysis of the epitope of the anti-HIV antibody 2F5 sheds light into its mechanism of neutralization and HIV fusion. J Mol Biol **330:**1101-15.

16. Barouch, D. H., S. Santra, M. J. Kuroda, J. E. Schmitz, R. Plishka, A. Buckler-White, A. E. Gaitan, R. Zin, J. H. Nam, L. S. Wyatt, M. A. Lifton, C. E. Nickerson, B. Moss, D. C. Montefiori, V. M. Hirsch, and N. L. Letvin. 2001. Reduction of simian-human immunodeficiency virus 89.6P viremia in rhesus monkeys by recombinant modified vaccinia virus Ankara vaccination. J Virol **75:**5151-8.

17. Beausejour, Y., and M. J. Tremblay. 2004. Interaction between the cytoplasmic domain of ICAM-1 and Pr55Gag leads to acquisition of host ICAM-1 by human immunodeficiency virus type 1. J Virol **78:**11916-25.

18. Beddows, S., S. Lister, R. Cheingsong, C. Bruck, and J. Weber. 1999. Comparison of the antibody repertoire generated in healthy volunteers following immunization with a monomeric recombinant gp120 construct derived from a CCR5/CXCR4-using human immunodeficiency virus type 1 isolate with sera from naturally infected individuals. J. Virol. **73:**1740-1745.

19. Beenhouwer, D. O., R. J. May, P. Valadon, and M. D. Scharff. 2002. High affinity mimotope of the polysaccharide capsule of Cryptococcus neoformans identified from an evolutionary phage peptide library. J Immunol **169:**6992-9.

20. Benjamin, D. C., J. A. Berzofsky, I. J. East, F. R. Gurd, C. Hannum, S. J. Leach, E. Margoliash, J. G. Michael, A. Miller, E. M. Prager, and et al. 1984. The antigenic structure of proteins: a reappraisal. Annu Rev Immunol **2:**67-101.

21. Berman, H. M., J. Westbrook, Z. Feng, G. Gilliland, T. N. Bhat, H. Weissig, I. N. Shindyalov, and P. E. Bourne. 2000. The Protein Data Bank. Nucleic Acids Res **28:**235-42.

22. Biacore. 1998. BIAapplications Handbook. Biacore AB, Uppsala, Sweden.

23. Biacore. 2004. BIAevaluation Software 4.1 Handbook. Biacore AB, Uppsala, Sweden.

24. Binley, J. M., C. S. Cayanan, C. Wiley, N. Schulke, W. C. Olson, and D. R. Burton. 2003. Redox-triggered infection by disulfide-shackled human immunodeficiency virus type 1 pseudovirions. J Virol **77:**5678-84.

25. Binley, J. M., R. W. Sanders, B. Clas, N. Schuelke, A. Master, Y. Guo, F. Kajumo, D. J. Anselma, P. J. Maddon, W. C. Olson, and J. P. Moore. 2000. A recombinant human immunodeficiency virus type 1 envelope glycoprotein complex stabilized by an intermolecular disulfide bond between the gp120 and gp41 subunits is an antigenic mimic of the trimeric virion-associated structure. J. Virol. **74:**627-643.

26. Binley, J. M., T. Wrin, B. Korber, M. B. Zwick, M. Wang, C. Chappey, G. Stiegler, R. Kunert, S. Zolla-Pazner, H. Katinger, C. J. Petropoulos, and D. R. Burton. 2004. Comprehensive cross-clade neutralization analysis of a panel of anti-human immunodeficiency virus type 1 monoclonal antibodies. J Virol **78:**13232-52.

27. Blake II, R. C., A. R. Pavlov, and D. A. Blake. 1999. Automated Kinetic Exclusion Assays to quantify protein binding interactions in homogeneous solution. Analytical Biochemistry **272:**123-134.

28. Blixt, O., S. Head, T. Mondala, C. Scanlan, M. E. Huflejt, R. Alvarez, M. C. Bryan, F. Fazio, D. Calarese, J. Stevens, N. Razi, D. J. Stevens, J. J. Skehel, I. van Die, D. R. Burton, I. A. Wilson, R. Cummings, N. Bovin, C. H. Wong, and J. C. Paulson. 2004. Printed covalent glycan array for ligand profiling of diverse glycan binding proteins. Proc Natl Acad Sci U S A **101:**17033-8.

29. Bolmstedt, A. J., B. R. O'Keefe, S. R. Shenoy, J. B. McMahon, and M. R. Boyd. 2001. Cyanovirin-N defines a new class of antiviral agent targeting N-linked, high-mannose glycans in an oligosaccharide-specific manner. Mol Pharmacol **59:**949-54.

30. Bonnycastle, L. L., J. S. Mehroke, M. Rashed, X. Gong, and J. K. Scott. 1996. Probing the basis of antibody reactivity with a panel of constrained peptide libraries displayed by filamentous phage. J Mol Biol **258:**747-62.

31. Bonnycastle, L. L., A. Menendez, and J. K. Scott. 2001. General phage methods. *In* C. F. Barbas, D. R. Burton, J. K. Scott, and G. J. Silverman (ed.), Phage Display. A Laboratory Manual. Cold Spring Harbor Laboratory Press, New York.

32. Bonnycastle, L. L., A. Menendez, and J. K. Scott. 2001. Production of peptide libraries. *In* C. F. Barbas, D. R. Burton, J. K. Scott, and G. J. Silverman (ed.), Phage Display. A Laboratory Manual. Cold Spring Harbor Laboratory Press, New York.

33. Borrow, P., H. Lewicki, B. H. Hahn, G. M. Shaw, and M. B. Oldstone. 1994. Virus-specific CD8+ cytotoxic T-lymphocyte activity associated with control of viremia in primary human immunodeficiency virus type 1 infection. J Virol **68:**6103-10.

34. Borrow, P., H. Lewicki, X. Wei, M. S. Horwitz, N. Peffer, H. Meyers, J. A. Nelson, J. E. Gairin, B. H. Hahn, M. B. Oldstone, and G. M. Shaw. 1997. Antiviral pressure exerted by HIV-1-specific cytotoxic T lymphocytes (CTLs) during primary infection demonstrated by rapid selection of CTL escape virus. Nat Med **3:**205-11.

35. Borrow, P., and G. M. Shaw. 1998. Cytotoxic T-lymphocyte escape viral variants: how important are they in viral evasion of immune clearance in vivo? Immunol Rev **164:**37-51.

36. Bouckaert, J., T. W. Hamelryck, L. Wyns, and R. Loris. 1999. The crystal structures of Man(alpha1-3)Man(alpha1-O)Me and Man(alpha1-6)Man(alpha1-O)Me in complex with concanavalin A. J Biol Chem **274:**29188-95.

37. Boyd, M. R., K. R. Gustafson, J. B. McMahon, R. H. Shoemaker, B. R. O'Keefe, T. Mori, R. J. Gulakowski, L. Wu, M. I. Rivera, C. M. Laurencot, M. J. Currens, J. H. Cardellina, 2nd, R. W. Buckheit, Jr., P. L. Nara, L. K. Pannell, R. C. Sowder, 2nd, and L. E. Henderson. 1997. Discovery of cyanovirin-N, a novel human immunodeficiency virus-inactivating protein that binds viral surface envelope glycoprotein gp120: potential applications to microbicide development. Antimicrob Agents Chemother **41:**1521-30.

38. Boyer, J. D., A. D. Cohen, S. Vogt, K. Schumann, B. Nath, L. Ahn, K. Lacy, M. L. Bagarazzi, T. J. Higgins, Y. Baine, R. B. Ciccarelli, R. S. Ginsberg, R. R. MacGregor, and D. B. Weiner. 2000. Vaccination of seronegative volunteers with a human immunodeficiency virus type 1 env/rev DNA vaccine induces antigen-specific proliferation and lymphocyte production of beta-chemokines. J Infect Dis **181:**476-83.

39. Bradney, A. P., S. Scheer, J. M. Crawford, S. P. Buchbinder, and D. Montefiori. 1999. Neutralization escape in human immunodeficiency virus type 1 infected long-term non progressors. J. Infect. Dis. **179:**1264-1267.

40. Broliden, P. A., A. von Gegerfelt, P. Clapham, J. Rosen, E. M. Fenyo, B. Wahren, and K. Broliden. 1992. Identification of human neutralization-inducing regions of the

human immunodeficiency virus type 1 envelope glycoproteins. Proc Natl Acad Sci U S A **89:**461-5.

41. Brunger, A. T., P. D. Adams, G. M. Clore, W. L. DeLano, P. Gros, R. W. Grosse-Kunstleve, J. S. Jiang, J. Kuszewski, M. Nilges, N. S. Pannu, R. J. Read, L. M. Rice, T. Simonson, and G. L. Warren. 1998. Crystallography & NMR system: A new software suite for macromolecular structure determination. Acta Crystallogr D Biol Crystallogr **54 (Pt 5):**905-21.

42. Buchacher, A., R. Predl, K. Strutzenberger, W. Steinfellner, A. Trkola, M. Purtscher, G. Gruber, C. Tauer, F. Steindl, A. Jungbauer, and H. Katinger. 1994. Generation of human monoclonal antibodies against HIV-1 proteins; electrofusion and Epstein-Bar virus transformation for periferal blood lynphocyte immortalization. AIDS Res. Hum. Retrov. **10:**359-369.

43. Burritt, J. B., S. C. Busse, D. Gizachew, D. W. Siemsen, M. T. Quinn, C. W. Bond, E. A. Dratz, and A. J. Jesaitis. 1998. Antibody imprint of a membrane protein surface. Phagocyte flavocytochrome b. J Biol Chem **273:**24847-52.

44. Burton, D. R., C. F. Barbas , III, M. A. A. Persson, S. Koening, R. M. Chanock, and R. A. Lerner. 1991. A large array of human monoclonal antibodies to type 1 human immunodeficiency virus from combinatorial libraries of asymptomatic seropositive individuals. Proc. Natl. Acad. Sci. USA **88:**10134-10137.

45. Burton, D. R., J. Pyati, R. Koduri, S. J. Sharp, G. B. Thornton, P. W. Parren, L. S. Sawyer, R. M. Hendry, N. Dunlop, P. L. Nara, and et al. 1994. Efficient neutralization of primary isolates of HIV-1 by a recombinant human monoclonal antibody. Science **266:**1024-7.

46. Calarese, D. A., C. N. Scanlan, M. B. Zwick, S. Deechongkit, Y. Mimura, R. Kunert, P. Zhu, M. R. Wormald, R. L. Stanfield, K. H. Roux, J. W. Kelly, P. M. Rudd, R. A. Dwek, H. Katinger, D. R. Burton, and I. A. Wilson. 2003. Antibody domain exchange is an immunological solution to carbohydrate cluster recognition. Science **300:**2065-71.

47. Calarota, S., M. Jansson, M. Levi, K. Broliden, O. Libonatti, H. Wigzell, and B. Wahren. 1996. Immunodominant glycoprotein 41 epitope identified by seroreactivity in HIV type 1-infected individuals. AIDS Res Hum Retroviruses **12:**705-13.

48. Cao, J., L. Bergeron, E. Helseth, M. Thali, H. Repke, and J. Sodroski. 1993. Effects of amino acid changes in the extracellular domain of the human immunodeficiency virus type 1 gp41 envelope glycoprotein. J Virol **67:**2747-55.

49. Cardoso, R. M., M. B. Zwick, R. L. Stanfield, R. Kunert, J. M. Binley, H. Katinger, D. R. Burton, and I. A. Wilson. 2005. Broadly neutralizing anti-HIV antibody 4E10 recognizes a helical conformation of a highly conserved fusion-associated motif in gp41. Immunity **22:**163-73.

50. Cavacini, L., J. E. Peterson, E. Nappi, M. Duval, R. Goldstein, K. Mayer, and M. R. Posner. 1999. Minimal incidence of serum antibodies reactive with intact primary isolate virions in human immunodeficiency virus type 1 infected individuals. J. Virol. **73:**9638-9641.

51. Center, R. J., P. Schuck, R. D. Leapman, L. O. Arthur, P. L. Earl, B. Moss, and J. Lebowitz. 2001. Oligomeric structure of virion-associated and soluble forms of the simian immunodeficiency virus envelope protein in the prefusion activated conformation. Proc Natl Acad Sci U S A **98:**14877-82.

52. Chamat, S., P. Nara, L. Berquist, A. Whalley, W. J. Morrow, H. Kohler, and C. Y. Kang. 1992. Two major groups of neutralizing anti-gp120 antibodies exist in HIV-infected individuals. Evidence for epitope diversity around the CD4 attachment site. J Immunol **149:**649-54.

53. Chan, D. C., D. Fass, J. M. Berger, and P. S. Kim. 1997. Core structure of gp41 from the HIV envelope glycoprotein. Cell **89:**263-73.

54. Chan, D. C., and P. S. Kim. 1998. HIV entry and its inhibition. Cell **93:**681-4.

55. Chargelegue, D., O. E. Obeid, S. C. Hsu, M. D. Shaw, A. N. Denbury, G. Taylor, and M. W. Steward. 1998. A peptide mimic of a protective epitope of respiratory syncytial virus selected from a combinatorial library induces virus-neutralizing antibodies and reduces viral load in vivo. J Virol **72:**2040-6.

56. Chen, B., E. M. Vogan, H. Gong, J. J. Skehel, D. C. Wiley, and S. C. Harrison. 2005. Structure of an unliganded simian immunodeficiency virus gp120 core. Nature **433:**834-41.

57. Chertova, E., J. W. Bess Jr, Jr., B. J. Crise, I. R. Sowder, T. M. Schaden, J. M. Hilburn, J. A. Hoxie, R. E. Benveniste, J. D. Lifson, L. E. Henderson, and L. O. Arthur. 2002. Envelope glycoprotein incorporation, not shedding of surface envelope glycoprotein (gp120/SU), Is the primary determinant of SU content of purified human immunodeficiency virus type 1 and simian immunodeficiency virus. J Virol **76:**5315-25.

58. Chirinos-Rojas, C. L., M. W. Steward, and C. D. Partidos. 1999. A phage-displayed mimotope inhibits tumour necrosis factor-alpha-induced cytotoxicity more effectively than the free mimotope. Immunology **96:**109-13.

59. Christensen, L. L. 1997. Theoretical analysis of protein concentration determination using biosensor technology under conditions of partial mass transport limitation. Anal Biochem **249:**153-64.

60. Chun, T. W., D. Engel, M. M. Berrey, T. Shea, L. Corey, and A. S. Fauci. 1998. Early establishment of a pool of latently infected, resting CD4(+) T cells during primary HIV-1 infection. Proc Natl Acad Sci U S A **95:**8869-73.

61. Clements-Mann, M. L., K. Weinhold, T. J. Matthews, B. S. Graham, G. J. Gorse, M. C. Keefer, M. J. McElrath, R. H. Hsieh, J. Mestecky, S. Zolla-Pazner, J. Mascola, D. Schwartz, R. Siliciano, L. Corey, P. F. Wright, R. Belshe, R. Dolin, S. Jackson, S. Xu, P. Fast, M. C. Walker, D. Stablein, J. L. Excler, J. Tartaglia, E. Paoletti, and et al. 1998. Immune responses to human immunodeficiency virus (HIV) type 1 induced by canarypox expressing HIV-1MN gp120, HIV-1SF2 recombinant gp120, or both vaccines in seronegative adults. NIAID AIDS Vaccine Evaluation Group. J Infect Dis **177:**1230-46.

62. Clotet, B. 2004. Strategies for overcoming resistance in HIV-1 infected patients receiving HAART. AIDS Rev **6:**123-30.

63. Coeffier, E., J. M. Clement, V. Cussac, N. Khodaei-Boorane, M. Jehanno, M. Rojas, A. Dridi, M. Latour, R. El Habib, F. Barre-Sinoussi, M. Hofnung, and C. Leclerc. 2000. Antigenicity and immunogenicity of the HIV-1 gp41 epitope ELDKWA inserted into permissive sites of the MalE protein. Vaccine **19:**684-93.

64. Conley, A. J., J. A. Kessler, 2nd, L. J. Boots, J. S. Tung, B. A. Arnold, P. M. Keller, A. R. Shaw, and E. A. Emini. 1994. Neutralization of divergent human immunodeficiency virus type 1 variants and primary isolates by IAM-41-2F5, an anti-gp41 human monoclonal antibody. Proc Natl Acad Sci U S A **91:**3348-52.

65. Connolly, M. L. 1983. Solvent-accessible surfaces of proteins and nucleic acids. Science **221:**709-13.

66. Connor, R. I., B. T. Korber, B. S. Graham, B. H. Hahn, D. D. Ho, B. D. Walker, A. U. Neumann, S. H. Vermund, J. Mestecky, S. Jackson, E. Fenamore, Y. Cao, F. Gao, S. Kalams, K. J. Kunstman, D. McDonald, N. McWilliams, A. Trkola, J. P. Moore, and S. M. Wolinsky. 1998. Immunological and virological analyses of persons infected by human immunodeficiency virus type 1 while participating in trials of recombinant gp120 subunit vaccines. Journal of Virology **72:**1552-15576.

67. Corcoran, A., B. P. Mahon, and S. Doyle. 2004. B cell memory is directed toward conformational epitopes of parvovirus B19 capsid proteins and the unique region of VP1. J Infect Dis **189:**1873-80.

68. Coulon, S., J. Y. Metais, M. Chartier, J. P. Briand, and D. Baty. 2004. Cyclic peptides selected by phage display mimic the natural epitope recognized by a monoclonal anti-colicin A antibody. J Pept Sci **10:**648-58.

69. Craig, L., P. C. Sanschagrin, A. Rozek, S. Lackie, L. A. Kuhn, and J. K. Scott. 1998. The role of structure in antibody cross-reactivity between peptides and folded proteins. J Mol Biol **281:**183-201.

70. D'Souza, M. P., P. Durda, C. V. Hanson, and G. Milman. 1991. Evaluation of monoclonal antibodies to HIV-1 by neutralization and serological assays: an international collaboration. Collaborating Investigators. Aids **5:**1061-70.

71. D'Souza, M. P., D. Livnat, J. A. Bradac, S. H. Bridges, and a. C. I. The AIDS Clinical Trials Group Antibody Selection Working Group. 1997. Evaluation of monoclonal antibodies to human immunodeficiency virus type 1 primary isolates by neutralization assays: Performance criteria for selecting candidate antibodies for clinical trials. J. Infec. Dis. **197:**1056-1062.

72. da Silva, J. 2003. The evolutionary adaptation of HIV-1 to specific immunity. Curr HIV Res **1:**363-71.

73. Dale, C. J., R. De Rose, I. Stratov, S. Chea, D. C. Montefiori, S. Thomson, I. A. Ramshaw, B. E. Coupar, D. B. Boyle, M. Law, and S. J. Kent. 2004. Efficacy of DNA and fowlpox virus priming/boosting vaccines for simian/human immunodeficiency virus. J Virol **78:**13819-28.

74. Dalgleish, A. G., P. C. Beverley, P. R. Clapham, D. H. Crawford, M. F. Greaves, and R. A. Weiss. 1984. The CD4 (T4) antigen is an essential component of the receptor for the AIDS retrovirus. Nature **312:**763-7.

75. Daniel, M. D., F. Kirchhoff, S. C. Czajak, P. K. Sehgal, and R. C. Desrosiers. 1992. Protective effects of a live attenuated SIV vaccine with a deletion in the nef gene. Science **258:**1938-41.

76. Davenport, M. P., R. M. Ribeiro, D. L. Chao, and A. S. Perelson. 2004. Predicting the impact of a nonsterilizing vaccine against human immunodeficiency virus. J Virol **78:**11340-51.

77. Davenport, M. P., R. M. Ribeiro, and A. S. Perelson. 2004. Kinetics of virus-specific CD8+ T cells and the control of human immunodeficiency virus infection. J Virol **78:**10096-103.

78. Davis, N. L., I. J. Caley, K. W. Brown, M. R. Betts, D. M. Irlbeck, K. M. McGrath, M. J. Connell, D. C. Montefiori, J. A. Frelinger, R. Swanstrom, P. R. Johnson, and R. E. Johnston. 2000. Vaccination of macaques against pathogenic simian immunodeficiency virus with Venezuelan equine encephalitis virus replicon particles. J Virol **74:**371-8.

79. Delamstro, P., A. Meola, P. Monaci, R. Cortese, and G. Galfrè. 1997. Immunogenicity of filamentous phage displaying peptide mimotopes after oral administration. Vaccine **11:**1276-1285.

80. Demangel, C., P. Lafaye, and J. C. Mazie. 1996. Reproducing the immune response against the Plasmodium vivax merozoite surface protein 1 with mimotopes selected from a phage-displayed peptide library. Mol Immunol **33:**909-16.

81. Derewenda, Z., J. Yariv, J. R. Helliwell, A. J. Kalb, E. J. Dodson, M. Z. Papiz, T. Wan, and J. Campbell. 1989. The structure of the saccharide-binding site of concanavalin A. Embo J **8:**2189-93.

82. Doan, L. X., M. Li, C. Chen, and Q. Yao. 2005. Virus-like particles as HIV-1 vaccines. Rev Med Virol **15:**75-88.

83. Dominguez, V., G. Gevorkian, T. Govezensky, H. Rodriguez, M. Viveros, G. Cocho, Y. Macotela, F. Masso, M. Pacheco, J. L. Estrada, C. Lavalle, and C. Larralde. 1998. Antigenic homology of HIV-1 GP41 and human platelet glycoprotein GPIIIa (integrin beta3). J Acquir Immune Defic Syndr Hum Retrovirol **17:**385-90.

84. Dong, M., P. F. Zhang, F. Grieder, J. Lee, G. Krishnamurthy, T. VanCott, C. Broder, V. R. Polonis, X. F. Yu, Y. Shao, D. Faix, P. Valente, and G. V. Quinnan, Jr. 2003. Induction of primary virus-cross-reactive human immunodeficiency virus type 1-neutralizing antibodies in small animals by using an alphavirus-derived in vivo expression system. J Virol **77:**3119-30.

85. Doranz, B. J., S. S. Baik, and R. W. Doms. 1999. Use of a gp120 binding assay to dissect the requirements and kinetics of human immunodeficiency virus fusion events. J Virol **73:**10346-58.

86. Dorgham, K., I. Dogan, N. Bitton, C. Parizot, V. Cardona, P. Debre, O. Hartley, and G. Gorochov. 2005. Immunogenicity of HIV type 1 gp120 CD4 binding site phage mimotopes. AIDS Res Hum Retroviruses **21:**82-92.

87. Drake, A. W., D. G. Myszka, and S. L. Klakamp. 2004. Characterizing high-affinity antigen/antibody complexes by kinetic- and equilibrium-based methods. Anal Biochem **328:**35-43.

88. Dreyer, K., E. G. Kallas, V. Planelles, D. Montefiori, M. P. McDermott, M. S. Hasan, and T. G. Evans. 1999. Primary isolate neutralization by HIV type 1-infected patient sera in the era of highly active antiretroviral therapy. AIDS Res. Hum. Retrov. **15:**1563-1571.

89. Dudkin, V. Y., M. Orlova, X. Geng, M. Mandal, W. C. Olson, and S. J. Danishefsky. 2004. Toward fully synthetic carbohydrate-based HIV antigen design: on the critical role of bivalency. J Am Chem Soc **126:**9560-2.

90. Earl, P. L., R. W. Doms, and B. Moss. 1990. Oligomeric structure of the human immunodeficiency virus type 1 envelope glycoprotein. Proc Natl Acad Sci U S A **87:**648-52.

91. Eckert, D. M., and P. S. Kim. 2001. Mechanisms of viral membrane fusion and its inhibition. Annu Rev Biochem **70:**777-810.

92. Eckhart, L., W. Raffelsberger, B. Ferko, A. Klima, M. Purtscher, H. Katinger, and F. Ruker. 1996. Immunogenic presentation of a conserved gp41 epitope of human immunodeficiency virus type 1 on recombinant surface antigen of hepatitis B virus. J Gen Virol **77 (Pt 9):**2001-8.

93. Elgavish, S., and B. Shaanan. 1997. Lectin-carbohydrate interactions: different folds, common recognition principles. Trends Biochem Sci **22:**462-7.

94. Enterprise, C. C. o. t. G. H. A. V. 2005. The global HIV/AIDS vaccine enterprise: Scientific strategic plan. PLoS Medicine **2:**111-121.

95. Esnouf, R. M. 1999. Further additions to MolScript version 1.4, including reading and contouring of electron-density maps. Acta Crystallographica **D55:**938-940.

96. Esser, M. T., T. Mori, I. Mondor, Q. J. Sattentau, B. Dey, E. A. Berger, M. R. Boyd, and J. D. Lifson. 1999. Cyanovirin-N binds to gp120 to interfere with CD4-dependent human immunodeficiency virus type 1 virion binding, fusion, and infectivity but does not affect the CD4 binding site on gp120 or soluble CD4-induced conformational changes in gp120. J Virol **73:**4360-71.

97. Estcourt, M. J., A. J. McMichael, and T. Hanke. 2004. DNA vaccines against human immunodeficiency virus type 1. Immunol Rev **199:**144-55.

98. Evans, D. T., L. M. Chen, J. Gillis, K. C. Lin, B. Harty, G. P. Mazzara, R. O. Donis, K. G. Mansfield, J. D. Lifson, R. C. Desrosiers, J. E. Galan, and R. P. Johnson. 2003. Mucosal priming of simian immunodeficiency virus-specific cytotoxic T-lymphocyte responses in rhesus macaques by the Salmonella type III secretion antigen delivery system. J Virol **77:**2400-9.

99. Evans, D. T., D. H. O'Connor, P. Jing, J. L. Dzuris, J. Sidney, J. da Silva, T. M. Allen, H. Horton, J. E. Venham, R. A. Rudersdorf, T. Vogel, C. D. Pauza, R. E. Bontrop, R. DeMars, A. Sette, A. L. Hughes, and D. I. Watkins. 1999. Virus-specific cytotoxic T-lymphocyte responses select for amino-acid variation in simian immunodeficiency virus Env and Nef. Nat Med **5:**1270-6.

100. Farzan, M., H. Choe, E. Desjardins, Y. Sun, J. Kuhn, J. Cao, D. Archambault, P. Kolchinsky, M. Koch, R. Wyatt, and J. Sodroski. 1998. Stabilization of human immunodeficiency virus type 1 envelope glycoprotein trimers by disulfide bonds introduced into the gp41 glycoprotein ectodomain. J Virol **72:**7620-5.

101. Fassina, G., A. Verdoliva, G. Palombo, M. Ruvo, and G. Cassani. 1998. Immunoglobulin specificity of TG19318: a novel synthetic ligand for antibody affinity purification. J Mol Recognit **11:**128-33.

102. Ferko, B., D. Katinger, A. Grassauer, A. Egorov, J. Romanova, B. Niebler, H. Katinger, and T. Muster. 1998. Chimeric influenza virus replicating predominantly in the murine upper respiratory tract induces local immune responses against human immunodeficiency virus type 1 in the genital tract. J Infect Dis **178:**1359-68.

103. Ferrantelli, F., R. Hofmann-Lehmann, R. A. Rasmussen, T. Wang, W. Xu, P. L. Li, D. C. Montefiori, L. A. Cavacini, H. Katinger, G. Stiegler, D. C. Anderson, H. M. McClure, and R. M. Ruprecht. 2003. Post-exposure prophylaxis with human

monoclonal antibodies prevented SHIV89.6P infection or disease in neonatal macaques. Aids **17**:301-9.

104. Flynn, N. M., D. N. Forthal, C. D. Harro, F. N. Judson, K. H. Mayer, and M. F. Para. 2005. Placebo-controlled phase 3 trial of a recombinant glycoprotein 120 vaccine to prevent HIV-1 infection. J Infect Dis **191**:654-65.

105. Fouts, T. R., J. M. Binley, A. Trkola, J. E. Robinson, and J. P. Moore. 1997. Neutralization of the human immunodeficiency virus type 1 primary isolate JR-FL by human monoclonal antibodies correlates with antibody binding to the oligomeric form of the envelope glycoprotein complex. J. Virol. **71**:2779-2785.

106. Fransen, M., P. P. Van Veldhoven, and S. Subramani. 1999. Identification of peroxisomal proteins by using M13 phage protein VI phage display: molecular evidence that mammalian peroxisomes contain a 2,4-dienoyl-CoA reductase. Biochem J **340 (Pt 2)**:561-8.

107. Gallo, S. A., C. M. Finnegan, M. Viard, Y. Raviv, A. Dimitrov, S. S. Rawat, A. Puri, S. Durell, and R. Blumenthal. 2003. The HIV Env-mediated fusion reaction. Biochim Biophys Acta **1614**:36-50.

108. Gao, C., S. Mao, C. H. Lo, P. Wirsching, R. A. Lerner, and K. D. Janda. 1999. Making artificial antibodies: a format for phage display of combinatorial heterodimeric arrays. Proc Natl Acad Sci U S A **96**:6025-30.

109. Gaschen, B., J. Taylor, K. Yusim, B. Foley, F. Gao, D. Lang, V. Novitsky, B. Haynes, B. H. Hahn, T. Bhattacharya, and B. Korber. 2002. Diversity considerations in HIV-1 vaccine selection. Science **296**:2354-60.

110. Gauduin, M. C., P. W. Parren, R. Weir, C. F. Barbas, D. R. Burton, and R. A. Koup. 1997. Passive immunization with a human monoclonal antibody protects hu-PBL-SCID mice against challenge by primary isolates of HIV-1. Nat Med **3**:1389-93.

111. Gazarian, T. G., B. Selisko, G. B. Gurrola, R. Hernandez, L. D. Possani, and K. G. Gazarian. 2003. Potential of peptides selected from random phage-displayed libraries to mimic conformational epitopes: a study on scorpion toxin Cn2 and the neutralizing monoclonal antibody BCF2. Comb Chem High Throughput Screen **6**:119-32.

112. Geffin, R. B., G. B. Scott, M. Melenwick, C. Hutto, S. Lai, L. J. Boots, P. M. McKenna, J. A. Kessler, 2nd, and A. J. Conley. 1998. Association of antibody reactivity to ELDKWA, a glycoprotein 41 neutralization epitope, with disease progression in children perinatally infected with HIV type 1. AIDS Res Hum Retroviruses **14**:579-90.

113. Geijtenbeek, T. B., D. S. Kwon, R. Torensma, S. J. van Vliet, G. C. van Duijnhoven, J. Middel, I. L. Cornelissen, H. S. Nottet, V. N. KewalRamani, D. R.

Littman, C. G. Figdor, and Y. van Kooyk. 2000. DC-SIGN, a dendritic cell-specific HIV-1-binding protein that enhances trans-infection of T cells. Cell **100:**587-97.

114. Gelderblom, H. R. 1991. Assembly and morphology of HIV: potential effect of structure on viral function. Aids **5:**617-37.

115. Geng, X., V. Y. Dudkin, M. Mandal, and S. J. Danishefsky. 2004. In pursuit of carbohydrate-based HIV vaccines, part 2: The total synthesis of high-mannose-type gp120 fragments--evaluation of strategies directed to maximal convergence. Angew Chem Int Ed Engl **43:**2562-5.

116. Geysen, H. M., S. J. Barteling, and R. H. Meloen. 1985. Small peptides induce antibodies with a sequence and structural requirement for binding antigen comparable to antibodies raised against the native protein. Proc Natl Acad Sci U S A **82:**178-82.

117. Geysen, H. M., R. H. Meloen, and S. J. Barteling. 1984. Use of peptide synthesis to probe viral antigens for epitopes to a resolution of a single amino acid. Proc Natl Acad Sci U S A **81:**3998-4002.

118. Gloster, S. E., P. Newton, D. Cornforth, J. D. Lifson, I. Williams, G. M. Shaw, and P. Borrow. 2004. Association of strong virus-specific CD4 T cell responses with efficient natural control of primary HIV-1 infection. Aids **18:**749-55.

119. Gomez-Roman, V. R., L. J. Patterson, D. Venzon, D. Liewehr, K. Aldrich, R. Florese, and M. Robert-Guroff. 2005. Vaccine-elicited antibodies mediate antibody-dependent cellular cytotoxicity correlated with significantly reduced acute viremia in rhesus macaques challenged with SIVmac251. J Immunol **174:**2185-9.

120. Gorny, M. K., T. C. VanCott, C. Williams, K. Revesz, and S. Zolla-Pazner. 2000. Effects of oligomerization on the epitopes of the human immunodeficiency virus type 1 envelope glycoproteins. Virology **267:**220-228.

121. Gorny, M. K., and S. Zolla-Pazner. 2000. Recognition by human monoclonal antibodies of free and complexed peptides representing the prefusogenic and fusogenic forms of human immunodeficiency virus type 1 gp41. J Virol **74:**6186-92.

122. Gorse, G. J., S. E. Frey, G. Patel, F. K. Newman, and R. B. Belshe. 1994. Vaccine-induced antibodies to native and recombinant human immunodeficiency virus type 1 envelope glycoproteins. NIAID AIDS Vaccine Clinical Trials Network. Vaccine **12:**912-8.

123. Goudsmit, J., R. H. Meloen, and R. Brasseur. 1990. Map of sequential B cell epitopes of the HIV-1 transmembrane protein using human antibodies as probe. Intervirology **31:**327-38.

124. Green, L. L. 1999. Antibody engineering via genetic engineering of the mouse: XenoMouse strains are a vehicle for the facile generation of therapeutic human monoclonal antibodies. J Immunol Methods **231:**11-23.

125. Grovit-Ferbas, K., J. F. Hsu, J. Ferbas, V. Gudeman, and I. S. Chen. 2000. Enhanced binding of antibodies to neutralization epitopes following thermal and chemical inactivation of human immunodeficiency virus type 1. J Virol **74:**5802-9.

126. Grundner, C., T. Mirzabekov, J. Sodroski, and R. Wyatt. 2002. Solid-phase proteoliposomes containing human immunodeficiency virus envelope glycoproteins. J Virol **76:**3511-21.

127. Haaparanta, T., and W. D. Huse. 1995. A combinatorial method for constructing libraries of long peptides displayed by filamentous phage. Mol Divers **1:**39-52.

128. Haigwood, N. L. 2004. Predictive value of primate models for AIDS. AIDS Rev **6:**187-98.

129. Hammarstedt, M., and H. Garoff. 2004. Passive and active inclusion of host proteins in human immunodeficiency virus type 1 gag particles during budding at the plasma membrane. J Virol **78:**5686-97.

130. Han, Z., J. T. Simpson, M. J. Fivash, R. Fisher, and T. Mori. 2004. Identification and characterization of peptides that bind to cyanovirin-N, a potent human immunodeficiency virus-inactivating protein. Peptides **25:**551-61.

131. Harlow, E., and D. Lane. 1988. Antibodies. A laboratory manual. Cold Spring Harbor Laboratory, New York.

132. Harris, S. L., L. Craig, J. S. Mehroke, M. Rashed, M. B. Zwick, K. Kenar, E. J. Toone, N. Greenspan, F. I. Auzanneau, J. R. Marino-Albernas, B. M. Pinto, and J. K. Scott. 1997. Exploring the basis of peptide-carbohydrate crossreactivity: Evidence for discrimination by peptides between closely related anti carbohydrate antibodies. Proc. Natl. Acad. Sci USA **94:**2454-2459.

133. Haynes, B. F., J. Fleming, E. W. St Clair, H. Katinger, G. Stiegler, R. Kunert, J. Robinson, R. M. Scearce, K. Plonk, H. F. Staats, T. L. Ortel, H. X. Liao, and S. M. Alam. 2005. Cardiolipin polyspecific autoreactivity in two broadly neutralizing HIV-1 antibodies. Science **308:**1906-8.

134. Helseth, E., U. Olshevsky, C. Furman, and J. Sodroski. 1991. Human immunodeficiency virus type 1 gp120 envelope glycoprotein regions important for association with the gp41 transmembrane glycoprotein. J Virol **65:**2119-23.

135. Herrera, C., C. Spenlehauer, M. S. Fung, D. R. Burton, S. Beddows, and J. P. Moore. 2003. Nonneutralizing antibodies to the CD4-binding site on the gp120 subunit of human immunodeficiency virus type 1 do not interfere with the activity of a neutralizing antibody against the same site. J Virol **77:**1084-91.

136. Hezareh, M., A. J. Hessell, R. C. Jensen, J. G. van de Winkel, and P. W. Parren. 2001. Effector function activities of a panel of mutants of a broadly neutralizing antibody against human immunodeficiency virus type 1. J Virol **75:**12161-8.

137. Ho, J., R. A. Uger, M. B. Zwick, M. A. Luscher, B. H. Barber, and K. S. MacDonald. 2005. Conformational constraints imposed on a pan-neutralizing HIV-1 antibody epitope result in increased antigenicity but not neutralizing response. Vaccine **23:**1559-73.

138. Hoffmuller, U., T. Knaute, M. Hahn, W. Hohne, J. Schneider-Mergener, and A. Kramer. 2000. Evolutionary transition pathways for changing peptide ligand specificity and structure. Embo J **19:**4866-74.

139. Hofmann-Lehmann, R., J. Vlasak, R. A. Rasmussen, S. Jiang, P. L. Li, T. W. Baba, D. C. Montefiori, B. J. Bernacky, T. A. Rizvi, R. Schmidt, L. R. Hill, M. E. Keeling, H. Katinger, G. Stiegler, L. A. Cavacini, M. R. Posner, and R. M. Ruprecht. 2002. Postnatal pre- and postexposure passive immunization strategies: protection of neonatal macaques against oral simian-human immunodeficiency virus challenge. J Med Primatol **31:**109-19.

140. Hofmann-Lehmann, R., J. Vlasak, R. A. Rasmussen, B. A. Smith, T. W. Baba, V. Liska, F. Ferrantelli, D. C. Montefiori, H. M. McClure, D. C. Anderson, B. J. Bernacky, T. A. Rizvi, R. Schmidt, L. R. Hill, M. E. Keeling, H. Katinger, G. Stiegler, L. A. Cavacini, M. R. Posner, T. C. Chou, J. Andersen, and R. M. Ruprecht. 2001. Postnatal passive immunization of neonatal macaques with a triple combination of human monoclonal antibodies against oral simian-human immunodeficiency virus challenge. J Virol **75:**7470-80.

141. Hong, S. S., N. A. Habib, L. Franqueville, S. Jensen, and P. A. Boulanger. 2003. Identification of adenovirus (ad) penton base neutralizing epitopes by use of sera from patients who had received conditionally replicative ad (addl1520) for treatment of liver tumors. J Virol **77:**10366-75.

142. Horal, P., B. Svennerholm, S. Jeansson, L. Rymo, W. W. Hall, and A. Vahlne. 1991. Continuous epitopes of the human immunodeficiency virus type 1 (HIV-1) transmembrane glycoprotein and reactivity of human sera to synthetic peptides representing various HIV-1 isolates. J Virol **65:**2718-23.

143. Hu, S. L., P. N. Fultz, H. M. McClure, J. W. Eichberg, E. K. Thomas, J. Zarling, M. C. Singhal, S. G. Kosowski, R. B. Swenson, D. C. Anderson, and et al. 1987. Effect of immunization with a vaccinia-HIV env recombinant on HIV infection of chimpanzees. Nature **328:**721-3.

144. Hulskotte, E. G., A. M. Geretti, K. H. Siebelink, G. van Amerongen, M. P. Cranage, E. W. Rud, S. G. Norley, P. de Vries, and A. D. Osterhaus. 1995. Vaccine-induced virus-neutralizing antibodies and cytotoxic T cells do not protect macaques from experimental infection with simian immunodeficiency virus SIVmac32H (J5). J Virol **69:**6289-96.

145. Hunter, E. 1997. gp41, a multifunctional protein involved in HIV entry and pathogenesis. *In* B. Korber, C. Brander, B. Haynes, R. A. Koup, J. P. Moore, and B.

Walker (ed.), HIV Molecular Immunology Database. Theoretical Biology and Biophysics Group, Los Alamos National Laboratory, Los Alamos.

146. Irving, M. B., O. Pan, and J. K. Scott. 2001. Random-peptide libraries and antigen-fragment libraries for epitope mapping and the development of vaccines and diagnostics. Curr Opin Chem Biol **5:**314-24.

147. Ito, H. O., T. Nakashima, T. So, M. Hirata, and M. Inoue. 2003. Immunodominance of conformation-dependent B-cell epitopes of protein antigens. Biochem Biophys Res Commun **308:**770-6.

148. Jacobs, J. M., B. W. Bailey, J. B. Burritt, S. G. Morrison, R. P. Morrison, E. A. Dratz, A. J. Jesaitis, and M. Teintze. 2003. QSYP peptide sequence is selected from phage display libraries by bovine IgG contaminants in monoclonal antibody preparations. Biotechniques **34:**132-4, 137-41.

149. Jain, D., K. Kaur, B. Sundaravadivel, and D. M. Salunke. 2000. Structural and functional consequences of peptide-carbohydrate mimicry. Crystal structure of a carbohydrate-mimicking peptide bound to concanavalin A. J Biol Chem **275:**16098-102.

150. Jain, D., K. J. Kaur, and D. M. Salunke. 2001. Plasticity in protein-peptide recognition: crystal structures of two different peptides bound to concanavalin A. Biophys J **80:**2912-21.

151. Jelinek, R., T. D. Terry, J. J. Gesell, P. Malik, R. N. Perham, and S. J. Opella. 1997. NMR structure of the principal neutralizing determinant of HIV-1 displayed in filamentous bacteriophage coat protein. J Mol Biol **266:**649-55.

152. Jespers, L. S., J. H. Messens, A. De Keyser, D. Eeckhout, I. Van den Brande, Y. G. Gansemans, M. J. Lauwereys, G. P. Vlasuk, and P. E. Stanssens. 1995. Surface expression and ligand-based selection of cDNAs fused to filamentous phage gene VI. Biotechnology (N Y) **13:**378-82.

153. Ji, J., and L. A. Loeb. 1994. Fidelity of HIV-1 reverse transcriptase copying a hypervariable region of the HIV-1 env gene. Virology **199:**323-30.

154. Jiang, B., W. Liu, H. Qu, L. Meng, S. Song, T. Ouyang, and C. Shou. 2005. A novel peptide isolated from a phage display peptide library with trastuzumab can mimic antigen epitope of HER-2. J Biol Chem **280:**4656-62.

155. Jin, L., B. M. Fendly, and J. A. Wells. 1992. High resolution functional analysis of antibody-antigen interactions. J Mol Biol **226:**851-65.

156. Jolivet-Reynaud, C., A. Adida, S. Michel, G. Deleage, G. Paranhos-Baccala, V. Gonin, N. Battail-Poirot, X. Lacoux, and D. Rolland. 2004. Characterization of mimotopes mimicking an immunodominant conformational epitope on the hepatitis C virus NS3 helicase. J Med Virol **72:**385-95.

157. Jones, A. T. 1978. A graphics model building and refinement system for macromolecules. Journal of Applied Crystallography **11:**268-272.

158. Jones, N. A., X. Wei, D. R. Flower, M. Wong, F. Michor, M. S. Saag, B. H. Hahn, M. A. Nowak, G. M. Shaw, and P. Borrow. 2004. Determinants of human immunodeficiency virus type 1 escape from the primary CD8+ cytotoxic T lymphocyte response. J Exp Med **200:**1243-56.

159. Jones, P. L., T. Korte, and R. Blumenthal. 1998. Conformational changes in cell surface HIV-1 envelope glycoproteins are triggered by cooperation between cell surface CD4 and co-receptors. J Biol Chem **273:**404-9.

160. Jones, T. A. 1982. p. 303-317. *In* D. Sayre (ed.), Computational Crystallography. Oxford University Press.

161. Jones, T. A., J. Y. Zou, S. W. Cowan, and Kjeldgaard. 1991. Improved methods for building protein models in electron density maps and the location of errors in these models. Acta Crystallogr A **47 (Pt 2):**110-9.

162. Jouault, T., C. Fradin, F. Dzierszinski, M. Borg-Von-Zepelin, S. Tomavo, R. Corman, P. A. Trinel, J. P. Kerckaert, and D. Poulain. 2001. Peptides that mimic Candida albicans-derived beta-1,2-linked mannosides. Glycobiology **11:**693-701.

163. Joyce, J. G., W. M. Hurni, M. J. Bogusky, V. M. Garsky, X. Liang, M. P. Citron, R. C. Danzeisen, M. D. Miller, J. W. Shiver, and P. M. Keller. 2002. Enhancement of alpha -helicity in the HIV-1 inhibitory peptide DP178 leads to an increased affinity for human monoclonal antibody 2F5 but does not elicit neutralizing responses in vitro. Implications for vaccine design. J Biol Chem **277:**45811-20.

164. Kahn, J. O., D. W. Cherng, K. Mayer, H. Murray, and S. Lagakos. 2000. Evaluation of HIV-1 immunogen, an immunologic modifier, administered to patients infected with HIV having 300 to 549 x 10(6)/L CD4 cell counts: A randomized controlled trial. Jama **284:**2193-202.

165. Karlsson, R. 1994. Real-time competitive kinetic analysis of interactions between low-molecular-weight ligands in solution and surface-immobilized receptors. Anal Biochem **221:**142-51.

166. Karnasuta, C., R. M. Paris, J. H. Cox, S. Nitayaphan, P. Pitisuttithum, P. Thongcharoen, A. E. Brown, S. Gurunathan, J. Tartaglia, W. L. Heyward, J. G. McNeil, D. L. Birx, and M. S. de Souza. 2005. Antibody-dependent cell-mediated cytotoxic responses in participants enrolled in a phase I/II ALVAC-HIV/AIDSVAX B/E prime-boost HIV-1 vaccine trial in Thailand. Vaccine **23:**2522-9.

167. Keitel, T., A. Kramer, H. Wessner, C. Scholz, J. Schneider-Mergener, and W. Hohne. 1997. Crystallographic analysis of anti-p24 (HIV-1) monoclonal antibody cross-reactivity and polyspecificity. Cell **91:**811-20.

168. Kitabwalla, M., F. Ferrantelli, T. Wang, A. Chalmers, H. Katinger, G. Stiegler, L. A. Cavacini, T. C. Chou, and R. M. Ruprecht. 2003. Primary African HIV clade A and D isolates: effective cross-clade neutralization with a quadruple combination of human monoclonal antibodies raised against clade B. AIDS Res Hum Retroviruses **19:**125-31.

169. Kostrikis, L. G., Y. Cao, H. Ngai, J. P. Moore, and D. D. Ho. 1996. Quantitative analysis of serum neutralization of human immunodeficiency virus type 1 from subtypes A, B, C, D, E, F, and I: lack of direct correlation between neutralization serotypes and genetic subtypes and evidence for prevalent serum-dependent infectivity enhancement. J Virol **70:**445-58.

170. Koup, R. A., J. T. Safrit, Y. Cao, C. A. Andrews, G. McLeod, W. Borkowsky, C. Farthing, and D. D. Ho. 1994. Temporal association of cellular immune responses with the initial control of viremia in primary human immunodeficiency virus type 1 syndrome. J Virol **68:**4650-5.

171. Kramer, A., T. Keitel, K. Winkler, W. Stocklein, W. Hohne, and J. Schneider-Mergener. 1997. Molecular basis for the binding promiscuity of an anti-p24 (HIV-1) monoclonal antibody. Cell **91:**799-809.

172. Kuby, J. 1994. Immunology, 2nd ed. W. H. freeman and Company, New York.

173. Kunert, R., F. Ruker, and H. Katinger. 1998. Molecular characterization of five neutralizing anti-HIV type 1 antibodies: identification of nonconventional D segments in the human monoclonal antibodies 2G12 and 2F5. AIDS Res Hum Retroviruses **14:**1115-28.

174. Kunkel, T. A., K. Bebenek, and J. McClary. 1991. Efficient site-directed mutagenesis using uracil-containing DNA. Methods Enzymol **204:**125-39.

175. Kwong, P. D., M. L. Doyle, D. J. Casper, C. Cicala, S. A. Leavitt, S. Majeed, T. D. Steenbeke, M. Venturi, I. Chaiken, M. Fung, H. Katinger, P. W. Parren, J. Robinson, D. Van Ryk, L. Wang, D. R. Burton, E. Freire, R. Wyatt, J. Sodroski, W. A. Hendrickson, and J. Arthos. 2002. HIV-1 evades antibody-mediated neutralization through conformational masking of receptor-binding sites. Nature **420:**678-82.

176. Kwong, P. D., R. Wyatt, J. Robinson, R. W. Sweet, J. Sodroski, and W. A. Hendrickson. 1998. Structure of an HIV gp120 envelope glycoprotein in complex with the CD4 receptor and a neutralizing human antibody. Nature **393:**648-59.

177. Kwong, P. D., R. Wyatt, Q. J. Sattentau, J. Sodroski, and W. A. Hendrickson. 2000. Oligomeric modeling and electrostatic analysis of the gp120 envelope glycoprotein of human immunodeficiency virus. J Virol **74:**1961-72.

178. Lathey, J. L., R. D. Pratt, and S. A. Spector. 1997. Appearance of autologous neutralizing antibody correlates with reduction of viral load and phenotype switch

during primary infection with human immunodeficiency virus. J. Infect. Dis **175:**231-232.

179. Layne, S. P., M. J. Merges, M. Dembo, J. L. Spouge, S. R. Conley, J. P. Moore, J. L. Raina, H. Renz, H. R. Gelderblom, and P. L. Nara. 1992. Factors underlying spontaneous inactivation and susceptibility to neutralization of human immunodeficiency virus. Virology **189:**695-714.

180. Lee, H. K., C. N. Scanlan, C. Y. Huang, A. Y. Chang, D. A. Calarese, R. A. Dwek, P. M. Rudd, D. R. Burton, I. A. Wilson, and C. H. Wong. 2004. Reactivity-based one-pot synthesis of oligomannoses: defining antigens recognized by 2G12, a broadly neutralizing anti-HIV-1 antibody. Angew Chem Int Ed Engl **43:**1000-3.

181. Lesinski, G. B., S. L. Smithson, N. Srivastava, D. Chen, G. Widera, and M. A. Westerink. 2001. A DNA vaccine encoding a peptide mimic of Streptococcus pneumoniae serotype 4 capsular polysaccharide induces specific anti-carbohydrate antibodies in Balb/c mice. Vaccine **19:**1717-26.

182. Letvin, N. L., D. H. Barouch, and D. C. Montefiori. 2002. Prospects for vaccine protection against HIV-1 infection and AIDS. Annu Rev Immunol **20:**73-99.

183. Levine, A. M., S. Groshen, J. Allen, K. M. Munson, D. J. Carlo, A. E. Daigle, F. Ferre, F. C. Jensen, S. P. Richieri, R. J. Trauger, J. W. Parker, P. L. Salk, and J. Salk. 1996. Initial studies on active immunization of HIV-infected subjects using a gp120-depleted HIV-1 Immunogen: long-term follow-up. J Acquir Immune Defic Syndr Hum Retrovirol **11:**351-64.

184. Levy, D. N., G. M. Aldrovandi, O. Kutsch, and G. M. Shaw. 2004. Dynamics of HIV-1 recombination in its natural target cells. Proc Natl Acad Sci U S A **101:**4204-9.

185. Li, H., and L. X. Wang. 2004. Design and synthesis of a template-assembled oligomannose cluster as an epitope mimic for human HIV-neutralizing antibody 2G12. Org Biomol Chem **2:**483-8.

186. Liang, X., S. Munshi, J. Shendure, G. Mark, 3rd, M. E. Davies, D. C. Freed, D. C. Montefiori, and J. W. Shiver. 1999. Epitope insertion into variable loops of HIV-1 gp120 as a potential means to improve immunogenicity of viral envelope protein. Vaccine **17:**2862-72.

187. Locher, C. P., R. M. Grant, E. A. Collisson, G. Reyes-Teran, T. Elbeik, J. O. Kahn, and J. A. Levy. 1999. Antibody and cellular immune responses in breakthrough infection subjects after HIV type 1 glycoprotein 120 vaccination. AIDS Res Hum Retroviruses **15:**1685-9.

188. Lorin, C., L. Mollet, F. Delebecque, C. Combredet, B. Hurtrel, P. Charneau, M. Brahic, and F. Tangy. 2004. A single injection of recombinant measles virus vaccines expressing human immunodeficiency virus (HIV) type 1 clade B envelope

glycoproteins induces neutralizing antibodies and cellular immune responses to HIV. J Virol **78:**146-57.

189. Lou, Q., and I. Pastan. 1999. A Lewis(y) epitope mimicking peptide induces anti-Lewis(y) immune responses in rabbits and mice. J Pept Res **53:**252-60.

190. MacCallum, R. M., A. C. Martin, and J. M. Thornton. 1996. Antibody-antigen interactions: contact analysis and binding site topography. J Mol Biol **262:**732-45.

191. Mackewicz, C., L. C. Yang, J. D. Lifson, and a. J. A. Levy. 1994. Non-cytolytic CD8 T-cell anti-HIV responses in primary HIV-1 infection. Lancet **344:**1671-1673.

192. Maerz, A. L., H. E. Drummer, K. A. Wilson, and P. Poumbourios. 2001. Functional analysis of the disulfide-bonded loop/chain reversal region of human immunodeficiency virus type 1 gp41 reveals a critical role in gp120-gp41 association. J Virol **75:**6635-44.

193. Manaresi, E., G. Gallinella, A. M. Morselli Labate, P. Zucchelli, D. Zaccarelli, S. Ambretti, S. Delbarba, M. Zerbini, and M. Musiani. 2004. Seroprevalence of IgG against conformational and linear capsid antigens of parvovirus B19 in Italian blood donors. Epidemiol Infect **132:**857-62.

194. Mandal, M., V. Y. Dudkin, X. Geng, and S. J. Danishefsky. 2004. In pursuit of carbohydrate-based HIV vaccines, part 1: The total synthesis of hybrid-type gp120 fragments. Angew Chem Int Ed Engl **43:**2557-61.

195. Marchalonis, J. J., M. K. Adelman, I. F. Robey, S. F. Schluter, and A. B. Edmundson. 2001. Exquisite specificity and peptide epitope recognition promiscuity, properties shared by antibodies from sharks to humans. J Mol Recognit **14:**110-21.

196. Mascola, J. R., M. G. Lewis, G. Stiegler, D. Harris, T. C. VanCott, D. Hayes, M. K. Louder, C. R. Brown, C. V. Sapan, S. S. Frankel, Y. Lu, M. L. Robb, H. Katinger, and D. L. Birx. 1999. Protection of Macaques against pathogenic simian/human immunodeficiency virus 89.6PD by passive transfer of neutralizing antibodies. J Virol **73:**4009-18.

197. Mascola, J. R., M. G. Lewis, T. C. VanCott, G. Stiegler, H. Katinger, M. Seaman, K. Beaudry, D. H. Barouch, B. Korioth-Schmitz, G. Krivulka, A. Sambor, B. Welcher, D. C. Douek, D. C. Montefiori, J. W. Shiver, P. Poignard, D. R. Burton, and N. L. Letvin. 2003. Cellular immunity elicited by human immunodeficiency virus type 1/ simian immunodeficiency virus DNA vaccination does not augment the sterile protection afforded by passive infusion of neutralizing antibodies. J Virol **77:**10348-56.

198. Mascola, J. R., M. K. Louder, T. C. VanCott, C. V. Sapan, J. S. Lambert, L. R. Muenz, B. Bunow, D. L. Birx, and M. L. Robb. 1997. Potent and synergistic neutralization of human immunodeficiency virus (HIV) type 1 primary isolates by

hyperimmune anti-HIV immunoglobulin combined with monoclonal antibodies 2F5 and 2G12. J Virol **71:**7198-206.

199. Mascola, J. R., B. J. Mathieson, P. M. Zack, M. C. Walker, S. B. Halstead, and D. S. Burke. 1993. Summary report: workshop on the potential risks of antibody-dependent enhancement in human HIV vaccine trials. AIDS Res Hum Retroviruses **9:**1175-84.

200. Mascola, J. R., S. W. Snyder, O. S. Weislow, S. M. Belay, R. B. Belshe, D. H. Schwartz, M. L. Clements, R. Dolin, B. S. Graham, G. J. Gorse, M. C. Keefer, M. J. McElrath, M. C. Walker, K. F. Wagner, J. G. McNeil, F. E. McCutchan, and D. S. Burke. 1996. Immunization with envelope subunit vaccine products elicits neutralizing antibodies against laboratory-adapted but not primary isolates of human immunodeficiency virus type 1. J. Infect. Dis. **173:**340-348.

201. Mascola, J. R., G. Stiegler, T. C. VanCott, H. Katinger, C. B. Carpenter, C. E. Hanson, H. Beary, D. Hayes, S. S. Frankel, D. L. Birx, and M. G. Lewis. 2000. Protection of macaques against vaginal transmission of a pathogenic HIV 1/SIV chimeric virus by passive infusion of neutralizing antibodies. Nature Med. **6:**207-210.

202. McCormack, S., A. Tilzey, A. Carmichael, F. Gotch, J. Kepple, A. Newberry, G. Jones, S. Lister, S. Beddows, R. Cheingsong, A. Rees, A. Babiker, J. Banatvala, C. Bruck, J. Darbyshire, D. Tyrrell, C. Van Hoecke, and J. Weber. 2000. A phase I trial in HIV negative healthy volunteers evaluating the effect of potent adjuvants on immunogenicity of a recombinant gp120W61D derived from dual tropic R5X4 HIV-1ACH320. Vaccine **18:**1166-77.

203. McGaughey, G. B., M. Citron, R. C. Danzeisen, R. M. Freidinger, V. M. Garsky, W. M. Hurni, J. G. Joyce, X. Liang, M. Miller, J. Shiver, and M. J. Bogusky. 2003. HIV-1 vaccine development: constrained peptide immunogens show improved binding to the anti-HIV-1 gp41 MAb. Biochemistry **42:**3214-23.

204. Meloen, R. H., W. C. Puijk, and J. W. Slootstra. 2000. Mimotopes: realization of an unlikely concept. J Mol Recognit **13:**352-9.

205. Menendez, A., L. L. Bonnycastle, C. C. O. Pan, and J. K. Scott. 2001. Screening peptide libraries. *In* C. F. Barbas, D. R. Burton, J. K. Scott, and G. J. Silverman (ed.), Phage Display. A Laboratory Manual. Cold Spring Harbor Laboratory Press, New York.

206. Menendez, A., K. C. Chow, O. C. Pan, and J. K. Scott. 2004. Human immunodeficiency virus type 1-neutralizing monoclonal antibody 2F5 is multispecific for sequences flanking the DKW core epitope. J Mol Biol **338:**311-27.

207. Menendez, A., and J. K. Scott. 2005. The nature of target-unrelated peptides recovered in the screening of phage-displayed random peptide libraries with antibodies. Anal Biochem **336:**145-57.

208. Montefiori, D. C., G. Pantaleo, L. M. Fink, J. T. Zhou, J. Y. Zhou, M. Bilska, G. D. Miralles, and A. S. Fauci. 1996. Neutralizing and infection-enhancing antibody responses to human immunodeficiency virus type 1 in long-term nonprogressors. J. Infect. Dis. **173:**60-67.

209. Moog, C., H. J. Fleury, I. Pellegrin, A. Kirn, and A. M. Aubertin. 1997. Autologous and heterologous neutralizing antibody responses following initial seroconversion in human immunodeficiency virus type 1-infected individuals. J Virol **71:**3734-41.

210. Moore, J. P., Y. Cao, L. Qing, Q. J. Sattentau, J. Pyati, R. Koduri, J. Robinson, C. F. Barbas, 3rd, D. R. Burton, and D. D. Ho. 1995. Primary isolates of human immunodeficiency virus type 1 are relatively resistant to neutralization by monoclonal antibodies to gp120, and their neutralization is not predicted by studies with monomeric gp120. J Virol **69:**101-9.

211. Moore, J. P., and D. D. Ho. 1993. Antibodies to discontinuous or conformationally sensitive epitopes on the gp120 glycoprotein of human immunodeficiency virus type 1 are highly prevalent in sera of infected humans. J Virol **67:**863-75.

212. Moore, J. P., and J. Sodroski. 1996. Antibody cross-competition analysis of the human immunodeficiency virus type 1 gp120 exterior envelope glycoprotein. J. Virol. **70:**1863-1872.

213. Morens, D. M. 1994. Antibody-dependent enhancement of infection and the pathogenesis of viral disease. Clin. Infect. Dis. **19:**500-512.

214. Moss, R. B., F. Ferre, A. Levine, J. Turner, F. C. Jensen, A. E. Daigle, S. P. Richieri, A. Truckenbrod, R. J. Trauger, D. J. Carlo, and J. Salk. 1996. Viral load, CD4 percentage, and delayed-type hypersensitivity in subjects receiving the HIV-1 immunogen and antiviral drug therapy. J Clin Immunol **16:**266-71.

215. Mossman, S. P., F. Bex, P. Berglund, J. Arthos, S. P. O'Neil, D. Riley, D. H. Maul, C. Bruck, P. Momin, A. Burny, P. N. Fultz, J. I. Mullins, P. Liljestrom, and E. A. Hoover. 1996. Protection against lethal simian immunodeficiency virus SIVsmmPBj14 disease by a recombinant Semliki Forest virus gp160 vaccine and by a gp120 subunit vaccine. J Virol **70:**1953-60.

216. Muhlbacher, M., M. Spruth, F. Siegel, R. Zangerle, and M. P. Dierich. 1999. Longitudinal study of antibody reactivity against HIV-1 envelope and a peptide representing a conserved site on Gp41 in HIV-1-infected patients. Immunobiology **200:**295-305.

217. Muster, T., B. Ferko, A. Klima, M. Purtscher, A. Trkola, P. Schulz, A. Grassauer, O. G. Engelhardt, A. Garcia-Sastre, P. Palese, and et al. 1995. Mucosal model of

immunization against human immunodeficiency virus type 1 with a chimeric influenza virus. J Virol **69:**6678-86.

218. Muster, T., R. Guinea, A. Trkola, M. Purtscher, A. Klima, F. Steindl, P. Palese, and H. Katinger. 1994. Cross-neutralizing activity against divergent human immunodeficiency virus type 1 isolates induced by the gp41 sequence ELDKWAS. J Virol **68:**4031-4.

219. Muster, T., F. Steindl, M. Purtscher, A. Trkola, A. Klima, G. Himmler, F. Ruker, and H. Katinger. 1993. A conserved neutralizing epitope on gp41 of human immunodeficiency virus type 1. J Virol **67:**6642-7.

220. Myszka, D. G., R. W. Sweet, P. Hensley, M. Brigham-Burke, P. D. Kwong, W. A. Hendrickson, R. Wyatt, J. Sodroski, and M. L. Doyle. 2000. Energetics of the HIV gp120-CD4 binding reaction. Proc Natl Acad Sci U S A **97:**9026-31.

221. Naismith, J. H., and R. A. Field. 1996. Structural basis of trimannoside recognition by concanavalin A. J Biol Chem **271:**972-6.

222. Navaza, J. 1994. AMoRe: An Automated Package for Molecular Replacement. Acta Crystallographica **A50:**157-163.

223. Negroni, M., and H. Buc. 2001. Mechanisms of retroviral recombination. Annu Rev Genet **35:**275-302.

224. Ni, J., R. Powell, I. V. Baskakov, A. DeVico, G. K. Lewis, and L. X. Wang. 2004. Synthesis, conformation, and immunogenicity of monosaccharide-centered multivalent HIV-1 gp41 peptides containing the sequence of DP178. Bioorg Med Chem **12:**3141-8.

225. Nieba, L., A. Krebber, and A. Pluckthun. 1996. Competition BIAcore for measuring true affinities: large differences from values determined from binding kinetics. Anal Biochem **234:**155-65.

226. Nyambi, P. N., P. Lewi , M. Peeters, W. Janssens, L. Heyndrickx, K. Fransen, K. Andries, M. Vanden Haesevelde, J. Heeney, P. Piot, and G. van der Groen. 1997. Study of the dynamics of neutralization escape mutants in a chimpanzee naturally infected with the simian immunodeficiency virus SIVcpz-ant. Journal of Virology **71:**2320-2330.

227. O'Shannessy, D. J., and D. J. Winzor. 1996. Interpretation of deviations from pseudo-first-order kinetic behavior in the characterization of ligand binding by biosensor technology. Anal Biochem **236:**275-83.

228. Ofek, G., M. Tang, A. Sambor, H. Katinger, J. R. Mascola, R. Wyatt, and P. D. Kwong. 2004. Structure and Mechanistic Analysis of the Anti-Human Immunodeficiency Virus Type 1 Antibody 2F5 in Complex with Its gp41 Epitope. J Virol **78:**10724-37.

229. Oldenburg, K. R., D. Loganathan, I. J. Goldstein, P. G. Schultz, and M. A. Gallop. 1992. Peptide ligands for a sugar-binding protein isolated from a random peptide library. Proc Natl Acad Sci U S A **89:**5393-7.

230. Otwinowski, Z., and W. Minor. 1997. Processing of X-ray difraction data collected in oscillation mode. Methods in Enzymology **276:**307-326.

231. Pai, E. F., M. H. Klein, P. Chong, and A. Pedyczak. 2000. Fab'-epitope complex from the HIV-1 cross-neutralizing monoclonal antibody 2F5.

232. Palker, T. J., M. E. Clark, A. J. Langlois, T. J. Matthews, K. J. Weinhold, R. R. Randall, D. P. Bolognesi, and B. F. Haynes. 1988. Type-specific neutralization of the human immunodeficiency virus with antibodies to env-encoded synthetic peptides. Proc Natl Acad Sci U S A **85:**1932-6.

233. Pantophlet, R., E. Ollmann Saphire, P. Poignard, P. W. Parren, I. A. Wilson, and D. R. Burton. 2003. Fine mapping of the interaction of neutralizing and nonneutralizing monoclonal antibodies with the CD4 binding site of human immunodeficiency virus type 1 gp120. J Virol **77:**642-58.

234. Pantophlet, R., I. A. Wilson, and D. R. Burton. 2003. Hyperglycosylated mutants of human immunodeficiency virus (HIV) type 1 monomeric gp120 as novel antigens for HIV vaccine design. J Virol **77:**5889-901.

235. Parker, C. E., L. J. Deterding, C. Hager-Braun, J. M. Binley, N. Schulke, H. Katinger, J. P. Moore, and K. B. Tomer. 2001. Fine definition of the epitope on the gp41 glycoprotein of human immunodeficiency virus type 1 for the neutralizing monoclonal antibody 2F5. J Virol **75:**10906-11.

236. Parmley, S. F., and G. P. Smith. 1988. Antibody-selectable filamentous fd phage vectors: affinity purification of target genes. Gene **73:**305-18.

237. Parren, P. W., and D. R. Burton. 2001. The antiviral activity of antibodies in vitro and in vivo. Adv Immunol **77:**195-262.

238. Parren, P. W., H. J. Ditzel, R. J. Gulizia, J. M. Binley, C. F. Barbas, 3rd, D. R. Burton, and D. E. Mosier. 1995. Protection against HIV-1 infection in hu-PBL-SCID mice by passive immunization with a neutralizing human monoclonal antibody against the gp120 CD4-binding site. Aids **9:**F1-6.

239. Parren, P. W., P. A. Marx, A. J. Hessell, A. Luckay, J. Harouse, C. Cheng-Mayer, J. P. Moore, and D. R. Burton. 2001. Antibody protects macaques against vaginal challenge with a pathogenic R5 simian/human immunodeficiency virus at serum levels giving complete neutralization in vitro. J Virol **75:**8340-7.

240. Parren, P. W., I. Mondor, D. Naniche, H. J. Ditzel, P. J. Klasse, D. R. Burton, and Q. J. Sattentau. 1998. Neutralization of human immunodeficiency virus type 1 by

antibody to gp120 is determined primarily by occupancy of sites on the virion irrespective of epitope specificity. J Virol **72:**3512-9.

241. Parren, P. W., J. P. Moore, D. R. Burton, and Q. J. Sattentau. 1999. The neutralizing antibody response to HIV-1: viral evasion and escape from humoral immunity. Aids **13 Suppl A:**S137-62.

242. Parren, P. W., M. Wang, A. Trkola, J. M. Binley, M. Purtscher, H. Katinger, J. P. Moore, and D. R. Burton. 1998. Antibody neutralization-resistant primary isolates of human immunodeficiency virus type 1. J Virol **72:**10270-4.

243. Parren, P. W. H. I., and D. R. Burton. 1997. HIV-1 antibody- debris or virion? Nature Med. **3:**366 367.

244. Pascual, R., M. R. Moreno, and J. Villalain. 2005. A Peptide Pertaining to the Loop Segment of Human Immunodeficiency Virus gp41 Binds and Interacts with Model Biomembranes: Implications for the Fusion Mechanism. J Virol **79:**5142-52.

245. Peisajovich, S. G., and Y. Shai. 2001. SIV gp41 binds to membranes both in the monomeric and trimeric states: consequences for the neuropathology and inhibition of HIV infection. J Mol Biol **311:**249-54.

246. Perales, M. A., D. H. Schwartz, J. A. Fabry, and J. Lieberman. 1995. A vaccinia-gp160-based vaccine but not a gp160 protein vaccine elicits anti-gp160 cytotoxic T lymphocytes in some HIV-1 seronegative vaccinees. J Acquir Immune Defic Syndr Hum Retrovirol **10:**27-35.

247. Phalipon, A., A. Folgori, J. Arondel, G. Sgaramella, P. Fortugno, R. Cortese, P. J. Sansonetti, and F. Felici. 1997. Induction of anti-carbohydrate antibodies by phage library-selected peptide mimics. Eur J Immunol **27:**2620-5.

248. Pialoux, G., J. L. Excler, Y. Rivier, G. Gonzalez-Canali, V. Feuillie, P. Coulaud, J. C. Gluckman, T. J. Matthews, B. Meigner, M. P. Kieny, P. Gonnet, I. Diaz, C. Meric, E. Paoletti, J. Tartaglia, H. Salomon, and S. Plotkin. 1995. A prime-boost approach to HIV preventive vaccine using a recombinant canarypox virus expressing glycoprotein 160 (MN) followed by a recombinant glycoprotein 160 (MN/LAI). AIDS Res. Hum. Retrov. **11:**373-381.

249. Pilgrim, A. K., G. Pantaleo, O. J. Cohen, L. M. Fink, J. Y. Zhou, J. T. Zhou, D. P. Bolognesi, A. S. Fauci, and D. C. Montefiori. 1997. Neutralizing antibody responses to human immunodeficiency virus type 1 in primary infection and long-term-nonprogressive infection. J Infect Dis **176:**924-32.

250. Pincus, S. H., M. J. Smith, H. J. Jennings, J. B. Burritt, and P. M. Glee. 1998. Peptides that mimic the group B streptococcal type III capsular polysaccharide antigen. J Immunol **160:**293-8.

251. Pinilla, C., S. Chendra, J. R. Appel, and R. A. Houghten. 1995. Elucidation of monoclonal antibody polyspecificity using a synthetic combinatorial library. Pept Res **8:**250-7.

252. Pohlmann, S., F. Baribaud, B. Lee, G. J. Leslie, M. D. Sanchez, K. Hiebenthal-Millow, J. Munch, F. Kirchhoff, and R. W. Doms. 2001. DC-SIGN interactions with human immunodeficiency virus type 1 and 2 and simian immunodeficiency virus. J Virol **75:**4664-72.

253. Poignard, P., M. Moulard, E. Golez, V. Vivona, M. Franti, S. Venturini, M. Wang, P. W. Parren, and D. R. Burton. 2003. Heterogeneity of envelope molecules expressed on primary human immunodeficiency virus type 1 particles as probed by the binding of neutralizing and nonneutralizing antibodies. J Virol **77:**353-65.

254. Poignard, P., R. Sabbe, G. R. Picchio, M. Wang, R. J. Gulizia, H. Katinger, P. W. Parren, D. E. Mosier, and D. R. Burton. 1999. Neutralizing antibodies have limited effects on the control of established HIV-1 infection in vivo. Immunity **10:**431-8.

255. Poignard, P., E. O. Saphire, P. W. Parren, and D. R. Burton. 2001. gp120: Biologic aspects of structural features. Annu Rev Immunol **19:**253-74.

256. Ponnuraj, E. M., J. Springer, A. R. Hayward, H. Wilson, and E. A. Simoes. 2003. Antibody-dependent enhancement, a possible mechanism in augmented pulmonary disease of respiratory syncytial virus in the Bonnet monkey model. J Infect Dis **187:**1257-63.

257. Popkov, M., R. G. Mage, C. B. Alexander, S. Thundivalappil, C. F. Barbas, 3rd, and C. Rader. 2003. Rabbit immune repertoires as sources for therapeutic monoclonal antibodies: the impact of kappa allotype-correlated variation in cysteine content on antibody libraries selected by phage display. J Mol Biol **325:**325-35.

258. Preston, B. D., B. J. Poiesz, and L. A. Loeb. 1988. Fidelity of HIV-1 reverse transcriptase. Science **242:**1168-71.

259. Prinz, D. M., S. L. Smithson, T. Kieber-Emmons, and M. A. Westerink. 2003. Induction of a protective capsular polysaccharide antibody response to a multiepitope DNA vaccine encoding a peptide mimic of meningococcal serogroup C capsular polysaccharide. Immunology **110:**242-9.

260. Prinz, D. M., S. L. Smithson, and M. A. Westerink. 2004. Two different methods result in the selection of peptides that induce a protective antibody response to Neisseria meningitidis serogroup C. J Immunol Methods **285:**1-14.

261. Purtscher, M., A. Trkola, A. Grassauer, P. M. Schulz, A. Klima, S. Dopper, G. Gruber, A. Buchacher, T. Muster, and H. Katinger. 1996. Restricted antigenic variability of the epitope recognized by the neutralizing gp41 antibody 2F5. Aids **10:**587-93.

262. Putterman, C., B. Deocharan, and B. Diamond. 2000. Molecular analysis of the autoantibody response in peptide-induced autoimmunity. J Immunol **164:**2542-9.

263. Pyle, S. W., J. W. Bess, Jr., W. G. Robey, P. J. Fischinger, R. V. Gilden, and L. O. Arthur. 1987. Purification of 120,000 dalton envelope glycoprotein from culture fluids of human immunodeficiency virus (HIV)-infected H9 cells. AIDS Res Hum Retroviruses **3:**387-400.

264. Quinnan, G. V., Jr., X. F. Yu, M. G. Lewis, P. F. Zhang, G. Sutter, P. Silvera, M. Dong, A. Choudhary, P. T. Sarkis, P. Bouma, Z. Zhang, D. C. Montefiori, T. C. Vancott, and C. C. Broder. 2005. Protection of rhesus monkeys against infection with minimally pathogenic simian-human immunodeficiency virus: correlations with neutralizing antibodies and cytotoxic T cells. J Virol **79:**3358-69.

265. Reimann, K. A., J. T. Li, R. Veazey, M. Halloran, I. W. Park, G. Karlsson, J. Sodroski, and N. Letvin. 1996. A chimeric simian/human immunodeficiency virus expressing a primary patient human immunodeficiency virus type 1 isolate *env* causes an AIDS-like disease after *in vivo* passage in *Rhesus* monkeys. J. Virol. **70:**6922-6928.

266. Richalet-Secordel, P. M., N. Rauffer-Bruyere, L. L. Christensen, B. Ofenloch-Haehnle, C. Seidel, and M. H. Van Regenmortel. 1997. Concentration measurement of unpurified proteins using biosensor technology under conditions of partial mass transport limitation. Anal Biochem **249:**165-73.

267. Richardson, T. M. J., B. L. Stryjewski, C. C. Broder, J. A. Hoxie, J. R. Mascola, P. L. Earl, and R. W. Doms. 1996. Humoral response to oligomeric human immunodeficiency virus type 1 envelope protein. J. Virol. **70:**753-762.

268. Richman, D. D., T. Wrin, S. J. Little, and C. J. Petropoulos. 2003. Rapid evolution of the neutralizing antibody response to HIV type 1 infection. Proc Natl Acad Sci U S A **100:**4144-9.

269. Roben, P., J. P. Moore, M. Thali, J. Sodroski, C. F. Barbas, 3rd, and D. R. Burton. 1994. Recognition properties of a panel of human recombinant Fab fragments to the CD4 binding site of gp120 that show differing abilities to neutralize human immunodeficiency virus type 1. J Virol **68:**4821-8.

270. Robey, I. F., A. B. Edmundson, S. F. Schluter, D. E. Yocum, and J. J. Marchalonis. 2002. Specificity mapping of human anti-T cell receptor monoclonal natural antibodies: defining the properties of epitope recognition promiscuity. Faseb J **16:**642-52.

271. Robey, W. G., B. Safai, S. Oroszlan, L. O. Arthur, M. A. Gonda, R. C. Gallo, and P. J. Fischinger. 1985. Characterization of envelope and core structural gene products of HTLV-III with sera from AIDS patients. Science **228:**593-5.

272. Rossio, J. L., M. T. Esser, K. Suryanarayana, D. K. Schneider, J. W. Bess, Jr., G. M. Vasquez, T. A. Wiltrout, E. Chertova, M. K. Grimes, Q. Sattentau, L. O. Arthur, L.

E. Henderson, and J. D. Lifson. 1998. Inactivation of human immunodeficiency virus type 1 infectivity with preservation of conformational and functional integrity of virion surface proteins. J Virol **72:**7992-8001.

273. Roux, K. H., P. Zhu, M. Seavy, H. Katinger, R. Kunert, and V. Seamon. 2004. Electron microscopic and immunochemical analysis of the broadly neutralizing HIV-1-specific, anti-carbohydrate antibody, 2G12. Mol Immunol **41:**1001-11.

274. Ruppach, H., P. Nara, I. Raudonat, Z. Elanjikal, H. Rubsamen-Waigmann, and U. Dietrich. 2000. Human immunodeficiency virus (HIV)-positive sera obtained shortly after seroconversion neutralize autologous HIV type 1 isolates on primary macrophages but not on lymphocytes. J Virol **74:**5403-11.

275. Salzwedel, K., J. T. West, and E. Hunter. 1999. A conserved tryptophan-rich motif in the membrane-proximal region of the human immunodeficiency virus type 1 gp41 ectodomain is important for Env-mediated fusion and virus infectivity. J Virol **73:**2469-80.

276. Sambrook, J., E. F. Fritsch, and T. Maniatis. 1989. Molecular Cloning. A Laboratory Manual. Cold Spring Harbor Laboratory Press, New York.

277. Sanders, R. W., M. Venturi, L. Schiffner, R. Kalyanaraman, H. Katinger, K. O. Lloyd, P. D. Kwong, and J. P. Moore. 2002. The mannose-dependent epitope for neutralizing antibody 2G12 on human immunodeficiency virus type 1 glycoprotein gp120. J Virol **76:**7293-305.

278. Sanders, R. W., M. Vesanen, N. Schuelke, A. Master, L. Schiffner, R. Kalyanaraman, M. Paluch, B. Berkhout, P. J. Maddon, W. C. Olson, M. Lu, and J. P. Moore. 2002. Stabilization of the soluble, cleaved, trimeric form of the envelope glycoprotein complex of human immunodeficiency virus type 1. J Virol **76:**8875-89.

279. Sanner, M. F. 1999. Python: a programming language for software integration and development. J Mol Graph Model **17:**57-61.

280. **Sanner, M. F., B. S. Duncan, C. J. Carrillo, and A. J. Olson.** 1999. Presented at the Pacific Symposium in Biocomputing, Mauna Lani, Hawaii, USA.

281. Sanner, M. F., A. J. Olson, and J. C. Spehner. 1996. Reduced surface: an efficient way to compute molecular surfaces. Biopolymers **38:**305-20.

282. Saphire, E. O., M. Montero, A. Menendez, N. V. van Houten, R. Pantophlet, M. B. Zwick, P. W. Parren, D. R. Burton, J. K. Scott, and W. I. A. Crystal structure of a broadly neutralizing anti-HIV-1 antibody in complex with a peptide: Mechanism of gp120 cross-reactivity.

283. Saphire, E. O., P. W. Parren, C. F. Barbas, 3rd, D. R. Burton, and I. A. Wilson. 2001. Crystallization and preliminary structure determination of an intact human

immunoglobulin, b12: an antibody that broadly neutralizes primary isolates of HIV-1. Acta Crystallogr D Biol Crystallogr **57:**168-71.

284. Saphire, E. O., P. W. Parren, R. Pantophlet, M. B. Zwick, G. M. Morris, P. M. Rudd, R. A. Dwek, R. L. Stanfield, D. R. Burton, and I. A. Wilson. 2001. Crystal structure of a neutralizing human IgG against HIV-1: a template for vaccine design. Science **293:**1155-9.

285. Saphire, E. O., R. L. Stanfield, M. D. Crispin, P. W. Parren, P. M. Rudd, R. A. Dwek, D. R. Burton, and I. A. Wilson. 2002. Contrasting IgG structures reveal extreme asymmetry and flexibility. J Mol Biol **319:**9-18.

286. Sattentau, Q. J., and J. P. Moore. 1995. Human immunodeficiency virus type 1 neutralization is determined by epitope exposure on the gp120 oligomer. J Exp Med **182:**185-96.

287. Sattentau, Q. J., S. Zolla-Pazner, and P. Poignard. 1995. Epitope exposure on functional, oligomeric HIV-1 gp41 molecules. Virology **206:**713-7.

288. Scala, G., X. Chen, W. Liu, J. N. Telles, O. J. Cohen, M. Vaccarezza , T. Igarashi, and A. S. Fauci. 1999. Selection of HIV-specific immunogenic epitopes by screening random peptide libraries with HIV-1-positive sera. J. Immunol. **162:**6155-6161.

289. Scanlan, C. N., R. Pantophlet, M. R. Wormald, E. Ollmann Saphire, R. Stanfield, I. A. Wilson, H. Katinger, R. A. Dwek, P. M. Rudd, and D. R. Burton. 2002. The broadly neutralizing anti-human immunodeficiency virus type 1 antibody 2G12 recognizes a cluster of alpha1-->2 mannose residues on the outer face of gp120. J Virol **76:**7306-21.

290. Scanlan, C. N., R. Pantophlet, M. R. Wormald, E. O. Saphire, D. Calarese, R. Stanfield, I. A. Wilson, H. Katinger, R. A. Dwek, D. R. Burton, and P. M. Rudd. 2003. The carbohydrate epitope of the neutralizing anti-HIV-1 antibody 2G12. Adv Exp Med Biol **535:**205-18.

291. Schibli, D. J., R. C. Montelaro, and H. J. Vogel. 2001. The membrane-proximal tryptophan-rich region of the HIV glycoprotein, gp41, forms a well-defined helix in dodecylphosphocholine micelles. Biochemistry **40:**9570-8.

292. Schneider, J., O. Kaaden, T. D. Copeland, S. Oroszlan, and G. Hunsmann. 1986. Shedding and interspecies type sero-reactivity of the envelope glycopolypeptide gp120 of the human immunodeficiency virus. J Gen Virol **67 (Pt 11):**2533-8.

293. Schulke, N., M. S. Vesanen, R. W. Sanders, P. Zhu, M. Lu, D. J. Anselma, A. R. Villa, P. W. Parren, J. M. Binley, K. H. Roux, P. J. Maddon, J. P. Moore, and W. C. Olson. 2002. Oligomeric and conformational properties of a proteolytically mature, disulfide-stabilized human immunodeficiency virus type 1 gp140 envelope glycoprotein. J Virol **76:**7760-76.

294. Scott, J. K., and C. F. Barbas , III. 2001. Phage-display vectors. *In* C. F. Barbas, D. R. Burton, J. K. Scott, and G. J. Silverman (ed.), Phage Display. A Laboratory Manual. Cold Spring Harbor Laboratory Press, New York.

295. Scott, J. K., D. Loganathan, R. B. Easley, X. Gong, and I. J. Goldstein. 1992. A family of concanavalin A-binding peptides from a hexapeptide epitope library. Proc Natl Acad Sci U S A **89:**5398-402.

296. Scott, J. K., and G. P. Smith. 1990. Searching for peptide ligands with an epitope library. Science **249:**386-90.

297. Seaman, M. S., L. Xu, K. Beaudry, K. L. Martin, M. H. Beddall, A. Miura, A. Sambor, B. K. Chakrabarti, Y. Huang, R. Bailer, R. A. Koup, J. R. Mascola, G. J. Nabel, and N. L. Letvin. 2005. Multiclade human immunodeficiency virus type 1 envelope immunogens elicit broad cellular and humoral immunity in rhesus monkeys. J Virol **79:**2956-63.

298. Sheppard, N., and Q. Sattentau. 2005. The prospects for vaccines against HIV-1: more than a field of long-term nonprogression? Expert Rev Mol Med **7:**1-21.

299. Simon, V., and D. D. Ho. 2003. HIV-1 dynamics in vivo: implications for therapy. Nat Rev Microbiol **1:**181-90.

300. Smith, G. P. 1985. Filamentous fusion phage: novel expression vectors that display cloned antigens on the virion surface. Science **228:**1315-7.

301. Stanfield, R. L., T. M. Fieser, R. A. Lerner, and I. A. Wilson. 1990. Crystal structures of an antibody to a peptide and its complex with peptide antigen at 2.8 A. Science **248:**712-9.

302. Stanfield, R. L., and I. A. Wilson. 1993. X-ray crystallographic studies of antibody-peptide complexes. Immunomethods **3:**211-221.

303. Steward, M. W., C. M. Stanley, and O. E. Obeid. 1995. A mimotope from a solid-phase peptide library induces a measles virus-neutralizing and protective antibody response. J Virol **69:**7668-73.

304. Stiegler, G., C. Armbruster, B. Vcelar, H. Stoiber, R. Kunert, N. L. Michael, L. L. Jagodzinski, C. Ammann, W. Jager, J. Jacobson, N. Vetter, and H. Katinger. 2002. Antiviral activity of the neutralizing antibodies 2F5 and 2G12 in asymptomatic HIV-1-infected humans: a phase I evaluation. Aids **16:**2019-25.

305. Stiegler, G., R. Kunert, M. Purtscher, S. Wolbank, R. Voglauer, F. Steindl, and H. Katinger. 2001. A potent cross-clade neutralizing human monoclonal antibody against a novel epitope on gp41 of human immunodeficiency virus type 1. AIDS Res Hum Retroviruses **17:**1757-65.

306. Sullivan, B. L., E. J. Knopoff, M. Saifuddin, D. M. Takefman, M. N. Saarloos, B. E. Sha, and G. T. Spear. 1996. Susceptibility of HIV-1 plasma virus to complement-mediated lysis. Evidence for a role in clearance of virus in vivo. J Immunol **157:**1791-8.

307. Sun, Y., K. Y. Fong, M. C. Chung, and Z. J. Yao. 2001. Peptide mimicking antigenic and immunogenic epitope of double-stranded DNA in systemic lupus erythematosus. Int Immunol **13:**223-32.

308. Sundberg, E. J., and R. A. Mariuzza. 2003. Molecular Recognition in Antibody-Antigen Complexes, p. 119-160. *In* J. Janin and S. J. Wodak (ed.), Advances in Protein Chemistry, vol. 61. Academic Press, San Diego.

309. Tafi, R., R. Bandi, C. Prezzi, M. U. Mondelli, R. Cortese, P. Monaci, and A. Nicosia. 1997. Identification of HCV core mimotopes: improved methods for the selection and use of disease-related phage-displayed peptides. Biol Chem **378:**495-502.

310. Theisen, M., D. Dodoo, A. Toure-Balde, S. Soe, G. Corradin, K. K. Koram, J. A. Kurtzhals, L. Hviid, T. Theander, B. Akanmori, M. Ndiaye, and P. Druilhe. 2001. Selection of glutamate-rich protein long synthetic peptides for vaccine development: antigenicity and relationship with clinical protection and immunogenicity. Infect Immun **69:**5223-9.

311. Tian, Y., C. V. Ramesh, X. Ma, S. Naqvi, T. Patel, T. Cenizal, M. Tiscione, K. Diaz, T. Crea, E. Arnold, G. F. Arnold, and J. W. Taylor. 2002. Structure-affinity relationships in the gp41 ELDKWA epitope for the HIV-1 neutralizing monoclonal antibody 2F5: effects of side-chain and backbone modifications and conformational constraints. J Pept Res **59:**264-76.

312. Tomlinson, I. M., G. Walter, P. T. Jones, P. H. Dear, E. L. Sonnhammer, and G. Winter. 1996. The imprint of somatic hypermutation on the repertoire of human germline V genes. J Mol Biol **256:**813-17.

313. Tonini, T., S. Barnett, J. Donnelly, and R. Rappuoli. 2005. Current approaches to developing a preventative HIV vaccine. Curr Opin Investig Drugs **6:**155-62.

314. Trkola, A., A. Grassauer, P. M. Schulz, A. Klima, S. Dopper, G. Gruber, A. Buchacher, T. Muster, and H. Katinger. 1996. Restricted antigenic variability of the epitope recognized by the neutralizing gp41 antibody 2F5. AIDS **10:**587-593.

315. Trkola, A., A. B. Pomales, H. Yuan, B. Korber, P. J. Maddon, G. P. Allaway, H. Katinger, C. F. Barbas, 3rd, D. R. Burton, D. D. Ho, and et al. 1995. Cross-clade neutralization of primary isolates of human immunodeficiency virus type 1 by human monoclonal antibodies and tetrameric CD4-IgG. J Virol **69:**6609-17.

316. Trkola, A., M. Purtscher, T. Muster, C. Ballaun, A. Buchacher, N. Sullivan, K. Srinivasan, J. Sodroski, J. P. Moore, and H. Katinger. 1996. Human monoclonal

antibody 2G12 defines a distinctive neutralization epitope on the gp120 glycoprotein of human immunodeficiency virus type 1. J Virol **70:**1100-8.

317. Turbica, I., F. Simon, and F. Barin. 1999. Antibodies to the CD4-binding site of HIV-1 gp120 in patients infected by variants belonging to the M or O group. J Acquir Immune Defic Syndr Hum Retrovirol **20:**95-7.

318. Ugen, K. E., J. J. Goedert, J. Boyer, Y. Refaeli, I. Frank, W. V. Williams, A. Willoughby, S. Landesman, H. Mendez, A. Rubinstein, and et al. 1992. Vertical transmission of human immunodeficiency virus (HIV) infection. Reactivity of maternal sera with glycoprotein 120 and 41 peptides from HIV type 1. J Clin Invest **89:**1923-30.

319. UNAIDS/WHO. 2004. AIDS Epidemic Update UNAIDS/04.45E. Joint United Nations Programme on HIV/AIDS (UNAIDS) and World health Organization (WHO).

320. Valadon, P., G. Nussbaum, L. F. Boyd, D. H. Margulies, and M. D. Scharff. 1996. Peptide libraries define the fine specificity of anti-polysaccharide antibodies to Cryptococcus neoformans. J Mol Biol **261:**11-22.

321. Valadon, P., G. Nussbaum, J. Oh, and M. D. Scharff. 1998. Aspects of antigen mimicry revealed by immunization with a peptide mimetic of Cryptococcus neoformans polysaccharide. J Immunol **161:**1829-36.

322. -van Houten, N. E., and J. K. Scott. in press. Phage Libraries for Developing Antibody-Targeted Diagnostics and Vaccines. *In* S. S. Sidhu (ed.), Phage Display in Biotechnology and Drug Discovery. Marcel Dekker, New York.

323. Vanhoorelbeke, K., H. Depraetere, R. A. Romijn, E. G. Huizinga, M. De Maeyer, and H. Deckmyn. 2003. A consensus tetrapeptide selected by phage display adopts the conformation of a dominant discontinuous epitope of a monoclonal anti-VWF antibody that inhibits the von Willebrand factor-collagen interaction. J Biol Chem **278:**37815-21.

324. Vanini, S., R. Longhi, A. Lazzarin, E. Vigo, A. G. Siccardi, and G. Viale. 1993. Discrete regions of HIV-1 gp41 defined by syncytia-inhibiting affinity-purified human antibodies. Aids **7:**167-74.

325. Vargas-Madrazo, E., F. Lara-Ochoa, and J. C. Almagro. 1995. Canonical structure repertoire of the antigen-binding site of immunoglobulins suggests strong geometrical restrictions associated to the mechanism of immune recognition. J. Mol. Biol. **254:**479-504.

326. Veazey, R. S., R. J. Shattock, M. Pope, J. C. Kirijan, J. Jones, Q. Hu, T. Ketas, P. A. Marx, P. J. Klasse, D. R. Burton, and J. P. Moore. 2003. Prevention of virus transmission to macaque monkeys by a vaginally applied monoclonal antibody to HIV-1 gp120. Nat Med **9:**343-6.

327. Viau, M., and M. Zouali. 2001. Molecular determinants of the human antibody response to HIV-1: implications for disease control. J Clin Immunol **21:**410-9.

328. Villen, J., E. Borras, W. M. Schaaper, R. H. Meloen, M. Davila, E. Domingo, E. Giralt, and D. Andreu. 2001. Synthetic peptides as functional mimics of a viral discontinuous antigenic site. Biologicals **29:**265-9.

329. Vincent, N., C. Genin, and E. Malvoisin. 2002. Identification of a conserved domain of the HIV-1 transmembrane protein gp41 which interacts with cholesteryl groups. Biochim Biophys Acta **1567:**157-64.

330. Vyas, N. K., M. N. Vyas, M. C. Chervenak, D. R. Bundle, B. M. Pinto, and F. A. Quiocho. 2003. Structural basis of peptide-carbohydrate mimicry in an antibody-combining site. Proc Natl Acad Sci U S A **100:**15023-8.

331. Vyas, N. K., M. N. Vyas, M. C. Chervenak, M. A. Johnson, B. M. Pinto, D. R. Bundle, and F. A. Quiocho. 2002. Molecular recognition of oligosaccharide epitopes by a monoclonal Fab specific for Shigella flexneri Y lipopolysaccharide: X-ray structures and thermodynamics. Biochemistry **41:**13575-86.

332. Wain-Hobson, S. 1993. The fastest genome evolution ever described: HIV variation in situ. Curr Opin Genet Dev **3:**878-83.

333. Wang, L. X., J. Ni, S. Singh, and H. Li. 2004. Binding of high-mannose-type oligosaccharides and synthetic oligomannose clusters to human antibody 2G12: implications for HIV-1 vaccine design. Chem Biol **11:**127-34.

334. Watkins, B. A., M. S. Reitz, Jr., C. A. Wilson, K. Aldrich, A. E. Davis, and M. Robert-Guroff. 1993. Immune escape by human immunodeficiency virus type 1 from neutralizing antibodies: evidence for multiple pathways. J Virol **67:**7493-500.

335. Wei, X., J. M. Decker, S. Wang, H. Hui, J. C. Kappes, X. Wu, J. F. Salazar-Gonzalez, M. G. Salazar, J. M. Kilby, M. S. Saag, N. L. Komarova, M. A. Nowak, B. H. Hahn, P. D. Kwong, and G. M. Shaw. 2003. Antibody neutralization and escape by HIV-1. Nature **422:**307-12.

336. Weissenhorn, W., A. Dessen, S. C. Harrison, J. J. Skehel, and D. C. Wiley. 1997. Atomic structure of the ectodomain from HIV-1 gp41. Nature **387:**426-30.

337. Whatmore, A. M., N. Cook, G. A. Hall, S. Sharpe, E. W. Rud, and M. P. Cranage. 1995. Repair and evolution of nef in vivo modulates simian immunodeficiency virus virulence. J Virol **69:**5117-23.

338. Wilson, I. A., J. M. Rini, D. H. Fremont, G. G. Fieser, and E. A. Stura. 1991. X-ray crystallographic analysis of free and antigen-complexed Fab fragments to investigate structural basis of immune recognition. Methods Enzymol **203:**153-76.

339. Wilson, I. A., and R. L. Stanfield. 1993. Antibody-antigen interactions. Current Opinion in Structural Biology **3:**113-118.

340. Wyatt, R., E. Desjardin, U. Olshevsky, C. Nixon, J. Binley, V. Olshevsky, and J. Sodroski. 1997. Analysis of the interaction of the human immunodeficiency virus type 1 gp120 envelope glycoprotein with the gp41 transmembrane glycoprotein. J Virol **71:**9722-31.

341. Wyatt, R., P. D. Kwong, E. Desjardins, R. W. Sweet, J. Robinson, W. A. Hendrickson, and J. G. Sodroski. 1998. The antigenic structure of the HIV gp120 envelope glycoprotein. Nature **393:**705-11.

342. Xiang, S. H., P. D. Kwong, R. Gupta, C. D. Rizzuto, D. J. Casper, R. Wyatt, L. Wang, W. A. Hendrickson, M. L. Doyle, and J. Sodroski. 2002. Mutagenic stabilization and/or disruption of a CD4-bound state reveals distinct conformations of the human immunodeficiency virus type 1 gp120 envelope glycoprotein. J Virol **76:**9888-99.

343. Yang, X., L. Florin, M. Farzan, P. Kolchinsky, P. D. Kwong, J. Sodroski, and R. Wyatt. 2000. Modifications that stabilize human immunodeficiency virus envelope glycoprotein trimers in solution. J Virol **74:**4746-54.

344. Yang, X., S. Kurteva, S. Lee, and J. Sodroski. 2005. Stoichiometry of antibody neutralization of human immunodeficiency virus type 1. J Virol **79:**3500-8.

345. Yasutomi, Y., S. Koenig, S. S. Haun, C. K. Stover, R. K. Jackson, P. Conard, A. J. Conley, E. A. Emini, T. R. Fuerst, and N. L. Letvin. 1993. Immunization with recombinant BCG-SIV elicits SIV-specific cytotoxic T lymphocytes in rhesus monkeys. J Immunol **150:**3101-7.

346. Young, A. C., P. Valadon, A. Casadevall, M. D. Scharff, and J. C. Sacchettini. 1997. The three-dimensional structures of a polysaccharide binding antibody to Cryptococcus neoformans and its complex with a peptide from a phage display library: implications for the identification of peptide mimotopes. J Mol Biol **274:**622-34.

347. Yu, M. W. N., J. K. Scott, A. Fournier, and P. J. Talbot. 2000. Characterization of murine corona virus neutralization epitopes with phage-displayed peptides. Virology **271:**182-196.

348. Zeder-Lutz, G., A. Benito, and M. H. Van Regenmortel. 1999. Active concentration measurements of recombinant biomolecules using biosensor technology. J Mol Recognit **12:**300-9.

349. Zeder-Lutz, G., J. Hoebeke, and M. H. Van Regenmortel. 2001. Differential recognition of epitopes present on monomeric and oligomeric forms of gp160 glycoprotein of human immunodeficiency virus type 1 by human monoclonal antibodies. Eur J Biochem **268:**2856-66.

350. Zhang, L., R. M. Ribeiro, J. R. Mascola, M. G. Lewis, G. Stiegler, H. Katinger, A. S. Perelson, and M. P. Davenport. 2004. Effects of antibody on viral kinetics in simian/human immunodeficiency virus infection: implications for vaccination. J Virol **78:**5520-2.

351. Zhong, G., G. P. Smith, J. Berry, and R. C. Brunham. 1994. Conformational mimicry of a chlamydial neutralization epitope on filamentous phage. J Biol Chem **269:**24183-8.

352. Zwick, M. B., L. L. Bonnycastle, A. Menendez, M. B. Irving, C. F. Barbas, 3rd, P. W. Parren, D. R. Burton, and J. K. Scott. 2001. Identification and characterization of a peptide that specifically binds the human, broadly neutralizing anti-human immunodeficiency virus type 1 antibody b12. J Virol **75:**6692-9.

353. Zwick, M. B., L. L. Bonnycastle, K. A. Noren, S. Venturini, E. Leong, C. F. Barbas, 3rd, C. J. Noren, and J. K. Scott. 1998. The maltose-binding protein as a scaffold for monovalent display of peptides derived from phage libraries. Anal Biochem **264:**87-97.

354. Zwick, M. B., R. Jensen, S. Church, M. Wang, G. Stiegler, R. Kunert, H. Katinger, and D. R. Burton. 2005. Anti-human immunodeficiency virus type 1 (HIV-1) antibodies 2F5 and 4E10 require surprisingly few crucial residues in the membrane-proximal external region of glycoprotein gp41 to neutralize HIV-1. J Virol **79:**1252-61.

355. Zwick, M. B., H. K. Komori, R. L. Stanfield, S. Church, M. Wang, P. W. Parren, R. Kunert, H. Katinger, I. A. Wilson, and D. R. Burton. 2004. The long third complementarity-determining region of the heavy chain is important in the activity of the broadly neutralizing anti-human immunodeficiency virus type 1 antibody 2F5. J Virol **78:**3155-61.

356. Zwick, M. B., A. F. Labrijn, M. Wang, C. Spenlehauer, E. O. Saphire, J. M. Binley, J. P. Moore, G. Stiegler, H. Katinger, D. R. Burton, and P. W. Parren. 2001. Broadly neutralizing antibodies targeted to the membrane-proximal external region of human immunodeficiency virus type 1 glycoprotein gp41. J Virol **75:**10892-905.

357. Zwick, M. B., P. W. Parren, E. O. Saphire, S. Church, M. Wang, J. K. Scott, P. E. Dawson, I. A. Wilson, and D. R. Burton. 2003. Molecular features of the broadly neutralizing immunoglobulin G1 b12 required for recognition of human immunodeficiency virus type 1 gp120. J Virol **77:**5863-76.

358. Zwick, M. B., J. Shen, and J. K. Scott. 2000. Homodimeric peptides displayed by the major coat protein of filamentous phage. J Mol Biol **300:**307-20.